PACIFIC EARTHQUAKE ENGINEERING
RESEARCH CENTER

Reinvestigation of Liquefaction and Nonliquefaction Case Histories from the 1976 Tangshan Earthquake

Robb Eric S. Moss
California Polytechnic State University
San Luis Obispo, California

Robert Kayen
U.S. Geological Survey

Liyuan Tong
Songyu Liu
Guojun Cai
Southeast University, Nanjing, People's Republic of China

Jiaer Wu
URS
Oakland, California

PEER 2009/102
AUGUST 2009

Reinvestigation of Liquefaction and Nonliquefaction Case Histories from the 1976 Tangshan Earthquake

Robb Eric S. Moss
California Polytechnic State University, San Luis Obispo

Robert E. Kayen
U.S. Geological Survey

Liyuan Tong, Songyu Liu, and Guojun Cai
Southeast University, Nanjing, People's Republic of China

Jiaer Wu
URS Oakland, California

PEER Report 2009/102
Pacific Earthquake Engineering Research Center
College of Engineering
University of California, Berkeley

August 2009

ABSTRACT

A field investigation was carried out to retest liquefaction and nonliquefaction sites from the 1976 Tangshan earthquake in the People's Republic of China (PRC). These sites were carefully investigated in 1978/1979 using standard penetration test (SPT) and cone penetration test (CPT) equipment; however the CPT measurements are obsolete because of the now nonstandard cone that was used at the time. In 2007 a modern cone was mobilized to retest 18 select sites that are particularly valuable because they experienced intense ground shaking, have high fines content, and are classified as nonliquefaction sites. Of the sites reinvestigated and carefully processed, 13 are considered accurate representative case histories that warrant being included in the worldwide CPT database. Two of the sites that were originally documented as exhibiting liquefaction and nonliquefaction have been reassessed as cyclic failure of fine-grained soil and removed from consideration for liquefaction triggering. The most important result of these field investigations are 3 nonliquefaction case histories that experienced intense ground shaking. These 3 case histories reside in a region of the liquefaction-triggering database that is poorly populated and will help constrain the upper bound of future liquefaction-triggering curves.

ACKNOWLEDGMENTS

This material is based upon work supported by the National Science Foundation under Grant No. 0633886. Funding in the People's Republic of China was provided by the National Natural Science Foundation of China (NSFC) Grant No. 40702047 and the Jiangsu Transportation Research Foundation Grant No. 8821006021. Publication of this report was supported by the Pacific Earthquake Engineering Research Center (PEER) with funding from the State of California. Any opinions, findings, and conclusions or recommendations expressed in this material are those of the authors and do not necessarily reflect the views of the funding agencies.

CONTENTS

ABSTRACT iii
ACKNOWLEDGMENTS iv
TABLE OF CONTENTS v
LIST OF FIGURES vii
LIST OF TABLES ix
1 INTRODUCTION 1
2 1976 TANGSHAN EARTHQUAKE 3
3 DATA COLLECTION 11
4 CASE HISTORY PROCESSING 15
5 TANGSHAN CASE HISTORIES 17
REFERENCES 23
APPENDIX A: TANGSHAN CASE HISTORY DATA A-1
APPENDIX B: DATA PROCESSING TECHNIQUES (CHAPTER 4 EXCERPT FROM MOSS ET AL. 2003) B-1
4.1 Introduction B-3
4.2 Field Observations B-3
4.3 Strength Parameters B-4
4.3.1 Choice of Log B-4
4.3.2 Case Selection B-5
4.3.3 Critical Layer Selection B-5
4.3.4 Index Measurements B-6
4.3.5 Masked Liquefaction B-7
4.3.6 Screening for Other Failure Mechanisms B-7
4.3.7 Normalization B-8
4.3.8 Thin Layer Correction B-8
4.3.9 Processed Strength Parameters B-9
4.4 Stress Parameters B-9
4.4.1 Cyclic Stress Ratio B-9

4.4.2 Peak Ground Acceleration B-10
4.4.3 Total and Effective Stress B-11
4.4.4 Nonlinear Shear Mass Participation Factor (r_d) B-12
4.4.5 Moment Magnitude B-12
4.5 Data Class B-13
4.6 Review Process B-14
4.7 Conclusion B-14

LIST OF FIGURES

Figure 2.1 GSHAP seismic hazard map showing 10% in 50 year estimate of peak ground acceleration. Tangshan region is circled 4

Figure 2.2 Chinese intensity map (Zhang and Zhou 1979). Intensity scale correlated to PGA using Chinese Building Code. Sites circled with associated site number. 6

Figure 2.3 Strong motion recordings of 1976 Tangshan event shown with respect to three well-known intraplate attenuation relationships and estimates of rock PGA ranges from Chinese intensity contours. Recordings were from both rock and soil sites and not corrected for nonlinear soil effects 7

Figure 2.4 Atkinson and Boore (1995, 1997) attenuation relationship is shown calibrated to recordings and estimated rock PGA ranges. Attenuation relationship converted from hypocentral to epicentral distance using depth to rupture of 14 km. 8

Figure 3.1 Regional view of sites investigated in this study....................12

Figure 3.2 Intercity view of sites investigated in this study. Tangshan sites, denoted by T and site number, are scattered in and around city. Lutai sites are located outside this city and are denoted by L and site number. 13

Figure 3.3 Investigated sites in proximity to Tangshan City 14

Figure 5.1 Tangshan District and Lutai District case histories shown against Moss et al. (2006) probabilistic liquefaction-triggering curves. X-axis is cone-tip resistance normalized for effective overburden pressure. Y-axis is cyclic stress ratio corrected for magnitude. 20

Figure 5.2 X-axis shows cone-tip resistance modified for “apparent” fines content as measured using friction ratio for proxy. 21

Figure 5.3 Tangshan District and Lutai District case histories with respect to worldwide CPT case history database (Moss et al. 2003). Tangshan District sites are particularly important for high CSR values and for nonliquefaction cases. Lutai District sites are interpreted as examples of cyclic failure of clay and not liquefaction. 22

LIST OF TABLES

Table 2.1 Estimated soil peak ground acceleration (PGA) using calibrated rock attenuation relationships and Stewart et al. (2003) site amplification factors for NEHRP site class D soil conditions. Distances reported in kilometers (km) and peak ground acceleration (PGA) in units of gravity. Minimum or saturation epicentral distance of 10 km used. 9

Table 5.1 Case history values for Tangshan District sites....17

Table 5.2 Case history values for Lutai District sites....17

Table 5.3 GPS coordinates of sites investigated....18

1 Introduction

The 1976 Tangshan, People's Republic of China, earthquake resulted in widespread liquefaction that was well documented at the time by Chinese researchers (Zhou and Guo 1979; Zhou and Zhang 1979). These reports accurately documented case histories of liquefaction and nonliquefaction with SPT (standard penetration test), CPT (cone penetration test), and soil borings to acquire subsurface samples for measuring water content, unit weight, and performing grain size analysis. The CPT measurements, however, were made using what is now an obsolete cone that measured only tip resistance. Current CPT–based liquefaction-triggering procedures (e.g., Moss et al. 2006; Youd et al. 2001) require sleeve friction measurements to make accurate liquefaction predictions. This report documents the efforts to re-acquire subsurface information using a modern cone (capable of measuring tip, sleeve, pore pressure, and shear wave velocity) so that these valuable case histories can be included in the worldwide CPT liquefaction database (Moss et al. 2003). The main focus of these field investigations was at sites providing the most informational content: sites that experienced high estimated ground shaking and soils that contained high fines content. High priority was given to nonliquefaction sites because these tend to be under-represented in the worldwide database.

This research was a collaborative effort between researchers in the United States and the People's Republic of China. The research was directed by Robb Moss (Cal Poly San Luis Obispo) with assistance from Robert Kayen (USGS). Southeast University in Nanjing, PRC, provided the ground support with a fully manned CPT rig and lab support for analyzing soil samples. Collaborators from Southeast University included Prof. Liyuan Tong, Prof. Du, and Guojun Cai. The CEA (China Earthquake Agency) in conjunction with IEM (Inst. Engineering Mechanics) in Harbin provided logistical support and assistance in locating and obtaining access to the sites. Collaborators from CEA-IEM included Prof. Yuan, Prof. Tow, Cao Zhengzhong, Shi Lijing, and several other student researchers. This research was truly a collaborative effort and would not have been successful without the contribution from every member of the research team.

2 1976 Tangshan Earthquake

The M_S=7.8 Tangshan earthquake occurred on July 8, 1976. The epicenter was located in the southern part of the city of Tangshan, and surface fault rupture progressed predominantly to the northeast through the town , with some additional rupture to the southwest. The fault rupture was primarily right-lateral strike-slip in nature. The event occurred in the early hours of the morning, and collapse of unreinforced masonry (URM) structures was the primary cause for fatalities that have recently been reassessed at upwards of 500,000. A detailed compilation of reports on the event and the aftermath can be found in (Liu et al. 2002).

This event occurred in an intraplate region of high seismicity dominated by strike-slip faulting. The global seismic hazard assessment program (GSHAP) (http://www.seismo.ethz.ch/GSHAP/) map of the region. Figure 2.1, shows the high seismicity of this region based on historical seismicity and regional tectonics. The source of crustal stress in this region may be due to the combined effects of the collision zone to the far southwest between the Eurasian plate and the Indian Plate as well as the subduction zone off the east coast between the Eurasian and Philippine plates. The intraplate region may be an old suture zone between accreted subplate sections (Liu et al. 2002).

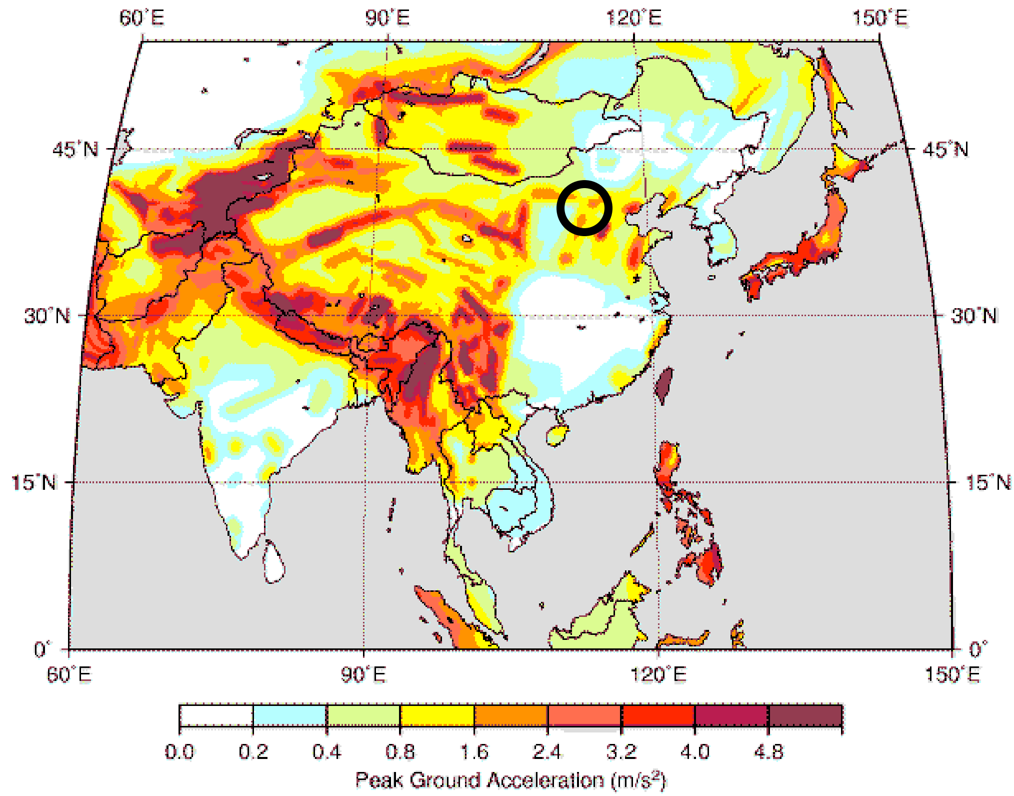

Fig. 2.1 GSHAP seismic hazard map showing 10% in 50 year estimate of peak ground acceleration. Tangshan region is circled.

The area affected by the earthquake is a piedmont region with many rivers and streams flowing to the Bay of Bo, which is connected to the Yellow Sea. The low hills inland from the current coast are the source of river sediment. It is apparent from the subsurface soil conditions that migrating river channels dominate the depositional environment. Flood plain silts are interlayered with sands having varying silt content. At certain locations are clay deposits indicating either past lacustrine depositional environment or sea level rise resulting in a marine depositional environment. Most of the liquefaction occurred in the upper few meters in loose to medium-dense silty fine sand or fine to medium clean sand. Most of the nonliquefaction sites were underlain by very dense clean sand. The sites around Tangshan City are in the Stone River watershed. The sites in the city of Lutai are in the watershed of the Li Yun River.

A calibrated attenuation relationship was used to improve estimates of peak ground acceleration (PGA) at each site. Six recordings (Liu et al. 2002) of the event were used along with correlated intensity contours to fit an intraplate attenuation relationship. The nearest recording was at 148 km epicentral distance, so the near-source fitting was made using rock PGA estimates from Chinese isoseismal intensity contours (Fig. 2.2). (Shibata and Teparaska 1988) correlated Chinese intensity to PGA using the following approximation from the Chinese building code; IX~0.4g, VIII~0.2g, and VI~0.1 g. To account for soil nonlinearity from basement rock to the ground surface, amplification factors by Stewart et al. (2003) were applied. An epicentral distance of 10 km was used as a minimum or lower cap because of the uncertainty in the location of the epicenter with respect to the sites. Figure 2.3 shows the recordings plotted against three well-known intraplate attenuation relationships, and the estimated PGA range from Chinese intensity contours. The three attenuation relationships evaluated were Atkinson and Boore (1995; 1997); Dahle et al. (1990); and Toro et al. (1997). A depth to rupture of 14 km (Liu et al. 2002) was used to convert between hypocentral and epicentral distance. By inspection, the Atkinson and Boore relationship provide the best fit to mean PGA for small and large epicentral distances. This attenuation relationship was then calibrated to the data (Fig. 2.4) to provide a better estimate of the ground shaking that occurred during the Tangshan event.

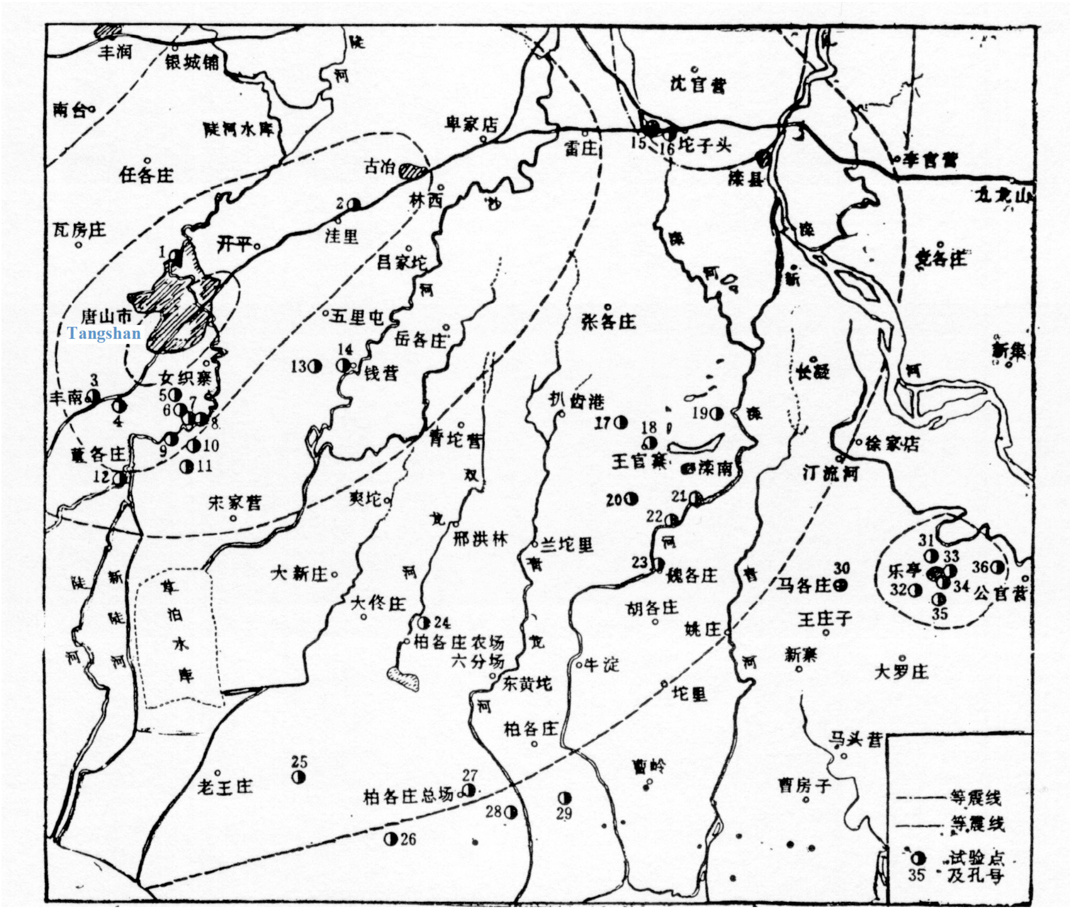

Fig. 2.2 Chinese intensity map (Zhang and Zhou 1979). Intensity scale correlated to PGA using Chinese Building Code. Sites circled with associated site number.

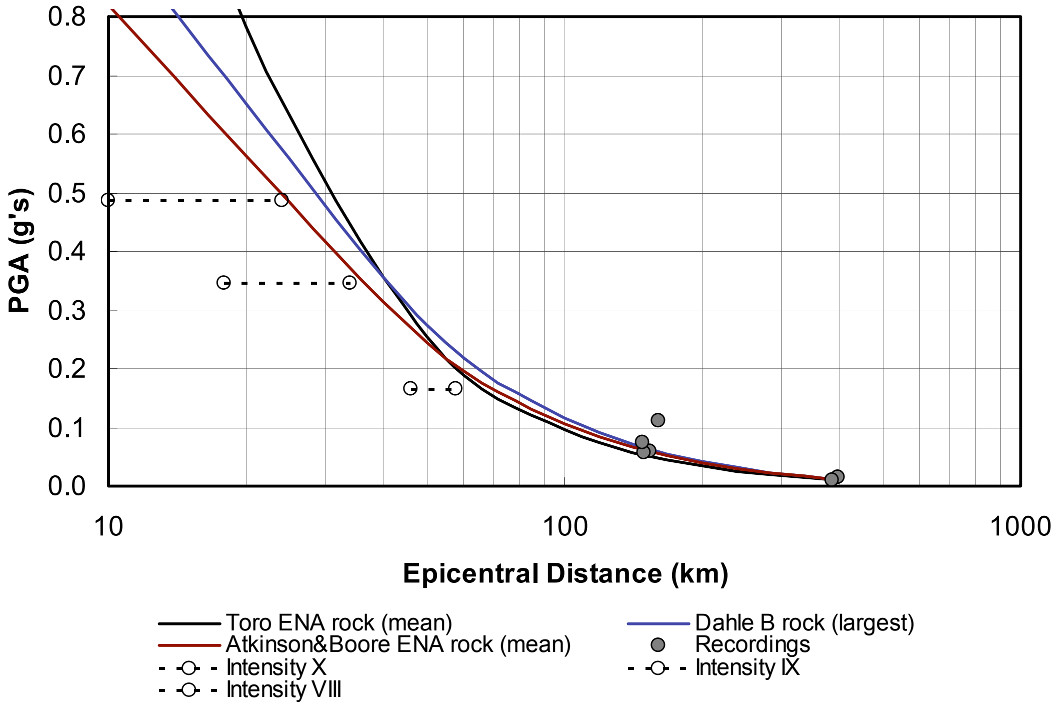

Fig. 2.3 Strong motion recordings of 1976 Tangshan event shown with respect to three well-known intraplate attenuation relationships and estimates of rock PGA ranges from Chinese intensity contours. Recordings were from both rock and soil sites and not corrected for nonlinear soil effects.

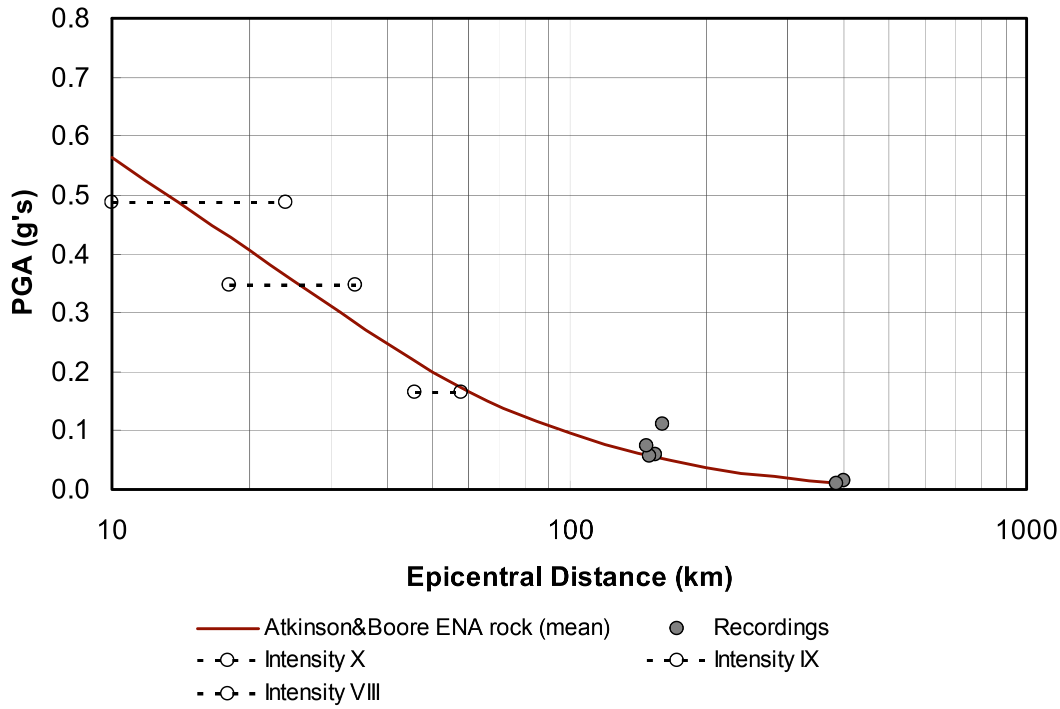

Fig. 2.4 Atkinson and Boore (1995, 1997) attenuation relationship is shown calibrated to recordings and estimated rock PGA ranges. Attenuation relationship converted from hypocentral to epicentral distance using depth to rupture of 14 km.

Table 2.1 Estimated soil peak ground acceleration (PGA) using calibrated rock attenuation relationships and Stewart et al. (2003) site amplification factors for NEHRP site class D soil conditions. Distances reported in kilometers (km) and peak ground acceleration (PGA) in units of gravity. Minimum or saturation epicentral distance of 10 km used.

Sites	Epicentral Distance	Minimum Distance	PGA Rock	Amplification	PGA Soil
T1	8	10	0.56	1.13	0.64
T2	16	16	0.46	1.14	0.53
T3	10	10	0.56	1.13	0.64
T4	9	10	0.56	1.13	0.64
T5	6	10	0.56	1.13	0.64
T6	7	10	0.56	1.13	0.64
T7	6	10	0.56	1.13	0.64
T8	8	10	0.56	1.13	0.64
T9	9	10	0.56	1.13	0.64
T10	9	10	0.56	1.13	0.64
T11	11	11	0.54	1.13	0.61
T12	13	13	0.51	1.14	0.58
T13	13	13	0.51	1.14	0.58
T14	15	15	0.47	1.14	0.54
T15	43	43	0.23	1.20	0.27
T16	46	46	0.22	1.21	0.26
L1	44	44	0.22	1.20	0.27
L2	44	44	0.22	1.20	0.27

3 Data Collection

Data collection involved using the CPT to measure tip resistance (qc), sleeve friction (fs), pore pressure (u), and incremental shear wave velocity. Soil samples were retrieved using a CPT soil sampler and hand auger. SASW (spectral analysis of surface waves) were made at the site previously.

The CPT rig is a Vertek-Hogentogler 200kN (20 ton) seismic piezocone penetrometer. The cones (adhering to ASTM 5778) used have a 10 cm2 base area with an apex angle of 60º. A friction sleeve, located behind the conical tip, has a standard area of 150 cm^2. A pressure transducer is located immediately behind the cone tip. A temperature sensor is also embedded in the cones, which is primarily used to correct data for thermal offset. A slope sensor is included in the cone design to monitor vertically during penetration. A small geophone or accelerometer located inside the cone, measures shear wave velocities. Data were collected at 50 mm intervals. Seismic shear wave velocity measurements were made every 1 m during brief pauses in the cone penetration.

Figures 3.1–3.3 show the geo-referenced locations of the sites from regional to city scale. The coordinates for each site are shown in Table 5.3.

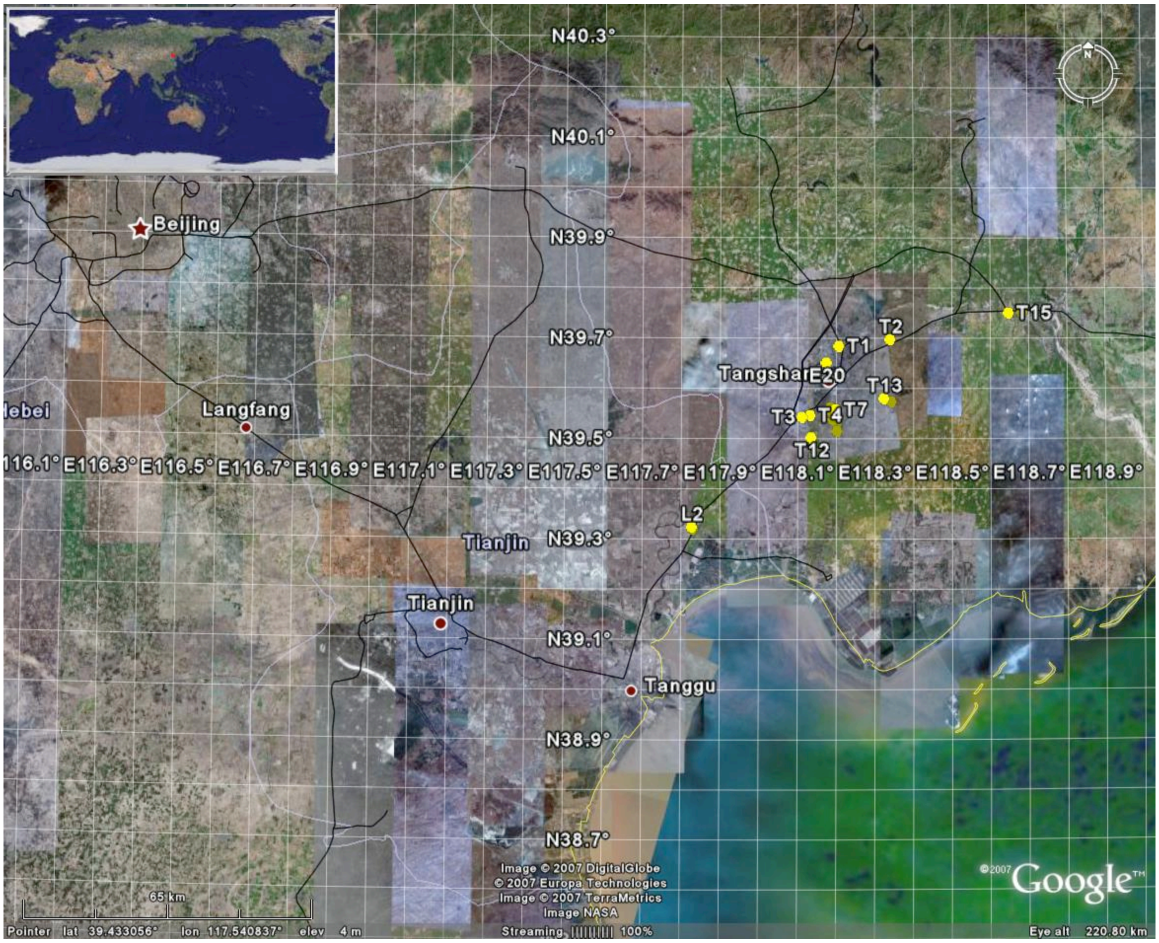

Fig. 3.1 Regional view of sites investigated in this study.

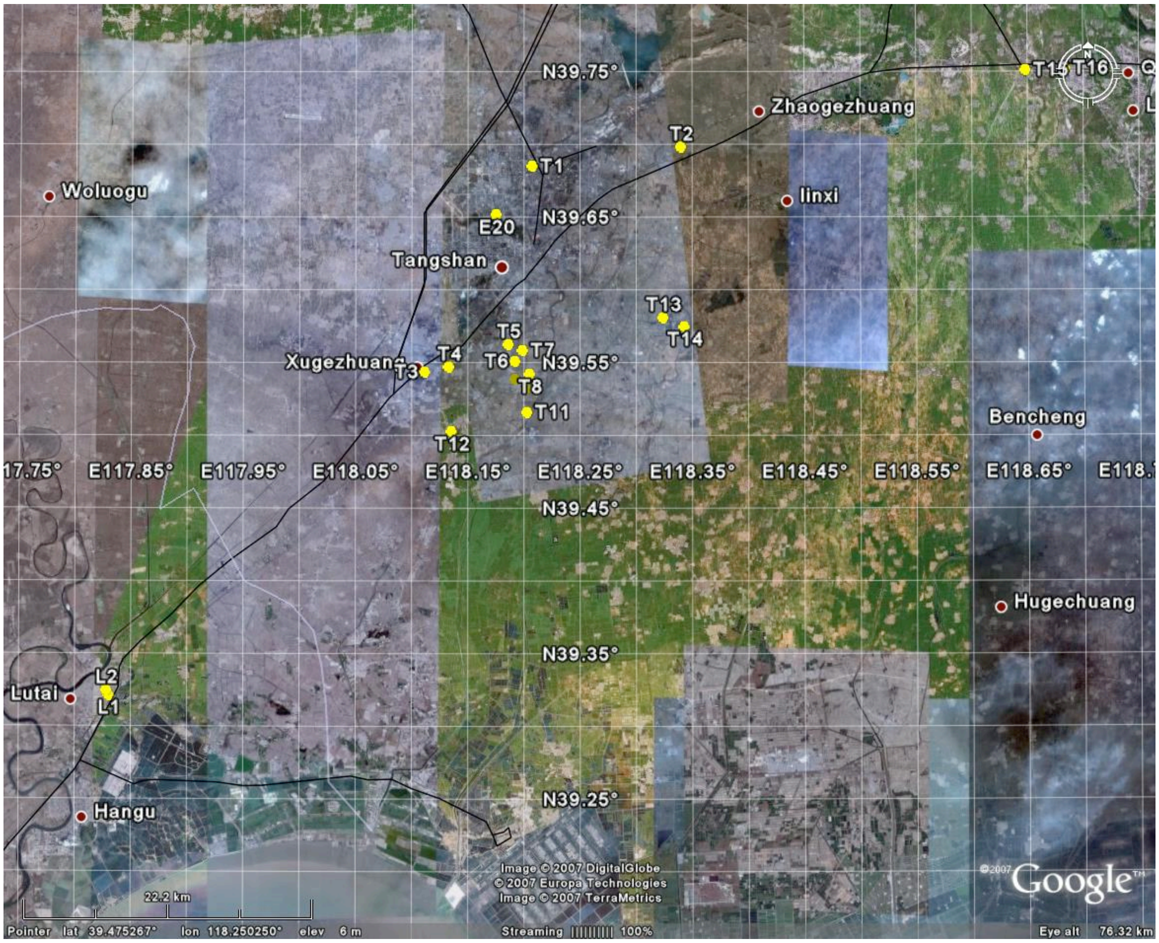

Fig. 3.2 Intercity view of sites investigated in this study. Tangshan sites, denoted by T and site number, are scattered in and around city. Lutai sites are located outside this city and are denoted by L and site number.

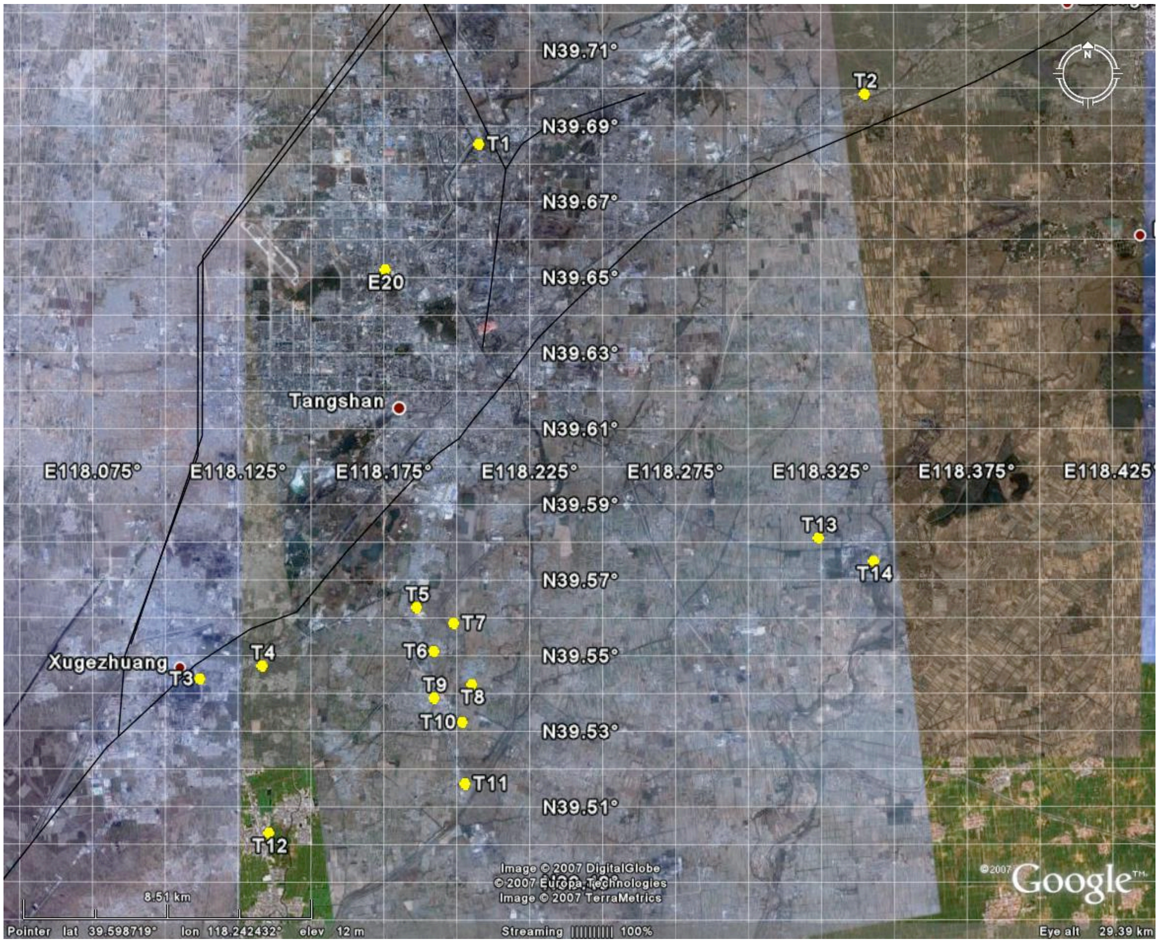

Fig. 3.3 Investigated sites in proximity to Tangshan City.

4 Case History Processing

The case histories from this investigation were processed according to the procedures outlined in Moss et al. (2006). This accounts for the uncertainties in the various input parameters and quantifies the impact of these uncertainties on the resulting liquefaction-triggering correlation. The results are a probabilistic estimate of cyclic loading and cyclic resistance for each site.

The sites investigated as part of this project contain uncertainties that are a byproduct of the subsurface investigations occurring so long after the 1976 earthquake. Reinvestigating liquefaction/nonliquefaction sites of past earthquakes has been carried out before with success (Moss et al. 2005). A key to reinvestigating a previous documented site is accurately locating the spot at which previous subsurface investigations were conducted. This is a function of how well the site was documented via maps, coordinates, ground and aerial photos, field notes, references to landmarks, and, in this case, the long-term memory of residents. The sites must also be relatively unmodified since the previous investigation.

The sites in this report are generally in rural agricultural areas with little land development having occurred since the time of the earthquake and surface elevations are considered to be close to the 1976 elevations, or post-earthquake elevations. Locating the sites consisted of driving to the town or landmark named in the logs by Zhou and Gou (1978) and Zhou and Zhang (1979), asking the residents who survived the earthquake to recall the event and subsequent subsurface investigations, and arriving at a group consensus about the location of the previous investigations. Although this appears to be an *ad hoc* method, the impression that a devastating earthquake and aftermath can have on people and their memories can be profound. This earthquake was not only the single most impressionable event for these people collectively, but in the aftermath they were asked detailed questions about their experiences by a group of investigators with government credentials and large sophisticated testing equipment for drilling the ground to collect subsurface information. In most cases there was little disagreement between the rural residents about where a previous location was, and when there was disagreement, the difference was usually only a few meters (e.g., this side of the pea patch or the other).

Confirmation of the right location can be assessed in a quantitative manner by observing the shape and trends in the 1978/1979 CPT soundings with respect to the recent sounding. Characteristic signatures of the site-specific stratigraphy can be identified and used to confirm that the subsurface conditions between the two soundings are similar. A statistical analysis could be used to provide a more quantitative analysis but this was not deemed a worthwhile investment of time and labor for this project.

The depth to water table is critical to liquefaction-triggering analysis. For this study the depth to water table is based on the measurements made in 1978/1979 by Zhang et al. Water table uncertainty in Moss et al. (2006) was assumed to be a fixed standard deviation of 0.3 m. Because of the uncertainty of the original surface elevation to the current surface elevation and uncertainty in the exact co-location of the previous and current borings, this fixed standard deviation was increased to 0.5 m for this study. It is interesting to note that the water table at the many sites visited have dropped several meters due to regional ground water pumping for agriculture, industrial, and residential use. Rebuilding after the 1976 earthquake has stimulated the regional economy with attendant growth in population and demand for water. Because of the drop in the water table, it is anticipated that liquefaction will be much reduced throughout the region when the next large earthquake occurs.

The critical layer depth is based on the 1978/1979 measurements because this better represents the static stress conditions at the time of the earthquake. There are case histories where the surface elevation has changed slightly since the previous measurements. This is probably due to man-made processes, particularly agricultural practices, since most of the sites are agrarian in nature. For these cases the critical layer trace is matched in the 2007 and 1978/1979 measurements using the characteristic shape of the trace. The 2007 CPT measurements are normalized using the current stress conditions, and the resulting normalized resistance is used to represent the soil resistance at the time of the earthquake.

The magnitude of the event was measured using surface waves at $M_s=7.8$ using the relationships presented in Heaton et al. (1986). Converting surface wave magnitude to moment magnitude results in $M_w=7.89$. Uncertainty from the moment magnitude was based on methods found in Moss et al. (2006).

5 Tangshan Case Histories

The case histories are shown in Appendix A as two pages for each site. These pages contain the pertinent calculations for the cyclic stress ratio (CSR) and cyclic resistance ratio (CRR). Appendix B contains a synopsis of the processing techniques excerpted from the Moss et al. (2003) summary report on the worldwide liquefaction database.

The first case history, site T1, shows an English translation of the subsurface logs from Zhou and Zhang (1979). The following tables show the resulting values and GPS coordinates.

Table 5.1 Case history values for Tangshan District sites.

Site	Liquefied?	Data Class	Median Depth Crit. Layer (m)	Median Depth GWT (m)	σ_{vo} (kPa)	σ_{vo}' (kPa)	a_{max} (g)	r_d	CSR	CSR*	q_{c1} (MPa)	R_f (%)	$q_{c1,mod}$ (MPa)
T1 Tangshan District	Y	C	4.75	3.70	83.38	73.07	0.64	0.82	0.39	0.42	6.85	2.27	8.79
T2 Tangshan District	Y	C	7.40	1.25	141.18	80.84	0.53	0.72	0.43	0.46	4.55	3.65	8.14
T6 Tangshan District	Y	C	5.10	1.50	95.70	60.38	0.64	0.80	0.53	0.57	12.37	0.86	12.81
T7 Tangshan District	Y	C	6.40	3.00	117.30	83.95	0.64	0.74	0.43	0.46	5.68	1.56	6.89
T8 Tangshan District	Y	C	5.25	2.20	96.88	66.95	0.64	0.79	0.48	0.51	10.37	0.84	10.77
T10 Tangshan District	Y	C	8.00	1.45	152.38	88.12	0.64	0.66	0.47	0.51	5.86	1.88	7.48
T11 Tangshan District	Y	C	2.10	0.85	38.83	26.56	0.61	0.94	0.54	0.58	6.65	1.36	7.71
T12 Tangshan District	Y	C	3.10	1.55	56.58	41.37	0.58	0.90	0.47	0.50	3.20	1.33	4.17
T13 Tangshan District	Y	C	7.00	1.05	133.88	75.51	0.58	0.72	0.48	0.52	14.12	0.96	14.67
T14 Tangshan District	NA	C	1.80	1.25	31.98	26.58	0.54	0.95	0.40	0.43	17.30	0.77	17.59
T15 Tangshan District	NA	C	2.40	1.00	44.30	30.57	0.27	0.95	0.24	0.26	16.18	0.74	16.40
T3 Tangshan District	NA	C	6.80	1.50	97.16	61.11	0.64	0.72	0.47	0.51	7.17	3.05	10.16
T4 Tangshan District	N	C	3.40	1.10	63.55	40.99	0.64	0.87	0.56	0.61	16.26	1.07	16.96
T5 Tangshan District	N	C	4.50	3.00	80.25	65.54	0.64	0.83	0.42	0.46	12.58	1.06	13.22
T9 Tangshan District	N	C	4.00	1.10	75.25	46.80	0.64	0.86	0.57	0.62	17.16	0.83	17.58
T16 Tangshan District	N	C	7.50	3.50	137.50	98.26	0.26	0.78	0.19	0.20	10.88	0.94	11.24

Table 5.2 Case history values for Lutai District sites.

Site	Liquefied?	Data Class	Median Depth Crit. Layer (m)	Median Depth GWT (m)	σ_{vo} (kPa)	σ_{vo}' (kPa)	a_{max} (g)	r_d	CSR	CSR*	q_{c1} (MPa)	R_f (%)	$q_{c1,mod}$ (MPa)	CSR^*_{cyclic}	CRR_{cyclic}
L1 Lutai District	N?	C	9.75	0.40	189.13	97.40	0.27	0.70	0.24	0.25	3.60	1.71	4.70	0.26	0.24
L2 Lutai District	Y?	ERR	12.50	0.21	243.23	122.66	0.27	0.63	0.22	0.24	3.32	1.31	4.03	0.26	0.17

In Table 5.1 a site that has NA in the Liquefied? column indicates that this site was removed from the database due to some problem with the data or the site. Specific reasons for a site being removed are described and highlighted on the data sheet for that site. The data processing techniques used for this analysis were the techniques developed by Moss et al.

(2003), Appendix B in this report. CSR is the simplified stress ratio, CSR* is the simplified stress ratio that has been corrected to M_w 7.5. In Table 5.2 CSR^*_{cyclic} and CRR_{cyclic} are the terms used in Boulanger and Idriss (2006) to define the cyclic stress ratio and cyclic resistance ratio of clay-like soils. Irrespective of the occurrence of cyclic failure, the coefficient of variation for Lutai L2 exceeds the acceptable criteria for uncertainty, and therefore in the Data Class column there is ERR, which means this would be removed from the liquefaction database.

Table 5.3 GPS coordinates of sites investigated.

Site	Lat	Lon
T1	N39.68541	E118.20774
T2	N39.69860	E118.34025
T3	N39.54396	E118.11207
T4	N39.54745	E118.13343
T5	N39.56293	E118.18641
T6	N39.56293	E118.18641
T7	N39.55876	E118.19913
T8	N39.54255	E118.20538
T9	N39.52287	E118.21356
T10	N39.53253	E118.20206
T11	N39.51628	E118.20302
T12	N39.50315	E118.13576
T13	N39.58128	E118.32427
T14	N39.57511	E118.34322
T15	N39.75145	E118.64855
T16	N39.75266	E118.68437
L1	N39.32172	E117.83062
L2	N39.32503	E117.82849

The summary of case history results are plotted against the probabilistic liquefaction-triggering curves as presented in Moss et al. (2006). Figures 5.1–5.3 show the processed liquefaction and nonliquefaction case histories against the probabilistic triggering curves and the existing worldwide database. The Tangshan District case histories are shown as squares and the Lutai District case histories are shown as triangles. The Tangshan sites agree well with the existing probabilistic triggering curves. The most valuable result from this study and what drove the research effort was acquiring the three nonliquefied sites in the high CSR range. This data region is poorly populated and any high CSR nonliquefied site is extremely useful in constraining the upper portion of the triggering curves. Granted the seismic loading in these cases has been approximated using a fitted attenuation relationship, but the additional uncertainty from this approach has been incorporated into each case history, resulting in confidence in the relative location of the median penetration resistance and cyclic stress ratio values for the site.

The Lutai cases L1 and L2 lie well to the left of the triggering curves, and the liquefaction and nonliquefaction cases are similar in the tip resistance and "apparent" fines content corrected tip resistance. This characteristic has been noticed in cases where there were observed ground deformations similar to liquefaction effects but the soil failed in a cyclic failure mode as discussed by Boulanger and Idriss (2006). This was the situation for case histories from the 1999 Kocaeli, Turkey, Adapazari sites and the 1999 Chi Chi, Taiwan, Wufeng sites. For these two Lutai sites the cyclic resistance ratio CRR was calculated using Boulanger and Idriss (2006). The cyclic failure results present a much more likely scenario than the liquefaction results, and these two cases are deemed as such. Zhou and Guo (1979) observed clay boils at L2, which is physically possible for cyclic failure. Cyclic failure of clay can produce an increase in excess pore pressures that results in ejecta, however the physics of cyclic failure is fundamentally different that the physics of liquefaction. It is conjectured that L2 was experiencing higher static driving shear stresses due to building loads than L1 which led to the manifestation of ground deformations and/or soil ejecta.

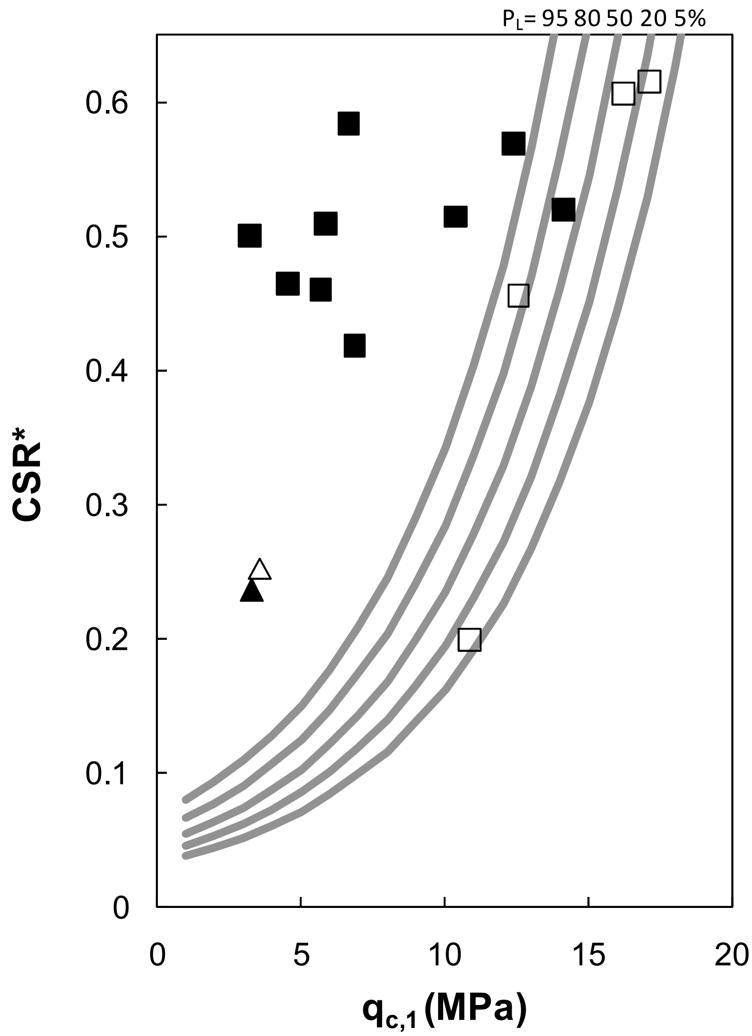

Fig. 5.1 Tangshan District (squares) and Lutai District (triangles) case histories shown against Moss et al. (2006) probabilistic liquefaction-triggering curves. X-axis is cone-tip resistance normalized for effective overburden pressure. Y-axis is cyclic stress ratio corrected for magnitude.

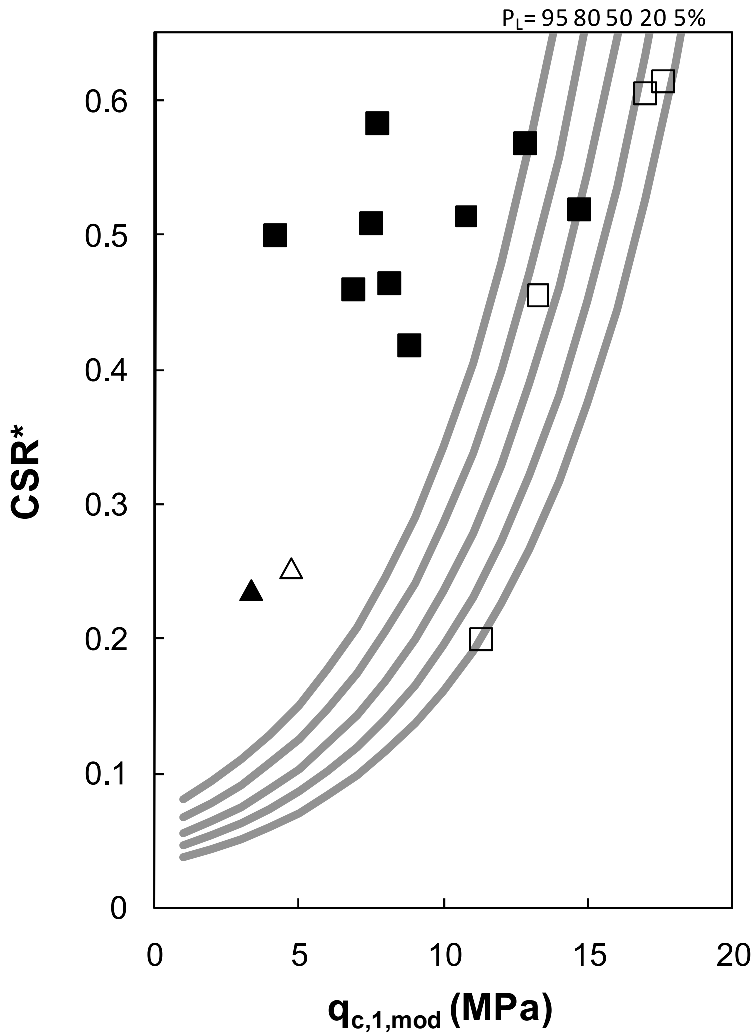

Fig. 5.2 X-axis shows cone-tip resistance modified for "apparent" fines content as measured using friction ratio for proxy.

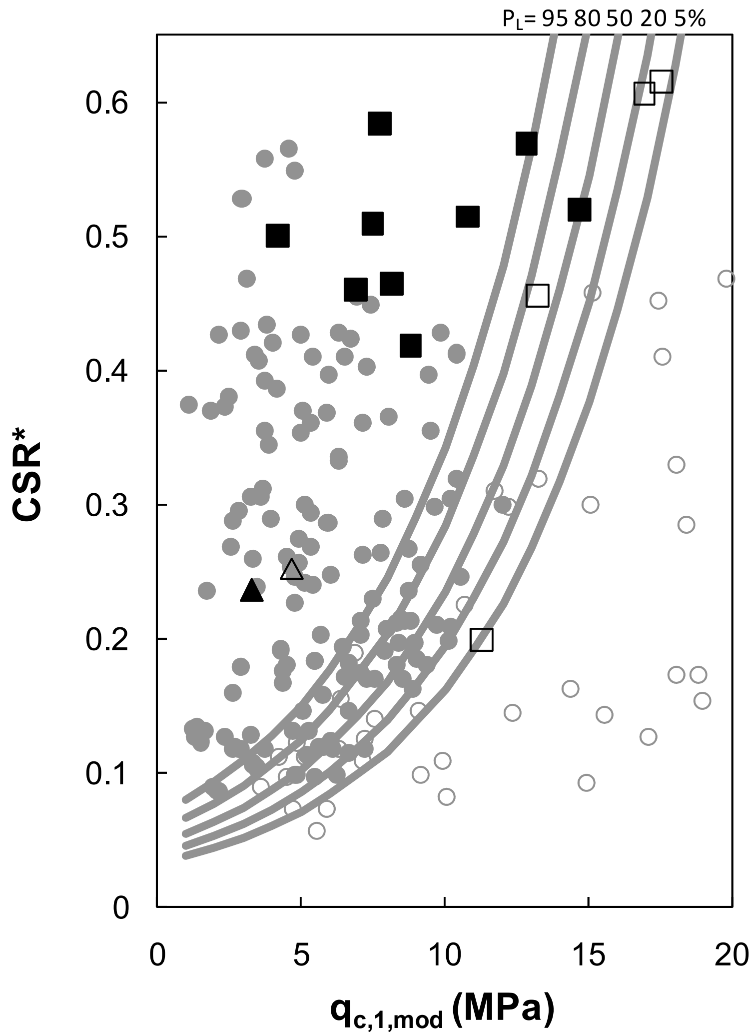

Fig. 5.3 Tangshan District and Lutai District case histories with respect to worldwide CPT case history database (Moss et al. 2003). Tangshan District sites are particularly important for high CSR values and for nonliquefaction cases. Lutai District sites are interpreted as examples of cyclic failure of clay and not liquefaction.

REFERENCES

Atkinson, G. M., and Boore, D. M. (1995). "New ground motion relations for eastern North America." *Bulletin of Seismological Society of America*, 85, 17-30.

Atkinson, G. M., and Boore, D. M. (1997). "Some comparisons between recent ground motion relations." *Seismological Research Letters*, 68, 24-40.

Boulanger, R.W., and Idriss, I.M. (2006). "Liquefaction Susceptibility Criteria for Silts and Clays." *Journal of Geotechnical and Geoenvironmental Engineering*, 132(11).

Dahle, A., Bungum, H., and Dvamme, L. G. (1990). "Attenuation models inferred from intraplate earthquake recordings." *Earthquake Engineering and Structural Dynamics*, 19, 1125-1141.

Liu, H., Housner, G. W., Xie, L., and He, D. (2002). *The Great Tangshan Earthquake of 1976*, Earthquake Engineering Research Library, Cal Tech, Pasadena. http://caltecheerl.library.caltech.edu/353/.

Moss, R. E. S., Collins, B. D., and Whang, D. H. (2005). "Retesting of Liquefaction/Nonliquefaction Case Histories in the Imperial Valley." *Earthquake Spectra*, 21(1), 179-196.

Moss, R. E. S., Seed, R. B., Kayen, R. E., Stewart, J. P., Der Kiureghian, A., and Cetin, K. O. (2006). "Probabilistic Seismic Soil Liquefaction Triggering Using the CPT." *Journal of Geotechnical and Geoenvironmental Engineering*, 132(8).

Moss, R. E. S., Seed, R. B., Kayen, R. E., Stewart, J. P., Youd, T. L., and Tokimatsu, K. (2003). "Field Case Histories for CPT-Based In Situ Liquefaction Potential Evaluation." *Berkeley Geoengineering Research Report No. UCB/GE-2003/04*.

Shengcong, F. and Tatsuoka, F. (1984). "Soil Liquefaction During Haicheng and Tangshan Earthquake in China; a Review." Soils and Foundations, Journal of the Japanese Society of Soil Mechanics and Foundation Engineering, 24(4), 11-29.

Shibata, T., and Teparaska, W. (1988). "Evaluation of Liquefaction Potential of Soils Using Cone Penetration Testing." Soils and Foundations, 28(2), 49-60.

Stewart, J. P., Liu, A. H., and Choi, Y. (2003). "Amplification Factors for Spectral Acceleration in Tectonically Active Regions." *Bulletin of Seismological Society of America*, 93(1), 332-352.

Toro, G. R., Abrahamson, N. A., and Schneider, J. F. (1997). "Model of strong ground motions from earthquakes in central and eastern North America: best estimates and uncertainties." *Seismological Research Letters*, 68, 41-57.

Youd, T. L., Idriss, I. M., Andrus, R. D., Arango, I., Castro, G., Christian, J. T., Dobry, R., Finn, W. D. L., Harder, L. F., Hynes, M. E., Ishihara, K., Koester, J. P., Liao, S. S. C., Marcuson, W. F., III, Martin, G. R., Mitchell, J. K., Moriwaki, Y., Power, M. S., Robertson, P. K., Seed, R. B., and Stokoe, K. H., II,. (2001). "Liquefaction Resistance of Soils: Summary Report from the 1996 NCEER and 1998 NCEER/NSF Workshops on Evaluation of Liquefaction Resistance of Soils." *Journal of Geotechnical and Geoenvironmental Engineering*, 127(10).

Zhou, S. G., and Guo, L. J. (1979). "Liquefaction Investigation in Lutai District." Ministry of Railway, China (in Chinese).

Zhou, S. G., and Zhang, S. M. (1979). "Liquefaction Investigations in Tangshan District." Ministry of Railway, China (in Chinese).

Appendix A: Tangshan Case History Data

Earthquake:	1976 Tanshan, China
Magnitude:	M_S=7.8
Location:	T1 Tangshan District
References:	Zhou & Zhang (1979), Shibata & Teparaska (1988)
Nature of Failure:	Suface evidence

Comments:

Dou He River near park, 250 m upstream bridge.
Bridge collapse, lateral spreading, and widespread liquefaction documeted by Zhou and Zhang.

Sloping free face at the site 8-10 m high.
CPT measurements 50 m back from top of bank.

Case history previously evaluated Moss et al. (2003)

Depths are inconsistent between logs but traces of tip resistance agree on stratigraphy.

Stress		**Strength**			
Liquefied	Y	N (bpf) from 78/79	9		
Data Class	C	V_S (m/s)			
Critical Layer (m)	4.0 to 5.5				
Median Depth (m)	4.75				
st.dev.	0.08	q_c (MPa)	6.49		
Depth to GWT (m)	3.70	st.dev.	1.42		
st.dev.	0.30	f_s (kPa)	146.99		
σ_v (kPa)	83.38	st.dev.	51.51		
st.dev.	3.04	norm. exp. initial	0.42		
σ_v' (kPa)	73.07	norm. exp. step	0.41		
st.dev.	3.35	norm. exp. Final	0.41		
a_{max} (g)	0.64	difference	0.00		
st.dev.	0.26	C_q, C_f	1.06		
r_d	0.82	C_{thin}	1.00		
st.dev.	0.09	f_{s1} (kPa)	155.17		
M_w	7.89	st.dev.	54.38	**1979 cone data**	
st.dev.	0.10	q_{c1} (MPa)	6.85	q_{c1} (MPa)	5.95
CSR_{eq}	0.39	st.dev.	1.50	st.dev.	1.29
st.dev.	0.16	R_f (%)	2.27		
$C.O.V._{CSR}$	0.42	stdev	0.87		
DWF (Moss et al.)	0.93	del qc	1.94		
DWF (Youd et al.)	0.88	qc1,mod	8.79		
CSR*	0.42	CRR	0.14		

T1 Tangshan District

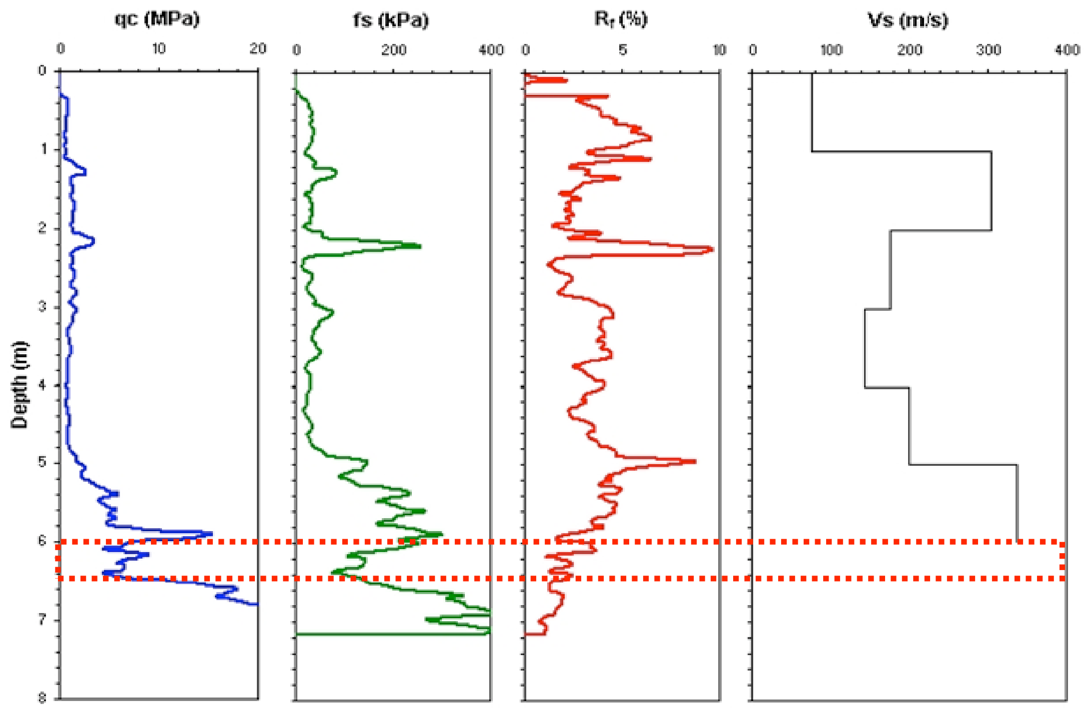

表 3　1 号孔勘探结果

（唐山陡河桥，Ⅹ度区，地下水位3.7米，液化，1977.8）

Water Table (m)

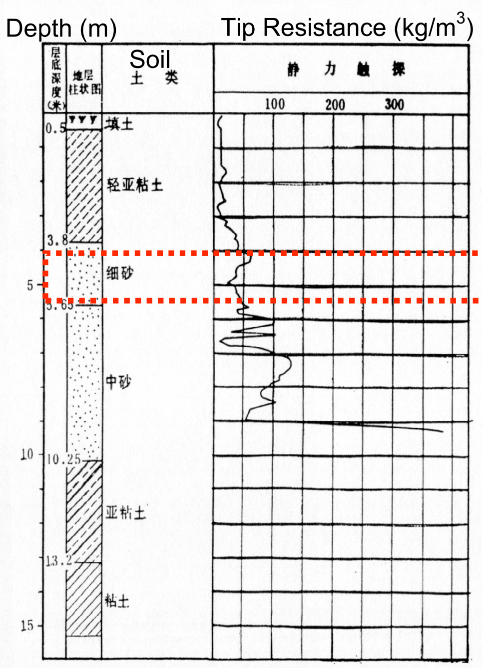

标准贯入试验 SPT		取　样　试　验								
		取样深度 Depth (m)	含水量 Water Content	容重	颗粒分析 Grain Size (mm) / Percent Finer (%)					
深度	击数				10—2	2—0.5	0.5—0.25	0.25—0.1	<0.1	0.1—0.05
3.5	4	2.5	23.6	1.84						
4.6	9									
5.85	14	4.1	11.3	1.68		2.5	30.5	59.0	8.0	
7.6	30	5.4	19.7	2.01	9.0	47.5	27.5	11.5	4.5	
9.5	50	7.3	19.9	2.05	1.7	48.0	39.9	8.9	1.5	
10.5	40									
11.9	17	9.9	17.3	1.88		38.0	40.0	16.5	5.5	
13.1	16	10.2	13.6	2.17		12.0	46.3	29.5	12.5	

Earthquake:	1976 Tanshan, China
Magnitude:	M_S=7.8
Location:	T2 Tangshan District
References:	Zhou & Zhang (1979), Shibata & Teparaska (1988)
Nature of Failure:	Suface evidence

Comments: Liquefaction documented by Zhou and Zhang.

Traces match at the stiff later starting at 5.5 m from 78/79 trace and starting at 7.5 m in 08 trace. 2 m increase differeince in elev (dipping bed?).

Critical layer that corresponds with 1988 and 2003 interpretation has friction ratio that exceeds database boundaries for liquefiable soil.
Shear wave velocity is high for liquefiable layer?

Case history previously evaluated Moss et al (2003)

Stress		**Strength**			
Liquefied	Y	N (bpf) from 78/79			
Data Class	C	V_S (m/s)	554		
Critical Layer (m)	7.0 to 7.8				
Median Depth (m)	7.40				
st.dev.	0.13	q_c (MPa)	4.17		
Depth to GWT (m)	1.25	st.dev.	1.65		
st.dev.	0.30	f_s (kPa)	152.08		
σ_v (kPa)	141.18	st.dev.	99.47		
st.dev.	4.84	norm. exp. initial	0.42		
σ_v' (kPa)	80.84	norm. exp. step	0.41		
st.dev.	4.68	norm. exp. Final	0.40		
a_{max} (g)	0.53	difference	0.00		
st.dev.	0.21	C_q, C_f	1.09		
r_d	0.72	C_{thin}	1.00		
st.dev.	0.13	f_{s1} (kPa)	165.73		
M_w	7.89	st.dev.	108.39	**1979 cone data**	
st.dev.	0.10	q_{c1} (MPa)	4.55	q_{c1} (MPa)	3.79
CSR_{eq}	0.43	st.dev.	1.80	st.dev.	1.56
st.dev.	0.19	R_f(%)	3.65		
$C.O.V._{CSR}$	0.44	stdev	0.94		
DWF (Moss et al.)	0.93	del qc	3.59		
DWF (Youd et al.)	0.88	qc1,mod	8.14		
CSR*	0.46	CRR	0.11		

T2 Tangshan District

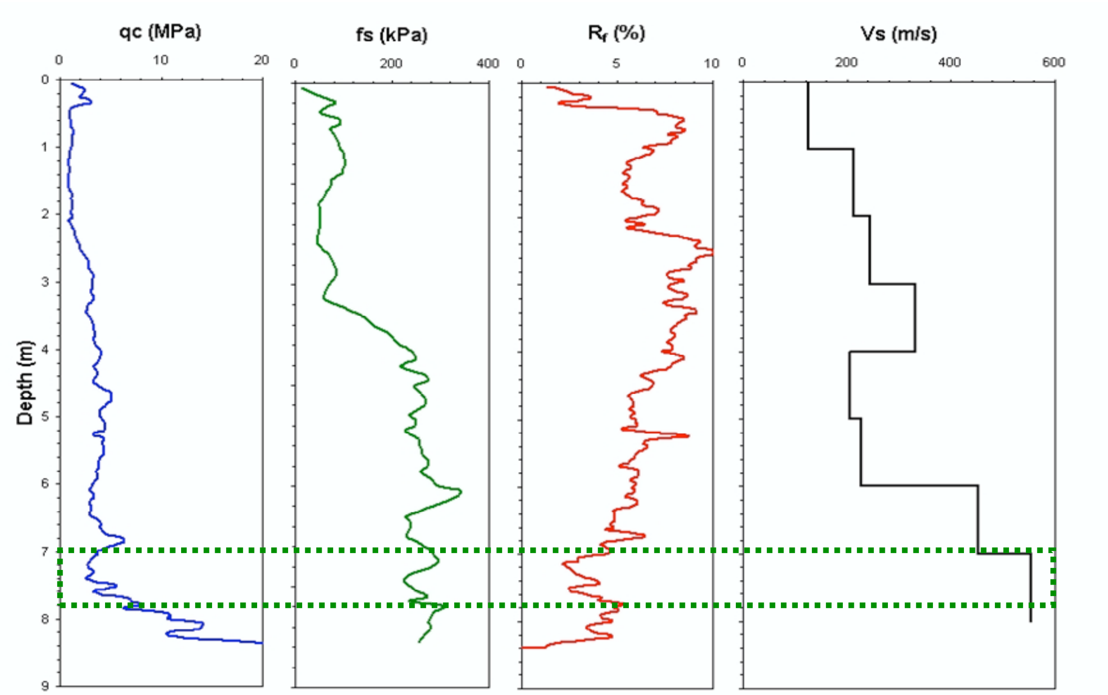

表 4　2 号孔勘探结果

（唐山洼里，Ⅹ度区，地下水位1.25米，液化，1977.8）

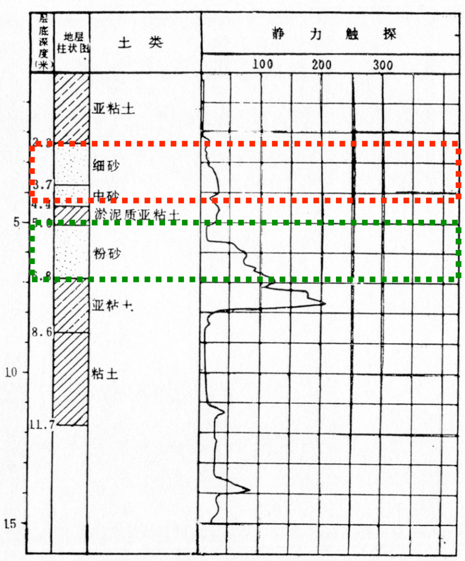

标准贯入试验		取样试验								
		取样深度	含水量	容重	颗粒分析					
深度	击数				10—2	2—0.5	0.5—0.25	0.25—0.1	＜0.1	0.1—0.05
2.8	10	2.0	26.3	1.97						
3.8	10	2.8	21.2	2.06		1.5	27	62	9.5	
4.8	11									
5.8	16									
6.15	23	3.8	21.0	2.04		4.2	81.0	14.5	0.3	
6.6	33	5.6	18.8	2.12		3.5	15.5	33.5	47.5	
7.15	7	6.2	19.1	2.04		4.5	26.5	30.5	38.5	

Earthquake:	1976 Tanshan, China
Magnitude:	M_S=7.8
Location:	T3 Tangshan District
References:	Zhou & Zhang (1979), Shibata & Teparaska (1988)
Nature of Failure:	No surface evidence

Comments:

Non-liquefaction documented by Zhou and Zhang.

CPT located approx. 140 m from SASW testing.

Next to coal facility developed since earthquake.
CPT started 1 m deep in hand augered hole.

Site conditions appear to have been altered since the earthquake. CPT traces are mismatched, case history eliminated.

Stress		**Strength**	
Liquefied	NA	Soil Class	
Data Class	C	LL	
Critical Layer (m)	6.3 to 7.3	PI	
Median Depth (m)	6.80		
st.dev.	0.17	q_c (MPa)	5.96
Depth to GWT (m)	1.50	st.dev.	0.55
st.dev.	0.30	f_s (kPa)	181.86
σ_v (kPa)	97.16	st.dev.	50.42
st.dev.	3.49	norm. exp. initial	0.39
σ_v' (kPa)	61.11	norm. exp. step	0.37
st.dev.	3.46	norm. exp. Final	0.37
a_{max} (g)	0.64	difference	0.00
st.dev.	0.26	C_q, C_f	1.20
r_d	0.72	C_{thin}	1.00
st.dev.	0.12	f_{s1} (kPa)	218.52
M_w	7.89	st.dev.	60.58
st.dev.	0.10	q_{c1} (MPa)	7.17
CSR_{eq}	0.47	st.dev.	0.67
st.dev.	0.21	R_f(%)	3.05
$C.O.V._{CSR}$	0.44	stdev	0.95
DWF (Moss et al.)	0.93	del qc	3.00
DWF (Youd et al.)	0.88	qc1,mod	10.16
CSR*	0.51	CRR	0.17

T3 Tangshan District

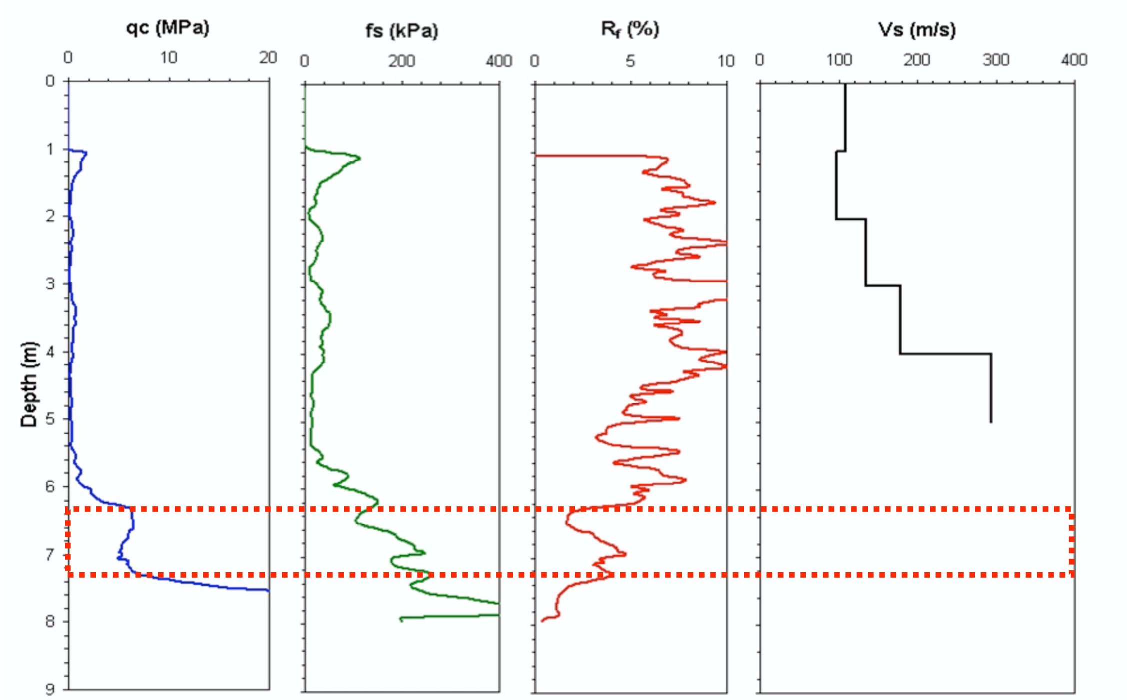

表5　3号孔勘探结果

（丰南县胥各庄，X度区，地下水位1.5米，未液化，1978.10）

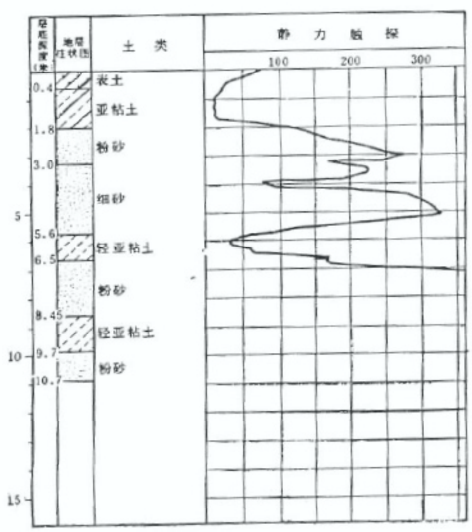

标准贯入试验		取样试验								
					颗粒分析					
深度	击数	取样深度	含水量	容重	10—2	2—0.5	0.5—0.25	0.25—0.1	0.1—0.05	<0.05
2.0	15	1.7				1	6	19	54	20
3.4	29	3.1			1	18	26	36	14	5
4.4	22	4.1				4	27	46	16	7
5.3	44	5.1				1	30	52	13	4
6.3	14	6.0				3	11	15	45	26
7.8	50	7.6					1	9	77	13
10.3	32	10				1	3	7	55	34

Earthquake:	1976 Tanshan, China
Magnitude:	M_S=7.8
Location:	T9 Tangshan District
References:	Zhou & Zhang (1979), Shibata & Teparaska (1988)
Nature of Failure:	
Comments:	Nonliquefaction documented by Zhou and Zhang.

Two soundings performed adjacent to each other.
T9-1 was 1.2m lower relative to T9-2.

Samples taken at 3m classified as SM

V_S profile in T9-1 appears to be incorrect.

Stress		**Strength**	
Liquefied	N	N (bpf) from 78/79	13
Data Class	C	V_S (m/s)	181
Critical Layer (m)	3.0 to 5.0		
Median Depth (m)	4.00		
st.dev.	0.33	q_c (MPa)	12.06
Depth to GWT (m)	1.10	st.dev.	2.94
st.dev.	0.30	f_s (kPa)	100.56
σ_v (kPa)	75.25	st.dev.	26.46
st.dev.	6.84	norm. exp. initial	0.49
σ_v' (kPa)	46.80	norm. exp. step	0.46
st.dev.	3.81	norm. exp. Final	0.46
a_{max} (g)	0.64	difference	0.00
st.dev.	0.26	C_q, C_f	1.42
r_d	0.86	C_{thin}	1.00
st.dev.	0.08	f_{s1} (kPa)	143.12
M_w	7.89	st.dev.	37.67
st.dev.	0.10	q_{c1} (MPa)	17.16
CSR_{eq}	0.57	st.dev.	4.18
st.dev.	0.24	R_f(%)	0.83
C.O.V.$_{CSR}$	0.43	stdev	0.15
DWF (Moss et al.)	0.93	del qc	0.42
DWF (Youd et al.)	0.88	qc1,mod	17.58
CSR*	0.62	CRR	0.71

T4 Tangshan District

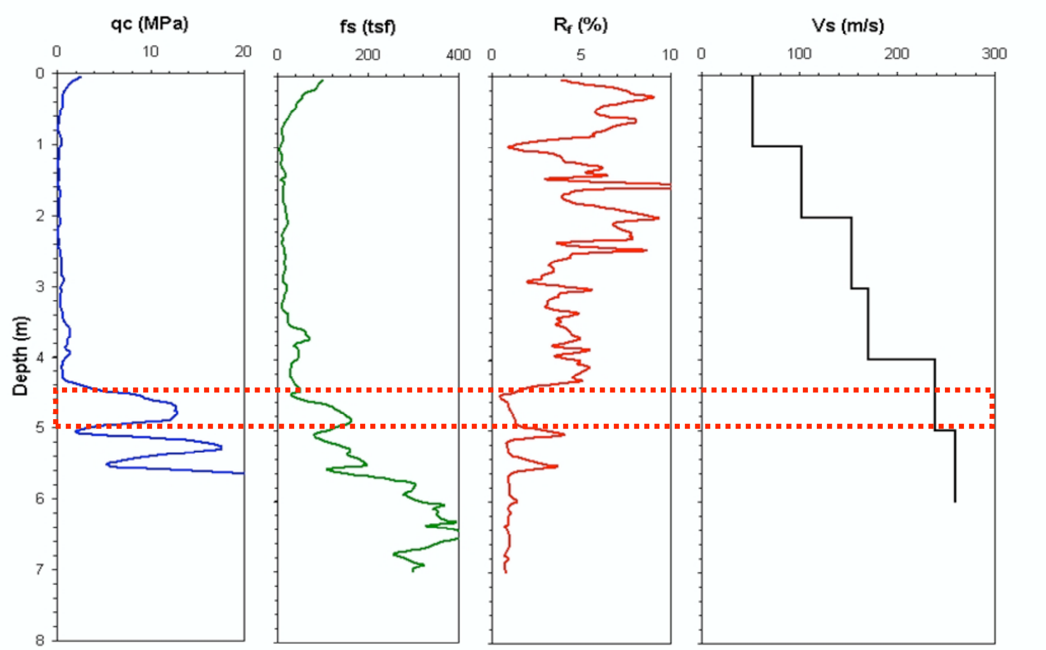

表 6　4号孔勘探结果

（丰南县高庄子，X度区，地下水位1.1米，未液化，1978.9）

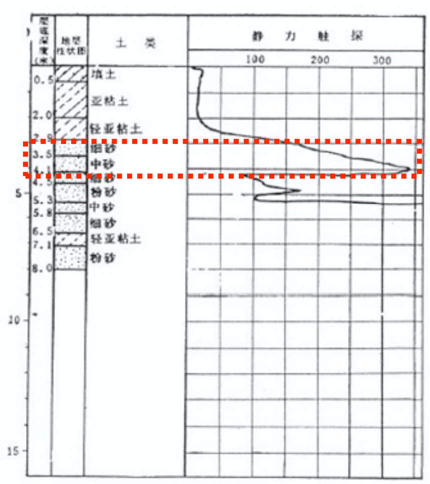

标准贯入试验		取样试验								
		取样深度	含水量	容重	颗粒分析					
深度	击数				10—2	2—0.5	0.5—0.25	0.25—0.1	0.1—0.05	<0.05
3.7	27	3.5				30	48	16	6	
4.8	27	4.5				1	5	43	37	14
5.9	50	5.7				4	21	56	16	3
7.9	48	7.5					1	13	73	13

Earthquake:	1976 Tanshan, China
Magnitude:	M_S=7.8
Location:	T5 Tangshan District
References:	Zhou & Zhang (1979), Shibata & Teparaska (1988)
Nature of Failure:	

Comments: Nonliquefaction documented by Zhou and Zhang.

Thin layer correction was applied to the entire layer 800mm thickiness and a ratio tip resistance of 5.

CPT soil sample taken at 5m

Silty clay soil transitioning to fine/med sand.

Critical layer differs from 1988 interpretation.

Stress		**Strength**	
Liquefied	N	N (bpf) from 78/79	21
Data Class	C	V_S (m/s)	393
Critical Layer (m)	4.0 to 5.0		
Median Depth (m)	4.50		
st.dev.	0.17	q_c (MPa)	7.76
Depth to GWT (m)	3.00	st.dev.	1.59
st.dev.	0.30	f_s (kPa)	98.72
σ_v (kPa)	80.25	st.dev.	19.51
st.dev.	3.97	norm. exp. initial	0.49
σ_v' (kPa)	65.54	norm. exp. step	0.45
st.dev.	3.29	norm. exp. Final	0.45
a_{max} (g)	0.64	difference	0.00
st.dev.	0.26	C_q, C_f	1.35
r_d	0.83	C_{thin}	1.20
st.dev.	0.08	f_{s1} (kPa)	133.42
M_w	7.89	st.dev.	26.37
st.dev.	0.10	q_{c1} (MPa)	12.58
CSR_{eq}	0.42	st.dev.	2.15
st.dev.	0.18	R_f(%)	1.06
$C.O.V._{CSR}$	0.42	stdev	0.30
DWF (Moss et al.)	0.93	del qc	0.64
DWF (Youd et al.)	0.88	qc1,mod	13.22
CSR*	0.46	CRR	0.33

T5 Tangshan District

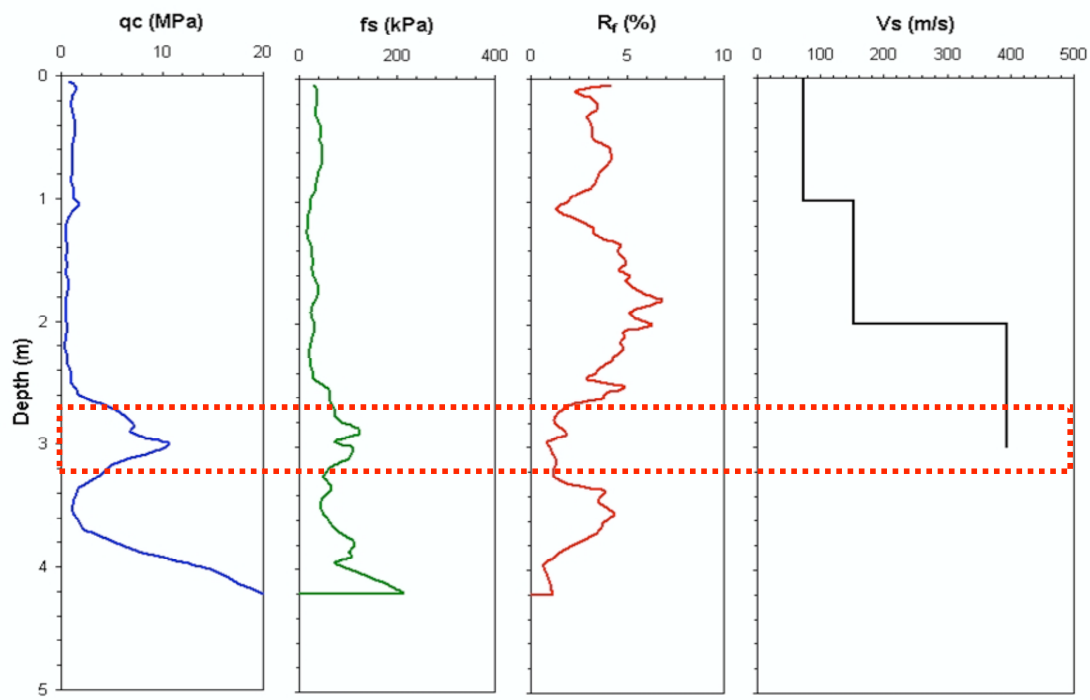

表 7　5 号孔勘探结果

（唐山良种场，X 度区，地下水位3.0米，未液化，1977.8）

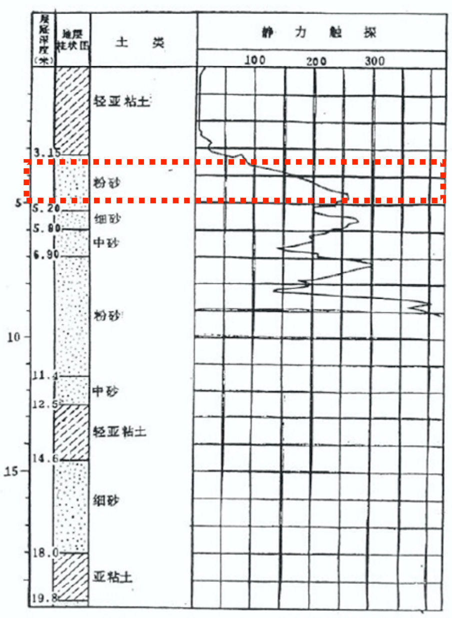

标准贯入试验		取样试验								
		取样	含水	容重	颗粒分析					
深度	击数	深度	量		10—2	2—0.5	0.5—0.25	0.25—0.1	<0.1	0.1—0.05
3.8	21	2.1		2.09						
4.8	36	4.0	24.2	2.03						
5.2	50	5.1	20.4	2.08						
5.8	50	6.6	20.3	2.05						
6.3	38	7.5	24.7	2.00		2.7	4.8	65.6	26.9	
6.9	44	9.6	29.3	1.98		4.8	14.0	32.8	48.4	
7.3	50	10.5	24.2	2.00			3.4	31.8	64.8	
7.8	46	11.5	18.4	2.10	1.1	36.5	26.0	21.1	15.3	
8.3	31	13.9		2.20						
8.8	50	15.0	15.6	2.11	0.9	3.7	29.7	45.9	19.8	
9.3	50	16.1	20.4	2.08						
9.8	50	17.0	19.9	2.05		2.5	41.5	50.4	5.6	
10.8	50									
12.7	50									
14.4	26									
16.3	50									
17.4	50									
18.3	13									

Earthquake:	1976 Tanshan, China
Magnitude:	M_S=7.8
Location:	T6 Tangshan District
References:	Zhou & Zhang (1979), Shibata & Teparaska (1988)
Nature of Failure:	Surface evidence

Comments: Liquefaction documented by Zhou and Zhang.

Approx. 130m from intersection where 78/79 measurements and SASW measurements were performed.

Interlayered silt, silty sand, and fine sand.

Hand auger samples at 2.5 and 3.1m.

Stress		**Strength**	
Liquefied	Y	N (bpf) from 78/79	15
Data Class	C	V_S (m/s)	191
Critical Layer (m)	4.4 to 5.8		
Median Depth (m)	5.10		
st.dev.	0.23	q_c (MPa)	7.68
Depth to GWT (m)	1.50	st.dev.	1.21
st.dev.	0.30	f_s (kPa)	66.12
σ_v (kPa)	95.70	st.dev.	15.93
st.dev.	5.24	norm. exp. initial	0.52
σ_v' (kPa)	60.38	norm. exp. step	0.48
st.dev.	3.72	norm. exp. Final	0.48
a_{max} (g)	0.64	difference	0.00
st.dev.	0.26	C_q, C_f	1.61
r_d	0.80	C_{thin}	1.00
st.dev.	0.09	f_{s1} (kPa)	106.56
M_w	7.89	st.dev.	25.67
st.dev.	0.10	q_{c1} (MPa)	12.37
CSR_{eq}	0.53	st.dev.	1.95
st.dev.	0.22	R_f(%)	0.86
$C.O.V._{CSR}$	0.42	stdev	0.31
DWF (Moss et al.)	0.93	del qc	0.44
DWF (Youd et al.)	0.88	qc1,mod	12.81
CSR*	0.57	CRR	0.31

T6 Tangshan District

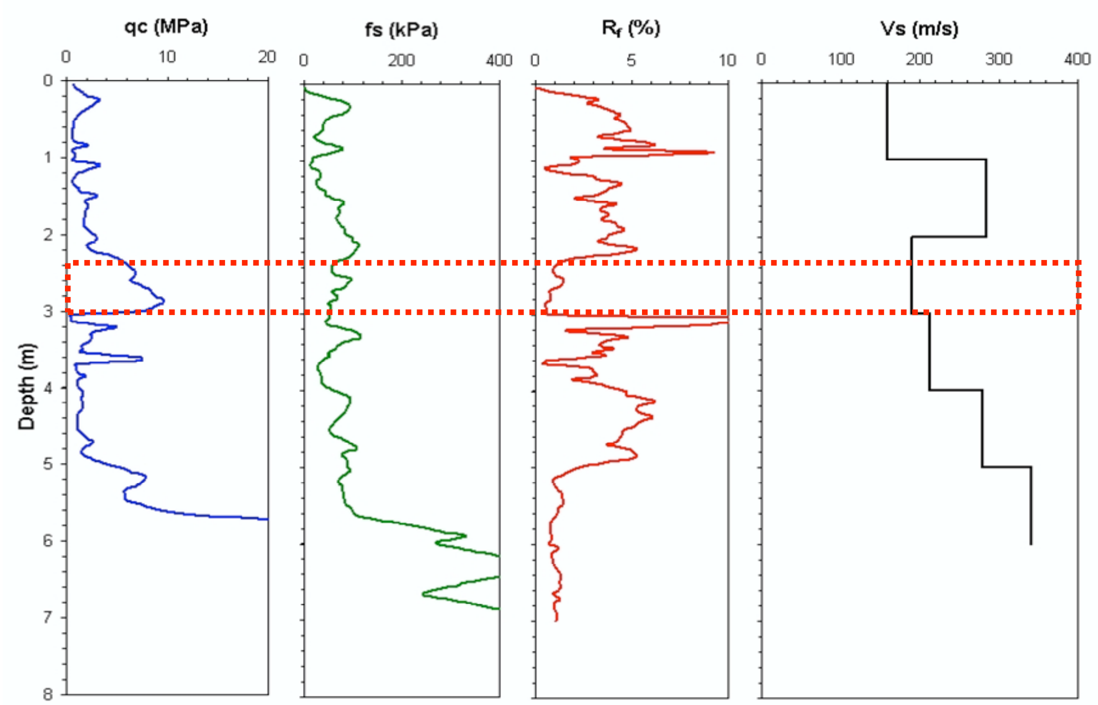

表 8　6 号孔勘探结果

（唐山西大夫坨，X 度区，地下水位1.5米，液化，1977.8）

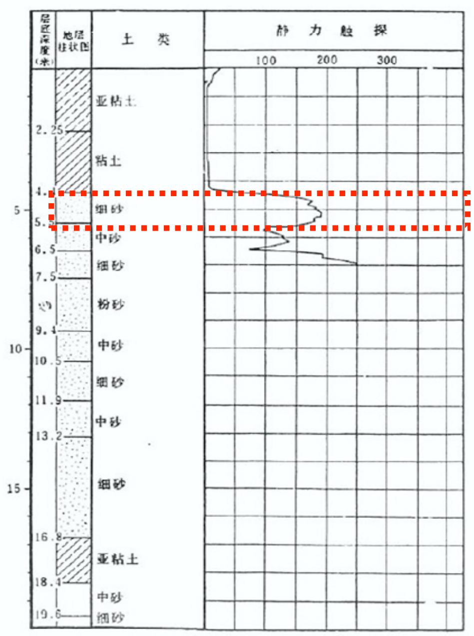

标准贯入试验		取样试验								
		取样深度	含水量	容重	颗粒分析					
深度	击数				10—2	2—0.5	0.5—0.25	0.25—0.1	<0.1	0.1—0.05
4.65	15	3.1		1.85						
5.65	32	5.0	21.0	2.03		2.2	31.8	61.6	4.4	
6.65	29	5.5	18.8	2.03		5.6	48.2	41.0	5.2	
7.65	42	6.5	14.6	2.12		2.0	25.1	51.0	21.9	
8.65	25	7.5	25.5	1.96			12.7	48.9	38.4	32.5
9.65	50	8.6	24.2	1.98			7.7	38.5	53.8	47.6
10.65	38	9.6	18.6	2.06		15.2	47.5	27.4	9.9	
11.8	47	10.7	21.3	2.04			3.5	65.6	29.9	24.7
12.65	50	11.6	22.3	2.02		1.1	9.2	56.0	33.7	31.9
13.65	28	12.5	17.1	2.08		24.9	59.7	11.0	4.4	
14.65	50	13.5	10.7	2.25		8.9	41.0	34.2	15.9	7.8
15.65	50	14.7	20.5	2.09			5.4	75.8	18.8	16.8
16.65	50	15.5	20.0	2.08		1.3	39.2	48.7	10.8	
19.0	50	16.5	19.6	2.10			15.9	74.6	9.5	
20.0	50	18.8	15.5	2.17		8.6	54.7	31.3	5.4	
		19.9	19.7	2.00			2.2	84.6	13.2	

Earthquake: 1976 Tanshan, China
Magnitude: M_S=7.8
Location: T7 Tangshan District
References: Zhou & Zhang (1979), Shibata & Teparaska (1988)
Nature of Failure: Surface evidence

Comments: Liquefaction documented by Zhou and Zhang.

Stress		**Strength**	
Liquefied	Y	N (bpf) from 78/79	12
Data Class	C	V_S (m/s)	173
Critical Layer (m)	5.3 to 7.5		
Median Depth (m)	6.40		
st.dev.	0.37	q_c (MPa)	4.27
Depth to GWT (m)	3.00	st.dev.	0.29
st.dev.	0.30	f_s (kPa)	66.59
σ_v (kPa)	117.30	st.dev.	21.48
st.dev.	7.75	norm. exp. initial	0.51
σ_v' (kPa)	83.95	norm. exp. step	0.48
st.dev.	4.49	norm. exp. Final	0.47
a_{max} (g)	0.64	difference	0.00
st.dev.	0.26	C_q, C_f	1.33
r_d	0.74	C_{thin}	1.00
st.dev.	0.11	f_{s1} (kPa)	88.53
M_w	7.89	st.dev.	28.55
st.dev.	0.10	q_{c1} (MPa)	5.68
CSR_{eq}	0.43	st.dev.	0.38
st.dev.	0.19	R_f(%)	1.56
C.O.V.$_{CSR}$	0.44	stdev	0.62
DWF (Moss et al.)	0.93	del qc	1.20
DWF (Youd et al.)	0.88	qc1,mod	6.89
CSR*	0.46	CRR	0.11

T7 Tangshan District

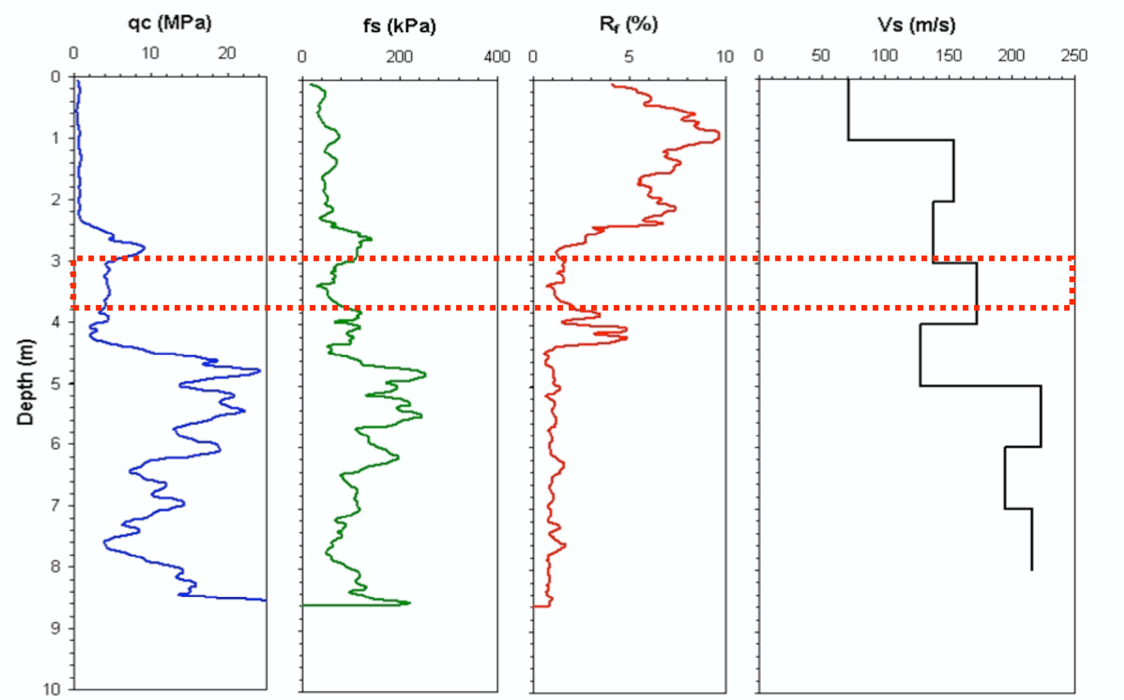

表 9　7 号孔勘探结果

（唐山东大夫坨，X 度区，地下水位3.0米，液化，1977.8）

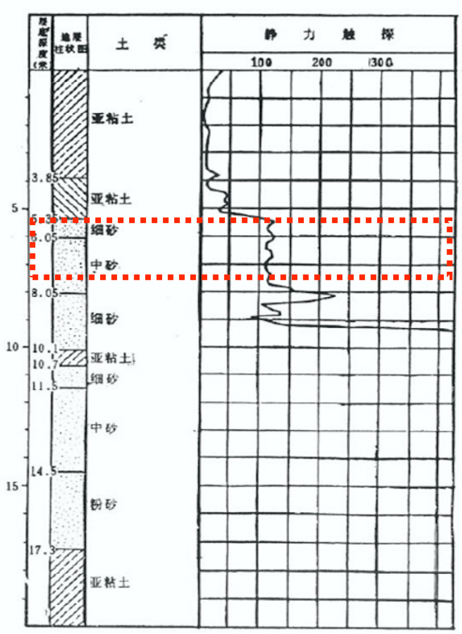

标准贯入试验 深度	标准贯入试验 击数	取样试验 取样深度	取样试验 含水量	取样试验 容重	颗粒分析 10—2	颗粒分析 2—0.5	颗粒分析 0.5—0.25	颗粒分析 0.25—0.1	颗粒分析 <0.1	颗粒分析 0.1—0.05
6.3	12	6.4	22.3	2.03			72.4	26.4	1.2	
7.4	28	7.3	19.5	2.06	2.6	22.5	52.2	21.0	1.1	
8.4	42	8.3	21.3	2.07			34.4	55.6	10.0	
9.3	50	9.3	12.2	2.19		6.5	38.1	31.3	23.8	16.4
10.3	18	11.3	20.3	2.09		9.9	34.4	41.9	13.8	
11.45	48	12.2	19.1	2.01		7.1	46.4	30.7	15.8	12.9
12.3	50	13.3	17.0	2.10		2.7	46.0	37.8	13.5	11.3
13.3	50	14.3	17.3	2.11	1.4	14.9	38.2	41.2	4.3	
14.3	50	15.3	27.5	1.92				4.1	95.9	77.0
16.55	50									
17.55	11									

Earthquake:	1976 Tanshan, China
Magnitude:	M_S=7.8
Location:	T8 Tangshan District
References:	Zhou & Zhang (1979), Shibata & Teparaska (1988)
Nature of Failure:	Surface evidence
Comments:	Liquefaction documented by Zhou and Zhang. Survivors reported wide spread liquefaction with sand blows issuing white sand ejecta.

Stress		**Strength**			
Liquefied	Y	N (bpf) from 78/79	5.5		
Data Class	C	V_S (m/s)	187		
Critical Layer (m)	4.5 to 6.0				
Median Depth (m)	5.25				
st.dev.	0.25	q_c (MPa)	9.08		
Depth to GWT (m)	2.20	st.dev.	2.95		
st.dev.	0.30	f_s (kPa)	76.24		
σ_v (kPa)	96.88	st.dev.	26.03		
st.dev.	5.49	norm. exp. initial	0.51		
σ_v' (kPa)	66.95	norm. exp. step	0.50		
st.dev.	3.72	norm. exp. Final	0.50		
a_{max} (g)	0.64	difference	0.00		
st.dev.	0.26	C_q, C_f	1.14		
r_d	0.79	C_{thin}	1.00		
st.dev.	0.10	f_{s1} (kPa)	87.07		
M_w	7.89	st.dev.	29.73	**1979 cone data**	
st.dev.	0.10	q_{c1} (MPa)	10.37	q_{c1} (MPa)	8.03
CSR_{eq}	0.48	st.dev.	3.37	st.dev.	3.68
st.dev.	0.20	R_f(%)	0.84		
C.O.V.$_{CSR}$	0.42	stdev	0.36		
DWF (Moss et al.)	0.93	del qc	0.40		
DWF (Youd et al.)	0.88	qc1,mod	10.77		
CSR*	0.51	CRR	0.21		

T8 Tangshan District

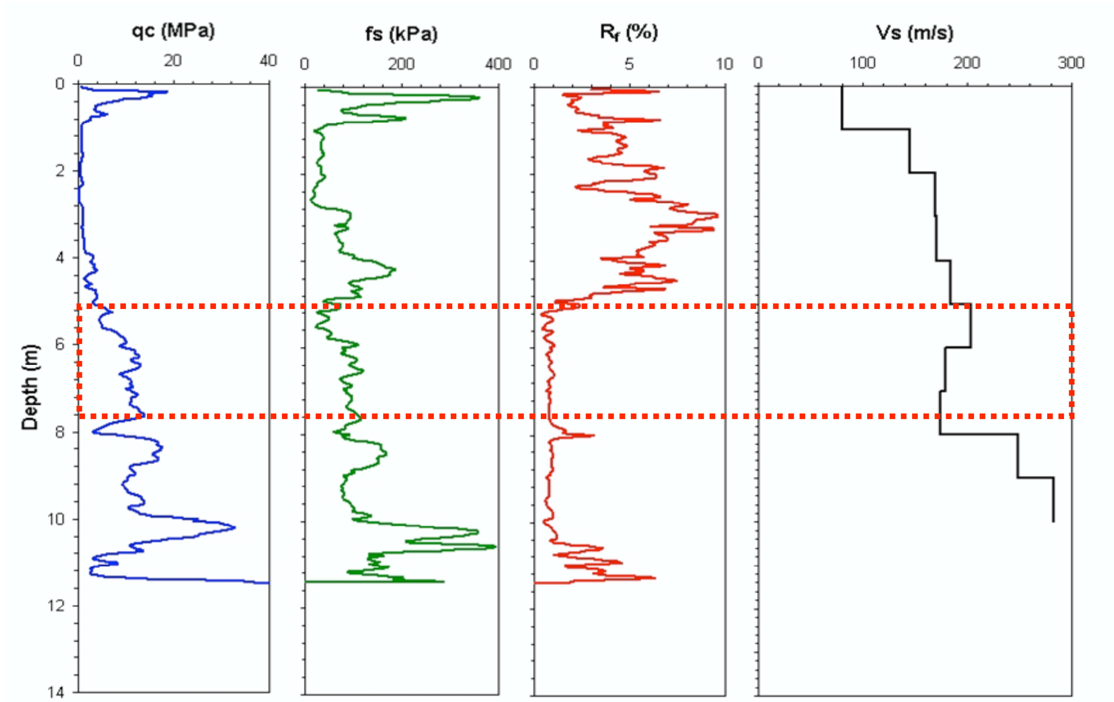

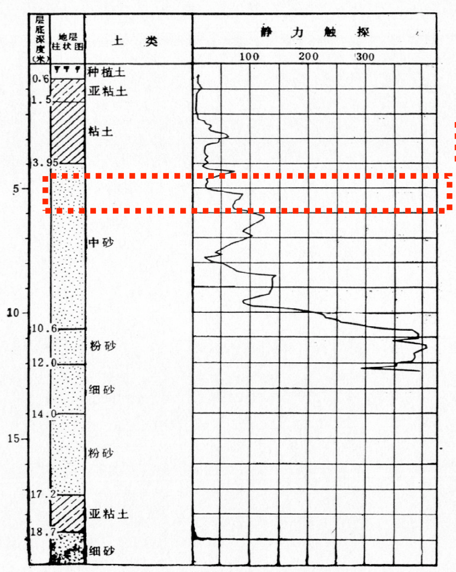

表10　8号孔勘探结果

（唐山老边庄，Ⅹ度区，地下水位2.2米，液化，1977.8）

标准贯入试验		取样试验								
					颗粒分析					
深度	击数	取样深度	含水量	容重	10—2	2—0.5	0.5—0.25	0.25—0.1	<0.1	0.1—0.05
3.6	12	2.0	32.1	1.83						
4.65	8	4.4	19.6	2.05		36.7	57.2	2.5	3.6	
5.65	3	6.2	21.1	2.06		22.0	72.0	5.3	0.7	
6.65	11	7.1	19.6	2.05	1.6	54.0	38.7	2.9	2.8	
7.65	18	8.1	22.4	1.90	1.1	34.1	53.8	9.4	1.6	
8.64	16	9.9	19.6	1.93			0.4	55.5	44.0	41.7
9.55	15	10.8	24.9	1.88			2.0	63.5	34.5	2.8
10.5	50	11.5	22.6	2.01		1.0	34.1	54.9	10.0	
11.1	50	12.6	18.6	2.10		2.1	21.7	63.0	13.2	
11.55	50	13.5	19.6	2.09			3.1	42.1	54.8	46.6
12.5	50	14.5	24.9	2.10		10.1	21.8	44.7	23.4	19.1
13.5	50	15.5	17.5	2.07			15.9	57.3	26.8	24.1
14.5	50	17.9	16.5	2.15		4.4	45.5	38.0	12.1	
15.5	50	19.5	19.1	1.99		26.1	64.6	8.4	0.9	
16.5	50									
17.5	30									
18.5	50									
19.6	50									

Earthquake: 1976 Tanshan, China
Magnitude: M_S=7.8
Location: T9 Tangshan District
References: Zhou & Zhang (1979), Shibata & Teparaska (1988)
Nature of Failure:

Comments: Nonliquefaction documented by Zhou and Zhang.

Two soundings performed adjacent to each other.
T9-1 was 1.2m lower relative to T9-2.

Samples taken at 3m classified as SM

V_S profile in T9-1 appears to be incorrect.

Stress		**Strength**	
Liquefied	N	N (bpf) from 78/79	13
Data Class	C	V_S (m/s)	181
Critical Layer (m)	3.0 to 5.0		
Median Depth (m)	4.00		
st.dev.	0.33	q_c (MPa)	12.06
Depth to GWT (m)	1.10	st.dev.	2.94
st.dev.	0.30	f_s (kPa)	100.56
σ_v (kPa)	75.25	st.dev.	26.46
st.dev.	6.84	norm. exp. initial	0.49
σ_v' (kPa)	46.80	norm. exp. step	0.46
st.dev.	3.81	norm. exp. Final	0.46
a_{max} (g)	0.64	difference	0.00
st.dev.	0.26	C_q, C_f	1.42
r_d	0.86	C_{thin}	1.00
st.dev.	0.08	f_{s1} (kPa)	143.12
M_w	7.89	st.dev.	37.67
st.dev.	0.10	q_{c1} (MPa)	17.16
CSR_{eq}	0.57	st.dev.	4.18
st.dev.	0.24	R_f(%)	0.83
$C.O.V._{CSR}$	0.43	stdev	0.15
DWF (Moss et al.)	0.93	del qc	0.42
DWF (Youd et al.)	0.88	qc1,mod	17.58
CSR*	0.62	CRR	0.71

T9 Tangshan District

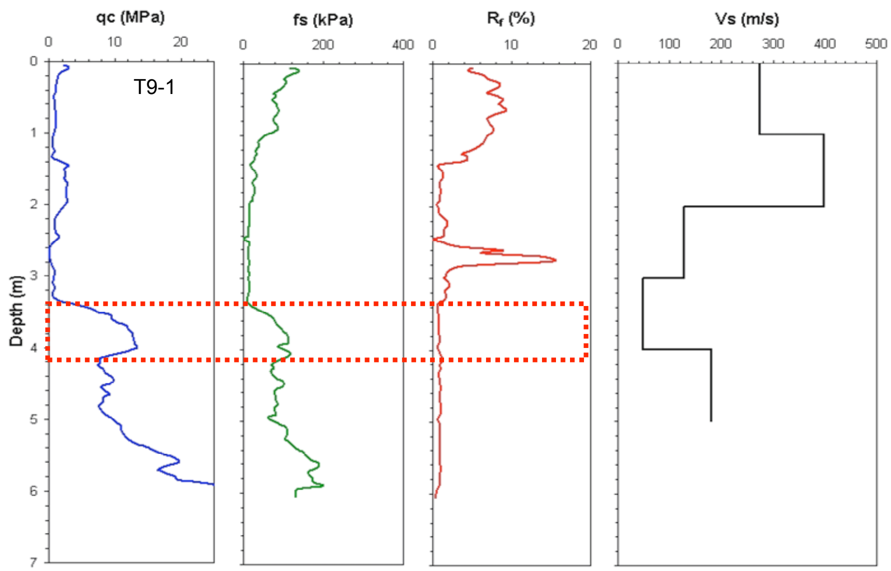

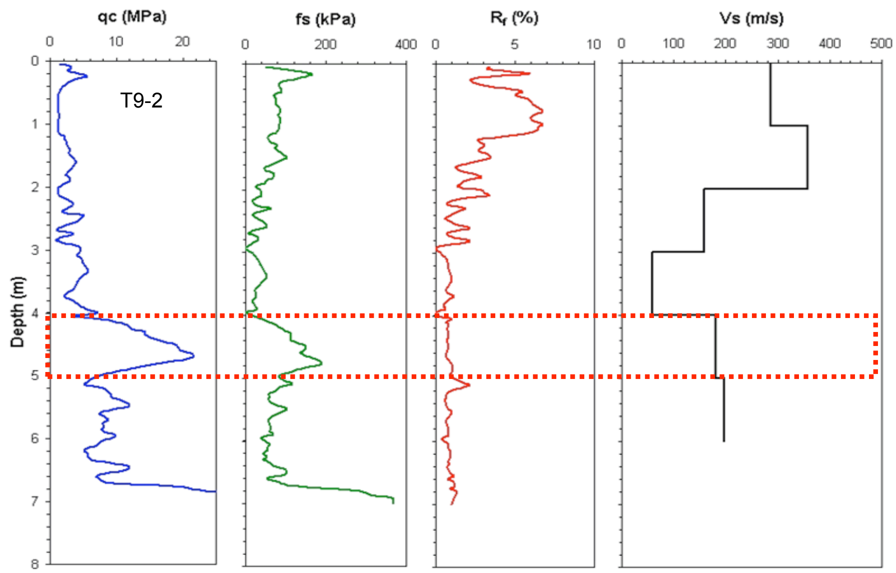

表11　9号孔勘探结果

（丰南县稻地，X度区，地下水位1.1米，未液化，1978.9）

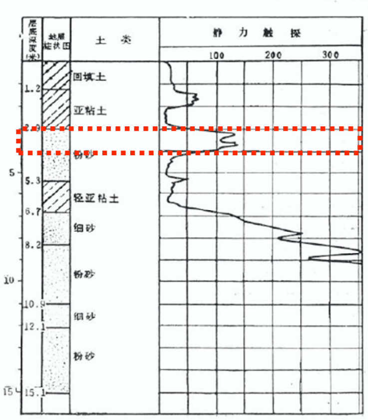

标准贯入试验		取样试验								
					颗粒分析					
深度	击数	取样深度	含水量	容重	10—2	2—0.5	0.5—0.25	0.25—0.1	0.1—0.05	<0.05
4.0	13	3.8					3	69	21	7
7.0	31	6.7				14	19	47	14	6
7.6	30	7.5				6	19	56	14	5
8.4	27	8.2				3	9	48	29	11
9.1	41	9.0				1	4	52	39	4
10.2	48	10.1			1	7	15	54	19	4
11.8	50	11.8			3	10	23	45	15	4
13.9	50	13.8				3	13	55	24	5
14.6	50	14.5				2	13	57	20	8

Earthquake: 1976 Tanshan, China
Magnitude: M_S=7.8
Location: T10 Tangshan District
References: Zhou & Zhang (1979), Shibata & Teparaska (1988)
Nature of Failure: Liquefaction

Comments: Liquefaction documented by Zhou and Zhang.

Stress		**Strength**			
Liquefied	Y	N (bpf) from 78/79	10.3		
Data Class	C	V_S (m/s)	148		
Critical Layer (m)	6.5 to 9.5				
Median Depth (m)	8.00				
st.dev.	0.50	q_c (MPa)	4.95		
Depth to GWT (m)	1.45	st.dev.	2.23		
st.dev.	0.30	f_s (kPa)	93.01		
σ_v (kPa)	152.38	st.dev.	32.21		
st.dev.	10.68	norm. exp. initial	0.47		
σ_v' (kPa)	88.12	norm. exp. step	0.45		
st.dev.	6.01	norm. exp. Final	0.45		
a_{max} (g)	0.64	difference	0.00		
st.dev.	0.26	C_q, C_f	1.18		
r_d	0.66	C_{thin}	1.00		
st.dev.	0.14	f_{s1} (kPa)	110.02		
M_w	7.89	st.dev.	38.10	**1979 cone data**	
st.dev.	0.10	q_{c1} (MPa)	5.86	qc1 (MPa)	5.90
CSR_{eq}	0.47	st.dev.	2.63	st.dev.	1.01
st.dev.	0.22	R_f(%)	1.88		
C.O.V.$_{CSR}$	0.46	stdev	0.89		
DWF (Moss et al.)	0.93	del qc	1.62		
DWF (Youd et al.)	0.88	qc1,mod	7.48		
CSR*	0.51	CRR	0.11		

T10 Tangshan District

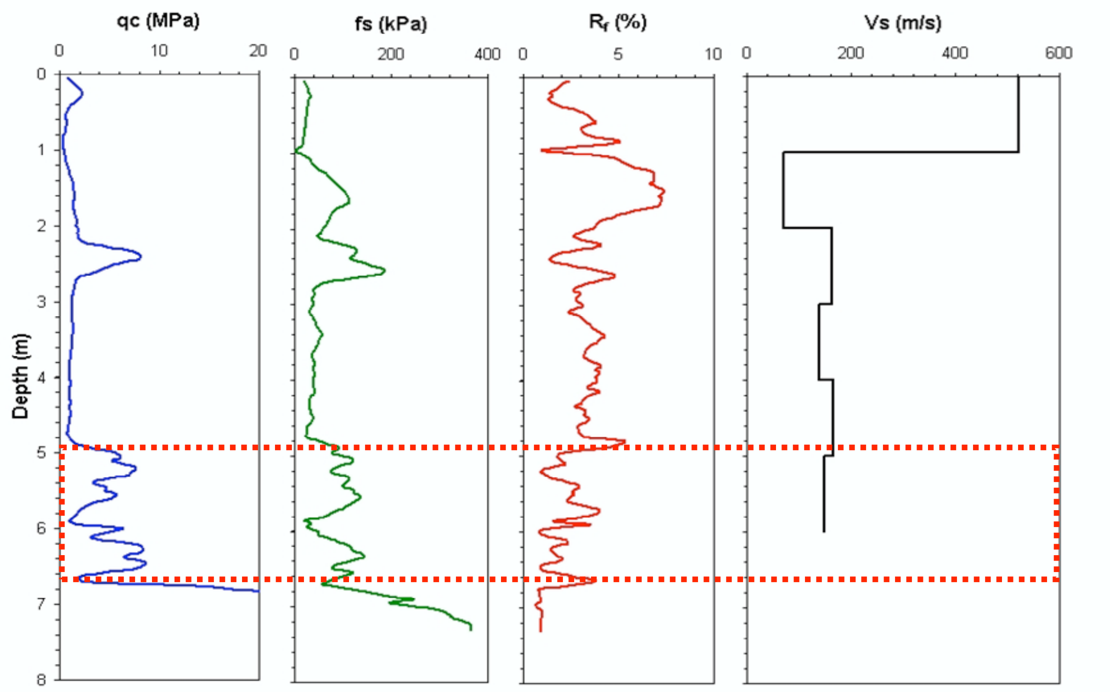

—312—

表12 10号孔勘探结果

(丰南县景庄，Ⅸ度区，地下水位1.45米，液化，1978.9)

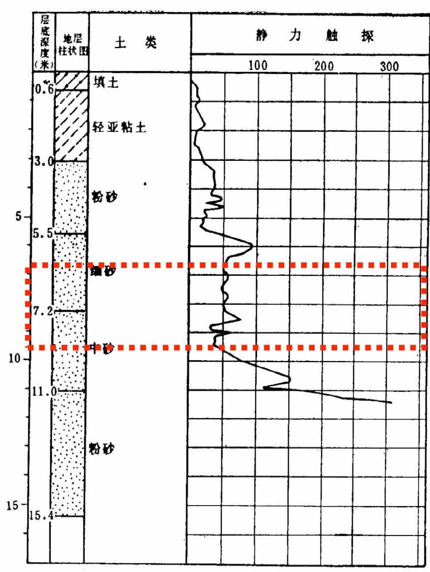

标准贯入试验 深度	标准贯入试验 击数	取样深度	含水量	容重	颗粒分析 10—2	2—0.5	0.5—0.25	0.25—0.1	0.1—0.05	<0.05
3.3	8	3.0					1	8	58	33
3.8	8	3.7					1	2	45	52
4.6	8.5	4.4						1	47	52
5.4	5	5.1							56	44
5.8	18	5.7				1	54	41	4	
6.3	9	6.2				2	48	47	3	
6.9	9	6.8				3	43	50	4	
7.3	13	7.2				5	52	41	2	
7.8	10	7.7				16	39	41	4	
8.8	9	8.7				15	64	18	3	
9.7	11	9.5				15	56	27	2	
10.9	22	10.6				8	35	50	7	

Earthquake:	1976 Tanshan, China
Magnitude:	M_S=7.8
Location:	T11 Tangshan District
References:	Zhou & Zhang (1979), Shibata & Teparaska (1988)
Nature of Failure:	Liquefaction
Comments:	Liquefaction documented by Zhou and Zhang. Hand auger samples at 1.5, 2.0, and 3.0 m. Soil grading from silty clay to sandy silt to silty sand to fine sand with depth.

Stress		**Strength**	
Liquefied	Y	N (bpf) from 78/79	14.3
Data Class	C	V_S (m/s)	157
Critical Layer (m)	1.2 to 3.0		
Median Depth (m)	2.10		
st.dev.	0.30	q_c (MPa)	3.91
Depth to GWT (m)	0.85	st.dev.	0.56
st.dev.	0.30	f_s (kPa)	53.37
σ_v (kPa)	38.83	st.dev.	19.33
st.dev.	5.98	norm. exp. initial	0.54
σ_v' (kPa)	26.56	norm. exp. step	0.48
st.dev.	3.22	norm. exp. Final	0.47
a_{max} (g)	0.61	difference	0.00
st.dev.	0.24	C_q, C_f	1.70
r_d	0.94	C_{thin}	1.00
st.dev.	0.04	f_{s1} (kPa)	90.72
M_w	7.89	st.dev.	32.86
st.dev.	0.10	q_{c1} (MPa)	6.65
CSR_{eq}	0.54	st.dev.	0.96
st.dev.	0.24	R_f(%)	1.36
C.O.V.$_{CSR}$	0.45	stdev	0.80
DWF (Moss et al.)	0.93	del qc	1.06
DWF (Youd et al.)	0.88	qc1,mod	7.71
CSR*	0.58	CRR	0.12

T11 Tangshan District

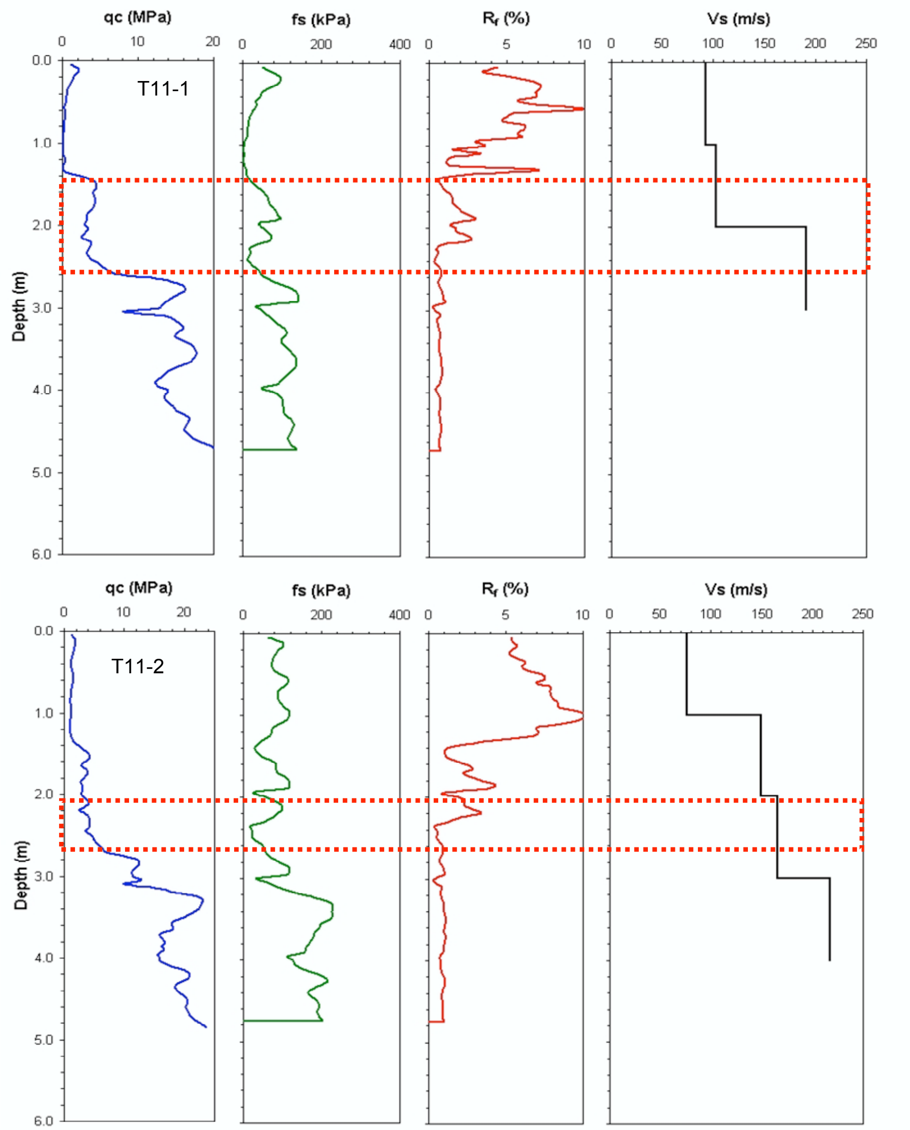

表13　11号孔勘探结果
（丰南县范庄，Ⅸ度区，地下水位0.85米，液化，1978.9）

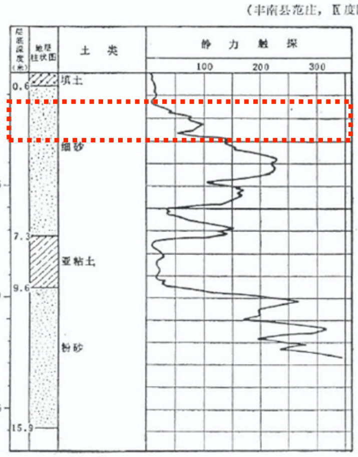

标准贯入试验		取样试验								
					颗粒分析					
深度	击数	取样深度	含水量	容重	10—2	2—0.5	0.5—0.25	0.25—0.1	0.1—0.05	<0.05
2.3	14	2.0				1	10	75	11	3
2.8	15	2.6				3	25	58	8	6
3.3	14	3.0				1	9	81	9	
4.3	39	4.3				1	15	76	8	
5.4	29	5.2				2	12	77	9	
6.3	25	6.2				6	22	64	8	

Earthquake:	1976 Tanshan, China
Magnitude:	M_S=7.8
Location:	T12 Tangshan District
References:	Zhou & Zhang (1979), Shibata & Teparaska (1988)
Nature of Failure:	Liquefaction

Comments: Liquefaction documented by Zhou and Zhang.

Hand auger samples at 2.0 and 2.5m
Soil grading from silt to silty sand and fine sand.

Up to 50m from 78/79 data, but coincident with SASW measurements.

V_S measurements appear incorrect.

Stress		**Strength**	
Liquefied	Y	N (bpf) from 78/79	6.5
Data Class	C	V_S (m/s)	
Critical Layer (m)	2.4 to 3.8		
Median Depth (m)	3.10		
st.dev.	0.23	q_c (MPa)	1.94
Depth to GWT (m)	1.55	st.dev.	0.68
st.dev.	0.30	f_s (kPa)	25.77
σ_v (kPa)	56.58	st.dev.	6.00
st.dev.	4.82	norm. exp. initial	0.67
σ_v' (kPa)	41.37	norm. exp. step	0.58
st.dev.	3.10	norm. exp. Final	0.57
a_{max} (g)	0.58	difference	0.01
st.dev.	0.23	C_q, C_f	1.65
r_d	0.90	C_{thin}	1.00
st.dev.	0.06	f_{s1} (kPa)	42.61
M_w	7.89	st.dev.	9.93
st.dev.	0.10	q_{c1} (MPa)	3.20
CSR_{eq}	0.47	st.dev.	1.13
st.dev.	0.20	R_f(%)	1.33
C.O.V.$_{CSR}$	0.42	stdev	0.79
DWF (Moss et al.)	0.93	del qc	0.97
DWF (Youd et al.)	0.88	qc1,mod	4.17
CSR*	0.50	CRR	0.07

T12 Tangshan District

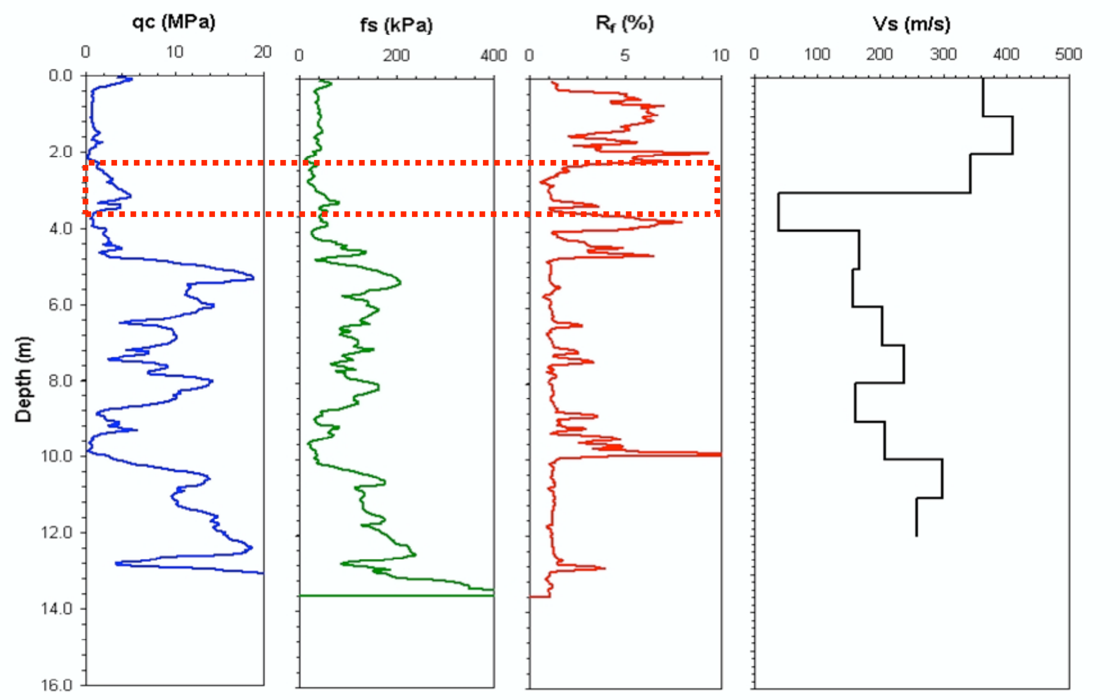

表14 12号孔勘探结果

（丰南县宣庄，Ⅸ度区，地下水位1.55米，液化，1978.9）

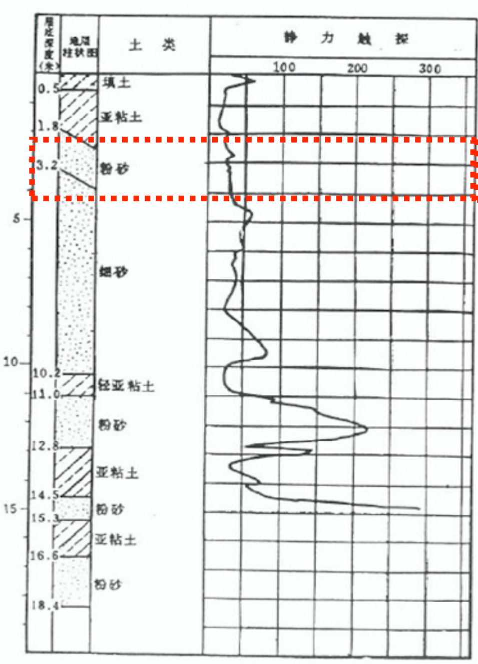

标准贯入试验		取样试验								
		取样	含水	容重	颗粒分析					
深度	击数	深度	量		10—2	2—0.5	0.5—0.25	0.25—0.1	0.1—0.05	<0.05
2.9	8	2.6					2	85	8	5
3.7	5	3.4					1	65	23	11
4.4	6	4.2					12	80	8	
5.0	10	4.7					8	84	8	
5.4	6	5.1					2	93	5	
5.9	5	6.1				1	2	91	6	
6.3	7	6.6					3	90	7	
6.9	10	7.1				1	10	79	10	
7.4	12	7.5					8	89	3	
7.8	7	7.9				1	6	80	8	5
8.2	14	8.4					8	89	3	
8.7	8	8.9				1	8	75	11	5
9.2	9	8.9				3	66	28	3	
10.9	16	10.6				3	13	18	44	22
12.5	30	12.2						2	73	25
12.8	15	12.7				1	3	1	53	42

Earthquake:	1976 Tanshan, China
Magnitude:	M_S=7.8
Location:	T13 Tangshan District
References:	Zhou & Zhang (1979), Shibata & Teparaska (1988)
Nature of Failure:	Liquefaction

Comments:

Liquefaction documented by Zhou and Zhang.

100m from SASW measurements.

Critical layer differs from 1988 interpretation of 2.0 to 2.7m because of high fines and clay content in that upper layer.

Shear wave velocity profile questionable.

Stress		**Strength**	
Liquefied	Y	N (bpf) from 78/79	
Data Class	C	V_S (m/s)	
Critical Layer (m)	6.0 to 8.0		
Median Depth (m)	7.00		
st.dev.	0.33	q_c (MPa)	11.47
Depth to GWT (m)	1.05	st.dev.	1.02
st.dev.	0.30	f_s (kPa)	110.64
σ_v (kPa)	133.88	st.dev.	12.62
st.dev.	7.60	norm. exp. initial	0.47
σ_v' (kPa)	75.51	norm. exp. step	0.46
st.dev.	5.05	norm. exp. Final	0.46
a_{max} (g)	0.58	difference	0.00
st.dev.	0.23	C_q, C_f	1.23
r_d	0.72	C_{thin}	1.00
st.dev.	0.12	f_{s1} (kPa)	136.20
M_w	7.89	st.dev.	15.54
st.dev.	0.10	q_{c1} (MPa)	14.12
CSR_{eq}	0.48	st.dev.	1.26
st.dev.	0.21	R_f(%)	0.96
C.O.V.$_{CSR}$	0.44	stdev	0.11
DWF (Moss et al.)	0.93	del qc	0.55
DWF (Youd et al.)	0.88	qc1,mod	14.67
CSR*	0.52	CRR	0.42

T13 Tangshan District

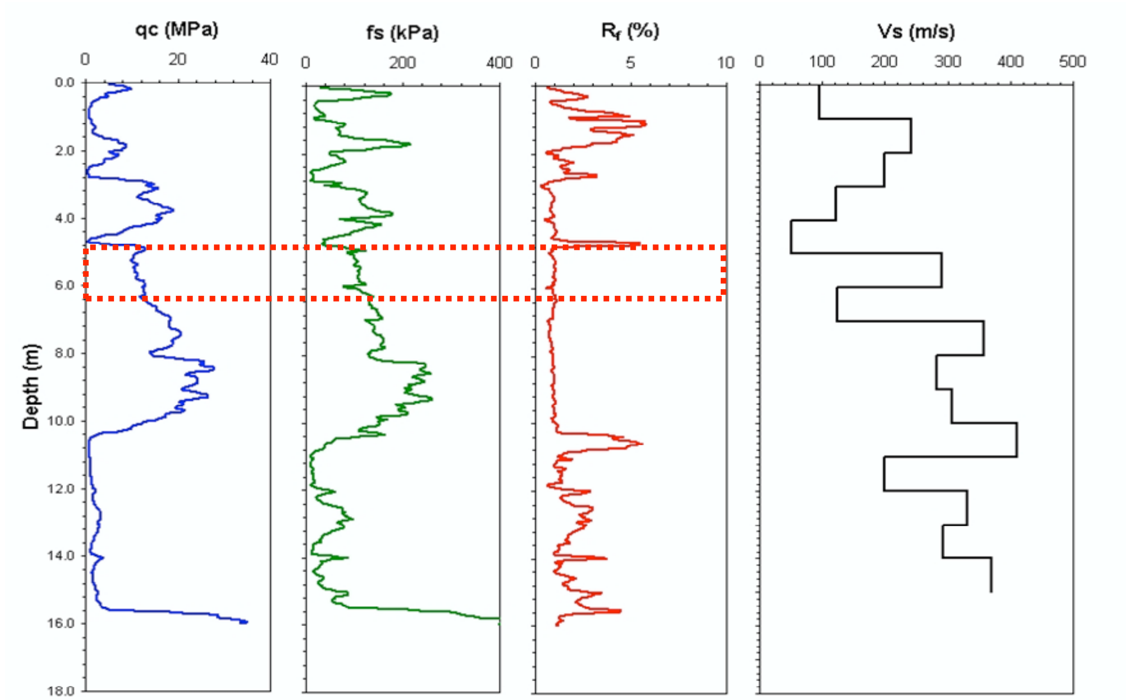

表15　13号孔勘探结果

（丰南县草各庄，Ⅱ度区，地下水位1.05米，液化，1978.9）

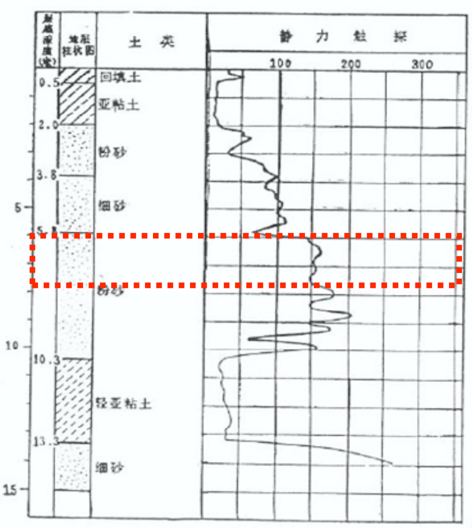

标准贯入试验 深度	标准贯入试验 击数	取样试验 取样深度	含水量	容重	颗粒分析 10—2	2—0.5	0.5—0.25	0.25—0.1	0.1—0.05	<0.05
2.5	10	2.3				1	10	48	19	22
4.3	19	4.1				1	6	74	15	4
5.3	16	5.0				7	22	57	11	3
5.9	9	5.7					12	36	45	7
6.3	27	6.0					5	40	49	6
7.4	21	7.1					4	48	45	3
7.8	27	7.5				1	5	54	37	3
9.3	29	9.0				2	21	65	8	4
9.8	29	9.5					2	70	21	7

Earthquake:	1976 Tanshan, China
Magnitude:	M_S=7.8
Location:	T14 Tangshan District
References:	Zhou & Zhang (1979), Shibata & Teparaska (1988)
Nature of Failure:	Liquefaction

Comments: Liquefaction documented by Zhou and Zhang.

Hand auger sample at 2m.

Liquefiable layer may have been at the deeper 7.5m layer, below 2007 measurements.

Based on the high penetration resistance it is difficult to interpret this site as a liquefaction case history. Detailed post-earthquake observations are needed to validate this case history as liquefied.

Stress		**Strength**	
Liquefied	NA	N (bpf) from 78/79	14
Data Class	C	V_S (m/s)	167
Critical Layer (m)	1.6 to 2.0		
Median Depth (m)	1.80		
st.dev.	0.07	q_c (MPa)	10.18
Depth to GWT (m)	1.25	st.dev.	0.49
st.dev.	0.30	f_s (kPa)	77.87
σ_v (kPa)	31.98	st.dev.	7.86
st.dev.	1.74	norm. exp. initial	0.52
σ_v' (kPa)	26.58	norm. exp. step	0.48
st.dev.	2.41	norm. exp. Final	0.48
a_{max} (g)	0.54	difference	0.00
st.dev.	0.22	C_q, C_f	1.70
r_d	0.95	C_{thin}	1.00
st.dev.	0.04	f_{s1} (kPa)	132.37
M_w	7.89	st.dev.	13.36
st.dev.	0.10	q_{c1} (MPa)	17.30
CSR_{eq}	0.40	st.dev.	0.84
st.dev.	0.17	R_f(%)	0.77
C.O.V.$_{CSR}$	0.42	stdev	0.05
DWF (Moss et al.)	0.93	del qc	0.30
DWF (Youd et al.)	0.88	qc1,mod	17.59
CSR*	0.43	CRR	0.71

T14 Tangshan District

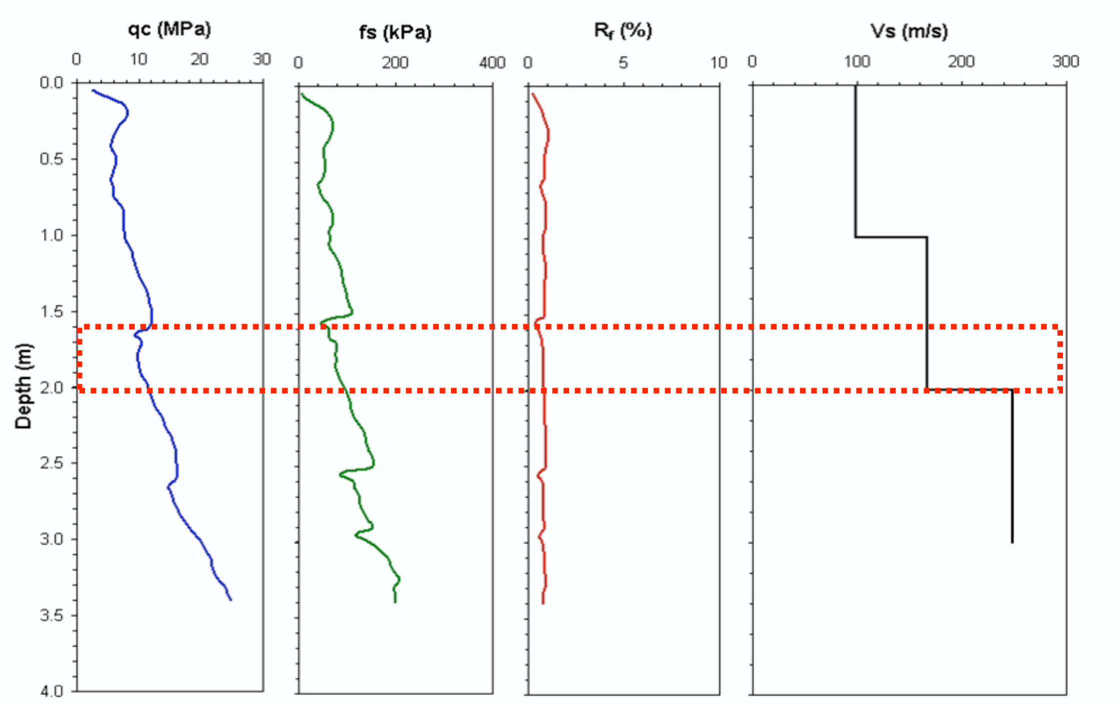

表16　14号孔勘探结果

（丰南县阎家庄，Ⅸ度区，地下水位1.25米，液化，1978.9）

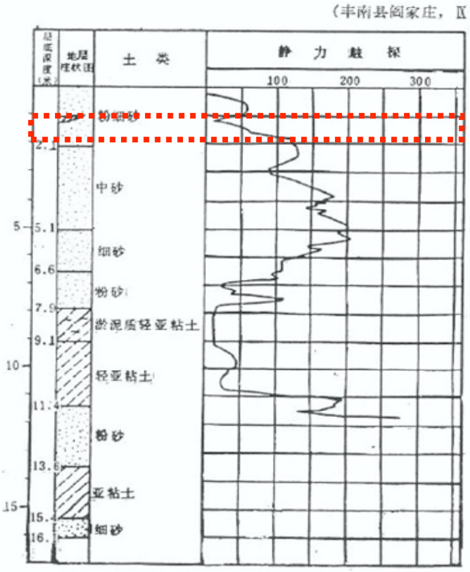

标准贯入试验		取样试验								
					颗粒分析					
深度	击数	取样深度	含水量	容重	10—2	2—0.5	0.5—0.25	0.25—0.1	0.1—0.05	<0.05
1.8	14	1.5					17	77	6	
2.8	15	2.5				8	51	39	2	
3.8	23	3.5				11	59	27	3	
4.8	23	4.5				1	24	71	4	
5.8	30	5.5				4	22	49	21	4
6.8	10	6.5						1	46	53

Earthquake:	1976 Tanshan, China
Magnitude:	M_S=7.8
Location:	T15 Tangshan District
References:	Zhou & Zhang (1979), Shibata & Teparaska (1988)
Nature of Failure:	Liquefaction

Comments: Liquefaction documented by Zhou and Zhang.

Very dense sand site, difficult to hand auger.

Based on the high penetration resistance it is difficult to interpret this site as a liquefaction case history. Detailed post-earthquake observations are needed to validate this case history as liquefied.

Stress		**Strength**	
Liquefied	NA	N (bpf) from 78/79	11
Data Class	C	V_S (m/s)	207
Critical Layer (m)	2.2 to 2.6		
Median Depth (m)	2.40		
st.dev.	0.07	q_c (MPa)	9.52
Depth to GWT (m)	1.00	st.dev.	0.24
st.dev.	0.30	f_s (kPa)	70.05
σ_v (kPa)	44.30	st.dev.	8.82
st.dev.	1.86	norm. exp. initial	0.53
σ_v' (kPa)	30.57	norm. exp. step	0.49
st.dev.	2.50	norm. exp. Final	0.49
a_{max} (g)	0.27	difference	0.00
st.dev.	0.11	C_q, C_f	1.70
r_d	0.95	C_{thin}	1.00
st.dev.	0.05	f_{s1} (kPa)	119.09
M_w	7.89	st.dev.	14.99
st.dev.	0.10	q_{c1} (MPa)	16.18
CSR_{eq}	0.24	st.dev.	0.40
st.dev.	0.10	R_f(%)	0.74
C.O.V.$_{CSR}$	0.41	stdev	0.10
DWF (Moss et al.)	0.93	del qc	0.22
DWF (Youd et al.)	0.88	qc1,mod	16.40
CSR*	0.26	CRR	0.58

T15 Tangshan District

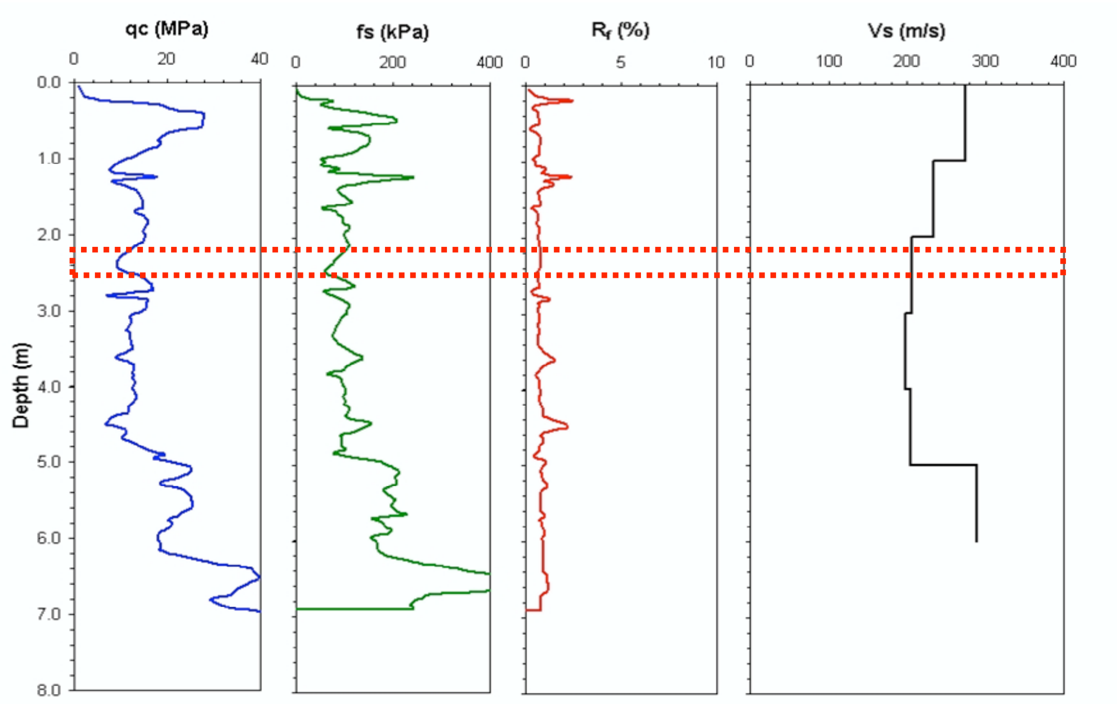

表17　15号孔勘探结果

（滦县佘庄，Ⅸ度区，地下水位1.0米，液化，1977.4）

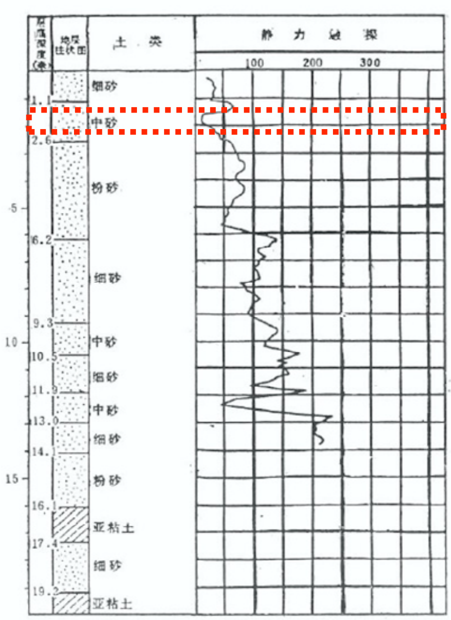

标准贯入试验		取样试验								
		取样	含水	容重	颗粒分析					
深度	击数	深度	量		10—2	2—0.5	0.5—0.25	0.25—0.1	<0.1	0.1—0.05
2.3	11	2.7	18.0	1.94	1.8	45.5	42.5	9.2	1.0	
3.25	15	3.4	22.7	2.01		0.7	7.7	62.2	29.4	27.9
4.3	24	4.3	23.5	1.89			16.8	65.8	17.4	14.5
5.25	23	5.3	22.8	2.07			9.5	60.9	29.6	24.2
6.25	26	6.3	19.3	2.08		2.8	36.7	47.1	13.4	11.1
7.20	43	7.4	20.4	2.05		2.1	46.2	48.2	3.5	
8.2	50	8.2	18.5	2.06		3.6	41.2	50.2	5.0	
9.3	50	9.3	21.1	2.07		4.4	46.9	43.2	5.5	
10.3	50	10.3	17.8	1.94		15.8	54.5	24.5	5.2	
11.3	50	11.3	16.7	2.09		10.6	32.7	49.5	7.2	
12.3	50	12.2	12.9	2.04	3.5	28.1	39.0	23.0	6.4	
13.3	50	13.1	21.4	2.05		0.5	36.3	54.5	8.7	
14.3	46	14.3	20.2	2.04		0.5	10.5	60.9	28.1	19.2
15.3	50	15.4	23.4	2.00		0.5	1.5	36.5	61.5	55.4
		16.4	19.2	2.00						
18.3	50	18.1	19.6	2.06		0.1	2.4	76.7	20.8	14.1

Earthquake:	1976 Tanshan, China
Magnitude:	M_S=7.8
Location:	T16 Tangshan District
References:	Zhou & Zhang (1979), Shibata & Teparaska (1988)
Nature of Failure:	
Comments:	Nonliquefaction documented by Zhou and Zhang.
	Encountered old brick foundation near the surface.

Stress		**Strength**	
Liquefied	N	N (bpf) from 78/79	32
Data Class	C	V_S (m/s)	267
Critical Layer (m)	7.2 to 8.2		
Median Depth (m)	7.50		
st.dev.	0.17	q_c (MPa)	10.26
Depth to GWT (m)	3.50	st.dev.	3.99
st.dev.	0.30	f_s (kPa)	96.78
σ_v (kPa)	137.50	st.dev.	50.72
st.dev.	4.76	norm. exp. initial	0.48
σ_v' (kPa)	98.26	norm. exp. step	0.48
st.dev.	4.22	norm. exp. Final	0.48
a_{max} (g)	0.26	difference	0.00
st.dev.	0.10	C_q, C_f	1.06
r_d	0.78	C_{thin}	1.00
st.dev.	0.13	f_{s1} (kPa)	102.62
M_w	7.89	st.dev.	53.78
st.dev.	0.10	q_{c1} (MPa)	10.88
CSR_{eq}	0.19	st.dev.	4.23
st.dev.	0.08	R_f(%)	0.94
C.O.V.$_{CSR}$	0.44	stdev	0.24
DWF (Moss et al.)	0.93	del qc	0.36
DWF (Youd et al.)	0.88	qc1,mod	11.24
CSR*	0.20	CRR	0.24

T16 Tangshan District

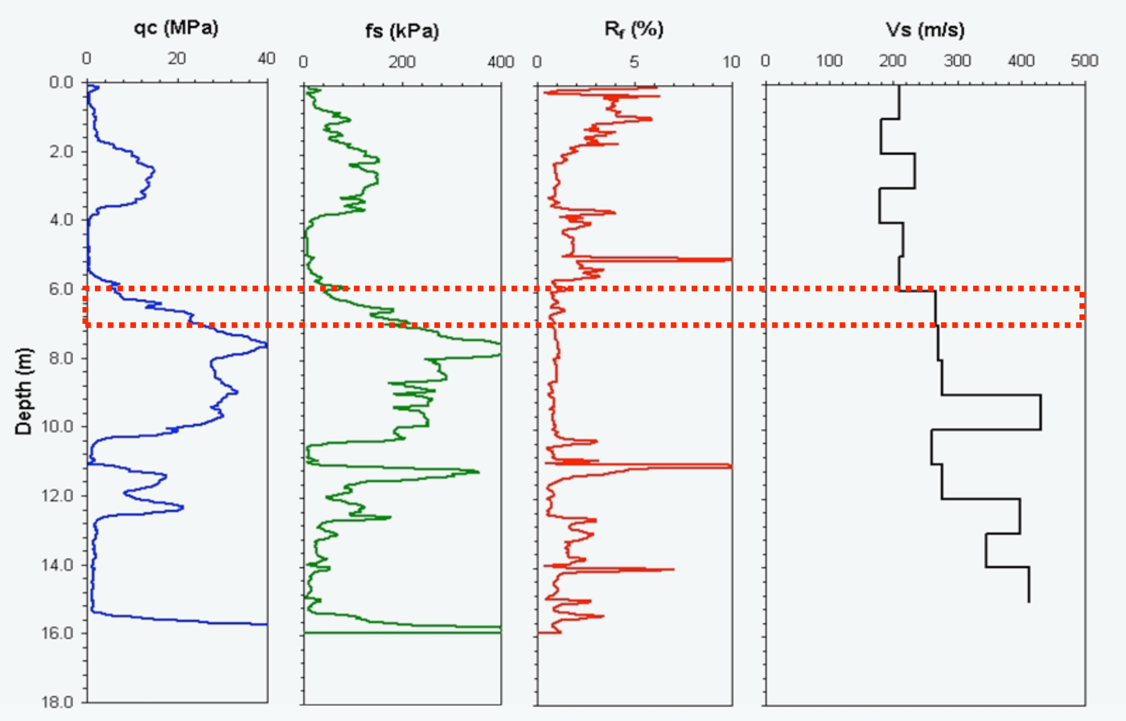

表18　16号孔勘探结果

（滦县东坨子头，Ⅸ度区，地下水位3.5米，未液化，1977.4）

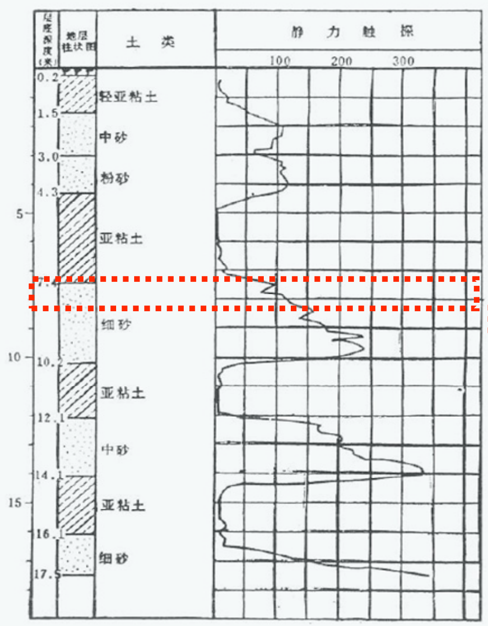

标准贯入试验		取样试验								
					颗粒分析					
深度	击数	取样深度	含水量	容重	10—2	2—0.5	0.5—0.25	0.25—0.1	<0.1	0.1—0.05
1.2	14	2.1	11.3	2.10		15.5	38.5	33.0	13.0	
2.25	22	3.0	19.8	1.96		0.1	10.0	60.0	29.9	25.9
3.25	23	4.1	19.6	2.13		2.4	24.8	48.9	23.9	22.1
4.25	31	7.6	14.2	2.17	0.4	10.2	31.4	38.8	19.2	15.6
5.45	10	8.2	14.6	2.09		5.4	32.4	45.2	17.0	14.5
6.3	7	9.1	19.7	2.05		0.5	36.0	47.5	16.0	12.8
7.35	32	12.1	14.7	2.12		17.2	47.0	27.7	8.1	
8.35	31	13.0	15.7	2.16		13.5	45.8	31.7	9.0	
9.3	50									
10.3	8									
12.3	46									
13.3	50									
14.3	10									
15.3	35									
16.3	50									
17.4	50									

Earthquake:	1976 Tanshan, China
Magnitude:	M_S=7.8
Location:	L1 Lutai District
References:	Zhou & Gou (1979), Shibata & Teparaska (1988)
Nature of Failure:	No Failure

Comments: Non-liquefaction documented by Zhou and Gou

Zhou & Guo observed that a slight decrease in the PI determined what liquefied (L2) and what did not liquefy (L1).

They found silty clay ejecta that correlates to a layer at around 12m depth at L2 with a PI in the 4.7 to 5.7 range. The same layer at L1 has a PI around 8 and a slightly higher tip resistance.

Static Driving shear stresses may have contributed to the failure at L2 and not at L1.

Stress		**Strength**	
Liquefied	N?	N (bpf) from 78/79	5
Data Class	C	V_S (m/s)	148
Critical Layer (m)	7 to 12.0		
Median Depth (m)	9.75		
st.dev.	0.83	q_c (MPa)	3.55
Depth to GWT (m)	0.40	st.dev.	1.03
st.dev.	0.30	f_s (kPa)	60.68
σ_v (kPa)	189.13	st.dev.	44.69
st.dev.	17.33	norm. exp. initial	0.53
σ_v' (kPa)	97.40	norm. exp. step	0.52
st.dev.	8.75	norm. exp. Final	0.52
a_{max} (g)	0.27	difference	0.00
st.dev.	0.11	C_q, C_f	1.01
r_d	0.70	C_{thin}	1.00
st.dev.	0.16	f_{s1} (kPa)	61.52
M_w	7.80	st.dev.	45.31
st.dev.	0.10	q_{c1} (MPa)	3.60
CSR_{eq}	0.24	st.dev.	1.04
st.dev.	0.11	R_f(%)	1.71
$C.O.V._{CSR}$	0.48	stdev	0.85
DWF (Moss et al.)	0.95	del qc	1.11
DWF (Youd et al.)	0.90	qc1,mod	4.70
CSR*	0.25	CRR	0.07

L1 Lutai District

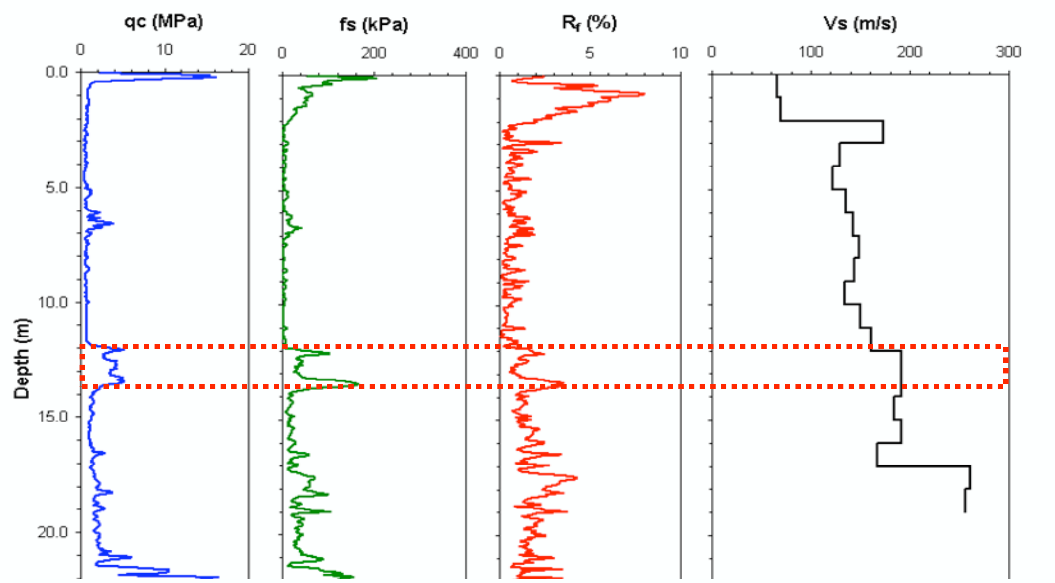

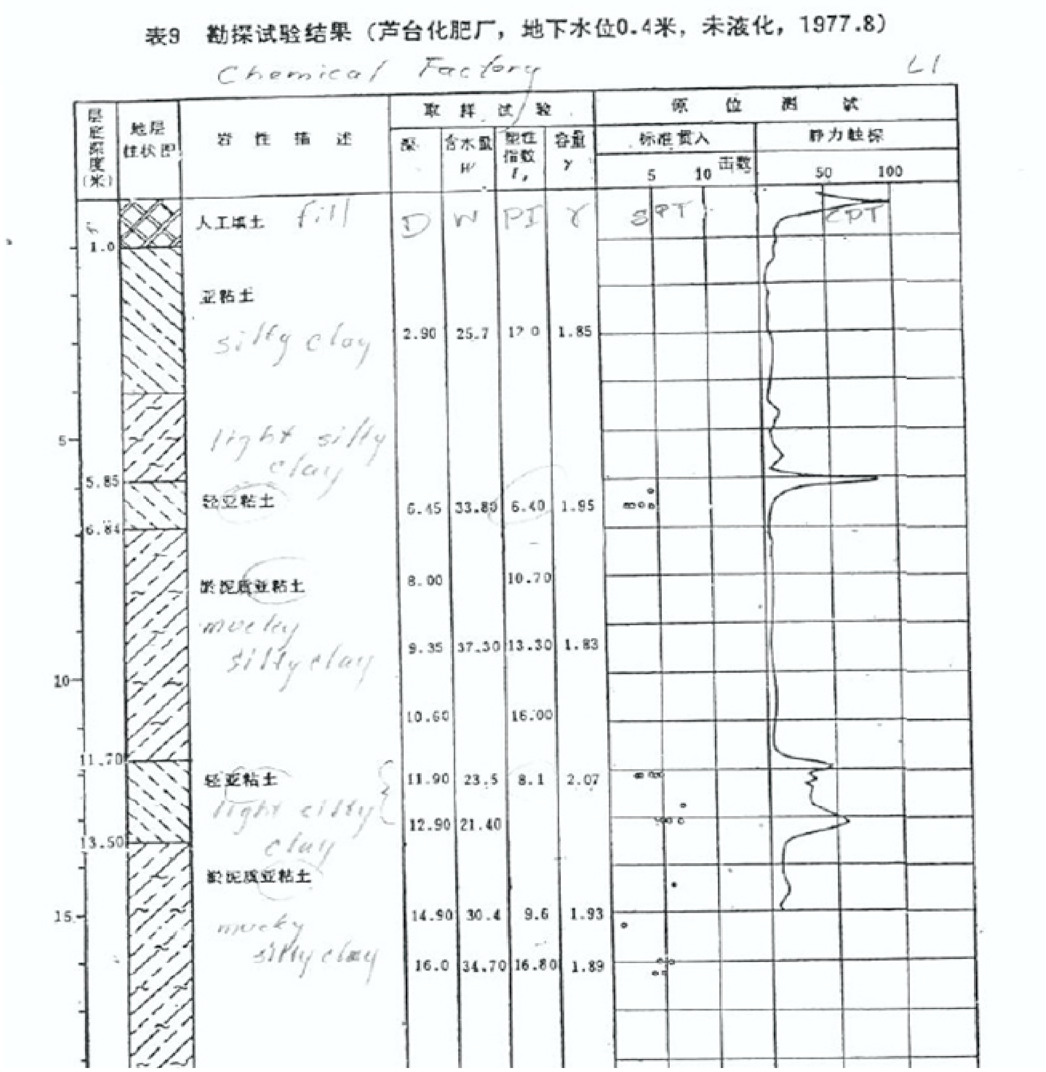

Earthquake:	1976 Tanshan, China
Magnitude:	M_S=7.8
Location:	L2 Lutai District
References:	Zhou & Guo (1979), Shibata & Teparaska (1988)
Nature of Failure:	Exhibited liquefaction traits

Comments: Liquefaction documented by Zhou and Guo.

Zhou & Guo observed that a slight decrease in the PI determined what liquefied (L2) and what did not liquefy (L1).

They found silty clay ejecta that correlates to a layer at around 12m depth at L2 with a PI in the 4.7 to 5.7 range. The same layer at L1 has a PI around 8 and a slightly higher tip resistance.

Static Driving shear stresses may have contributed to the failure at L2 and not at L1.

Stress		**Strength**	
Liquefied	Y?	N (bpf) from 78/79	
Data Class	ERR	V_S (m/s)	179
Critical Layer (m)	12.0 to 13.0		
Median Depth (m)	12.50		
st.dev.	0.17	q_c (MPa)	3.73
Depth to GWT (m)	0.21	st.dev.	1.30
st.dev.	0.30	f_s (kPa)	48.72
σ_v (kPa)	243.23	st.dev.	30.76
st.dev.	8.54	norm. exp. initial	0.55
σ_v' (kPa)	122.66	norm. exp. step	0.57
st.dev.	8.25	norm. exp. Final	0.57
a_{max} (g)	0.27	difference	0.00
st.dev.	0.11	C_q, C_f	0.89
r_d	0.63	C_{thin}	1.00
st.dev.	0.20	f_{s1} (kPa)	43.36
M_w	7.89	st.dev.	27.37
st.dev.	0.10	q_{c1} (MPa)	3.32
CSR_{eq}	0.22	st.dev.	1.16
st.dev.	0.11	R_f(%)	1.31
$C.O.V._{CSR}$	0.51	stdev	0.39
DWF (Moss et al.)	0.93	del qc	0.71
DWF (Youd et al.)	0.88	qc1,mod	4.03
CSR*	0.24	CRR	0.07

L2 Lutai District

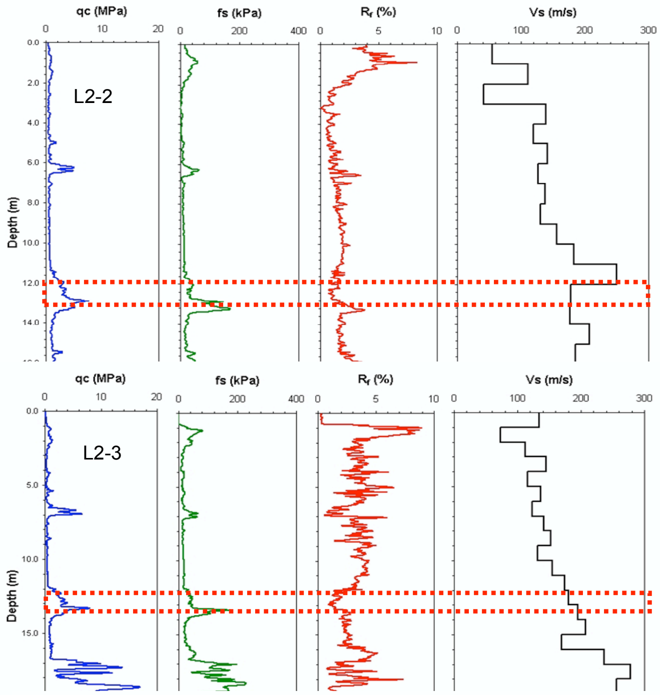

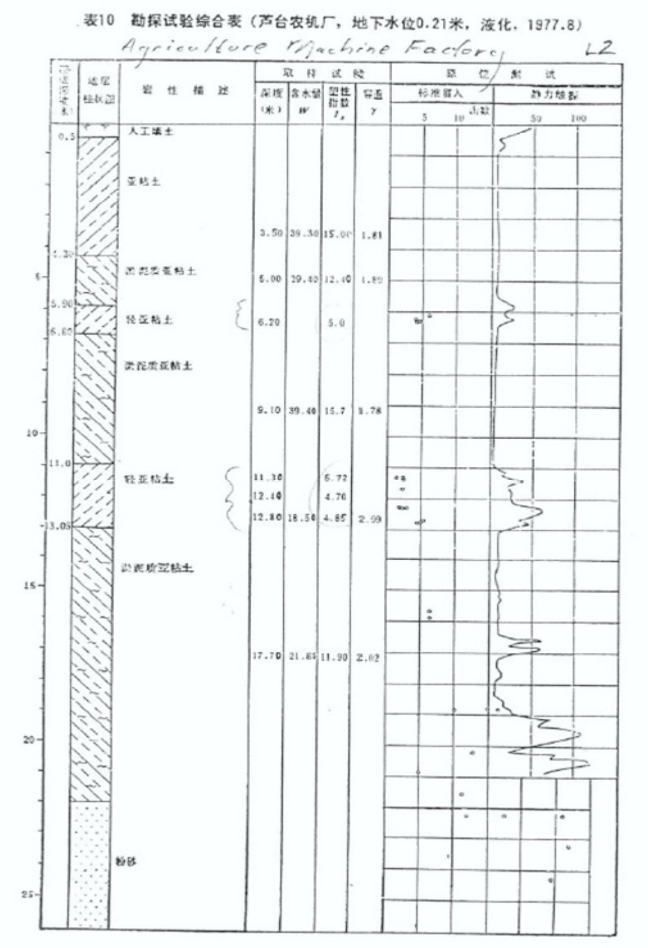

Cyclic failure calculations for L1 and L2 using Boulanger and Idriss (2006) method for CPT measurements.

L1-critical layer 7 to 11m depth

qc (MPa)	0.688065	
st.dev.	0.085278	
u (kPa)	278.0309	
st.dev.	97.83995	
a	1	area correction
qt (MPa)	0.688065	qc+(1-a)u
st.dev.	0.085278	
Nk	17.5	cone factor
su (kPa)	28.7894	(qt-sig_v)/Nk
st.dev.	4.972056	
Kalpha	1.00	
Ksigma	1.00	
CRR index	0.24	0.8*(su/p)
FS	0.93	against cyclic failure

L2-critical layer 7 to 11m depth

qc (MPa)	0.535308	
st.dev.	0.130259	
u (kPa)	251.6419	
st.dev.	143.1968	
a	1	area correction
qt (MPa)	0.535308	qc+(1-a)u
st.dev.	0.130259	
Nk	17.5	cone factor
su (kPa)	20.0333	(qt-sig_v)/Nk
st.dev.	7.459389	
Kalpha	1.00	
Ksigma	1.00	
CRR index	0.17	0.8*(su/p)
FS	0.66	against cyclic failure

Appendix B: Data Processing Techniques (Chapter 4 excerpt from Moss et al. 2003)

Chapter 4
Data Processing

4.1 INTRODUCTION

In order to have a robust unbiased estimate of the occurrence or nonoccurrence of liquefaction it is of preeminent importance to have the highest quality data. A probabilistic correlation requires powerful statistical techniques, but is only as good as the quality of data to which the techniques are applied. To this end, data processing was of utmost importance in this study. A considerable amount of time was spent processing and reviewing the database to minimize epistemic uncertainty that can creep in due to human error, biased interpretation, and poor analysis techniques.

4.2 FIELD OBSERVATIONS

The basis of a liquefaction correlation is a research engineer's observation of liquefaction or absence of liquefaction following a seismic event, and the index test measurements of the suspect critical layer. This basis is inherently fraught with uncertainty including lack of full coverage of affected area, misinterpretation of field evidence, poor index testing procedures, difficult field conditions, etc.

One of the primary discrepancies of a database of this type is that researchers tend to retrieve more liquefied than nonliquefied case histories. This can be attributed to the fact that testing in a liquefied area is much more appealing than testing at a site that hasn't experienced liquefaction. This unfortunately leads to a data bias, more liquefied case histories than nonliquefied case histories. To account for this data imbalance the procedure of bias weighting is used, as described in Chapter 5 on Bayesian analysis.

Liquefaction field correlations y are not based truly on the occurrence or nonoccurrence of liquefaction but on the observation of the manifestations of liquefaction at a particular location and the lack of manifestation at some other location. These manifestations can take the form of sand boils or sand blows, lateral spreading, building tilting or settlement, ground loss, broken lifelines, etc. Liquefaction can and does occur at depths where there is no surface evidence of the event. This of course does not make it into a liquefaction database; it fits the tree-falling-in-the-woods analogy.

The most content-rich sites are sites that are labeled as marginal. Marginal liquefaction does not exist, a soil deposit either liquefies or does not liquefy. Marginal is a research engineer's interpretation that at this location liquefaction was either incipient or occurred and resulted in minimal surface manifestations. These sites are included in the database and tend to have the most information content because they fall near the limit-state (threshold of liquefaction/nonliquefaction).

All these vagaries are incorporated into the database and can result in epistemic uncertainty. To minimize this uncertainty a panel of experts reviewed the database and came to a consensus on each site and the data it contained. This process of consensus results in a robust database that contains the best assessment of each variable to the highest standards of practice.

4.3 STRENGTH PARAMETERS

4.3.1 Choice of Logs

At any given site there can be multiple CPT and also corollary SPT logs to choose from. Proximity of the logs to the observed liquefaction/nonliquefaction is critical. The depositional environment and the properties that lead to liquefaction can vary significantly over a small distance and therefore it is important to be as close to the observed location as possible. Logs that are considered to be representative of the conditions are chosen. When there are multiple logs, the values (such as tip and sleeve resistance) are average.

CPT logs that were measured using a mechanical cone or a sleeveless cone are not used in this database because of the lack of sleeve measurements. However, when a sleeveless cone trace has a corollary SPT log that shows that the critical layer is composed of clean sand (FC<5%), then the tip resistance is used in conjunction with a prescribed median "clean sand" friction ratio ($R_f \cong 0.35\%$). This allows the use of important early CPT tip resistance data with a neutral friction ratio.

There are a few earthquake reconnaissance trips that utilized a Chinese cone. The report by Earth Technology (1985) showed that there is very little difference between tip and sleeve readings using the Chinese cone and a cone following ASTM specifications (D3441 and D5778); therefore the Chinese cone was treated no differently in this database.

4.3.2 Case Selection

The objective in case selection in this study was to end up with a group of statistically independent data points. Some previous correlations have used multiple liquefaction or nonliquefaction cases from a single site to generate more statistical data for analysis. This method can be incorrect for two reasons. First, given a site with consistent stratigraphy and a uniform depositional environment, selecting two liquefied or two nonliquefied cases from the same critical layer results in cross-correlation of these two data points. The cross-correlation must be accounted for in any form of statistical analysis and will result in much higher uncertainty or much reduced informational content for each data point. Second, if a particular layer within the site does liquefy, this then modifies the incoming seismic energy for the layers above through seismic isolation and below by blocking full reflection off the surface. This leads to a modified CSR for other layers at the site which can be difficult to determine.

4.3.3 Critical Layer Selection

Selection of the critical layer is an important step in estimating the seismic strength of a particular soil deposit. The criteria for selection is finding the strata of soil that is the weakest-link-in-the-chain from a liquefaction perspective. Finding the weakest link requires observing the tip resistance and friction ratio in conjunction, with the addition of a SPT log, for soil classification, if one is available. For most depositional environments this can be a simple matter of looking for the smallest continuous stretch of tip resistance with low friction ratio that agrees with the SPT log in terms of a liquefiable material. It can be a difficult proposal for fluvial depositional environments where the strata are thin, interbedded, and discontinuous both horizontally and vertically. A final criteria for identifying a critical layer is comparing the suspect layers to previous correlations. This aids in the more difficult sites where determining which of multiple layers liquefied or didn't liquefy.

One issue that is not commonly addressed in liquefaction correlations is that the *in situ* data are usually acquired post ground shaking. Particularly for the liquefied cases, the soil strength and properties have most likely been modified due to the process of liquefaction. Chameau et al. (1991) looked at sites that were affected by the Loma Prieta Earthquake in which previous CPT data existed. Post event CPT data were acquired and compared to the pre-event CPT data. They found that loose materials experienced the most alteration in tip resistance due to the ground shaking and subsequent liquefaction. This comes as no surprise. Recent work involving large scale liquefaction blast tests have and are being performed in Japan where pre- and post-liquefaction CPT measurements are made. Hopefully these data will resolve the bias and allow for proper accounting of the changes that occur within a liquefied layer.

If it can be assumed that tip resistance has a positive correlation with relative density for clean sands (Schmertmann 1978), then the greater the tip resistance the greater the relative density. In a critical state framework, given a constant confining stress, the higher the relative density (lower the void ratio), the less capacity the soil has for contractive behavior. Liquefaction is premised on this contractive behavior of soils. Therefore, the closer a point lies to the limit-state or liquefaction boundary the less contractive it is, and the less pre- to post-liquefaction change in resistance it is likely to experience. On the nonliquefaction side of the limit-state it is assumed that the resistance is unmodified by the ground shaking because no liquefaction has occurred. Another issue is that if a CSR value is determined for a liquefied site using the post-liquefaction *in situ* measurements for site response analysis, the value may be slightly higher than pre-liquefaction conditions because of the stiffening that has occurred.

Given all these pre- and post-liquefaction considerations, it is conjectured that the limit-state function is totally unaffected by post-liquefaction densification because:

1. near the limit-state the soils are near the critical state (small state parameter) and therefore have not significantly densified,
2. nonliquefied soils will have no post-event densification and therefore are unaffected by the event and will maintain their position near the limit-state.

The soils most affected by liquefaction, which will give vastly different post-event resistance measurements, are the loose or low tip resistance soils, and these have little impact on the limit-state function in a Bayesian-type analysis.

4.3.4 Index Measurements

Once the critical layer has been selected it is a matter of determining the appropriate statistics of the measurements within the layer. Kulansingam, Boulanger, and Idriss (1999) studied various procedures for estimating an average tip resistance over a standardized distance of cone travel. They looked at different standardized distances and came to the conclusion that having a preset distance over which the resistance is averaged works poorly.

The approach used in this study was to let the depositional environment dictate. Using the procedures described above for identifying the critical layer, the maximum distance over which the soil deposit lies is often apparent. The top and bottom depths are taken as extrema. The distribution of the tip and sleeve resistances are assumed to be normal, and the averages and standard deviations are calculated from a digitized form of the trace. Raw sleeve and tip measurements are used to calculate the friction ratio in order to eliminate aliasing that may have occurred in the field calculations.

Induced pore pressure can have an affect on the tip and sleeve measurements. This affect is pronounced in soils that respond in an undrained manner to the strain imposed by the advancing cone (i.e., fine-grained soils). For most soils that are susceptible to liquefaction, fully drained cone penetration is assumed (Lunne et al. 1997). Therefore, in general, no pore pressure corrections are necessary for materials that are potentially liquefiable. The assumption of fully drained response was checked using pore pressure measurements, when available, for each site.

4.3.5 Masked Liquefaction

In certain situations liquefaction may occur at depth but evidence may not reach the ground surface due to the monolithic or unified nature of overlying nonliquefiable strata. This masked liquefaction situation was researched and presented by Ishihara (1985). The results from that research are used to screen sites that are found to be liquefiable in terms of the index measurements, has overlying nonliquefiable material that fits the Ishihara (1985) thickness criteria, showed no surface manifestation of liquefaction, and was reported as a nonliquefied site. For reference, at a site experiencing a low level of ground shaking (PGA < 0.2 g) with a 2 m thick liquefiable layer, an overlying nonliquefiable layer of approximately 2 m could eliminate all surface manifestation of liquefaction.

4.3.6 Screening for Other Failure Mechanisms

Certain soil types are not susceptible to liquefaction but may deform via cyclic softening. These soils may exhibit surface manifestations that can appear quite similar to what may be observed in "classic" liquefaction, such as lateral spreading, and building tilting, punching, and settlement. However it has been shown that the failure mechanism is quite different from liquefaction and is primarily a function asymmetrical driving shear stresses (K_α). The soils that are susceptible to cyclic softening tend to have a high percentage of fines and these fines will tend to behave in a plastic manner. Several cases like this were observed in the 2001 Kocaeli, Turkey, earthquake and the 2001 Chi-Chi, Taiwan, earthquake. Since the limit-state and the overall correlation is based on "classic" liquefaction, it is not appropriate to include these cases in the analysis.

A criteria for screening these cases is based on research of fines content and plasticity in relation to liquefaction susceptibility (Andrews and Matin 2000; Andrianopoulos et al. 2001; Guo and Prakash 1999; Perlea 2000; Polito 2001; Sancio et al. 2003; Yamamuro and Lade 1998, Youd and Gilstrap 1999; to name a few). The criteria for soils not susceptible to liquefaction used in this study are shown graphically in Figure 4.1.

4.3.7 Normalization

The tip and sleeve are normalized using the variable normalization scheme presented with this study in Chapter 3, on Normalization. Note that the tip and sleeve values are normalized equivalently, which results in no change for a normalized friction ratio ($R_{f,1} = R_f$).

4.3.8 Thin Layer Correction

Thin layer corrections, if they were required, are performed using the method proposed in this study in Chapter 2, on Thin Layer Correction. Note that only 4% of the cases in the database required a thin layer correction. For database purposes the thin layer correction was limited to a maximum of 1.5 ($C_{thin} \leq 1.5$).

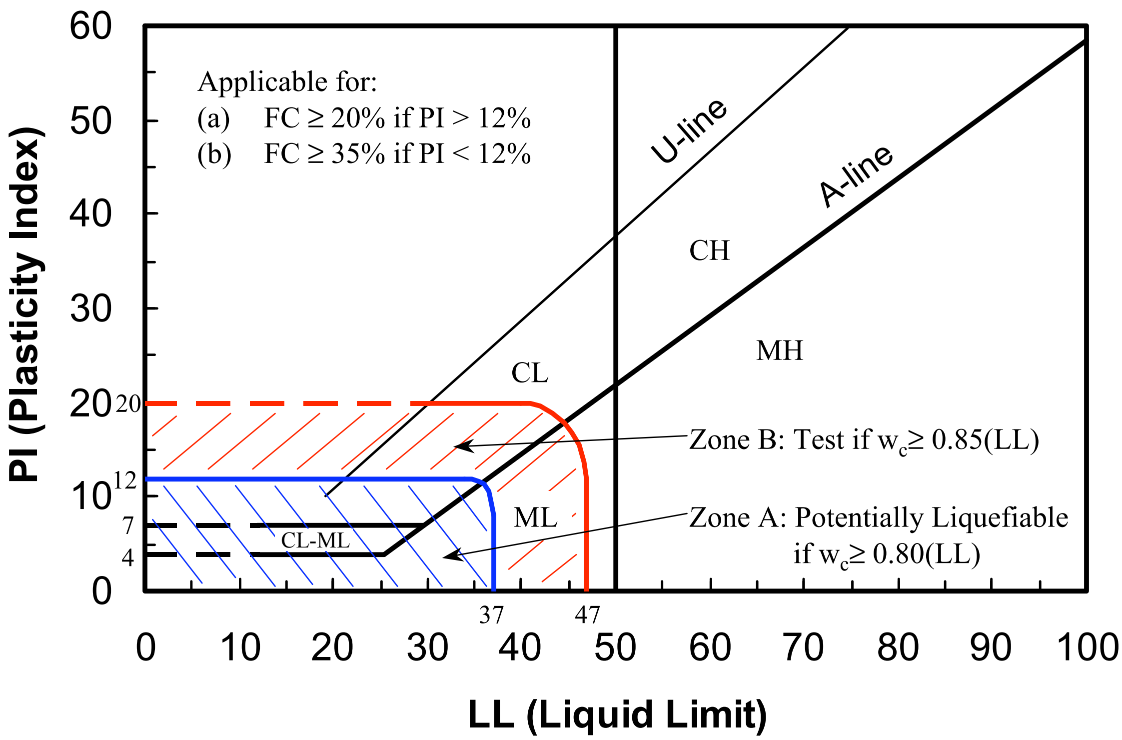

Fig. 4.1 Screening criteria for failure mechanism other than liquefaction.

4.3.9 Processed Strength Parameters

The result of this processing procedure is unbiased, statistically independent $q_{c,1}$, $f_{s,1}$, and R_f values for the liquefied and nonliquefied cases. These are mean resistance values and variances over the extent of the critical layer which have been normalized to one atmosphere and corrected for thin layer issue if required.

4.4 STRESS PARAMETERS

4.4.1 Cyclic Stress Ratio

The dynamic stress that the critical layer experienced is determined using the simplified uniform cyclic stress ratio as defined by Seed and Idriss (1971),

$$CSR = 0.65 \cdot \frac{a_{max}}{g} \cdot \frac{\sigma_v}{\sigma'_v} \cdot r_d \tag{4.1}$$

The CSR value calculated using Equation 4.1 is assumed to be the average or mean of a normally distributed random variable as in Equation 4.2. The variance of CSR is calculated via equation 4.3, where the coefficient of variation is equal to the standard deviation divided by the mean. Both Equation 4.2 and 4.3 are using first-order Taylor series expansions about the mean point, including only the first two terms.

$$CSR \cong 0.65 \cdot \frac{a_{max}}{g} \cdot \frac{\sigma_v}{\sigma'_v} \cdot r_d \tag{4.2}$$

$$\delta_{CSR}^2 \cong \delta_{a\,max}^2 + \delta_{rd}^2 + \delta_{\sigma v}^2 + \delta_{\sigma' v}^2 - 2 \cdot \rho_{\sigma v \sigma' v} \cdot \delta_{\sigma v} \cdot \delta_{\sigma' v} \tag{4.3}$$

Total and effective stress are correlated parameters, therefore the inclusion of the correlation coefficient term for these two variables is necessary.

4.4.2 Peak Ground Acceleration

The geometric mean of the peak ground acceleration is based on the best estimation of ground shaking possible. The methods of estimation are strong motion recordings, site response, calibrated attenuation relationships, adjustment of estimated site pga through general site response modeling, and general attenuation relationships. Using a calibrated attenuation relationship means using all available recordings to tune general attenuation relationships for event-specific variations and azimuth specifics when recordings permit.

The coefficient of variation of the peak ground acceleration is fixed according to the method of ground shaking estimation;

$\delta < 0.10$ for sites with strong motion stations less than 100m from site,

$\delta = 0.10$ to 0.25 for sites with strong motion stations within 100 to 500m from site or where site response analysis was performed using a nearby rock recording as input base motion ,

$\delta = 0.25$ to 0.35 for sites with strong motion stations within 500 m to 1000 m and/or estimates from calibrated attenuation relationships,

$\delta = 0.35$ to 0.5 for others.

This is a subjective determination of the variance of the ground shaking but is based on typical uncertainty bands from general attenuation relationships that have coefficient of variations of between 0.3 and 0.5 (e.g., Abrahamson and Silva 1997).

4.4.3 Total and Effective Stress

The total and effective vertical stress are correlated variables and this correlation must be accounted. The critical layer is selected using the procedures outlined above. From this the total extent of the critical layer is used to calculate the mean and variance of the critical layer, assuming that it is normally distributed. The variance is estimated using a 6 sigma approach, where the extrema of the layer are assumed to be three standard deviations away from the mean on either side. The total variance is then divided by six to give an estimate of the standard deviation.

A deterministic estimate is made of the mean unit weight of the soil above and below the water table. The variance is based on statistical studies of the measured variability of soil unit weight and is set at $\delta \cong 0.1$ (Kulhawy and Trautman 1996). The water table mean is taken as the reported field measured value (with consideration given for the depth of water table during the seismic event) and the variance is set at a fixed standard deviation of $\sigma = 0.3$ m., a reasonable estimate of water table fluctuations given relatively stable groundwater conditions. An estimate of the total and effective vertical stresses, their respective variances, and covariance can then be calculated using the expansion Equations 4.4–4.9:

$$ {}_{\sigma_v} \cong {}_{\gamma 1} \cdot {}_{h_w} + {}_{\gamma 2} \cdot \left({}_{h} - {}_{hw} \right) \tag{4.4}$$

$$ {}_{\sigma_v'} \cong {}_{\gamma 1} \cdot {}_{hw} + \left({}_{\gamma 2} - \gamma_w \right) \cdot \left({}_{h} - {}_{hw} \right) \tag{4.5}$$

$$ \sigma^2_{\sigma_v} \cong {}^{2}_{hw} \cdot \sigma^2_{\gamma 1} + \left({}_{h} - {}_{hw} \right)^2 \cdot \sigma^2_{\gamma 2} + {}^{2}_{\gamma 2} \cdot \sigma^2_{h} + \left({}_{\gamma 1} - {}_{\gamma 2} \right)^2 \cdot \sigma^2_{hw} \tag{4.6}$$

$$ \sigma^2_{\sigma_v'} \cong {}^{2}_{hw} \cdot \sigma^2_{\gamma 1} + \left({}_{h} - {}_{hw} \right)^2 \cdot \sigma^2_{\gamma 2} + \left({}_{\gamma 2} - \gamma_w \right)^2 \cdot \sigma^2_{h} + \left({}_{\gamma 1} + \gamma_w - {}_{\gamma 2} \right)^2 \cdot \sigma^2_{hw} \tag{4.7}$$

$$ Cov[\sigma_v, \sigma_v'] \cong \left({}^{2}_{hw} \cdot \sigma^2_{\gamma 1} \right) + \left({}_{\gamma 1} - {}_{\gamma 2} \right) \cdot \left({}_{\gamma 1} + \gamma_w - {}_{\gamma 2} \right) \cdot \sigma^2_{hw} + \left({}_{h} - {}_{hw} \right)^2 \cdot \sigma^2_{\gamma 2} + {}_{\gamma 2} \cdot \left({}_{\gamma 2} - \gamma_w \right) \cdot \sigma^2_{h} \tag{4.8}$$

$$ \rho_{\sigma_v \sigma_v'} = \frac{Cov[\sigma_v, \sigma_v']}{Var[\sigma_v] \cdot Var[\sigma_v']} \tag{4.9}$$

4.4.4 Nonlinear Shear Mass Participation Factor (r_d)

The nonlinear shear mass participation factor accounts for nonlinear response within a soil column and reduces the peak ground acceleration at the surface to reflect the ground acceleration that is experienced at the critical depth. This factor, denoted as r_d, has been derived from ground response analyses. In recent work, 2153 site response analyses were run using 50 sites and 42 ground motions covering a comprehensive suite of motions and soil profiles (Cetin and Seed 2000). This brute force approach allows for careful statistical analysis of the median response given the depth, peak ground acceleration, moment magnitude, and indicative shear wave velocity of the site. The variance was estimated from the dispersion of these simulations. The median values can be estimated using Equations 4.10 and 4.11, and the variance from Equations 4.12 and 4.13,

d < 65 ft (4.10)

$$r_d(d, M_w, a_{\max}) = \frac{\left[1 + \dfrac{-9.147 - 4.173 \cdot a_{\max} + 0.652 \cdot M_w}{10.567 + 0.089 \cdot e^{0.089 \cdot (-d - 7.760 \cdot a_{\max} + 78.576)}}\right]}{\left[1 + \dfrac{-9.147 - 4.173 \cdot PGA + 0.652 \cdot M_w}{10.567 + 0.089 \cdot e^{0.089 \cdot (-7.760 \cdot a_{\max} + 78.576)}}\right]} \pm \sigma_{\varepsilon r_d}$$

d ≥ 65 ft (4.11)

$$r_d(d, M_w, a_{\max}) = \frac{\left[1 + \dfrac{-9.147 - 4.173 \cdot a_{\max} + 0.652 \cdot M_w}{10.567 + 0.089 \cdot e^{0.089 \cdot (-d - 7.760 \cdot a_{\max} + 78.576)}}\right]}{\left[1 + \dfrac{-9.147 - 4.173 \cdot a_{\max} + 0.652 \cdot M_w}{10.567 + 0.089 \cdot e^{0.089 \cdot (-7.760 \cdot a_{\max} + 78.576)}}\right]} \pm \sigma_{\varepsilon r_d}$$

d < 40 ft

$$\sigma_{\varepsilon r_d}(d) = d^{0.864} \cdot 0.00814 \quad (4.12)$$

d ≥ 40 ft

$$\sigma_{\varepsilon r_d}(d) = 40^{0.864} \cdot 0.00814 \quad (4.13)$$

4.4.5 Moment Magnitude

Moment magnitude is a value that is usually reported by seismological laboratories following an event and iterated on for a week or two until the final value is set in stone. Calculating the moment magnitude involves an inverse problem to determine the seismic moment. The uncertainty in these calculations comes from the nonunique inversion based on seismograms that are recorded at various teleseismic stations. The dimensions of the fault plane and the amount of slip associated with larger magnitude events tend to be easier to define than with smaller magnitude events. A simple equation Equation 4.14, based on the variance of a series of previous events (1989 Loma Prieta, 1994 Northridge, 1999 Tehuacan, 1999 Kocaeli, 1999 Taiwan, 2001 Denali), was used to estimate this epistemic uncertainty,

$$\sigma_{M_w} \cong 0.5 - 0.45 \cdot \log(M_w) \qquad (4.14)$$

4.5 DATA CLASS

After the case histories have been selected and processed they are classified according to the quality of the informational content. Four classes of data are used to group the data, A through D, with D being substandard and therefore not included in the final database. The criteria for the data classes are as follows:

Class A

1. Original CPT trace with q_c and f_s/R_f, using a ASTM D3441 and D5778 spec. cone.
2. No thin layer correction required
3. $\delta_{CSR} \leq 0.20$

Class B

1. Original CPT trace with q_c and f_s/R_f, using a ASTM D3441 and D5778 spec. cone.
2. Thin layer correction.
3. $0.20 < \delta_{CSR} \leq 0.35$

Class C

1. Original CPT trace with q_c and f_s/R_f, but using a nonstandard cone (e.g., Chinese cone or mechanical cone).
2. No sleeve data but FC ≤ 5% (i.e., “clean” sand).
3. $0.35 < \delta_{CSR} \leq 0.50$

Class D

1. Not satisfying the criteria for Classes A, B, or C.

4.6 REVIEW PROCESS

The final step in processing the data is an extensive review procedure. Each case in the database is reviewed a minimum of three times. A panel of qualified experts was assembled to do the review, this included in addition to the author and Prof. Raymond B. Seed; Prof. Jon Stewart, Prof. Les Youd, Dr. Rob Kayen, and Prof. Kohji Tokimatsu. Each case was reviewed by the author, Ray Seed, and at least one of the four independent reviewers. The objective was to remove as much human error and epistemic error from the database as possible.

A final note on the review process includes the review of the analytical and statistical procedures. The application of Bayesian analysis to SPT-based liquefaction-triggering correlations and the techniques used was reviewed extensively by the Pacific Earthquake Engineering Research Center (PEER), and peer reviewed as journal publications in the *Journal of Geotechnical and Geoenvironmental Engineering* and the *Journal of Structural Reliability*. The CPT-based liquefaction-triggering correlation, and the associated Bayesian analysis and methodology, was also reviewed extensively by PEER at quarterly meetings that included as a review panel Prof. Les Youd, Prof. Geoff Martin, and Prof. I. M. Idriss.

It is the author's belief that the power of the Bayesian framework in engineering application is to incorporate all forms of information and that the review process is one of the more important and congenial steps in reducing epistemic uncertainty.

4.7 CONCLUSION

This chapter includes all the details and procedures used to process data for an unbiased liquefaction-triggering correlation within a Bayesian framework. The methods used to generate the best estimates of the representative statistics for each parameter are presented in their entirety. Figures 4.2 through 4.4 show the processed data in $q_{c,1}$ vs. CSR space. The task of developing accurate and appropriate processing techniques was both important and involved, and the final correlation attests to the time well spent.

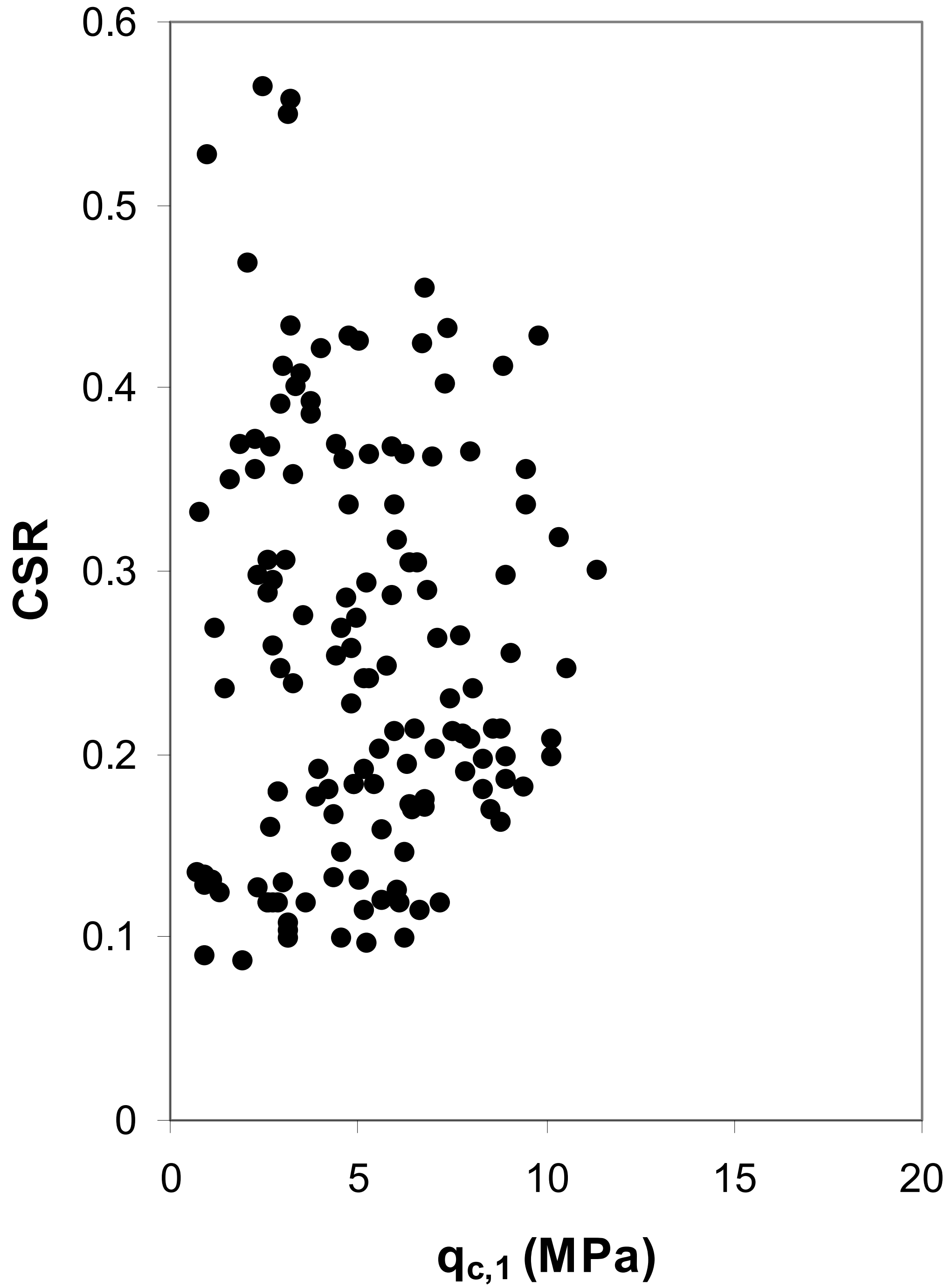

Fig. 4.2 Plot showing mean location of liquefied data points.

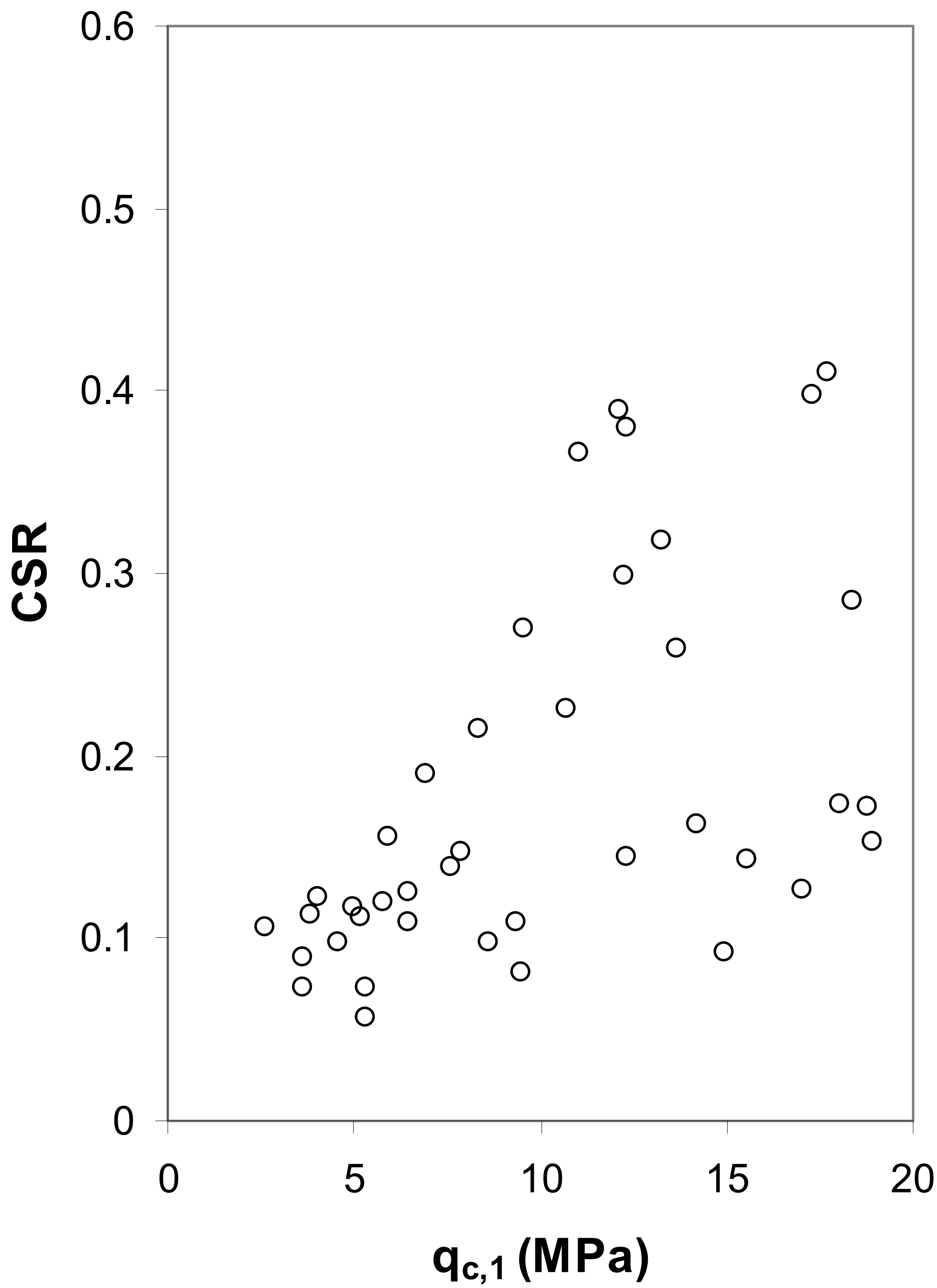

Fig. 4.3 Plot showing mean location of nonliquefied data points.

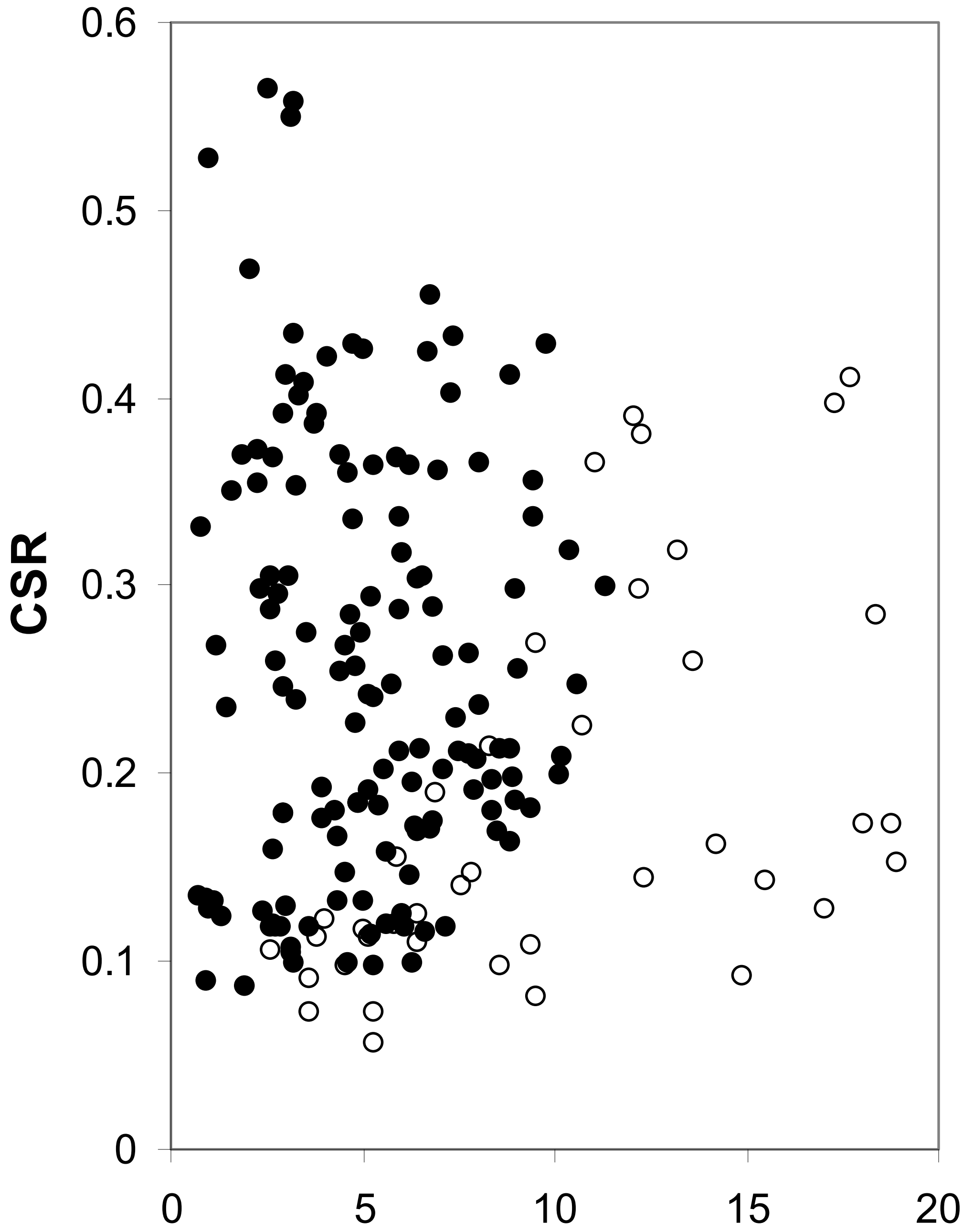

Fig. 4.4 Plot showing mean location of both liquefied (dots) and nonliquefied (circles) data points.

PEER REPORTS

PEER reports are available individually or by yearly subscription. PEER reports can be ordered at http://peer.berkeley.edu/publications/peer_reports.html or by contacting the Pacific Earthquake Engineering Research Center, 1301 South 46th Street, Richmond, CA 94804-4698. Tel.: (510) 665-3448; Fax: (510) 665-3456; Email: peer_editor@berkeley.edu

PEER 2009/01 *Evaluation of Ground Motion Selection and Modification Methods: Predicting Median Interstory Drift Response of Buildings.* Curt B. Haselton, Ed. June 2009.

PEER 2008/10 *Technical Manual for Strata.* Albert R. Kottke and Ellen M. Rathje. February 2009.

PEER 2008/09 *NGA Model for Average Horizontal Component of Peak Ground Motion and Response Spectra.* Brian S.-J. Chiou and Robert R. Youngs. November 2008.

PEER 2008/08 *Toward Earthquake-Resistant Design of Concentrically Braced Steel Structures.* Patxi Uriz and Stephen A. Mahin. November 2008.

PEER 2008/07 *Using OpenSees for Performance-Based Evaluation of Bridges on Liquefiable Soils.* Stephen L. Kramer, Pedro Arduino, and HyungSuk Shin. November 2008.

PEER 2008/06 *Shaking Table Tests and Numerical Investigation of Self-Centering Reinforced Concrete Bridge Columns.* Hyung IL Jeong, Junichi Sakai, and Stephen A. Mahin. September 2008.

PEER 2008/05 *Performance-Based Earthquake Engineering Design Evaluation Procedure for Bridge Foundations Undergoing Liquefaction-Induced Lateral Ground Displacement.* Christian A. Ledezma and Jonathan D. Bray. August 2008.

PEER 2008/04 *Benchmarking of Nonlinear Geotechnical Ground Response Analysis Procedures.* Jonathan P. Stewart, Annie On-Lei Kwok, Yousseff M. A. Hashash, Neven Matasovic, Robert Pyke, Zhiliang Wang, and Zhaohui Yang. August 2008.

PEER 2008/03 *Guidelines for Nonlinear Analysis of Bridge Structures in California.* Ady Aviram, Kevin R. Mackie, and Božidar Stojadinović. August 2008.

PEER 2008/02 *Treatment of Uncertainties in Seismic-Risk Analysis of Transportation Systems.* Evangelos Stergiou and Anne S. Kiremidjian. July 2008.

PEER 2008/01 *Seismic Performance Objectives for Tall Buildings.* William T. Holmes, Charles Kircher, William Petak, and Nabih Youssef. August 2008.

PEER 2007/12 *An Assessment to Benchmark the Seismic Performance of a Code-Conforming Reinforced Concrete Moment-Frame Building.* Curt Haselton, Christine A. Goulet, Judith Mitrani-Reiser, James L. Beck, Gregory G. Deierlein, Keith A. Porter, Jonathan P. Stewart, and Ertugrul Taciroglu. August 2008.

PEER 2007/11 *Bar Buckling in Reinforced Concrete Bridge Columns.* Wayne A. Brown, Dawn E. Lehman, and John F. Stanton. February 2008.

PEER 2007/10 *Computational Modeling of Progressive Collapse in Reinforced Concrete Frame Structures.* Mohamed M. Talaat and Khalid M. Mosalam. May 2008.

PEER 2007/09 *Integrated Probabilistic Performance-Based Evaluation of Benchmark Reinforced Concrete Bridges.* Kevin R. Mackie, John-Michael Wong, and Božidar Stojadinović. January 2008.

PEER 2007/08 *Assessing Seismic Collapse Safety of Modern Reinforced Concrete Moment-Frame Buildings.* Curt B. Haselton and Gregory G. Deierlein. February 2008.

PEER 2007/07 *Performance Modeling Strategies for Modern Reinforced Concrete Bridge Columns.* Michael P. Berry and Marc O. Eberhard. April 2008.

PEER 2007/06 *Development of Improved Procedures for Seismic Design of Buried and Partially Buried Structures.* Linda Al Atik and Nicholas Sitar. June 2007.

PEER 2007/05 *Uncertainty and Correlation in Seismic Risk Assessment of Transportation Systems.* Renee G. Lee and Anne S. Kiremidjian. July 2007.

PEER 2007/04 *Numerical Models for Analysis and Performance-Based Design of Shallow Foundations Subjected to Seismic Loading.* Sivapalan Gajan, Tara C. Hutchinson, Bruce L. Kutter, Prishati Raychowdhury, José A. Ugalde, and Jonathan P. Stewart. May 2008.

PEER 2007/03 *Beam-Column Element Model Calibrated for Predicting Flexural Response Leading to Global Collapse of RC Frame Buildings.* Curt B. Haselton, Abbie B. Liel, Sarah Taylor Lange, and Gregory G. Deierlein. May 2008.

PEER 2007/02 *Campbell-Bozorgnia NGA Ground Motion Relations for the Geometric Mean Horizontal Component of Peak and Spectral Ground Motion Parameters.* Kenneth W. Campbell and Yousef Bozorgnia. May 2007.

PEER 2007/01 *Boore-Atkinson NGA Ground Motion Relations for the Geometric Mean Horizontal Component of Peak and Spectral Ground Motion Parameters.* David M. Boore and Gail M. Atkinson. May. May 2007.

PEER 2006/12 *Societal Implications of Performance-Based Earthquake Engineering.* Peter J. May. May 2007.

PEER 2006/11 *Probabilistic Seismic Demand Analysis Using Advanced Ground Motion Intensity Measures, Attenuation Relationships, and Near-Fault Effects.* Polsak Tothong and C. Allin Cornell. March 2007.

PEER 2006/10 *Application of the PEER PBEE Methodology to the I-880 Viaduct.* Sashi Kunnath. February 2007.

PEER 2006/09 *Quantifying Economic Losses from Travel Forgone Following a Large Metropolitan Earthquake.* James Moore, Sungbin Cho, Yue Yue Fan, and Stuart Werner. November 2006.

PEER 2006/08 *Vector-Valued Ground Motion Intensity Measures for Probabilistic Seismic Demand Analysis*. Jack W. Baker and C. Allin Cornell. October 2006.

PEER 2006/07 *Analytical Modeling of Reinforced Concrete Walls for Predicting Flexural and Coupled–Shear-Flexural Responses.* Kutay Orakcal, Leonardo M. Massone, and John W. Wallace. October 2006.

PEER 2006/06 *Nonlinear Analysis of a Soil-Drilled Pier System under Static and Dynamic Axial Loading.* Gang Wang and Nicholas Sitar. November 2006.

PEER 2006/05 *Advanced Seismic Assessment Guidelines.* Paolo Bazzurro, C. Allin Cornell, Charles Menun, Maziar Motahari, and Nicolas Luco. September 2006.

PEER 2006/04 *Probabilistic Seismic Evaluation of Reinforced Concrete Structural Components and Systems.* Tae Hyung Lee and Khalid M. Mosalam. August 2006.

PEER 2006/03 *Performance of Lifelines Subjected to Lateral Spreading.* Scott A. Ashford and Teerawut Juirnarongrit. July 2006.

PEER 2006/02 *Pacific Earthquake Engineering Research Center Highway Demonstration Project.* Anne Kiremidjian, James Moore, Yue Yue Fan, Nesrin Basoz, Ozgur Yazali, and Meredith Williams. April 2006.

PEER 2006/01 *Bracing Berkeley. A Guide to Seismic Safety on the UC Berkeley Campus.* Mary C. Comerio, Stephen Tobriner, and Ariane Fehrenkamp. January 2006.

PEER 2005/16 *Seismic Response and Reliability of Electrical Substation Equipment and Systems*. Junho Song, Armen Der Kiureghian, and Jerome L. Sackman. April 2006.

PEER 2005/15 *CPT-Based Probabilistic Assessment of Seismic Soil Liquefaction Initiation.* R. E. S. Moss, R. B. Seed, R. E. Kayen, J. P. Stewart, and A. Der Kiureghian. April 2006.

PEER 2005/14 *Workshop on Modeling of Nonlinear Cyclic Load-Deformation Behavior of Shallow Foundations.* Bruce L. Kutter, Geoffrey Martin, Tara Hutchinson, Chad Harden, Sivapalan Gajan, and Justin Phalen. March 2006.

PEER 2005/13 *Stochastic Characterization and Decision Bases under Time-Dependent Aftershock Risk in Performance-Based Earthquake Engineering.* Gee Liek Yeo and C. Allin Cornell. July 2005.

PEER 2005/12 *PEER Testbed Study on a Laboratory Building: Exercising Seismic Performance Assessment.* Mary C. Comerio, editor. November 2005.

PEER 2005/11 *Van Nuys Hotel Building Testbed Report: Exercising Seismic Performance Assessment.* Helmut Krawinkler, editor. October 2005.

PEER 2005/10 *First NEES/E-Defense Workshop on Collapse Simulation of Reinforced Concrete Building Structures.* September 2005.

PEER 2005/09 *Test Applications of Advanced Seismic Assessment Guidelines.* Joe Maffei, Karl Telleen, Danya Mohr, William Holmes, and Yuki Nakayama. August 2006.

PEER 2005/08 *Damage Accumulation in Lightly Confined Reinforced Concrete Bridge Columns.* R. Tyler Ranf, Jared M. Nelson, Zach Price, Marc O. Eberhard, and John F. Stanton. April 2006.

PEER 2005/07 *Experimental and Analytical Studies on the Seismic Response of Freestanding and Anchored Laboratory Equipment.* Dimitrios Konstantinidis and Nicos Makris. January 2005.

PEER 2005/06 *Global Collapse of Frame Structures under Seismic Excitations.* Luis F. Ibarra and Helmut Krawinkler. September 2005.

PEER 2005//05 *Performance Characterization of Bench- and Shelf-Mounted Equipment.* Samit Ray Chaudhuri and Tara C. Hutchinson. May 2006.

PEER 2005/04 *Numerical Modeling of the Nonlinear Cyclic Response of Shallow Foundations.* Chad Harden, Tara Hutchinson, Geoffrey R. Martin, and Bruce L. Kutter. August 2005.

PEER 2005/03 *A Taxonomy of Building Components for Performance-Based Earthquake Engineering.* Keith A. Porter. September 2005.

PEER 2005/02 *Fragility Basis for California Highway Overpass Bridge Seismic Decision Making*. Kevin R. Mackie and Božidar Stojadinović. June 2005.

PEER 2005/01 *Empirical Characterization of Site Conditions on Strong Ground Motion.* Jonathan P. Stewart, Yoojoong Choi, and Robert W. Graves. June 2005.

PEER 2004/09 *Electrical Substation Equipment Interaction: Experimental Rigid Conductor Studies.* Christopher Stearns and André Filiatrault. February 2005.

PEER 2004/08 *Seismic Qualification and Fragility Testing of Line Break 550-kV Disconnect Switches.* Shakhzod M. Takhirov, Gregory L. Fenves, and Eric Fujisaki. January 2005.

PEER 2004/07 *Ground Motions for Earthquake Simulator Qualification of Electrical Substation Equipment.* Shakhzod M. Takhirov, Gregory L. Fenves, Eric Fujisaki, and Don Clyde. January 2005.

PEER 2004/06 *Performance-Based Regulation and Regulatory Regimes.* Peter J. May and Chris Koski. September 2004.

PEER 2004/05 *Performance-Based Seismic Design Concepts and Implementation: Proceedings of an International Workshop.* Peter Fajfar and Helmut Krawinkler, editors. September 2004.

PEER 2004/04 *Seismic Performance of an Instrumented Tilt-up Wall Building.* James C. Anderson and Vitelmo V. Bertero. July 2004.

PEER 2004/03 *Evaluation and Application of Concrete Tilt-up Assessment Methodologies.* Timothy Graf and James O. Malley. October 2004.

PEER 2004/02 *Analytical Investigations of New Methods for Reducing Residual Displacements of Reinforced Concrete Bridge Columns.* Junichi Sakai and Stephen A. Mahin. August 2004.

PEER 2004/01 *Seismic Performance of Masonry Buildings and Design Implications.* Kerri Anne Taeko Tokoro, James C. Anderson, and Vitelmo V. Bertero. February 2004.

PEER 2003/18 *Performance Models for Flexural Damage in Reinforced Concrete Columns.* Michael Berry and Marc Eberhard. August 2003.

PEER 2003/17 *Predicting Earthquake Damage in Older Reinforced Concrete Beam-Column Joints.* Catherine Pagni and Laura Lowes. October 2004.

PEER 2003/16 *Seismic Demands for Performance-Based Design of Bridges.* Kevin Mackie and Božidar Stojadinović. August 2003.

PEER 2003/15 *Seismic Demands for Nondeteriorating Frame Structures and Their Dependence on Ground Motions.* Ricardo Antonio Medina and Helmut Krawinkler. May 2004.

PEER 2003/14 *Finite Element Reliability and Sensitivity Methods for Performance-Based Earthquake Engineering.* Terje Haukaas and Armen Der Kiureghian. April 2004.

PEER 2003/13 *Effects of Connection Hysteretic Degradation on the Seismic Behavior of Steel Moment-Resisting Frames.* Janise E. Rodgers and Stephen A. Mahin. March 2004.

PEER 2003/12 *Implementation Manual for the Seismic Protection of Laboratory Contents: Format and Case Studies.* William T. Holmes and Mary C. Comerio. October 2003.

PEER 2003/11 *Fifth U.S.-Japan Workshop on Performance-Based Earthquake Engineering Methodology for Reinforced Concrete Building Structures.* February 2004.

PEER 2003/10 *A Beam-Column Joint Model for Simulating the Earthquake Response of Reinforced Concrete Frames*. Laura N. Lowes, Nilanjan Mitra, and Arash Altoontash. February 2004.

PEER 2003/09 *Sequencing Repairs after an Earthquake: An Economic Approach.* Marco Casari and Simon J. Wilkie. April 2004.

PEER 2003/08 *A Technical Framework for Probability-Based Demand and Capacity Factor Design (DCFD) Seismic Formats*. Fatemeh Jalayer and C. Allin Cornell. November 2003.

PEER 2003/07 *Uncertainty Specification and Propagation for Loss Estimation Using FOSM Methods.* Jack W. Baker and C. Allin Cornell. September 2003.

PEER 2003/06 *Performance of Circular Reinforced Concrete Bridge Columns under Bidirectional Earthquake Loading*. Mahmoud M. Hachem, Stephen A. Mahin, and Jack P. Moehle. February 2003.

PEER 2003/05 *Response Assessment for Building-Specific Loss Estimation.* Eduardo Miranda and Shahram Taghavi. September 2003.

PEER 2003/04 *Experimental Assessment of Columns with Short Lap Splices Subjected to Cyclic Loads*. Murat Melek, John W. Wallace, and Joel Conte. April 2003.

PEER 2003/03 *Probabilistic Response Assessment for Building-Specific Loss Estimation.* Eduardo Miranda and Hesameddin Aslani. September 2003.

PEER 2003/02 *Software Framework for Collaborative Development of Nonlinear Dynamic Analysis Program.* Jun Peng and Kincho H. Law. September 2003.

PEER 2003/01 *Shake Table Tests and Analytical Studies on the Gravity Load Collapse of Reinforced Concrete Frames.* Kenneth John Elwood and Jack P. Moehle. November 2003.

PEER 2002/24 *Performance of Beam to Column Bridge Joints Subjected to a Large Velocity Pulse.* Natalie Gibson, André Filiatrault, and Scott A. Ashford. April 2002.

PEER 2002/23 *Effects of Large Velocity Pulses on Reinforced Concrete Bridge Columns.* Greg L. Orozco and Scott A. Ashford. April 2002.

PEER 2002/22 *Characterization of Large Velocity Pulses for Laboratory Testing.* Kenneth E. Cox and Scott A. Ashford. April 2002.

PEER 2002/21 *Fourth U.S.-Japan Workshop on Performance-Based Earthquake Engineering Methodology for Reinforced Concrete Building Structures*. December 2002.

PEER 2002/20 *Barriers to Adoption and Implementation of PBEE Innovations.* Peter J. May. August 2002.

PEER 2002/19 *Economic-Engineered Integrated Models for Earthquakes: Socioeconomic Impacts.* Peter Gordon, James E. Moore II, and Harry W. Richardson. July 2002.

PEER 2002/18 *Assessment of Reinforced Concrete Building Exterior Joints with Substandard Details.* Chris P. Pantelides, Jon Hansen, Justin Nadauld, and Lawrence D. Reaveley. May 2002.

PEER 2002/17 *Structural Characterization and Seismic Response Analysis of a Highway Overcrossing Equipped with Elastomeric Bearings and Fluid Dampers: A Case Study.* Nicos Makris and Jian Zhang. November 2002.

PEER 2002/16 *Estimation of Uncertainty in Geotechnical Properties for Performance-Based Earthquake Engineering.* Allen L. Jones, Steven L. Kramer, and Pedro Arduino. December 2002.

PEER 2002/15 *Seismic Behavior of Bridge Columns Subjected to Various Loading Patterns*. Asadollah Esmaeily-Gh. and Yan Xiao. December 2002.

PEER 2002/14 *Inelastic Seismic Response of Extended Pile Shaft Supported Bridge Structures.* T.C. Hutchinson, R.W. Boulanger, Y.H. Chai, and I.M. Idriss. December 2002.

PEER 2002/13 *Probabilistic Models and Fragility Estimates for Bridge Components and Systems.* Paolo Gardoni, Armen Der Kiureghian, and Khalid M. Mosalam. June 2002.

PEER 2002/12 *Effects of Fault Dip and Slip Rake on Near-Source Ground Motions: Why Chi-Chi Was a Relatively Mild M7.6 Earthquake.* Brad T. Aagaard, John F. Hall, and Thomas H. Heaton. December 2002.

PEER 2002/11 *Analytical and Experimental Study of Fiber-Reinforced Strip Isolators*. James M. Kelly and Shakhzod M. Takhirov. September 2002.

PEER 2002/10 *Centrifuge Modeling of Settlement and Lateral Spreading with Comparisons to Numerical Analyses***.** Sivapalan Gajan and Bruce L. Kutter. January 2003.

PEER 2002/09 *Documentation and Analysis of Field Case Histories of Seismic Compression during the 1994 Northridge, California, Earthquake.* Jonathan P. Stewart, Patrick M. Smith, Daniel H. Whang, and Jonathan D. Bray. October 2002.

PEER 2002/08 *Component Testing, Stability Analysis and Characterization of Buckling-Restrained Unbonded Braces™.* Cameron Black, Nicos Makris, and Ian Aiken. September 2002.

PEER 2002/07 *Seismic Performance of Pile-Wharf Connections.* Charles W. Roeder, Robert Graff, Jennifer Soderstrom, and Jun Han Yoo. December 2001.

PEER 2002/06 *The Use of Benefit-Cost Analysis for Evaluation of Performance-Based Earthquake Engineering Decisions*. Richard O. Zerbe and Anthony Falit-Baiamonte. September 2001.

PEER 2002/05 *Guidelines, Specifications, and Seismic Performance Characterization of Nonstructural Building Components and Equipment*. André Filiatrault, Constantin Christopoulos, and Christopher Stearns. September 2001.

PEER 2002/04 *Consortium of Organizations for Strong-Motion Observation Systems and the Pacific Earthquake Engineering Research Center Lifelines Program: Invited Workshop on Archiving and Web Dissemination of Geotechnical Data, 4–5 October 2001*. September 2002.

PEER 2002/03 *Investigation of Sensitivity of Building Loss Estimates to Major Uncertain Variables for the Van Nuys Testbed.* Keith A. Porter, James L. Beck, and Rustem V. Shaikhutdinov. August 2002.

PEER 2002/02 *The Third U.S.-Japan Workshop on Performance-Based Earthquake Engineering Methodology for Reinforced Concrete Building Structures*. July 2002.

PEER 2002/01 *Nonstructural Loss Estimation: The UC Berkeley Case Study.* Mary C. Comerio and John C. Stallmeyer. December 2001.

PEER 2001/16 *Statistics of SDF-System Estimate of Roof Displacement for Pushover Analysis of Buildings.* Anil K. Chopra, Rakesh K. Goel, and Chatpan Chintanapakdee. December 2001.

PEER 2001/15 *Damage to Bridges during the 2001 Nisqually Earthquake.* R. Tyler Ranf, Marc O. Eberhard, and Michael P. Berry. November 2001.

PEER 2001/14 *Rocking Response of Equipment Anchored to a Base Foundation.* Nicos Makris and Cameron J. Black. September 2001.

PEER 2001/13 *Modeling Soil Liquefaction Hazards for Performance-Based Earthquake Engineering.* Steven L. Kramer and Ahmed-W. Elgamal. February 2001.

PEER 2001/12 *Development of Geotechnical Capabilities in OpenSees.* Boris Jeremi . September 2001.

PEER 2001/11 *Analytical and Experimental Study of Fiber-Reinforced Elastomeric Isolators*. James M. Kelly and Shakhzod M. Takhirov. September 2001.

PEER 2001/10 *Amplification Factors for Spectral Acceleration in Active Regions.* Jonathan P. Stewart, Andrew H. Liu, Yoojoong Choi, and Mehmet B. Baturay. December 2001.

PEER 2001/09 *Ground Motion Evaluation Procedures for Performance-Based Design.* Jonathan P. Stewart, Shyh-Jeng Chiou, Jonathan D. Bray, Robert W. Graves, Paul G. Somerville, and Norman A. Abrahamson. September 2001.

PEER 2001/08 *Experimental and Computational Evaluation of Reinforced Concrete Bridge Beam-Column Connections for Seismic Performance*. Clay J. Naito, Jack P. Moehle, and Khalid M. Mosalam. November 2001.

PEER 2001/07 *The Rocking Spectrum and the Shortcomings of Design Guidelines.* Nicos Makris and Dimitrios Konstantinidis. August 2001.

PEER 2001/06 *Development of an Electrical Substation Equipment Performance Database for Evaluation of Equipment Fragilities*. Thalia Agnanos. April 1999.

PEER 2001/05 *Stiffness Analysis of Fiber-Reinforced Elastomeric Isolators.* Hsiang-Chuan Tsai and James M. Kelly. May 2001.

PEER 2001/04 *Organizational and Societal Considerations for Performance-Based Earthquake Engineering.* Peter J. May. April 2001.

PEER 2001/03 *A Modal Pushover Analysis Procedure to Estimate Seismic Demands for Buildings: Theory and Preliminary Evaluation.* Anil K. Chopra and Rakesh K. Goel. January 2001.

PEER 2001/02 *Seismic Response Analysis of Highway Overcrossings Including Soil-Structure Interaction.* Jian Zhang and Nicos Makris. March 2001.

PEER 2001/01 *Experimental Study of Large Seismic Steel Beam-to-Column Connections.* Egor P. Popov and Shakhzod M. Takhirov. November 2000.

PEER 2000/10 *The Second U.S.-Japan Workshop on Performance-Based Earthquake Engineering Methodology for Reinforced Concrete Building Structures.* March 2000.

PEER 2000/09 *Structural Engineering Reconnaissance of the August 17, 1999 Earthquake: Kocaeli (Izmit), Turkey.* Halil Sezen, Kenneth J. Elwood, Andrew S. Whittaker, Khalid Mosalam, John J. Wallace, and John F. Stanton. December 2000.

PEER 2000/08 *Behavior of Reinforced Concrete Bridge Columns Having Varying Aspect Ratios and Varying Lengths of Confinement.* Anthony J. Calderone, Dawn E. Lehman, and Jack P. Moehle. January 2001.

PEER 2000/07 *Cover-Plate and Flange-Plate Reinforced Steel Moment-Resisting Connections.* Taejin Kim, Andrew S. Whittaker, Amir S. Gilani, Vitelmo V. Bertero, and Shakhzod M. Takhirov. September 2000.

PEER 2000/06 *Seismic Evaluation and Analysis of 230-kV Disconnect Switches.* Amir S. J. Gilani, Andrew S. Whittaker, Gregory L. Fenves, Chun-Hao Chen, Henry Ho, and Eric Fujisaki. July 2000.

PEER 2000/05 *Performance-Based Evaluation of Exterior Reinforced Concrete Building Joints for Seismic Excitation.* Chandra Clyde, Chris P. Pantelides, and Lawrence D. Reaveley. July 2000.

PEER 2000/04 *An Evaluation of Seismic Energy Demand: An Attenuation Approach.* Chung-Che Chou and Chia-Ming Uang. July 1999.

PEER 2000/03 *Framing Earthquake Retrofitting Decisions: The Case of Hillside Homes in Los Angeles.* Detlof von Winterfeldt, Nels Roselund, and Alicia Kitsuse. March 2000.

PEER 2000/02 *U.S.-Japan Workshop on the Effects of Near-Field Earthquake Shaking.* Andrew Whittaker, ed. July 2000.

PEER 2000/01 *Further Studies on Seismic Interaction in Interconnected Electrical Substation Equipment.* Armen Der Kiureghian, Kee-Jeung Hong, and Jerome L. Sackman. November 1999.

PEER 1999/14 *Seismic Evaluation and Retrofit of 230-kV Porcelain Transformer Bushings*. Amir S. Gilani, Andrew S. Whittaker, Gregory L. Fenves, and Eric Fujisaki. December 1999.

PEER 1999/13 *Building Vulnerability Studies: Modeling and Evaluation of Tilt-up and Steel Reinforced Concrete Buildings.* John W. Wallace, Jonathan P. Stewart, and Andrew S. Whittaker, editors. December 1999.

PEER 1999/12 *Rehabilitation of Nonductile RC Frame Building Using Encasement Plates and Energy-Dissipating Devices.* Mehrdad Sasani, Vitelmo V. Bertero, James C. Anderson. December 1999.

PEER 1999/11 *Performance Evaluation Database for Concrete Bridge Components and Systems under Simulated Seismic Loads.* Yael D. Hose and Frieder Seible. November 1999.

PEER 1999/10 *U.S.-Japan Workshop on Performance-Based Earthquake Engineering Methodology for Reinforced Concrete Building Structures.* December 1999.

PEER 1999/09 *Performance Improvement of Long Period Building Structures Subjected to Severe Pulse-Type Ground Motions*. James C. Anderson, Vitelmo V. Bertero, and Raul Bertero. October 1999.

PEER 1999/08 *Envelopes for Seismic Response Vectors.* Charles Menun and Armen Der Kiureghian. July 1999.

PEER 1999/07 *Documentation of Strengths and Weaknesses of Current Computer Analysis Methods for Seismic Performance of Reinforced Concrete Members.* William F. Cofer. November 1999.

PEER 1999/06 *Rocking Response and Overturning of Anchored Equipment under Seismic Excitations.* Nicos Makris and Jian Zhang. November 1999.

PEER 1999/05 *Seismic Evaluation of 550 kV Porcelain Transformer Bushings.* Amir S. Gilani, Andrew S. Whittaker, Gregory L. Fenves, and Eric Fujisaki. October 1999.

PEER 1999/04 *Adoption and Enforcement of Earthquake Risk-Reduction Measures.* Peter J. May, Raymond J. Burby, T. Jens Feeley, and Robert Wood.

PEER 1999/03 *Task 3 Characterization of Site Response General Site Categories*. Adrian Rodriguez-Marek, Jonathan D. Bray, and Norman Abrahamson. February 1999.

PEER 1999/02 *Capacity-Demand-Diagram Methods for Estimating Seismic Deformation of Inelastic Structures: SDF Systems*. Anil K. Chopra and Rakesh Goel. April 1999.

PEER 1999/01 *Interaction in Interconnected Electrical Substation Equipment Subjected to Earthquake Ground Motions.* Armen Der Kiureghian, Jerome L. Sackman, and Kee-Jeung Hong. February 1999.

PEER 1998/08 *Behavior and Failure Analysis of a Multiple-Frame Highway Bridge in the 1994 Northridge Earthquake.* Gregory L. Fenves and Michael Ellery. December 1998.

PEER 1998/07 *Empirical Evaluation of Inertial Soil-Structure Interaction Effects.* Jonathan P. Stewart, Raymond B. Seed, and Gregory L. Fenves. November 1998.

PEER 1998/06 *Effect of Damping Mechanisms on the Response of Seismic Isolated Structures.* Nicos Makris and Shih-Po Chang. November 1998.

PEER 1998/05 *Rocking Response and Overturning of Equipment under Horizontal Pulse-Type Motions.* Nicos Makris and Yiannis Roussos. October 1998.

PEER 1998/04 *Pacific Earthquake Engineering Research Invitational Workshop Proceedings, May 14–15, 1998: Defining the Links between Planning, Policy Analysis, Economics and Earthquake Engineering.* Mary Comerio and Peter Gordon. September 1998.

PEER 1998/03 *Repair/Upgrade Procedures for Welded Beam to Column Connections.* James C. Anderson and Xiaojing Duan. May 1998.

PEER 1998/02 *Seismic Evaluation of 196 kV Porcelain Transformer Bushings.* Amir S. Gilani, Juan W. Chavez, Gregory L. Fenves, and Andrew S. Whittaker. May 1998.

PEER 1998/01 *Seismic Performance of Well-Confined Concrete Bridge Columns.* Dawn E. Lehman and Jack P. Moehle. December 2000.

ONLINE REPORTS

The following PEER reports are available by Internet only at http://peer.berkeley.edu/publications/peer_reports.html

PEER 2009/103 *Performance Evaluation of Innovative Steel Braced Frames.* T. Y. Yang, Jack P. Moehle, and Božidar Stojadinović. August 2009.

PEER 2009/102 *Reinvestigation of Liquefaction and Nonliquefaction Case Histories from the 1976 Tangshan Earthquake.* Robb Eric Moss, Robert E. Kayen, Liyuan Tong, Songyu Liu, and Guojun Cai. August 2009.

PEER 2009/101 *Report of the First Joint Planning Meeting for the Second Phase of NEES/E-Defense Collaborative Research on Earthquake Engineering.* Stephen A. Mahin et al. July 2009.

PEER 2008/104 *Experimental and Analytical Study of the Seismic Performance of Retaining Structures.* Linda Al Atik and Nicholas Sitar. January 2009.

PEER 2008/103 *Experimental and Computational Evaluation of Current and Innovative In-Span Hinge Details in Reinforced Concrete Box-Girder Bridges. Part 1: Experimental Findings and Pre-Test Analysis.* Matias A. Hube and Khalid M. Mosalam. January 2009.

PEER 2008/102 *Modeling of Unreinforced Masonry Infill Walls Considering In-Plane and Out-of-Plane Interaction.* Stephen Kadysiewski and Khalid M. Mosalam. January 2009.

PEER 2008/101 *Seismic Performance Objectives for Tall Buildings.* William T. Holmes, Charles Kircher, William Petak, and Nabih Youssef. August 2008.

PEER 2007/101 *Generalized Hybrid Simulation Framework for Structural Systems Subjected to Seismic Loading.* Tarek Elkhoraibi and Khalid M. Mosalam. July 2007.

PEER 2007/100 *Seismic Evaluation of Reinforced Concrete Buildings Including Effects of Masonry Infill Walls.* Alidad Hashemi and Khalid M. Mosalam. July 2007.

Reinvestigation of Liquefaction and Nonliquefaction Case Histories from the 1976 Tangshan Earthquake

Robb Eric S. Moss
California Polytechnic State University, San Luis Obispo

Robert E. Kayen
U.S. Geological Survey

Liyuan Tong, Songyu Liu, and Guojun Cai
Southeast University, Nanjing, People's Republic of China

Jiaer Wu
URS Oakland, California

PEER Report 2009/102
Pacific Earthquake Engineering Research Center
College of Engineering
University of California, Berkeley

August 2009

ABSTRACT

A field investigation was carried out to retest liquefaction and nonliquefaction sites from the 1976 Tangshan earthquake in the People's Republic of China (PRC). These sites were carefully investigated in 1978/1979 using standard penetration test (SPT) and cone penetration test (CPT) equipment; however the CPT measurements are obsolete because of the now nonstandard cone that was used at the time. In 2007 a modern cone was mobilized to retest 18 select sites that are particularly valuable because they experienced intense ground shaking, have high fines content, and are classified as nonliquefaction sites. Of the sites reinvestigated and carefully processed, 13 are considered accurate representative case histories that warrant being included in the worldwide CPT database. Two of the sites that were originally documented as exhibiting liquefaction and nonliquefaction have been reassessed as cyclic failure of fine-grained soil and removed from consideration for liquefaction triggering. The most important result of these field investigations are 3 nonliquefaction case histories that experienced intense ground shaking. These 3 case histories reside in a region of the liquefaction-triggering database that is poorly populated and will help constrain the upper bound of future liquefaction-triggering curves.

ACKNOWLEDGMENTS

This material is based upon work supported by the National Science Foundation under Grant No. 0633886. Funding in the People's Republic of China was provided by the National Natural Science Foundation of China (NSFC) Grant No. 40702047 and the Jiangsu Transportation Research Foundation Grant No. 8821006021. Publication of this report was supported by the Pacific Earthquake Engineering Research Center (PEER) with funding from the State of California. Any opinions, findings, and conclusions or recommendations expressed in this material are those of the authors and do not necessarily reflect the views of the funding agencies.

CONTENTS

ABSTRACT iii
ACKNOWLEDGMENTS iv
TABLE OF CONTENTS v
LIST OF FIGURES vii
LIST OF TABLES ix
1 INTRODUCTION 1
2 1976 TANGSHAN EARTHQUAKE 3
3 DATA COLLECTION 11
4 CASE HISTORY PROCESSING 15
5 TANGSHAN CASE HISTORIES 17
REFERENCES 23
APPENDIX A: TANGSHAN CASE HISTORY DATA A-1
APPENDIX B: DATA PROCESSING TECHNIQUES (CHAPTER 4 EXCERPT FROM MOSS ET AL. 2003) B-1
4.1 Introduction B-3
4.2 Field Observations B-3
4.3 Strength Parameters B-4
4.3.1 Choice of Log B-4
4.3.2 Case Selection B-5
4.3.3 Critical Layer Selection B-5
4.3.4 Index Measurements B-6
4.3.5 Masked Liquefaction B-7
4.3.6 Screening for Other Failure Mechanisms B-7
4.3.7 Normalization B-8
4.3.8 Thin Layer Correction B-8
4.3.9 Processed Strength Parameters B-9
4.4 Stress Parameters B-9
4.4.1 Cyclic Stress Ratio B-9

4.4.2 Peak Ground Acceleration B-10
4.4.3 Total and Effective Stress B-10
4.4.4 Nonlinear Shear Mass Participation Factor (r_d) B-11
4.4.5 Moment Magnitude B-12
4.5 Data Class B-13
4.6 Review Process B-14
4.7 Conclusion B-14

LIST OF FIGURES

Figure 2.1 GSHAP seismic hazard map showing 10% in 50 year estimate of peak ground acceleration. Tangshan region is circled 4

Figure 2.2 Chinese intensity map (Zhang and Zhou 1979). Intensity scale correlated to PGA using Chinese Building Code. Sites circled with associated site number. 6

Figure 2.3 Strong motion recordings of 1976 Tangshan event shown with respect to three well-known intraplate attenuation relationships and estimates of rock PGA ranges from Chinese intensity contours. Recordings were from both rock and soil sites and not corrected for nonlinear soil effects 7

Figure 2.4 Atkinson and Boore (1995, 1997) attenuation relationship is shown calibrated to recordings and estimated rock PGA ranges. Attenuation relationship converted from hypocentral to epicentral distance using depth to rupture of 14 km. 8

Figure 3.1 Regional view of sites investigated in this study....12

Figure 3.2 Intercity view of sites investigated in this study. Tangshan sites, denoted by T and site number, are scattered in and around city. Lutai sites are located outside this city and are denoted by L and site number. 13

Figure 3.3 Investigated sites in proximity to Tangshan City 14

Figure 5.1 Tangshan District and Lutai District case histories shown against Moss et al. (2006) probabilistic liquefaction-triggering curves. X-axis is cone-tip resistance normalized for effective overburden pressure. Y-axis is cyclic stress ratio corrected for magnitude. 20

Figure 5.2 X-axis shows cone-tip resistance modified for “apparent” fines content as measured using friction ratio for proxy. 21

Figure 5.3 Tangshan District and Lutai District case histories with respect to worldwide CPT case history database (Moss et al. 2003). Tangshan District sites are particularly important for high CSR values and for nonliquefaction cases. Lutai District sites are interpreted as examples of cyclic failure of clay and not liquefaction. 22

LIST OF TABLES

Table 2.1 Estimated soil peak ground acceleration (PGA) using calibrated rock attenuation relationships and Stewart et al. (2003) site amplification factors for NEHRP site class D soil conditions. Distances reported in kilometers (km) and peak ground acceleration (PGA) in units of gravity. Minimum or saturation epicentral distance of 10 km used. 9

Table 5.1 Case history values for Tangshan District sites....17

Table 5.2 Case history values for Lutai District sites. 17

Table 5.3 GPS coordinates of sites investigated....18

1 Introduction

The 1976 Tangshan, People's Republic of China, earthquake resulted in widespread liquefaction that was well documented at the time by Chinese researchers (Zhou and Guo 1979; Zhou and Zhang 1979). These reports accurately documented case histories of liquefaction and nonliquefaction with SPT (standard penetration test), CPT (cone penetration test), and soil borings to acquire subsurface samples for measuring water content, unit weight, and performing grain size analysis. The CPT measurements, however, were made using what is now an obsolete cone that measured only tip resistance. Current CPT–based liquefaction-triggering procedures (e.g., Moss et al. 2006; Youd et al. 2001) require sleeve friction measurements to make accurate liquefaction predictions. This report documents the efforts to re-acquire subsurface information using a modern cone (capable of measuring tip, sleeve, pore pressure, and shear wave velocity) so that these valuable case histories can be included in the worldwide CPT liquefaction database (Moss et al. 2003). The main focus of these field investigations was at sites providing the most informational content: sites that experienced high estimated ground shaking and soils that contained high fines content. High priority was given to nonliquefaction sites because these tend to be under-represented in the worldwide database.

This research was a collaborative effort between researchers in the United States and the People's Republic of China. The research was directed by Robb Moss (Cal Poly San Luis Obispo) with assistance from Robert Kayen (USGS). Southeast University in Nanjing, PRC, provided the ground support with a fully manned CPT rig and lab support for analyzing soil samples. Collaborators from Southeast University included Prof. Liyuan Tong, Prof. Du, and Guojun Cai. The CEA (China Earthquake Agency) in conjunction with IEM (Inst. Engineering Mechanics) in Harbin provided logistical support and assistance in locating and obtaining access to the sites. Collaborators from CEA-IEM included Prof. Yuan, Prof. Tow, Cao Zhengzhong, Shi Lijing, and several other student researchers. This research was truly a collaborative effort and would not have been successful without the contribution from every member of the research team.

2 1976 Tangshan Earthquake

The M_S=7.8 Tangshan earthquake occurred on July 8, 1976. The epicenter was located in the southern part of the city of Tangshan, and surface fault rupture progressed predominantly to the northeast through the town , with some additional rupture to the southwest. The fault rupture was primarily right-lateral strike-slip in nature. The event occurred in the early hours of the morning, and collapse of unreinforced masonry (URM) structures was the primary cause for fatalities that have recently been reassessed at upwards of 500,000. A detailed compilation of reports on the event and the aftermath can be found in (Liu et al. 2002).

This event occurred in an intraplate region of high seismicity dominated by strike-slip faulting. The global seismic hazard assessment program (GSHAP) (http://www.seismo.ethz.ch/GSHAP/) map of the region. Figure 2.1, shows the high seismicity of this region based on historical seismicity and regional tectonics. The source of crustal stress in this region may be due to the combined effects of the collision zone to the far southwest between the Eurasian plate and the Indian Plate as well as the subduction zone off the east coast between the Eurasian and Philippine plates. The intraplate region may be an old suture zone between accreted subplate sections (Liu et al. 2002).

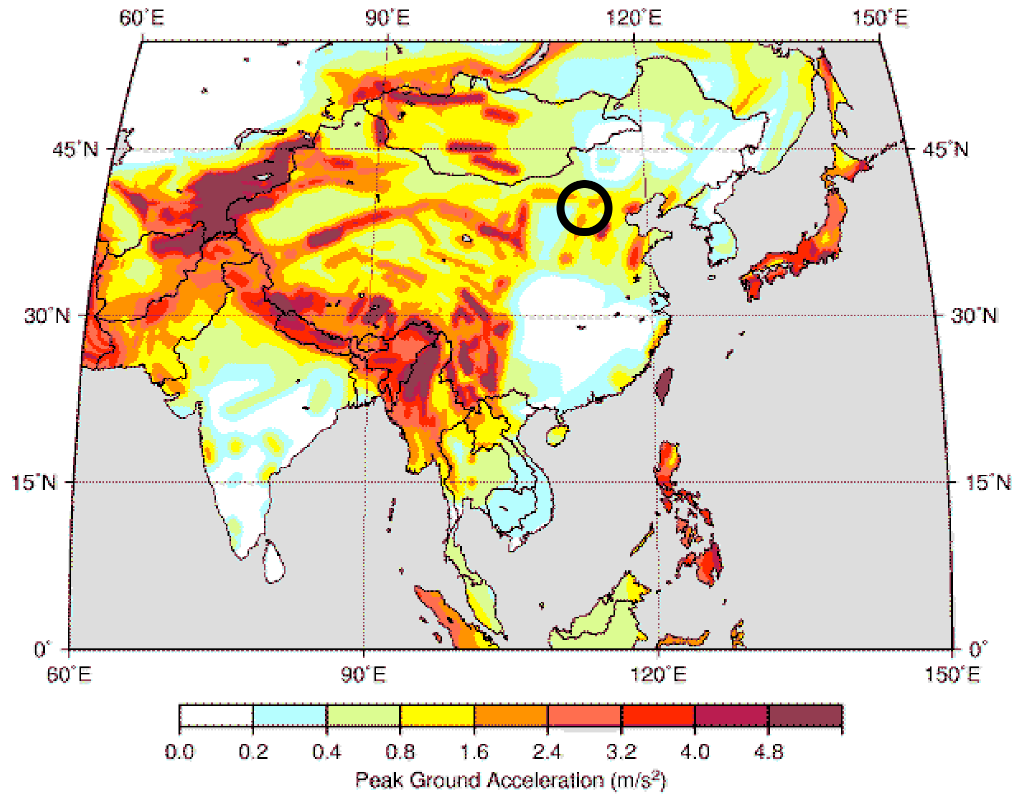

Fig. 2.1 GSHAP seismic hazard map showing 10% in 50 year estimate of peak ground acceleration. Tangshan region is circled.

The area affected by the earthquake is a piedmont region with many rivers and streams flowing to the Bay of Bo, which is connected to the Yellow Sea. The low hills inland from the current coast are the source of river sediment. It is apparent from the subsurface soil conditions that migrating river channels dominate the depositional environment. Flood plain silts are interlayered with sands having varying silt content. At certain locations are clay deposits indicating either past lacustrine depositional environment or sea level rise resulting in a marine depositional environment. Most of the liquefaction occurred in the upper few meters in loose to medium-dense silty fine sand or fine to medium clean sand. Most of the nonliquefaction sites were underlain by very dense clean sand. The sites around Tangshan City are in the Stone River watershed. The sites in the city of Lutai are in the watershed of the Li Yun River.

A calibrated attenuation relationship was used to improve estimates of peak ground acceleration (PGA) at each site. Six recordings (Liu et al. 2002) of the event were used along with correlated intensity contours to fit an intraplate attenuation relationship. The nearest recording was at 148 km epicentral distance, so the near-source fitting was made using rock PGA estimates from Chinese isoseismal intensity contours (Fig. 2.2). (Shibata and Teparaska 1988) correlated Chinese intensity to PGA using the following approximation from the Chinese building code; IX~0.4g, VIII~0.2g, and VI~0.1 g. To account for soil nonlinearity from basement rock to the ground surface, amplification factors by Stewart et al. (2003) were applied. An epicentral distance of 10 km was used as a minimum or lower cap because of the uncertainty in the location of the epicenter with respect to the sites. Figure 2.3 shows the recordings plotted against three well-known intraplate attenuation relationships, and the estimated PGA range from Chinese intensity contours. The three attenuation relationships evaluated were Atkinson and Boore (1995; 1997); Dahle et al. (1990); and Toro et al. (1997). A depth to rupture of 14 km (Liu et al. 2002) was used to convert between hypocentral and epicentral distance. By inspection, the Atkinson and Boore relationship provide the best fit to mean PGA for small and large epicentral distances. This attenuation relationship was then calibrated to the data (Fig. 2.4) to provide a better estimate of the ground shaking that occurred during the Tangshan event.

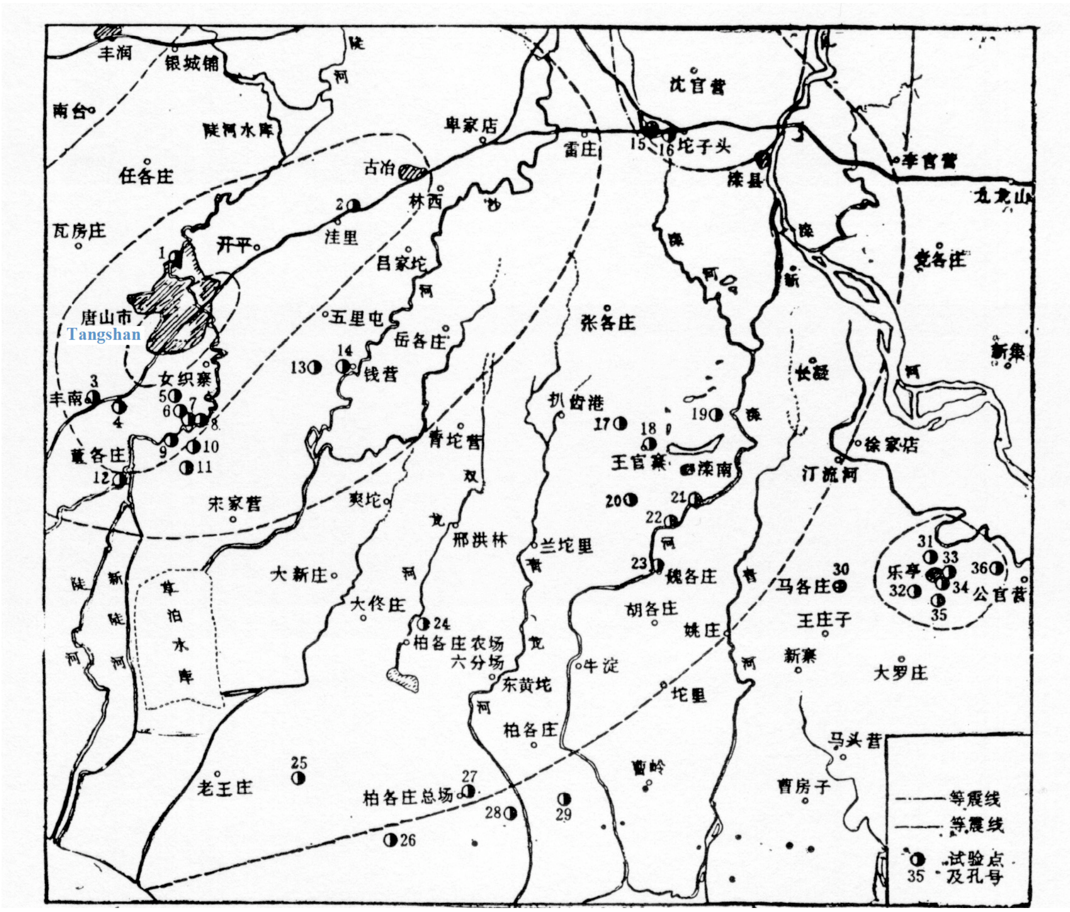

Fig. 2.2 Chinese intensity map (Zhang and Zhou 1979). Intensity scale correlated to PGA using Chinese Building Code. Sites circled with associated site number.

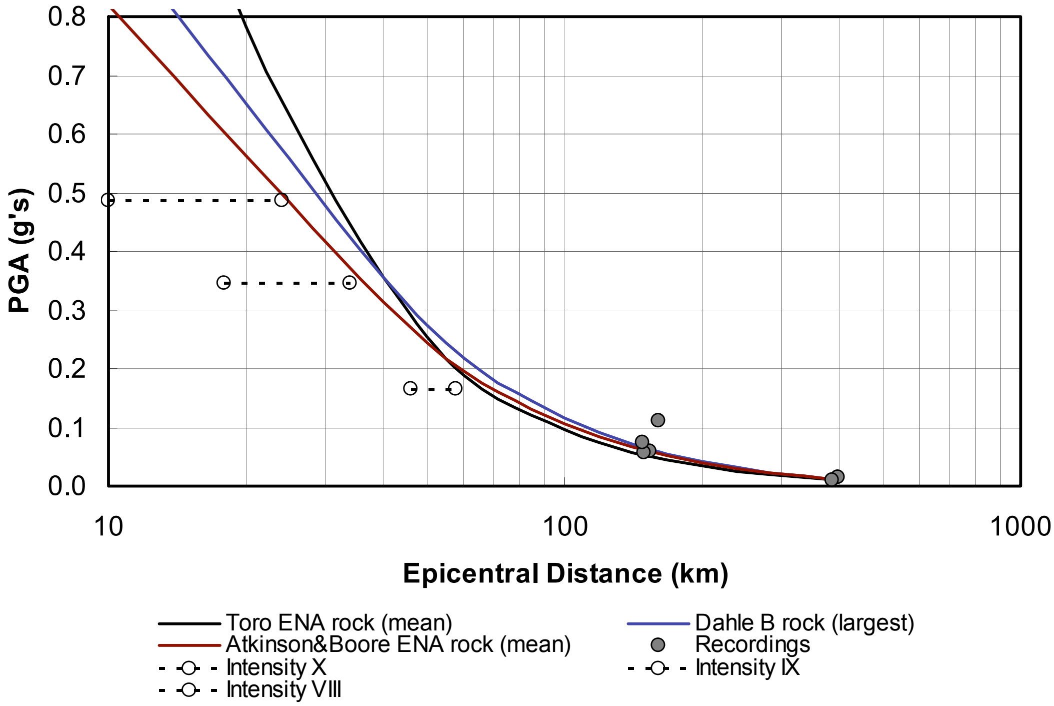

Fig. 2.3 Strong motion recordings of 1976 Tangshan event shown with respect to three well-known intraplate attenuation relationships and estimates of rock PGA ranges from Chinese intensity contours. Recordings were from both rock and soil sites and not corrected for nonlinear soil effects.

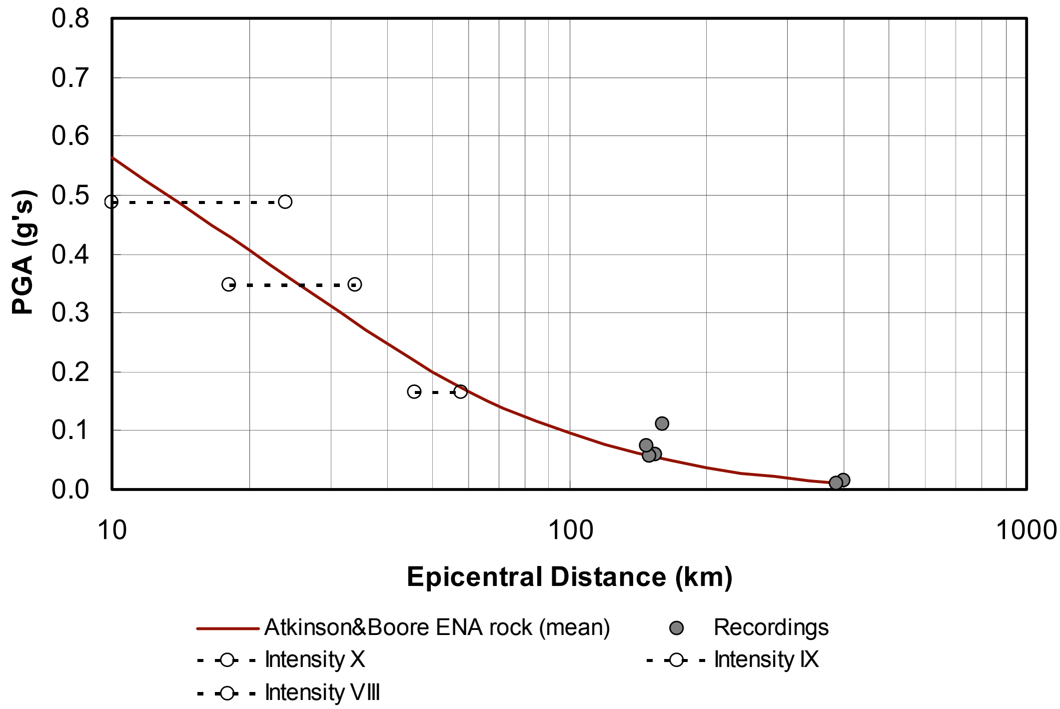

Fig. 2.4 Atkinson and Boore (1995, 1997) attenuation relationship is shown calibrated to recordings and estimated rock PGA ranges. Attenuation relationship converted from hypocentral to epicentral distance using depth to rupture of 14 km.

Table 2.1 Estimated soil peak ground acceleration (PGA) using calibrated rock attenuation relationships and Stewart et al. (2003) site amplification factors for NEHRP site class D soil conditions. Distances reported in kilometers (km) and peak ground acceleration (PGA) in units of gravity. Minimum or saturation epicentral distance of 10 km used.

Sites	Epicentral Distance	Minimum Distance	PGA Rock	Amplification	PGA Soil
T1	8	10	0.56	1.13	0.64
T2	16	16	0.46	1.14	0.53
T3	10	10	0.56	1.13	0.64
T4	9	10	0.56	1.13	0.64
T5	6	10	0.56	1.13	0.64
T6	7	10	0.56	1.13	0.64
T7	6	10	0.56	1.13	0.64
T8	8	10	0.56	1.13	0.64
T9	9	10	0.56	1.13	0.64
T10	9	10	0.56	1.13	0.64
T11	11	11	0.54	1.13	0.61
T12	13	13	0.51	1.14	0.58
T13	13	13	0.51	1.14	0.58
T14	15	15	0.47	1.14	0.54
T15	43	43	0.23	1.20	0.27
T16	46	46	0.22	1.21	0.26
L1	44	44	0.22	1.20	0.27
L2	44	44	0.22	1.20	0.27

3 Data Collection

Data collection involved using the CPT to measure tip resistance (qc), sleeve friction (fs), pore pressure (u), and incremental shear wave velocity. Soil samples were retrieved using a CPT soil sampler and hand auger. SASW (spectral analysis of surface waves) were made at the site previously.

The CPT rig is a Vertek-Hogentogler 200kN (20 ton) seismic piezocone penetrometer. The cones (adhering to ASTM 5778) used have a 10 cm2 base area with an apex angle of 60º. A friction sleeve, located behind the conical tip, has a standard area of 150 cm^2. A pressure transducer is located immediately behind the cone tip. A temperature sensor is also embedded in the cones, which is primarily used to correct data for thermal offset. A slope sensor is included in the cone design to monitor vertically during penetration. A small geophone or accelerometer located inside the cone, measures shear wave velocities. Data were collected at 50 mm intervals. Seismic shear wave velocity measurements were made every 1 m during brief pauses in the cone penetration.

Figures 3.1–3.3 show the geo-referenced locations of the sites from regional to city scale. The coordinates for each site are shown in Table 5.3.

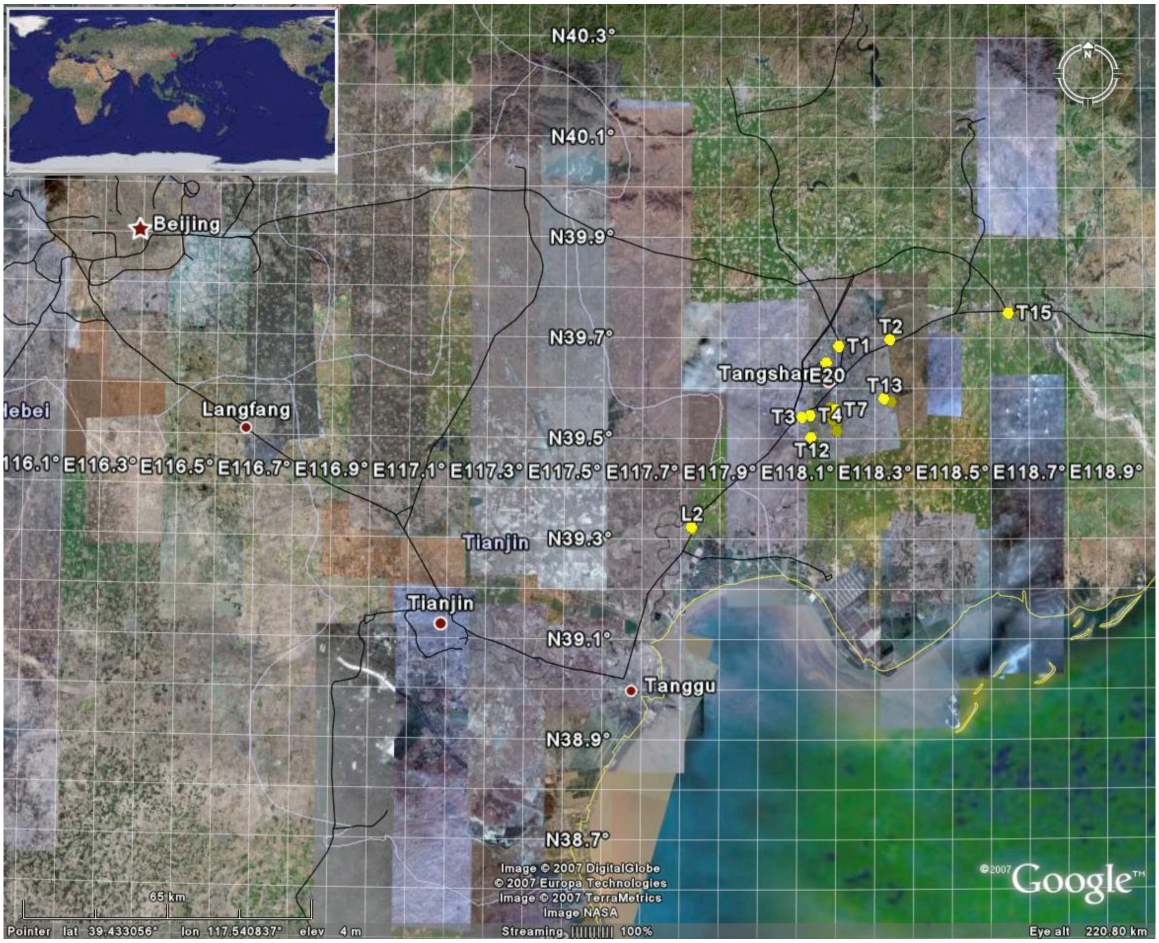

Fig. 3.1 Regional view of sites investigated in this study.

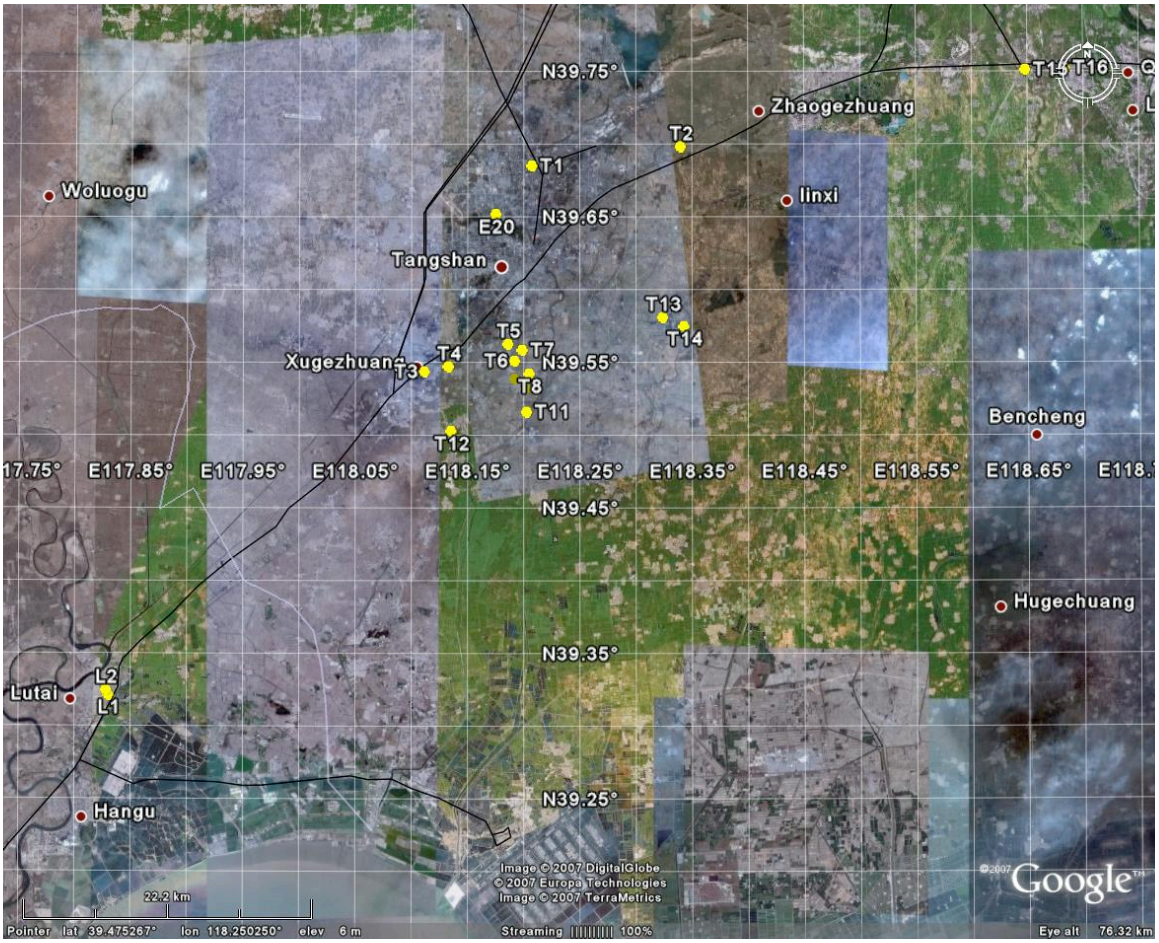

Fig. 3.2 Intercity view of sites investigated in this study. Tangshan sites, denoted by T and site number, are scattered in and around city. Lutai sites are located outside this city and are denoted by L and site number.

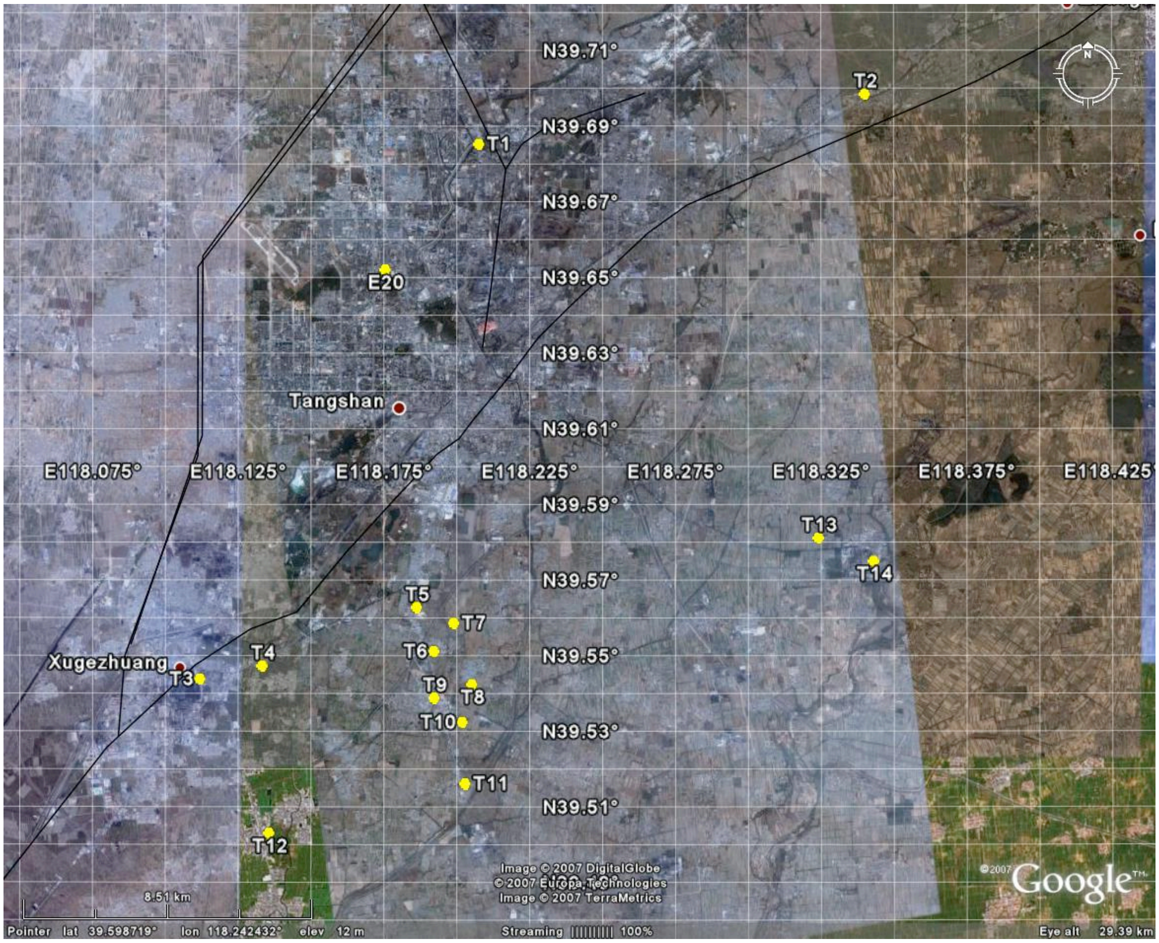

Fig. 3.3 Investigated sites in proximity to Tangshan City.

4 Case History Processing

The case histories from this investigation were processed according to the procedures outlined in Moss et al. (2006). This accounts for the uncertainties in the various input parameters and quantifies the impact of these uncertainties on the resulting liquefaction-triggering correlation. The results are a probabilistic estimate of cyclic loading and cyclic resistance for each site.

The sites investigated as part of this project contain uncertainties that are a byproduct of the subsurface investigations occurring so long after the 1976 earthquake. Reinvestigating liquefaction/nonliquefaction sites of past earthquakes has been carried out before with success (Moss et al. 2005). A key to reinvestigating a previous documented site is accurately locating the spot at which previous subsurface investigations were conducted. This is a function of how well the site was documented via maps, coordinates, ground and aerial photos, field notes, references to landmarks, and, in this case, the long-term memory of residents. The sites must also be relatively unmodified since the previous investigation.

The sites in this report are generally in rural agricultural areas with little land development having occurred since the time of the earthquake and surface elevations are considered to be close to the 1976 elevations, or post-earthquake elevations. Locating the sites consisted of driving to the town or landmark named in the logs by Zhou and Gou (1978) and Zhou and Zhang (1979), asking the residents who survived the earthquake to recall the event and subsequent subsurface investigations, and arriving at a group consensus about the location of the previous investigations. Although this appears to be an *ad hoc* method, the impression that a devastating earthquake and aftermath can have on people and their memories can be profound. This earthquake was not only the single most impressionable event for these people collectively, but in the aftermath they were asked detailed questions about their experiences by a group of investigators with government credentials and large sophisticated testing equipment for drilling the ground to collect subsurface information. In most cases there was little disagreement between the rural residents about where a previous location was, and when there was disagreement, the difference was usually only a few meters (e.g., this side of the pea patch or the other).

Confirmation of the right location can be assessed in a quantitative manner by observing the shape and trends in the 1978/1979 CPT soundings with respect to the recent sounding. Characteristic signatures of the site-specific stratigraphy can be identified and used to confirm that the subsurface conditions between the two soundings are similar. A statistical analysis could be used to provide a more quantitative analysis but this was not deemed a worthwhile investment of time and labor for this project.

The depth to water table is critical to liquefaction-triggering analysis. For this study the depth to water table is based on the measurements made in 1978/1979 by Zhang et al. Water table uncertainty in Moss et al. (2006) was assumed to be a fixed standard deviation of 0.3 m. Because of the uncertainty of the original surface elevation to the current surface elevation and uncertainty in the exact co-location of the previous and current borings, this fixed standard deviation was increased to 0.5 m for this study. It is interesting to note that the water table at the many sites visited have dropped several meters due to regional ground water pumping for agriculture, industrial, and residential use. Rebuilding after the 1976 earthquake has stimulated the regional economy with attendant growth in population and demand for water. Because of the drop in the water table, it is anticipated that liquefaction will be much reduced throughout the region when the next large earthquake occurs.

The critical layer depth is based on the 1978/1979 measurements because this better represents the static stress conditions at the time of the earthquake. There are case histories where the surface elevation has changed slightly since the previous measurements. This is probably due to man-made processes, particularly agricultural practices, since most of the sites are agrarian in nature. For these cases the critical layer trace is matched in the 2007 and 1978/1979 measurements using the characteristic shape of the trace. The 2007 CPT measurements are normalized using the current stress conditions, and the resulting normalized resistance is used to represent the soil resistance at the time of the earthquake.

The magnitude of the event was measured using surface waves at M_s=7.8 using the relationships presented in Heaton et al. (1986). Converting surface wave magnitude to moment magnitude results in M_w=7.89. Uncertainty from the moment magnitude was based on methods found in Moss et al. (2006).

5 Tangshan Case Histories

The case histories are shown in Appendix A as two pages for each site. These pages contain the pertinent calculations for the cyclic stress ratio (CSR) and cyclic resistance ratio (CRR). Appendix B contains a synopsis of the processing techniques excerpted from the Moss et al. (2003) summary report on the worldwide liquefaction database.

The first case history, site T1, shows an English translation of the subsurface logs from Zhou and Zhang (1979). The following tables show the resulting values and GPS coordinates.

Table 5.1 Case history values for Tangshan District sites.

Site	Liquefied?	Data Class	Median Depth Crit. Layer (m)	Median Depth GWT (m)	σ_{vo} (kPa)	σ_{vo}' (kPa)	a_{max} (g)	r_d	CSR	CSR*	q_{c1} (MPa)	R_f (%)	$q_{c1,mod}$ (MPa)
T1 Tangshan District	Y	C	4.75	3.70	83.38	73.07	0.64	0.82	0.39	0.42	6.85	2.27	8.79
T2 Tangshan District	Y	C	7.40	1.25	141.18	80.84	0.53	0.72	0.43	0.46	4.55	3.65	8.14
T6 Tangshan District	Y	C	5.10	1.50	95.70	60.38	0.64	0.80	0.53	0.57	12.37	0.86	12.81
T7 Tangshan District	Y	C	6.40	3.00	117.30	83.95	0.64	0.74	0.43	0.46	5.68	1.56	6.89
T8 Tangshan District	Y	C	5.25	2.20	96.88	66.95	0.64	0.79	0.48	0.51	10.37	0.84	10.77
T10 Tangshan District	Y	C	8.00	1.45	152.38	88.12	0.64	0.66	0.47	0.51	5.86	1.88	7.48
T11 Tangshan District	Y	C	2.10	0.85	38.83	26.56	0.61	0.94	0.54	0.58	6.65	1.36	7.71
T12 Tangshan District	Y	C	3.10	1.55	56.58	41.37	0.58	0.90	0.47	0.50	3.20	1.33	4.17
T13 Tangshan District	Y	C	7.00	1.05	133.88	75.51	0.58	0.72	0.48	0.52	14.12	0.96	14.67
T14 Tangshan District	NA	C	1.80	1.25	31.98	26.58	0.54	0.95	0.40	0.43	17.30	0.77	17.59
T15 Tangshan District	NA	C	2.40	1.00	44.30	30.57	0.27	0.95	0.24	0.26	16.18	0.74	16.40
T3 Tangshan District	NA	C	6.80	1.50	97.16	61.11	0.64	0.72	0.47	0.51	7.17	3.05	10.16
T4 Tangshan District	N	C	3.40	1.10	63.55	40.99	0.64	0.87	0.56	0.61	16.26	1.07	16.96
T5 Tangshan District	N	C	4.50	3.00	80.25	65.54	0.64	0.83	0.42	0.46	12.58	1.06	13.22
T9 Tangshan District	N	C	4.00	1.10	75.25	46.80	0.64	0.86	0.57	0.62	17.16	0.83	17.58
T16 Tangshan District	N	C	7.50	3.50	137.50	98.26	0.26	0.78	0.19	0.20	10.88	0.94	11.24

Table 5.2 Case history values for Lutai District sites.

Site	Liquefied?	Data Class	Median Depth Crit. Layer (m)	Median Depth GWT (m)	σ_{vo} (kPa)	σ_{vo}' (kPa)	a_{max} (g)	r_d	CSR	CSR*	q_{c1} (MPa)	R_f (%)	$q_{c1,mod}$ (MPa)	CSR^*_{cyclic}	CRR_{cyclic}
L1 Lutai District	N?	C	9.75	0.40	189.13	97.40	0.27	0.70	0.24	0.25	3.60	1.71	4.70	0.26	0.24
L2 Lutai District	Y?	ERR	12.50	0.21	243.23	122.66	0.27	0.63	0.22	0.24	3.32	1.31	4.03	0.26	0.17

In Table 5.1 a site that has NA in the Liquefied? column indicates that this site was removed from the database due to some problem with the data or the site. Specific reasons for a site being removed are described and highlighted on the data sheet for that site. The data processing techniques used for this analysis were the techniques developed by Moss et al.

(2003), Appendix B in this report. CSR is the simplified stress ratio, CSR* is the simplified stress ratio that has been corrected to M_w 7.5. In Table 5.2 CSR^*_{cyclic} and CRR_{cyclic} are the terms used in Boulanger and Idriss (2006) to define the cyclic stress ratio and cyclic resistance ratio of clay-like soils. Irrespective of the occurrence of cyclic failure, the coefficient of variation for Lutai L2 exceeds the acceptable criteria for uncertainty, and therefore in the Data Class column there is ERR, which means this would be removed from the liquefaction database.

Table 5.3 GPS coordinates of sites investigated.

Site	Lat	Lon
T1	N39.68541	E118.20774
T2	N39.69860	E118.34025
T3	N39.54396	E118.11207
T4	N39.54745	E118.13343
T5	N39.56293	E118.18641
T6	N39.56293	E118.18641
T7	N39.55876	E118.19913
T8	N39.54255	E118.20538
T9	N39.52287	E118.21356
T10	N39.53253	E118.20206
T11	N39.51628	E118.20302
T12	N39.50315	E118.13576
T13	N39.58128	E118.32427
T14	N39.57511	E118.34322
T15	N39.75145	E118.64855
T16	N39.75266	E118.68437
L1	N39.32172	E117.83062
L2	N39.32503	E117.82849

The summary of case history results are plotted against the probabilistic liquefaction-triggering curves as presented in Moss et al. (2006). Figures 5.1–5.3 show the processed liquefaction and nonliquefaction case histories against the probabilistic triggering curves and the existing worldwide database. The Tangshan District case histories are shown as squares and the Lutai District case histories are shown as triangles. The Tangshan sites agree well with the existing probabilistic triggering curves. The most valuable result from this study and what drove the research effort was acquiring the three nonliquefied sites in the high CSR range. This data region is poorly populated and any high CSR nonliquefied site is extremely useful in constraining the upper portion of the triggering curves. Granted the seismic loading in these cases has been approximated using a fitted attenuation relationship, but the additional uncertainty from this approach has been incorporated into each case history, resulting in confidence in the relative location of the median penetration resistance and cyclic stress ratio values for the site.

The Lutai cases L1 and L2 lie well to the left of the triggering curves, and the liquefaction and nonliquefaction cases are similar in the tip resistance and “apparent” fines content corrected tip resistance. This characteristic has been noticed in cases where there were observed ground deformations similar to liquefaction effects but the soil failed in a cyclic failure mode as discussed by Boulanger and Idriss (2006). This was the situation for case histories from the 1999 Kocaeli, Turkey, Adapazari sites and the 1999 Chi Chi, Taiwan, Wufeng sites. For these two Lutai sites the cyclic resistance ratio CRR was calculated using Boulanger and Idriss (2006). The cyclic failure results present a much more likely scenario than the liquefaction results, and these two cases are deemed as such. Zhou and Guo (1979) observed clay boils at L2, which is physically possible for cyclic failure. Cyclic failure of clay can produce an increase in excess pore pressures that results in ejecta, however the physics of cyclic failure is fundamentally different that the physics of liquefaction. It is conjectured that L2 was experiencing higher static driving shear stresses due to building loads than L1 which led to the manifestation of ground deformations and/or soil ejecta.

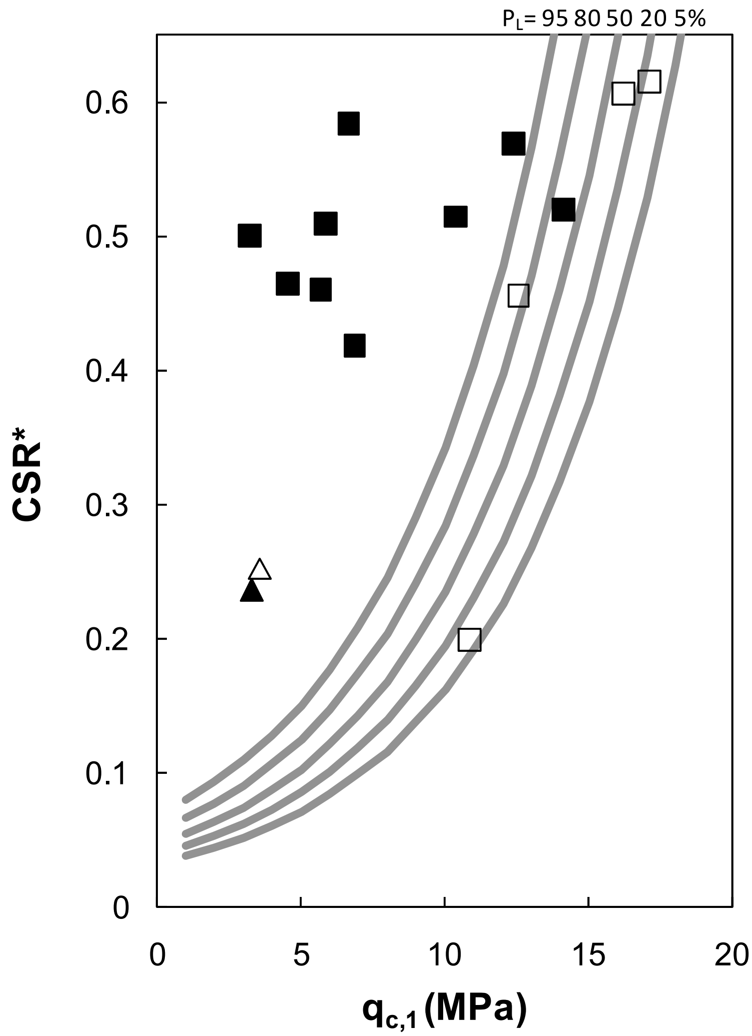

Fig. 5.1 Tangshan District (squares) and Lutai District (triangles) case histories shown against Moss et al. (2006) probabilistic liquefaction-triggering curves. X-axis is cone-tip resistance normalized for effective overburden pressure. Y-axis is cyclic stress ratio corrected for magnitude.

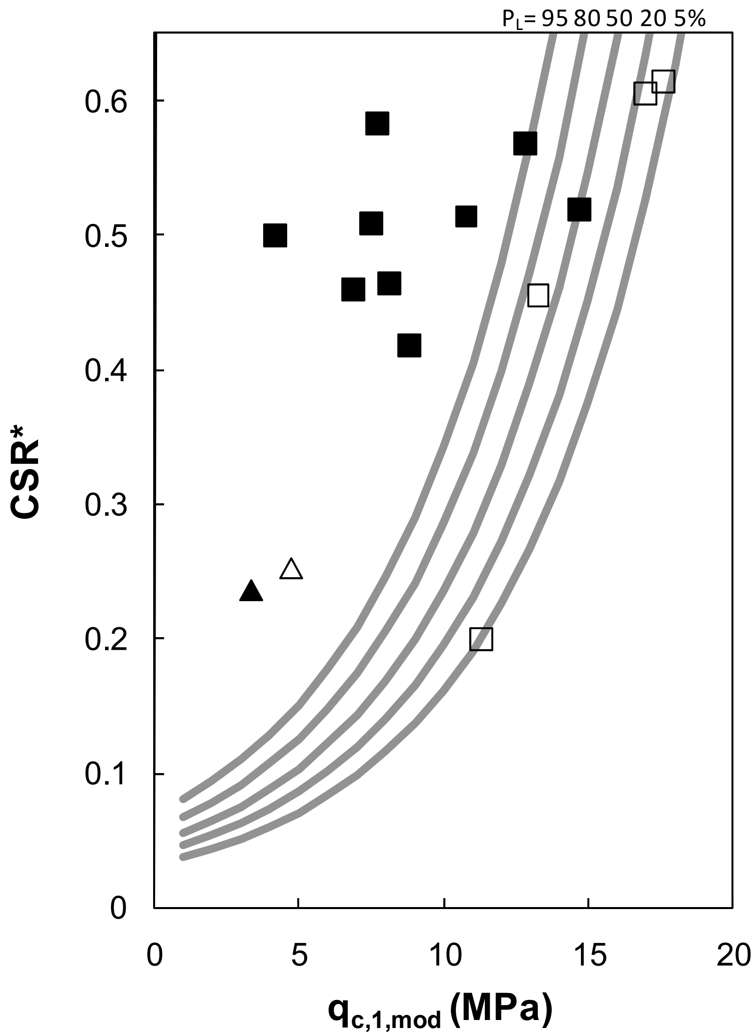

Fig. 5.2 X-axis shows cone-tip resistance modified for "apparent" fines content as measured using friction ratio for proxy.

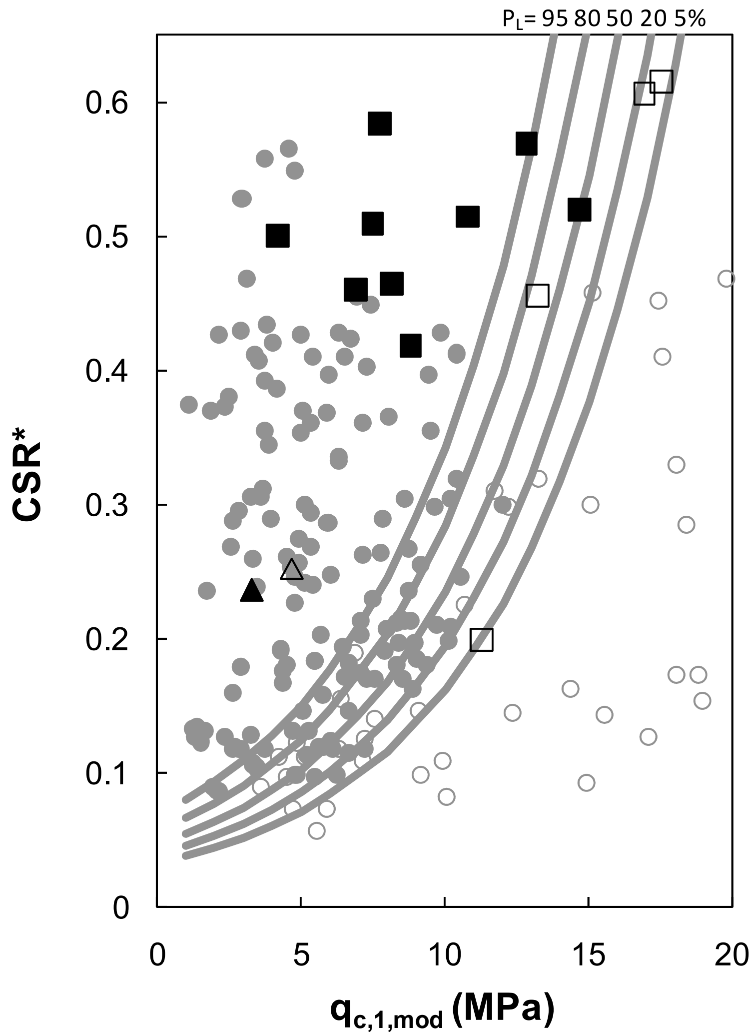

Fig. 5.3 Tangshan District and Lutai District case histories with respect to worldwide CPT case history database (Moss et al. 2003). Tangshan District sites are particularly important for high CSR values and for nonliquefaction cases. Lutai District sites are interpreted as examples of cyclic failure of clay and not liquefaction.

REFERENCES

Atkinson, G. M., and Boore, D. M. (1995). "New ground motion relations for eastern North America." *Bulletin of Seismological Society of America*, 85, 17-30.

Atkinson, G. M., and Boore, D. M. (1997). "Some comparisons between recent ground motion relations." *Seismological Research Letters*, 68, 24-40.

Boulanger, R.W., and Idriss, I.M. (2006). "Liquefaction Susceptibility Criteria for Silts and Clays." *Journal of Geotechnical and Geoenvironmental Engineering*, 132(11).

Dahle, A., Bungum, H., and Dvamme, L. G. (1990). "Attenuation models inferred from intraplate earthquake recordings." *Earthquake Engineering and Structural Dynamics*, 19, 1125-1141.

Liu, H., Housner, G. W., Xie, L., and He, D. (2002). *The Great Tangshan Earthquake of 1976*, Earthquake Engineering Research Library, Cal Tech, Pasadena. http://caltecheerl.library.caltech.edu/353/.

Moss, R. E. S., Collins, B. D., and Whang, D. H. (2005). "Retesting of Liquefaction/Nonliquefaction Case Histories in the Imperial Valley." *Earthquake Spectra*, 21(1), 179-196.

Moss, R. E. S., Seed, R. B., Kayen, R. E., Stewart, J. P., Der Kiureghian, A., and Cetin, K. O. (2006). "Probabilistic Seismic Soil Liquefaction Triggering Using the CPT." *Journal of Geotechnical and Geoenvironmental Engineering*, 132(8).

Moss, R. E. S., Seed, R. B., Kayen, R. E., Stewart, J. P., Youd, T. L., and Tokimatsu, K. (2003). "Field Case Histories for CPT-Based In Situ Liquefaction Potential Evaluation." *Berkeley Geoengineering Research Report No. UCB/GE-2003/04*.

Shengcong, F. and Tatsuoka, F. (1984). "Soil Liquefaction During Haicheng and Tangshan Earthquake in China; a Review." Soils and Foundations, Journal of the Japanese Society of Soil Mechanics and Foundation Engineering, 24(4), 11-29.

Shibata, T., and Teparaska, W. (1988). "Evaluation of Liquefaction Potential of Soils Using Cone Penetration Testing." Soils and Foundations, 28(2), 49-60.

Stewart, J. P., Liu, A. H., and Choi, Y. (2003). "Amplification Factors for Spectral Acceleration in Tectonically Active Regions." *Bulletin of Seismological Society of America*, 93(1), 332-352.

Toro, G. R., Abrahamson, N. A., and Schneider, J. F. (1997). "Model of strong ground motions from earthquakes in central and eastern North America: best estimates and uncertainties." *Seismological Research Letters*, 68, 41-57.

Youd, T. L., Idriss, I. M., Andrus, R. D., Arango, I., Castro, G., Christian, J. T., Dobry, R., Finn, W. D. L., Harder, L. F., Hynes, M. E., Ishihara, K., Koester, J. P., Liao, S. S. C., Marcuson, W. F., III, Martin, G. R., Mitchell, J. K., Moriwaki, Y., Power, M. S., Robertson, P. K., Seed, R. B., and Stokoe, K. H., II,. (2001). "Liquefaction Resistance of Soils: Summary Report from the 1996 NCEER and 1998 NCEER/NSF Workshops on Evaluation of Liquefaction Resistance of Soils." *Journal of Geotechnical and Geoenvironmental Engineering*, 127(10).

Zhou, S. G., and Guo, L. J. (1979). "Liquefaction Investigation in Lutai District." Ministry of Railway, China (in Chinese).

Zhou, S. G., and Zhang, S. M. (1979). "Liquefaction Investigations in Tangshan District." Ministry of Railway, China (in Chinese).

Appendix A: Tangshan Case History Data

Earthquake:	1976 Tanshan, China
Magnitude:	M_S=7.8
Location:	T1 Tangshan District
References:	Zhou & Zhang (1979), Shibata & Teparaska (1988)
Nature of Failure:	Suface evidence

Comments: Dou He River near park, 250 m upstream bridge. Bridge collapse, lateral spreading, and widespread liquefaction documeted by Zhou and Zhang.

Sloping free face at the site 8-10 m high.
CPT measurements 50 m back from top of bank.

Case history previously evaluated Moss et al. (2003)

Depths are inconsistent between logs but traces of tip resistance agree on stratigraphy.

Stress		**Strength**			
Liquefied	Y	N (bpf) from 78/79	9		
Data Class	C	V_S (m/s)			
Critical Layer (m)	4.0 to 5.5				
Median Depth (m)	4.75				
st.dev.	0.08	q_c (MPa)	6.49		
Depth to GWT (m)	3.70	st.dev.	1.42		
st.dev.	0.30	f_s (kPa)	146.99		
σ_v (kPa)	83.38	st.dev.	51.51		
st.dev.	3.04	norm. exp. initial	0.42		
σ_v' (kPa)	73.07	norm. exp. step	0.41		
st.dev.	3.35	norm. exp. Final	0.41		
a_{max} (g)	0.64	difference	0.00		
st.dev.	0.26	C_q, C_f	1.06		
r_d	0.82	C_{thin}	1.00		
st.dev.	0.09	f_{s1} (kPa)	155.17		
M_w	7.89	st.dev.	54.38	**1979 cone data**	
st.dev.	0.10	q_{c1} (MPa)	6.85	q_{c1} (MPa)	5.95
CSR_{eq}	0.39	st.dev.	1.50	st.dev.	1.29
st.dev.	0.16	R_f (%)	2.27		
$C.O.V._{CSR}$	0.42	stdev	0.87		
DWF (Moss et al.)	0.93	del qc	1.94		
DWF (Youd et al.)	0.88	qc1,mod	8.79		
CSR*	0.42	CRR	0.14		

T1 Tangshan District

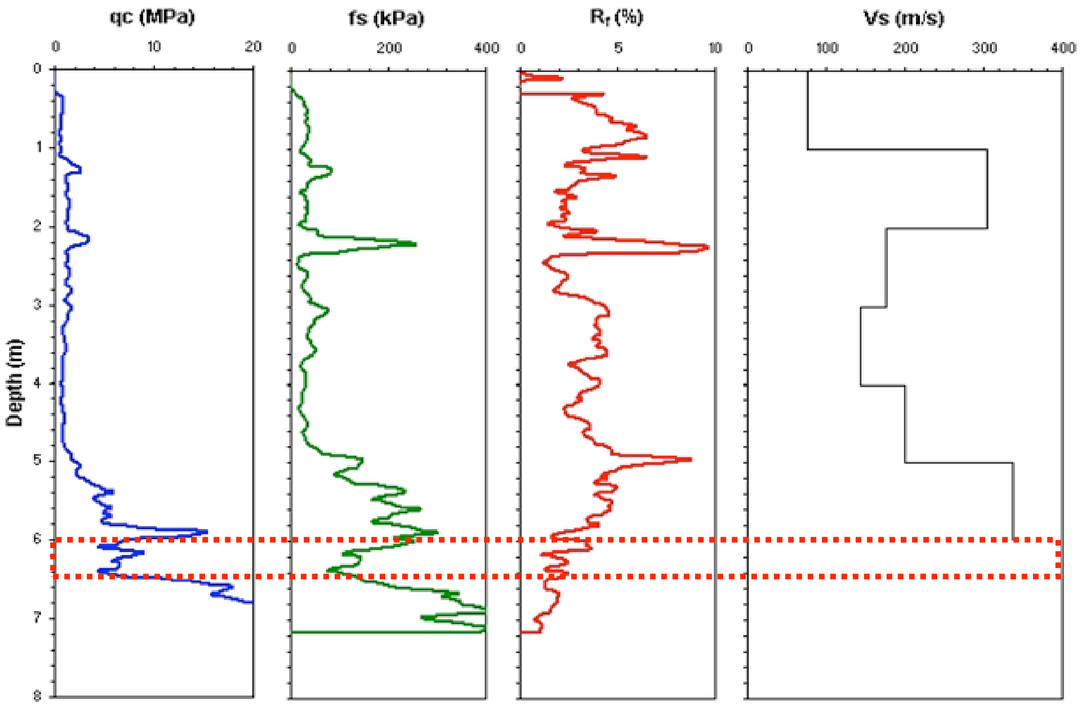

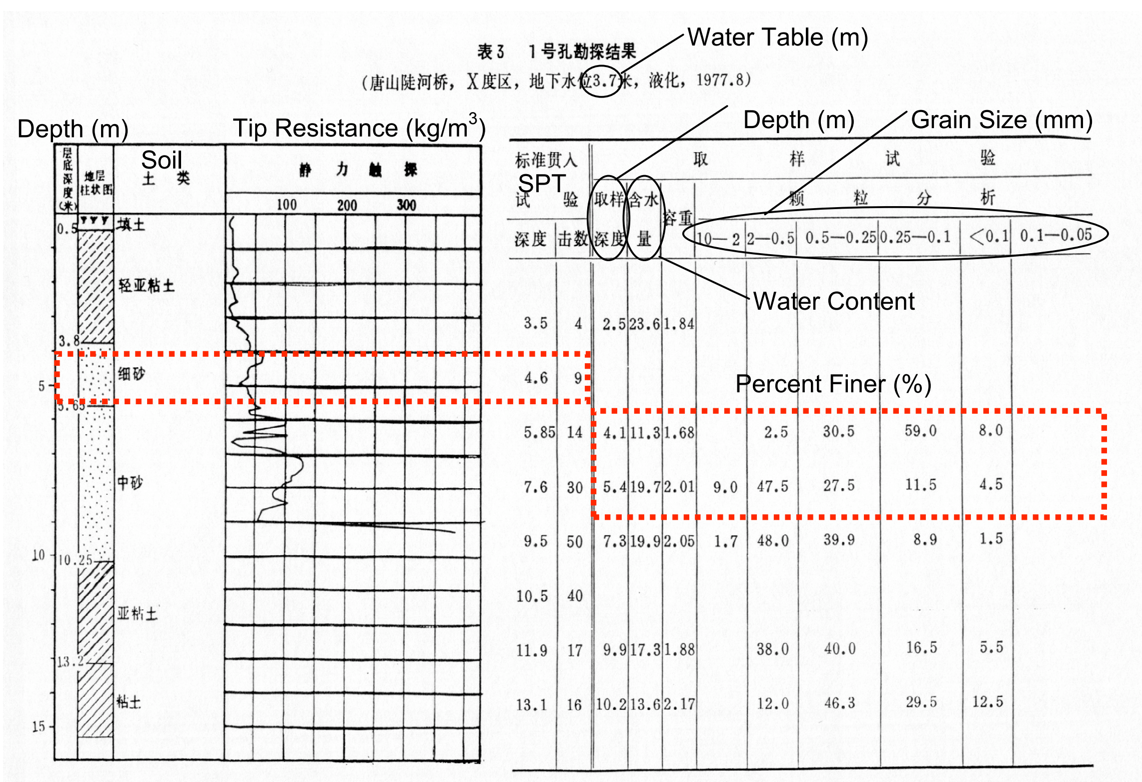

表3 1号孔勘探结果

（唐山陡河桥，Ⅹ度区，地下水位3.7米，液化，1977.8）

标准贯入试验 深度	标准贯入试验 击数	取样深度	含水量	容重	颗粒分析 10—2	2—0.5	0.5—0.25	0.25—0.1	<0.1	0.1—0.05
3.5	4	2.5	23.6	1.84						
4.6	9									
5.85	14	4.1	11.3	1.68		2.5	30.5	59.0	8.0	
7.6	30	5.4	19.7	2.01	9.0	47.5	27.5	11.5	4.5	
9.5	50	7.3	19.9	2.05	1.7	48.0	39.9	8.9	1.5	
10.5	40									
11.9	17	9.9	17.3	1.88		38.0	40.0	16.5	5.5	
13.1	16	10.2	13.6	2.17		12.0	46.3	29.5	12.5	

Earthquake:	1976 Tanshan, China
Magnitude:	M_S=7.8
Location:	T2 Tangshan District
References:	Zhou & Zhang (1979), Shibata & Teparaska (1988)
Nature of Failure:	Suface evidence

Comments: Liquefaction documented by Zhou and Zhang.

Traces match at the stiff later starting at 5.5 m
from 78/79 trace and starting at 7.5 m in 08 trace.
2 m increase differeince in elev (dipping bed?).

Critical layer that corresponds with 1988 and 2003
interpretation has friction ratio that exceeds
database boundaries for liquefiable soil.
Shear wave velocity is high for liquefiable layer?

Case history previously evaluated Moss et al (2003)

Stress		**Strength**			
Liquefied	Y	N (bpf) from 78/79			
Data Class	C	V_S (m/s)	554		
Critical Layer (m)	7.0 to 7.8				
Median Depth (m)	7.40				
st.dev.	0.13	q_c (MPa)	4.17		
Depth to GWT (m)	1.25	st.dev.	1.65		
st.dev.	0.30	f_s (kPa)	152.08		
σ_v (kPa)	141.18	st.dev.	99.47		
st.dev.	4.84	norm. exp. initial	0.42		
σ_v' (kPa)	80.84	norm. exp. step	0.41		
st.dev.	4.68	norm. exp. Final	0.40		
a_{max} (g)	0.53	difference	0.00		
st.dev.	0.21	C_q, C_f	1.09		
r_d	0.72	C_{thin}	1.00		
st.dev.	0.13	f_{s1} (kPa)	165.73		
M_w	7.89	st.dev.	108.39	**1979 cone data**	
st.dev.	0.10	q_{c1} (MPa)	4.55	q_{c1} (MPa)	3.79
CSR_{eq}	0.43	st.dev.	1.80	st.dev.	1.56
st.dev.	0.19	R_f(%)	3.65		
$C.O.V._{CSR}$	0.44	stdev	0.94		
DWF (Moss et al.)	0.93	del qc	3.59		
DWF (Youd et al.)	0.88	qc1,mod	8.14		
CSR*	0.46	CRR	0.11		

T2 Tangshan District

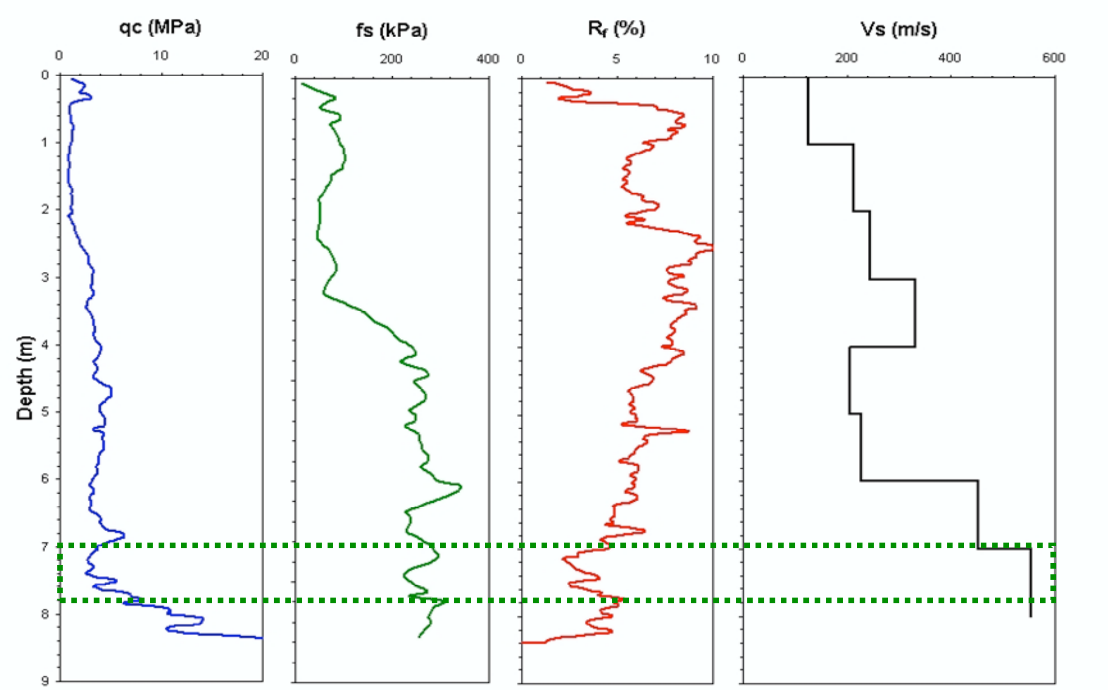

表 4　2号孔勘探结果

（唐山洼里，Ⅹ度区，地下水位1.25米，液化，1977.8）

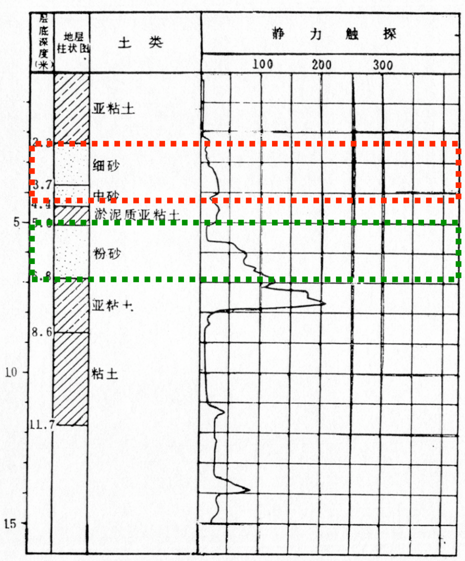

标准贯入试验 深度	标准贯入试验 击数	取样深度	含水量	容重	颗粒分析 10—2	2—0.5	0.5—0.25	0.25—0.1	<0.1	0.1—0.05
2.8	10	2.0	26.3	1.97						
3.8	10	2.8	21.2	2.06		1.5	27	62	9.5	
4.8	11									
5.8	16									
6.15	23	3.8	21.0	2.04		4.2	81.0	14.5	0.3	
6.6	33	5.6	18.8	2.12		3.5	15.5	33.5	47.5	
7.15	7	6.2	19.1	2.04		4.5	26.5	30.5	38.5	

Earthquake:	1976 Tanshan, China
Magnitude:	M_S=7.8
Location:	T3 Tangshan District
References:	Zhou & Zhang (1979), Shibata & Teparaska (1988)
Nature of Failure:	No surface evidence

Comments:

Non-liquefaction documented by Zhou and Zhang.

CPT located approx. 140 m from SASW testing.

Next to coal facility developed since earthquake.
CPT started 1 m deep in hand augered hole.

Site conditions appear to have been altered since the earthquake. CPT traces are mismatched, case history eliminated.

Stress		**Strength**	
Liquefied	NA	Soil Class	
Data Class	C	LL	
Critical Layer (m)	6.3 to 7.3	PI	
Median Depth (m)	6.80		
st.dev.	0.17	q_c (MPa)	5.96
Depth to GWT (m)	1.50	st.dev.	0.55
st.dev.	0.30	f_s (kPa)	181.86
σ_v (kPa)	97.16	st.dev.	50.42
st.dev.	3.49	norm. exp. initial	0.39
σ_v' (kPa)	61.11	norm. exp. step	0.37
st.dev.	3.46	norm. exp. Final	0.37
a_{max} (g)	0.64	difference	0.00
st.dev.	0.26	C_q, C_f	1.20
r_d	0.72	C_{thin}	1.00
st.dev.	0.12	f_{s1} (kPa)	218.52
M_w	7.89	st.dev.	60.58
st.dev.	0.10	q_{c1} (MPa)	7.17
CSR_{eq}	0.47	st.dev.	0.67
st.dev.	0.21	R_f(%)	3.05
C.O.V.$_{CSR}$	0.44	stdev	0.95
DWF (Moss et al.)	0.93	del qc	3.00
DWF (Youd et al.)	0.88	qc1,mod	10.16
CSR*	0.51	CRR	0.17

T3 Tangshan District

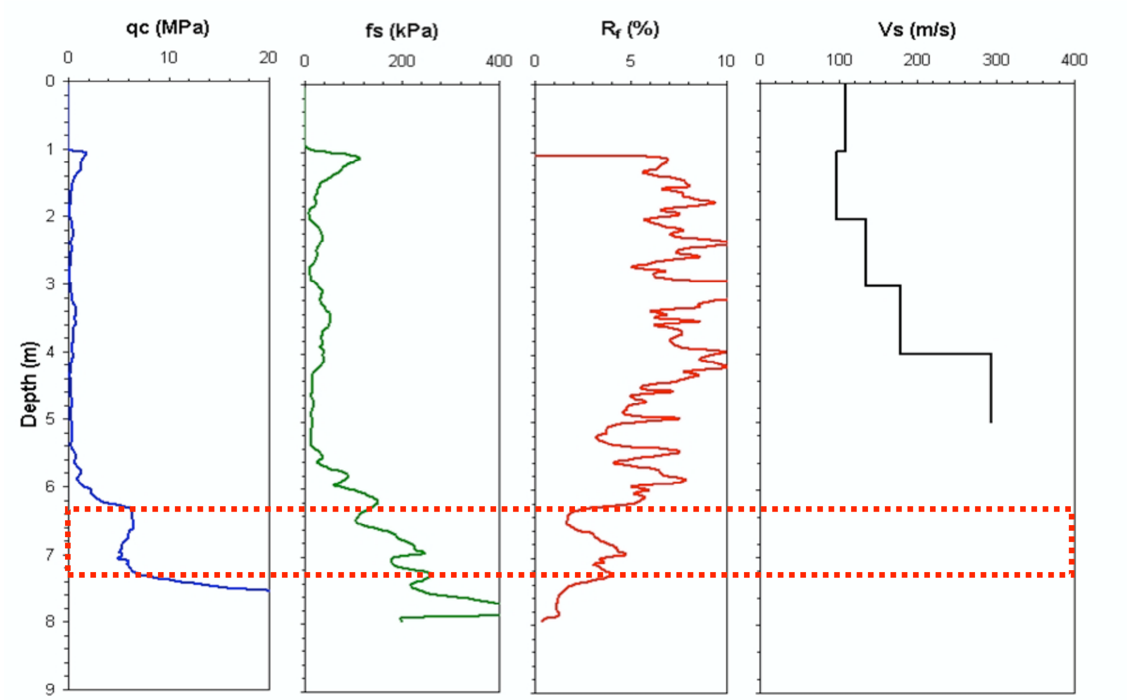

表 5　3 号孔勘探结果

(丰南县胥各庄，X度区，地下水位1.5米，未液化，1978.10)

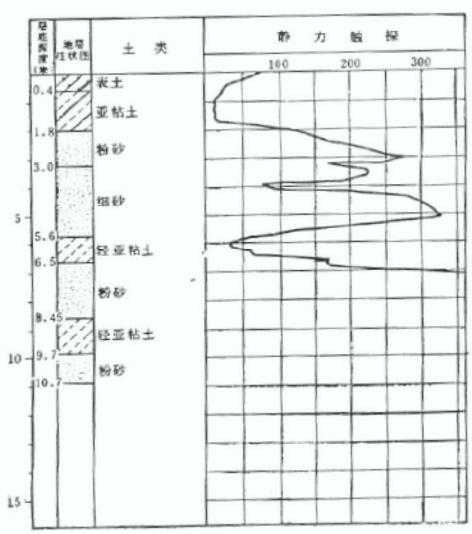

标准贯入试验		取样试验			颗粒分析					
深度	击数	取样深度	含水量	容重	10—2	2—0.5	0.5—0.25	0.25—0.1	0.1—0.05	<0.05
2.0	15	1.7				1	6	19	54	20
3.4	29	3.1			1	18	26	36	14	5
4.4	22	4.1				4	27	46	16	7
5.3	44	5.1				1	30	52	13	4
6.3	14	6.0				3	11	15	45	26
7.8	50	7.6					1	9	77	13
10.3	32	10				1	3	7	55	34

Earthquake:	1976 Tanshan, China
Magnitude:	M_S=7.8
Location:	T9 Tangshan District
References:	Zhou & Zhang (1979), Shibata & Teparaska (1988)
Nature of Failure:	
Comments:	Nonliquefaction documented by Zhou and Zhang.

Two soundings performed adjacent to each other.
T9-1 was 1.2m lower relative to T9-2.

Samples taken at 3m classified as SM

V_S profile in T9-1 appears to be incorrect.

Stress		**Strength**	
Liquefied	N	N (bpf) from 78/79	13
Data Class	C	V_S (m/s)	181
Critical Layer (m)	3.0 to 5.0		
Median Depth (m)	4.00		
st.dev.	0.33	q_c (MPa)	12.06
Depth to GWT (m)	1.10	st.dev.	2.94
st.dev.	0.30	f_s (kPa)	100.56
σ_v (kPa)	75.25	st.dev.	26.46
st.dev.	6.84	norm. exp. initial	0.49
σ_v' (kPa)	46.80	norm. exp. step	0.46
st.dev.	3.81	norm. exp. Final	0.46
a_{max} (g)	0.64	difference	0.00
st.dev.	0.26	C_q, C_f	1.42
r_d	0.86	C_{thin}	1.00
st.dev.	0.08	f_{s1} (kPa)	143.12
M_w	7.89	st.dev.	37.67
st.dev.	0.10	q_{c1} (MPa)	17.16
CSR_{eq}	0.57	st.dev.	4.18
st.dev.	0.24	R_f(%)	0.83
C.O.V.$_{CSR}$	0.43	stdev	0.15
DWF (Moss et al.)	0.93	del qc	0.42
DWF (Youd et al.)	0.88	qc1,mod	17.58
CSR*	0.62	CRR	0.71

T4 Tangshan District

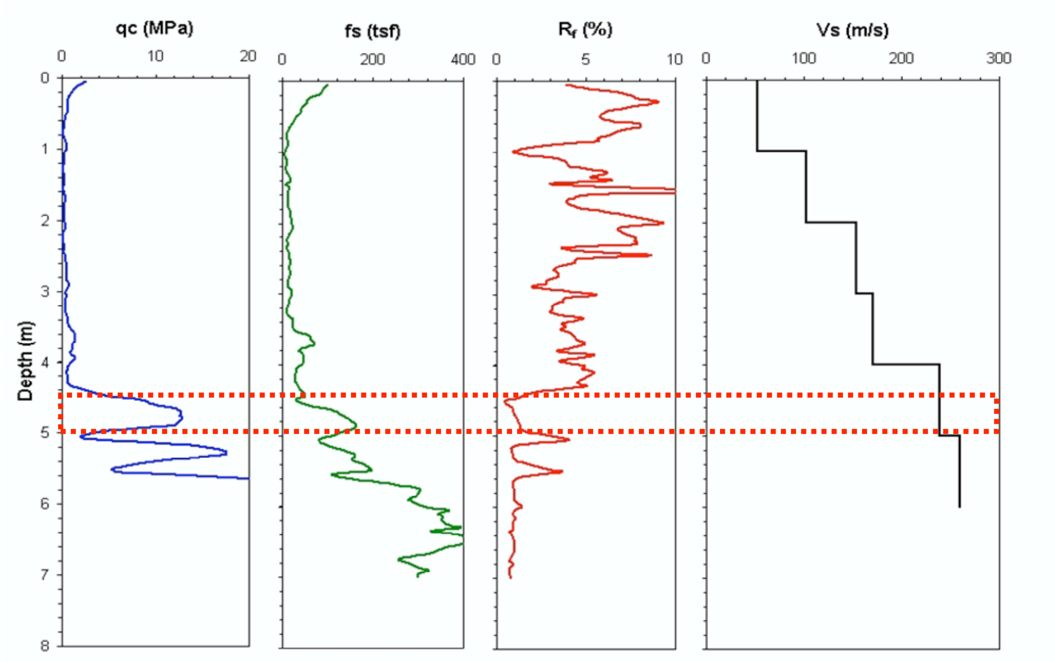

表6　4号孔勘探结果

(丰南县高庄子，Ⅹ度区，地下水位1.1米，未液化，1978.9)

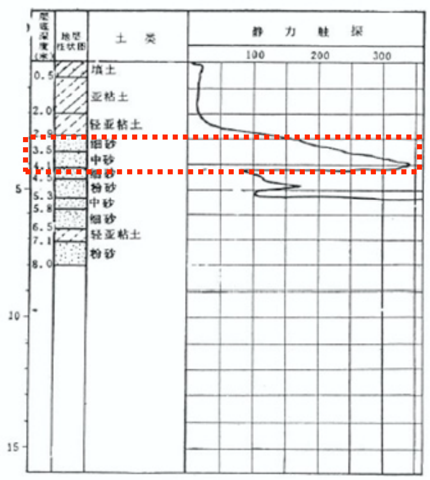

标准贯入试验		取样试验								
		取样深度	含水量	容重	颗粒分析					
深度	击数				10—2	2—0.5	0.5—0.25	0.25—0.1	0.1—0.05	<0.05
3.7	27	3.5				30	48	16	6	
4.8	27	4.5				1	5	43	37	14
5.9	50	5.7				4	21	56	16	3
7.9	48	7.5					1	13	73	13

Earthquake:	1976 Tanshan, China
Magnitude:	M_S=7.8
Location:	T5 Tangshan District
References:	Zhou & Zhang (1979), Shibata & Teparaska (1988)
Nature of Failure:	

Comments: Nonliquefaction documented by Zhou and Zhang.

Thin layer correction was applied to the entire layer 800mm thickiness and a ratio tip resistance of 5.

CPT soil sample taken at 5m

Silty clay soil transitioning to fine/med sand.

Critical layer differs from 1988 interpretation.

Stress		**Strength**	
Liquefied	N	N (bpf) from 78/79	21
Data Class	C	V_S (m/s)	393
Critical Layer (m)	4.0 to 5.0		
Median Depth (m)	4.50		
st.dev.	0.17	q_c (MPa)	7.76
Depth to GWT (m)	3.00	st.dev.	1.59
st.dev.	0.30	f_s (kPa)	98.72
σ_v (kPa)	80.25	st.dev.	19.51
st.dev.	3.97	norm. exp. initial	0.49
σ_v' (kPa)	65.54	norm. exp. step	0.45
st.dev.	3.29	norm. exp. Final	0.45
a_{max} (g)	0.64	difference	0.00
st.dev.	0.26	C_q, C_f	1.35
r_d	0.83	C_{thin}	1.20
st.dev.	0.08	f_{s1} (kPa)	133.42
M_w	7.89	st.dev.	26.37
st.dev.	0.10	q_{c1} (MPa)	12.58
CSR_{eq}	0.42	st.dev.	2.15
st.dev.	0.18	R_f(%)	1.06
C.O.V.$_{CSR}$	0.42	stdev	0.30
DWF (Moss et al.)	0.93	del qc	0.64
DWF (Youd et al.)	0.88	qc1,mod	13.22
CSR*	0.46	CRR	0.33

T5 Tangshan District

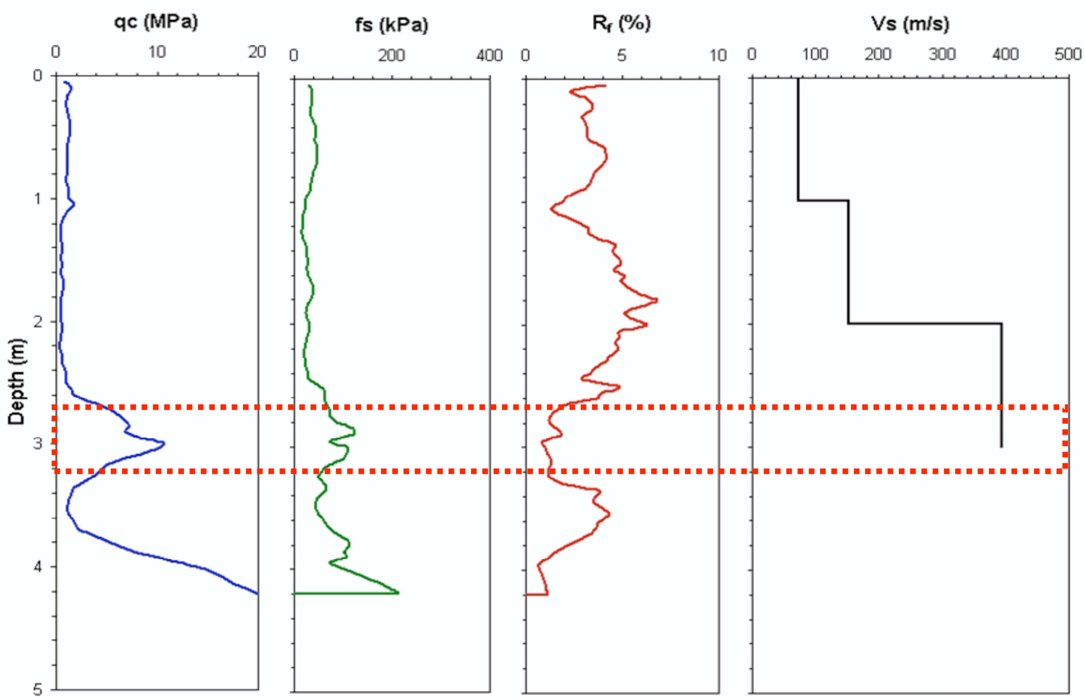

表 7　5 号孔勘探结果

（唐山良种场，X度区，地下水位3.0米，未液化，1977.8）

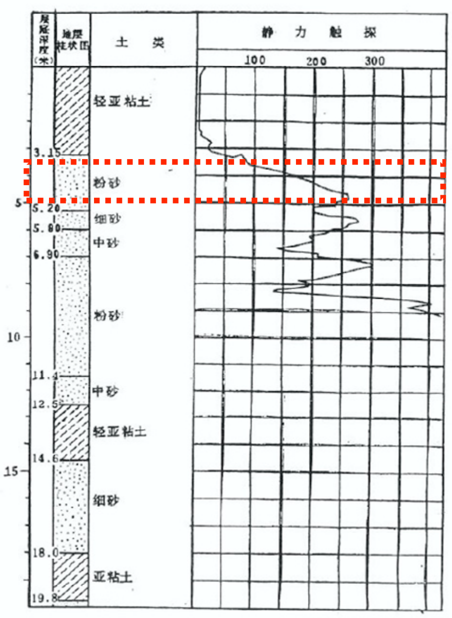

标准贯入试验		取样试验								
		取样深度	含水量	容重	颗粒分析					
深度	击数				10—2	2—0.5	0.5—0.25	0.25—0.1	<0.1	0.1—0.05
3.8	21	2.1		2.09						
4.8	36	4.0	24.2	2.03						
5.2	50	5.1	20.4	2.08						
5.8	50	6.6	20.3	2.05						
6.3	38	7.5	24.7	2.00		2.7	4.8	65.6	26.9	
6.9	44	9.6	29.3	1.98		4.8	14.0	32.8	48.4	
7.3	50	10.5	24.2	2.00			3.4	31.8	64.8	
7.8	46	11.5	18.4	2.10	1.1	36.5	26.0	21.1	15.3	
8.3	31	13.9		2.20						
8.8	50	15.0	15.6	2.11	0.9	3.7	29.7	45.9	19.8	
9.3	50	16.1	20.4	2.08						
9.8	50	17.0	19.9	2.05		2.5	41.5	50.4	5.6	
10.8	50									
12.7	50									
14.4	26									
16.3	50									
17.4	50									
18.3	13									

Earthquake:	1976 Tanshan, China
Magnitude:	M_S=7.8
Location:	T6 Tangshan District
References:	Zhou & Zhang (1979), Shibata & Teparaska (1988)
Nature of Failure:	Surface evidence

Comments: Liquefaction documented by Zhou and Zhang.

Approx. 130m from intersection where 78/79 measurements and SASW measurements were performed.

Interlayered silt, silty sand, and fine sand.

Hand auger samples at 2.5 and 3.1m.

Stress		**Strength**	
Liquefied	Y	N (bpf) from 78/79	15
Data Class	C	V_S (m/s)	191
Critical Layer (m)	4.4 to 5.8		
Median Depth (m)	5.10		
st.dev.	0.23	q_c (MPa)	7.68
Depth to GWT (m)	1.50	st.dev.	1.21
st.dev.	0.30	f_s (kPa)	66.12
σ_v (kPa)	95.70	st.dev.	15.93
st.dev.	5.24	norm. exp. initial	0.52
σ_v' (kPa)	60.38	norm. exp. step	0.48
st.dev.	3.72	norm. exp. Final	0.48
a_{max} (g)	0.64	difference	0.00
st.dev.	0.26	C_q, C_f	1.61
r_d	0.80	C_{thin}	1.00
st.dev.	0.09	f_{s1} (kPa)	106.56
M_w	7.89	st.dev.	25.67
st.dev.	0.10	q_{c1} (MPa)	12.37
CSR_{eq}	0.53	st.dev.	1.95
st.dev.	0.22	R_f(%)	0.86
C.O.V.$_{CSR}$	0.42	stdev	0.31
DWF (Moss et al.)	0.93	del qc	0.44
DWF (Youd et al.)	0.88	qc1,mod	12.81
CSR*	0.57	CRR	0.31

T6 Tangshan District

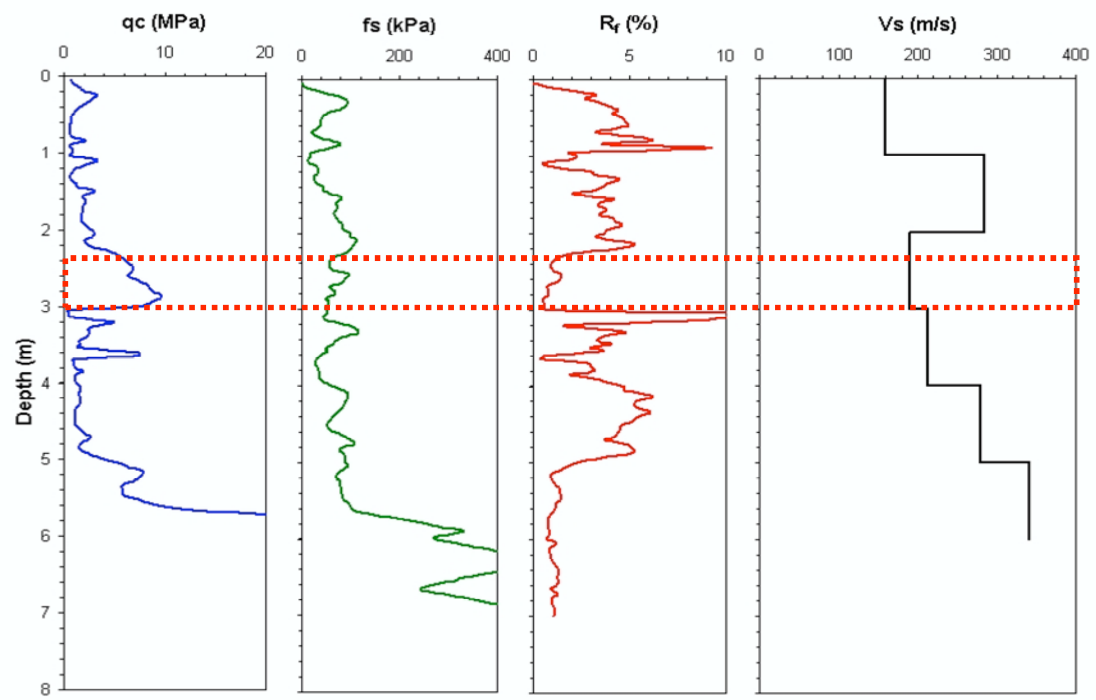

表 8　6号孔勘探结果

（唐山西大夫坨，Ⅹ度区，地下水位1.5米，液化，1977.8）

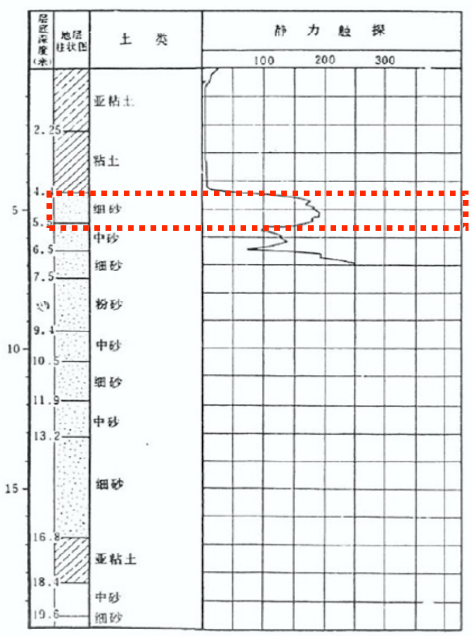

标准贯入试验		取样试验								
					颗粒分析					
深度	击数	取样深度	含水量	容重	10—2	2—0.5	0.5—0.25	0.25—0.1	<0.1	0.1—0.05
4.65	15	3.1		1.85						
5.65	32	5.0	21.0	2.03		2.2	31.8	61.6	4.4	
6.65	29	5.5	18.8	2.03		5.6	48.2	41.0	5.2	
7.65	42	6.5	14.6	2.12		2.0	25.1	51.0	21.9	
8.65	25	7.5	25.5	1.96			12.7	48.9	38.4	32.5
9.65	50	8.6	24.2	1.98			7.7	38.5	53.8	47.6
10.65	38	9.6	18.6	2.06		15.2	47.5	27.4	9.9	
11.8	47	10.7	21.3	2.04			3.5	65.6	29.9	24.7
12.65	50	11.6	22.3	2.02		1.1	9.2	56.0	33.7	31.9
13.65	28	12.5	17.1	2.08		24.9	59.7	11.0	4.4	
14.65	50	13.5	10.7	2.25		8.9	41.0	34.2	15.9	7.8
15.65	50	14.7	20.5	2.09			5.4	75.8	18.8	16.8
16.65	50	15.5	20.0	2.08		1.3	39.2	48.7	10.8	
19.0	50	16.5	19.6	2.10			15.9	74.6	9.5	
20.0	50	18.8	15.5	2.17		8.6	54.7	31.3	5.4	
		19.9	19.7	2.00			2.2	84.6	13.2	

Earthquake:	1976 Tanshan, China
Magnitude:	M_S=7.8
Location:	T7 Tangshan District
References:	Zhou & Zhang (1979), Shibata & Teparaska (1988)
Nature of Failure:	Surface evidence
Comments:	Liquefaction documented by Zhou and Zhang.

Stress		**Strength**	
Liquefied	Y	N (bpf) from 78/79	12
Data Class	C	V_S (m/s)	173
Critical Layer (m)	5.3 to 7.5		
Median Depth (m)	6.40		
st.dev.	0.37	q_c (MPa)	4.27
Depth to GWT (m)	3.00	st.dev.	0.29
st.dev.	0.30	f_s (kPa)	66.59
σ_v (kPa)	117.30	st.dev.	21.48
st.dev.	7.75	norm. exp. initial	0.51
σ_v' (kPa)	83.95	norm. exp. step	0.48
st.dev.	4.49	norm. exp. Final	0.47
a_{max} (g)	0.64	difference	0.00
st.dev.	0.26	C_q, C_f	1.33
r_d	0.74	C_{thin}	1.00
st.dev.	0.11	f_{s1} (kPa)	88.53
M_w	7.89	st.dev.	28.55
st.dev.	0.10	q_{c1} (MPa)	5.68
CSR_{eq}	0.43	st.dev.	0.38
st.dev.	0.19	R_f(%)	1.56
C.O.V.$_{CSR}$	0.44	stdev	0.62
DWF (Moss et al.)	0.93	del qc	1.20
DWF (Youd et al.)	0.88	qc1,mod	6.89
CSR*	0.46	CRR	0.11

T7 Tangshan District

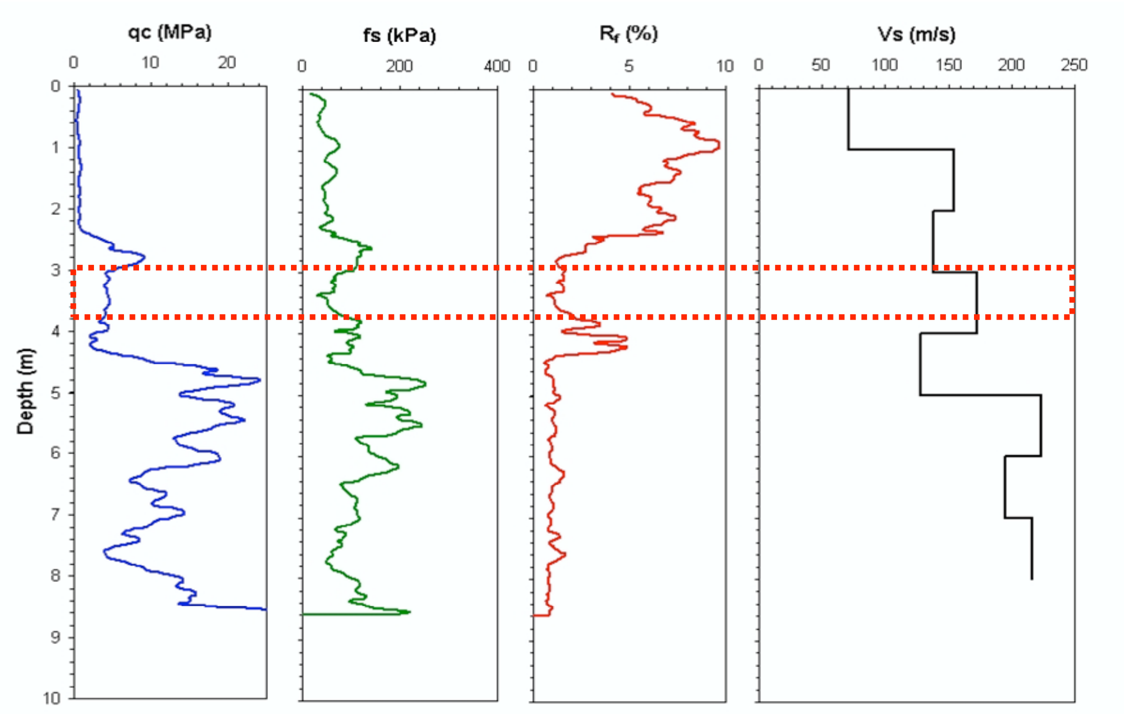

表 9　7 号孔勘探结果

（唐山东大夫坨，X 度区，地下水位3.0米，液化，1977.8）

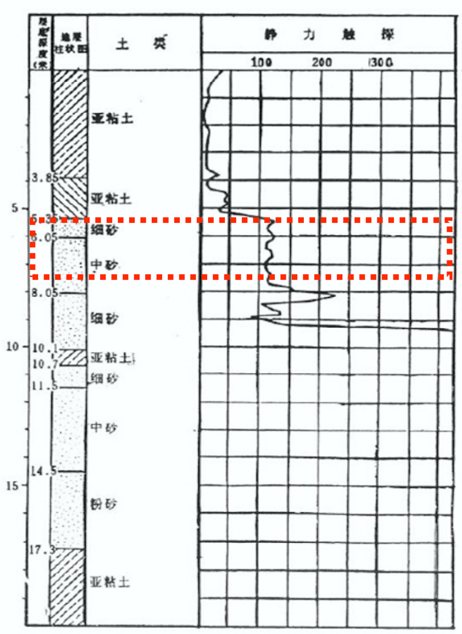

标准贯入试验		取样试验								
					颗粒分析					
深度	击数	取样深度	含水量	容重	10—2	2—0.5	0.5—0.25	0.25—0.1	<0.1	0.1—0.05
6.3	12	6.4	22.3	2.03			72.4	26.4	1.2	
7.4	28	7.3	19.5	2.06	2.6	22.5	52.2	21.0	1.1	
8.4	42	8.3	21.3	2.07			34.4	55.6	10.0	
9.3	50	9.3	12.2	2.19		6.5	38.1	31.3	23.8	16.4
10.3	18	11.3	20.3	2.09		9.9	34.4	41.9	13.8	
11.45	48	12.2	19.1	2.01		7.1	46.4	30.7	15.8	12.9
12.3	50	13.3	17.0	2.10		2.7	46.0	37.8	13.5	11.3
13.3	50	14.3	17.3	2.11	1.4	14.9	38.2	41.2	4.3	
14.3	50	15.3	27.5	1.92				4.1	95.9	77.0
16.55	50									
17.55	11									

Earthquake:	1976 Tanshan, China
Magnitude:	M_S=7.8
Location:	T8 Tangshan District
References:	Zhou & Zhang (1979), Shibata & Teparaska (1988)
Nature of Failure:	Surface evidence
Comments:	Liquefaction documented by Zhou and Zhang. Survivors reported wide spread liquefaction with sand blows issuing white sand ejecta.

Stress		**Strength**			
Liquefied	Y	N (bpf) from 78/79	5.5		
Data Class	C	V_S (m/s)	187		
Critical Layer (m)	4.5 to 6.0				
Median Depth (m)	5.25				
st.dev.	0.25	q_c (MPa)	9.08		
Depth to GWT (m)	2.20	st.dev.	2.95		
st.dev.	0.30	f_s (kPa)	76.24		
σ_v (kPa)	96.88	st.dev.	26.03		
st.dev.	5.49	norm. exp. initial	0.51		
σ_v' (kPa)	66.95	norm. exp. step	0.50		
st.dev.	3.72	norm. exp. Final	0.50		
a_{max} (g)	0.64	difference	0.00		
st.dev.	0.26	C_q, C_f	1.14		
r_d	0.79	C_{thin}	1.00		
st.dev.	0.10	f_{s1} (kPa)	87.07		
M_w	7.89	st.dev.	29.73	**1979 cone data**	
st.dev.	0.10	q_{c1} (MPa)	10.37	q_{c1} (MPa)	8.03
CSR_{eq}	0.48	st.dev.	3.37	st.dev.	3.68
st.dev.	0.20	R_f(%)	0.84		
C.O.V.$_{CSR}$	0.42	stdev	0.36		
DWF (Moss et al.)	0.93	del qc	0.40		
DWF (Youd et al.)	0.88	qc1,mod	10.77		
CSR*	0.51	CRR	0.21		

T8 Tangshan District

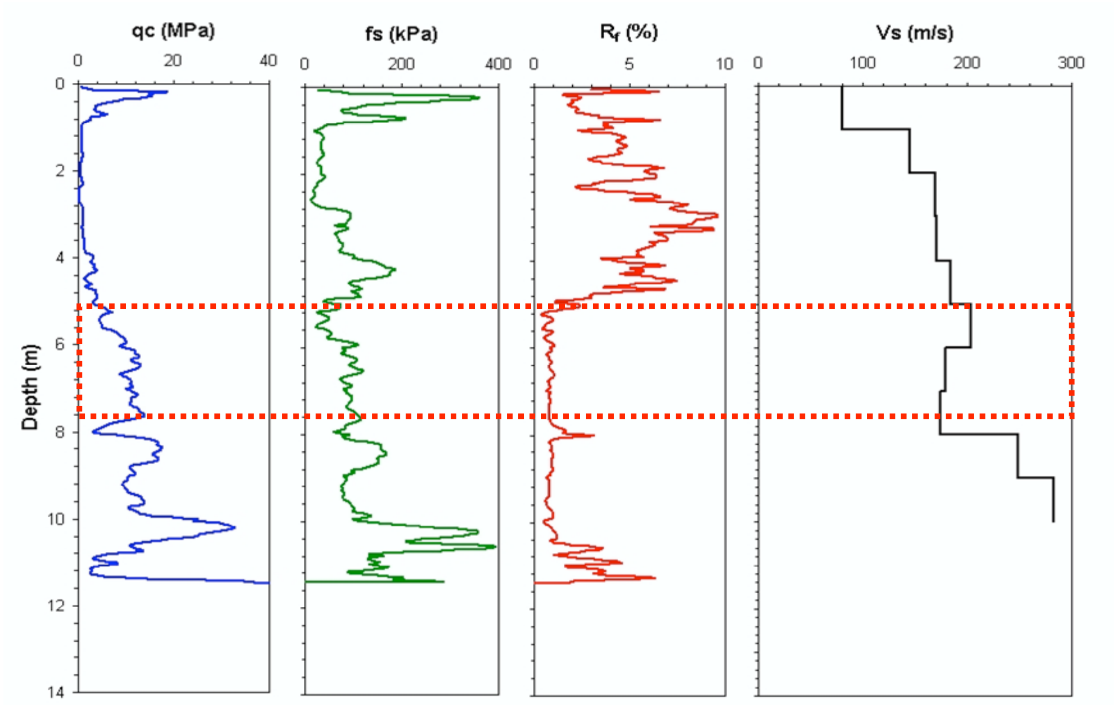

表10　8号孔勘探结果

（唐山老边庄，Ⅹ度区，地下水位2.2米，液化，1977.8）

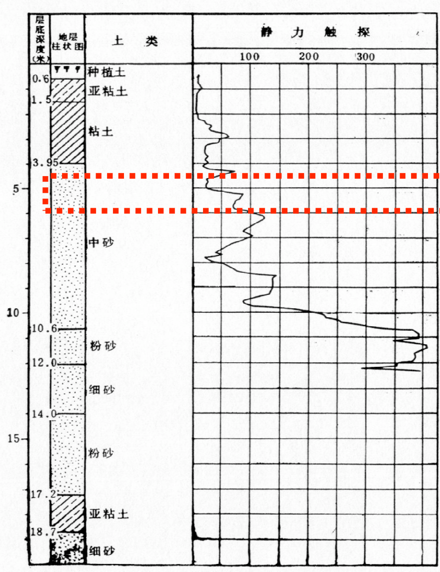

标准贯入试验		取样试验								
		取样深度	含水量	容重	颗粒分析					
深度	击数				10—2	2—0.5	0.5—0.25	0.25—0.1	<0.1	0.1—0.05
3.6	12	2.0	32.1	1.83						
4.65	8	4.4	19.6	2.05		36.7	57.2	2.5	3.6	
5.65	3	6.2	21.1	2.06		22.0	72.0	5.3	0.7	
6.65	11	7.1	19.6	2.05	1.6	54.0	38.7	2.9	2.8	
7.65	18	8.1	22.4	1.90	1.1	34.1	53.8	9.4	1.6	
8.64	16	9.9	19.6	1.93			0.4	55.5	44.0	41.7
9.55	15	10.8	24.9	1.88			2.0	63.5	34.5	2.8
10.5	50	11.5	22.6	2.01		1.0	34.1	54.9	10.0	
11.1	50	12.6	18.6	2.10		2.1	21.7	63.0	13.2	
11.55	50	13.5	19.6	2.09			3.1	42.1	54.8	46.6
12.5	50	14.5	24.9	2.10		10.1	21.8	44.7	23.4	19.1
13.5	50	15.5	17.5	2.07			15.9	57.3	26.8	24.1
14.5	50	17.9	16.5	2.15		4.4	45.5	38.0	12.1	
15.5	50	19.5	19.1	1.99		26.1	64.6	8.4	0.9	
16.5	50									
17.5	30									
18.5	50									
19.6	50									

Earthquake: 1976 Tanshan, China
Magnitude: M_S=7.8
Location: T9 Tangshan District
References: Zhou & Zhang (1979), Shibata & Teparaska (1988)
Nature of Failure:

Comments: Nonliquefaction documented by Zhou and Zhang.

Two soundings performed adjacent to each other.
T9-1 was 1.2m lower relative to T9-2.

Samples taken at 3m classified as SM

V_S profile in T9-1 appears to be incorrect.

Stress		**Strength**	
Liquefied	N	N (bpf) from 78/79	13
Data Class	C	V_S (m/s)	181
Critical Layer (m)	3.0 to 5.0		
Median Depth (m)	4.00		
st.dev.	0.33	q_c (MPa)	12.06
Depth to GWT (m)	1.10	st.dev.	2.94
st.dev.	0.30	f_s (kPa)	100.56
σ_v (kPa)	75.25	st.dev.	26.46
st.dev.	6.84	norm. exp. initial	0.49
σ_v' (kPa)	46.80	norm. exp. step	0.46
st.dev.	3.81	norm. exp. Final	0.46
a_{max} (g)	0.64	difference	0.00
st.dev.	0.26	C_q, C_f	1.42
r_d	0.86	C_{thin}	1.00
st.dev.	0.08	f_{s1} (kPa)	143.12
M_w	7.89	st.dev.	37.67
st.dev.	0.10	q_{c1} (MPa)	17.16
CSR_{eq}	0.57	st.dev.	4.18
st.dev.	0.24	R_f(%)	0.83
C.O.V.$_{CSR}$	0.43	stdev	0.15
DWF (Moss et al.)	0.93	del qc	0.42
DWF (Youd et al.)	0.88	qc1,mod	17.58
CSR*	0.62	CRR	0.71

T9 Tangshan District

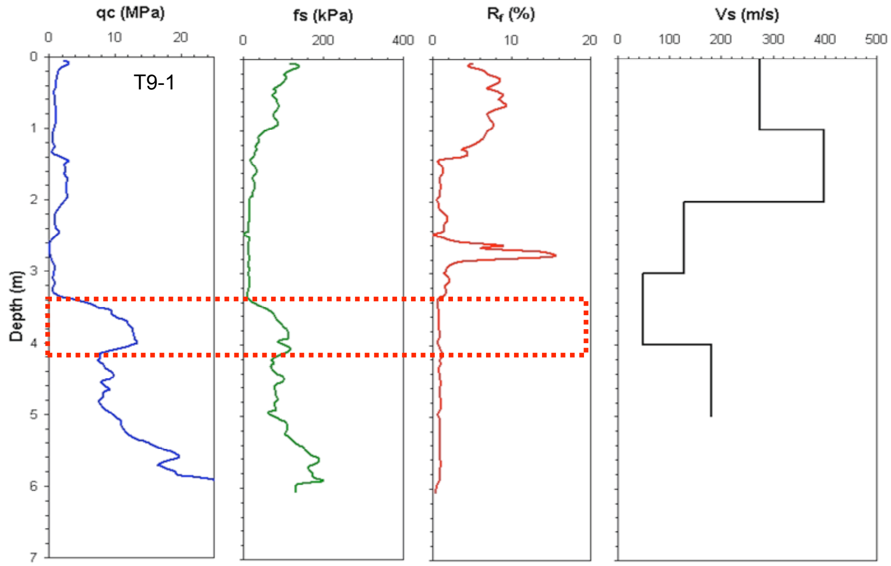

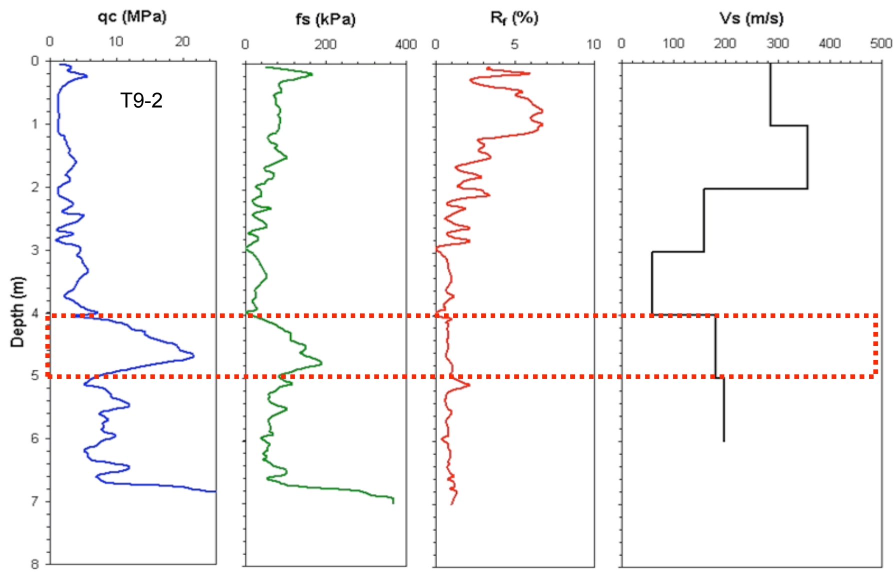

表11　9号孔勘探结果

(丰南县稻地，X度区，地下水位1.1米，未液化，1978.9)

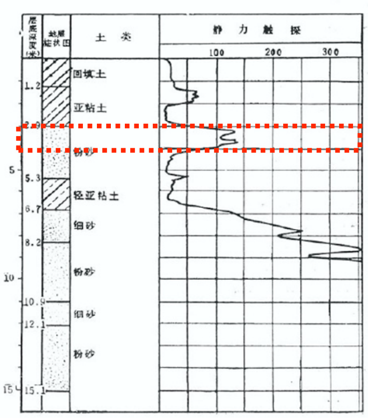

标准贯入试验		取样试验								
		取样	含水	容重	颗粒分析					
深度	击数	深度	量		10—2	2—0.5	0.5—0.25	0.25—0.1	0.1—0.05	<0.05
4.0	13	3.8					3	69	21	7
7.0	31	6.7				14	19	47	14	6
7.6	30	7.5				6	19	56	14	5
8.4	27	8.2				3	9	48	29	11
9.1	41	9.0				1	4	52	39	4
10.2	48	10.1			1	7	15	54	19	4
11.8	50	11.8			3	10	23	45	15	4
13.9	50	13.8				3	13	55	24	5
14.6	50	14.5				2	13	57	20	8

Earthquake: 1976 Tanshan, China
Magnitude: M_S=7.8
Location: T10 Tangshan District
References: Zhou & Zhang (1979), Shibata & Teparaska (1988)
Nature of Failure: Liquefaction

Comments: Liquefaction documented by Zhou and Zhang.

Stress		**Strength**			
Liquefied	Y	N (bpf) from 78/79	10.3		
Data Class	C	V_S (m/s)	148		
Critical Layer (m)	6.5 to 9.5				
Median Depth (m)	8.00				
st.dev.	0.50	q_c (MPa)	4.95		
Depth to GWT (m)	1.45	st.dev.	2.23		
st.dev.	0.30	f_s (kPa)	93.01		
σ_v (kPa)	152.38	st.dev.	32.21		
st.dev.	10.68	norm. exp. initial	0.47		
σ_v' (kPa)	88.12	norm. exp. step	0.45		
st.dev.	6.01	norm. exp. Final	0.45		
a_{max} (g)	0.64	difference	0.00		
st.dev.	0.26	C_q, C_f	1.18		
r_d	0.66	C_{thin}	1.00		
st.dev.	0.14	f_{s1} (kPa)	110.02		
M_w	7.89	st.dev.	38.10	**1979 cone data**	
st.dev.	0.10	q_{c1} (MPa)	5.86	qc1 (MPa)	5.90
CSR_{eq}	0.47	st.dev.	2.63	st.dev.	1.01
st.dev.	0.22	R_f(%)	1.88		
$C.O.V._{CSR}$	0.46	stdev	0.89		
DWF (Moss et al.)	0.93	del qc	1.62		
DWF (Youd et al.)	0.88	qc1,mod	7.48		
CSR*	0.51	CRR	0.11		

T10 Tangshan District

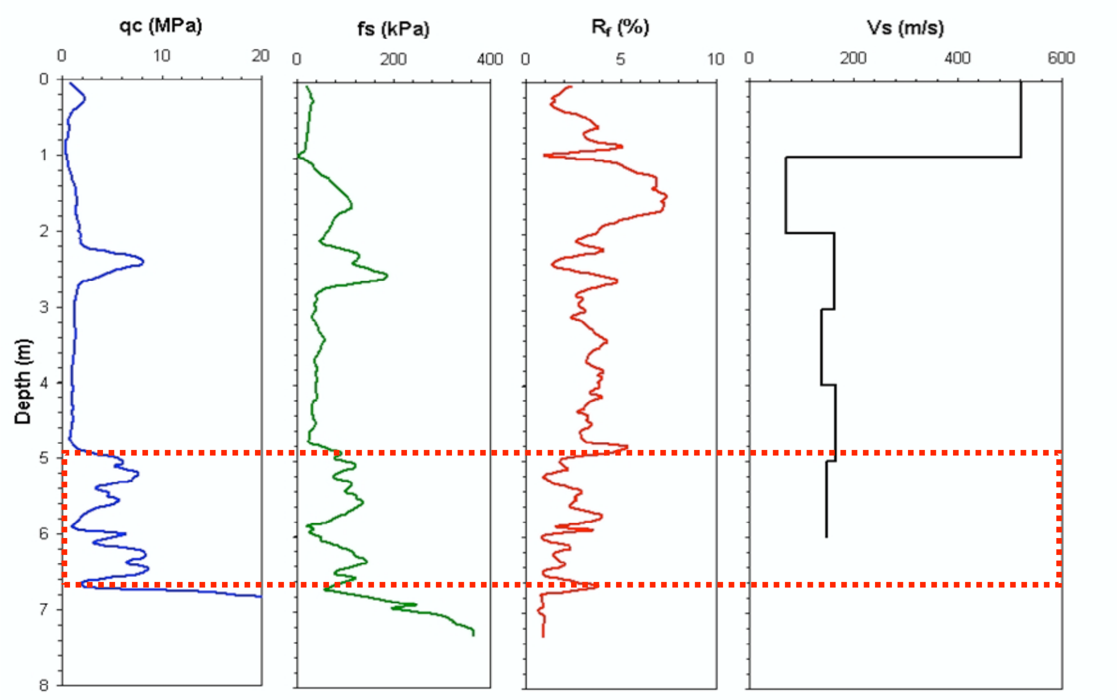

—312—

表12　10号孔勘探结果

（丰南县景庄，Ⅸ度区，地下水位1.45米，液化，1978.9）

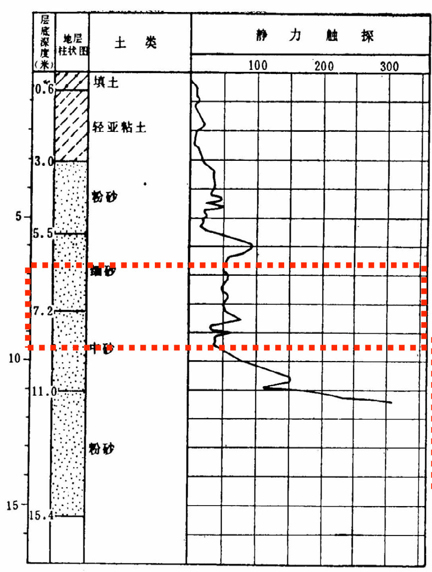

标准贯入试验 深度	标准贯入试验 击数	取样试验 取样深度	取样试验 含水量	取样试验 容重	取样试验 颗粒分析 10—2	取样试验 颗粒分析 2—0.5	取样试验 颗粒分析 0.5—0.25	取样试验 颗粒分析 0.25—0.1	取样试验 颗粒分析 0.1—0.05	取样试验 颗粒分析 <0.05
3.3	8	3.0					1	8	58	33
3.8	8	3.7					1	2	45	52
4.6	8.5	4.4						1	47	52
5.4	5	5.1							56	44
5.8	18	5.7				1	54	41	4	
6.3	9	6.2				2	48	47	3	
6.9	9	6.8				3	43	50	4	
7.3	13	7.2				5	52	41	2	
7.8	10	7.7				16	39	41	4	
8.8	9	8.7				15	64	18	3	
9.7	11	9.5				15	56	27	2	
10.9	22	10.6				8	35	50	7	

Earthquake:	1976 Tanshan, China
Magnitude:	M_S=7.8
Location:	T11 Tangshan District
References:	Zhou & Zhang (1979), Shibata & Teparaska (1988)
Nature of Failure:	Liquefaction
Comments:	Liquefaction documented by Zhou and Zhang. Hand auger samples at 1.5, 2.0, and 3.0 m. Soil grading from silty clay to sandy silt to silty sand to fine sand with depth.

Stress		**Strength**	
Liquefied	Y	N (bpf) from 78/79	14.3
Data Class	C	V_S (m/s)	157
Critical Layer (m)	1.2 to 3.0		
Median Depth (m)	2.10		
st.dev.	0.30	q_c (MPa)	3.91
Depth to GWT (m)	0.85	st.dev.	0.56
st.dev.	0.30	f_s (kPa)	53.37
σ_v (kPa)	38.83	st.dev.	19.33
st.dev.	5.98	norm. exp. initial	0.54
σ_v' (kPa)	26.56	norm. exp. step	0.48
st.dev.	3.22	norm. exp. Final	0.47
a_{max} (g)	0.61	difference	0.00
st.dev.	0.24	C_q, C_f	1.70
r_d	0.94	C_{thin}	1.00
st.dev.	0.04	f_{s1} (kPa)	90.72
M_w	7.89	st.dev.	32.86
st.dev.	0.10	q_{c1} (MPa)	6.65
CSR_{eq}	0.54	st.dev.	0.96
st.dev.	0.24	R_f(%)	1.36
C.O.V.$_{CSR}$	0.45	stdev	0.80
DWF (Moss et al.)	0.93	del qc	1.06
DWF (Youd et al.)	0.88	qc1,mod	7.71
CSR*	0.58	CRR	0.12

T11 Tangshan District

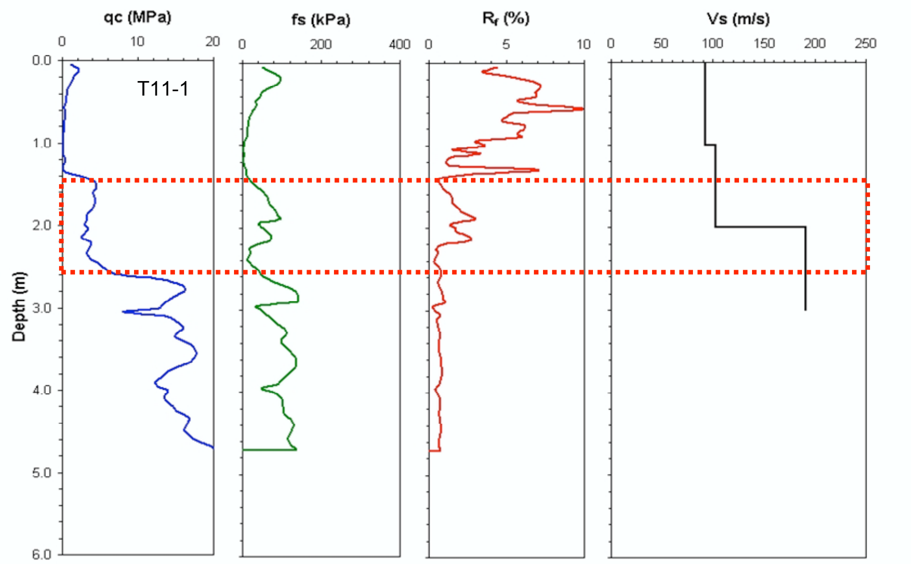

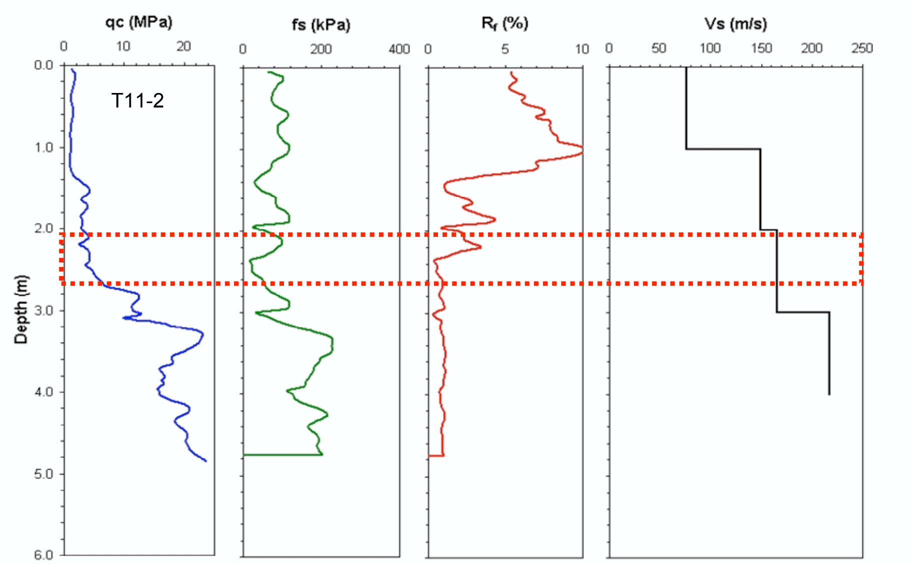

表13　11号孔勘探结果

（丰南县范庄，Ⅸ度区，地下水位0.85米，液化，1978.9）

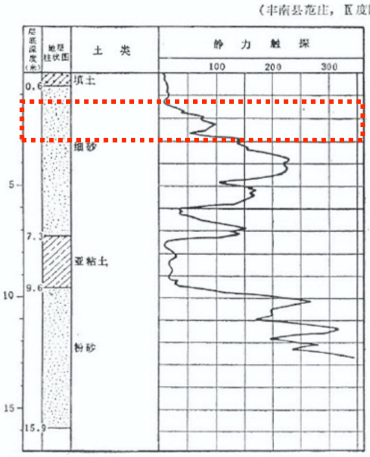

标准贯入试验		取样试验								
					颗粒分析					
深度	击数	取样深度	含水量	容重	10—2	2—0.5	0.5—0.25	0.25—0.1	0.1—0.05	<0.05
2.3	14	2.0				1	10	75	11	3
2.8	15	2.6				3	25	58	8	6
3.3	14	3.0				1	9	81	9	
4.3	39	4.3				1	15	76	8	
5.4	29	5.2				2	12	77	9	
6.3	25	6.2				6	22	64	8	

Earthquake:	1976 Tanshan, China
Magnitude:	M_S=7.8
Location:	T12 Tangshan District
References:	Zhou & Zhang (1979), Shibata & Teparaska (1988)
Nature of Failure:	Liquefaction

Comments: Liquefaction documented by Zhou and Zhang.

Hand auger samples at 2.0 and 2.5m
Soil grading from silt to silty sand and fine sand.

Up to 50m from 78/79 data, but coincident with SASW measurements.

V_S measurements appear incorrect.

Stress		**Strength**	
Liquefied	Y	N (bpf) from 78/79	6.5
Data Class	C	V_S (m/s)	
Critical Layer (m)	2.4 to 3.8		
Median Depth (m)	3.10		
st.dev.	0.23	q_c (MPa)	1.94
Depth to GWT (m)	1.55	st.dev.	0.68
st.dev.	0.30	f_s (kPa)	25.77
σ_v (kPa)	56.58	st.dev.	6.00
st.dev.	4.82	norm. exp. initial	0.67
σ_v' (kPa)	41.37	norm. exp. step	0.58
st.dev.	3.10	norm. exp. Final	0.57
a_{max} (g)	0.58	difference	0.01
st.dev.	0.23	C_q, C_f	1.65
r_d	0.90	C_{thin}	1.00
st.dev.	0.06	f_{s1} (kPa)	42.61
M_w	7.89	st.dev.	9.93
st.dev.	0.10	q_{c1} (MPa)	3.20
CSR_{eq}	0.47	st.dev.	1.13
st.dev.	0.20	R_f(%)	1.33
$C.O.V._{CSR}$	0.42	stdev	0.79
DWF (Moss et al.)	0.93	del qc	0.97
DWF (Youd et al.)	0.88	qc1,mod	4.17
CSR*	0.50	CRR	0.07

T12 Tangshan District

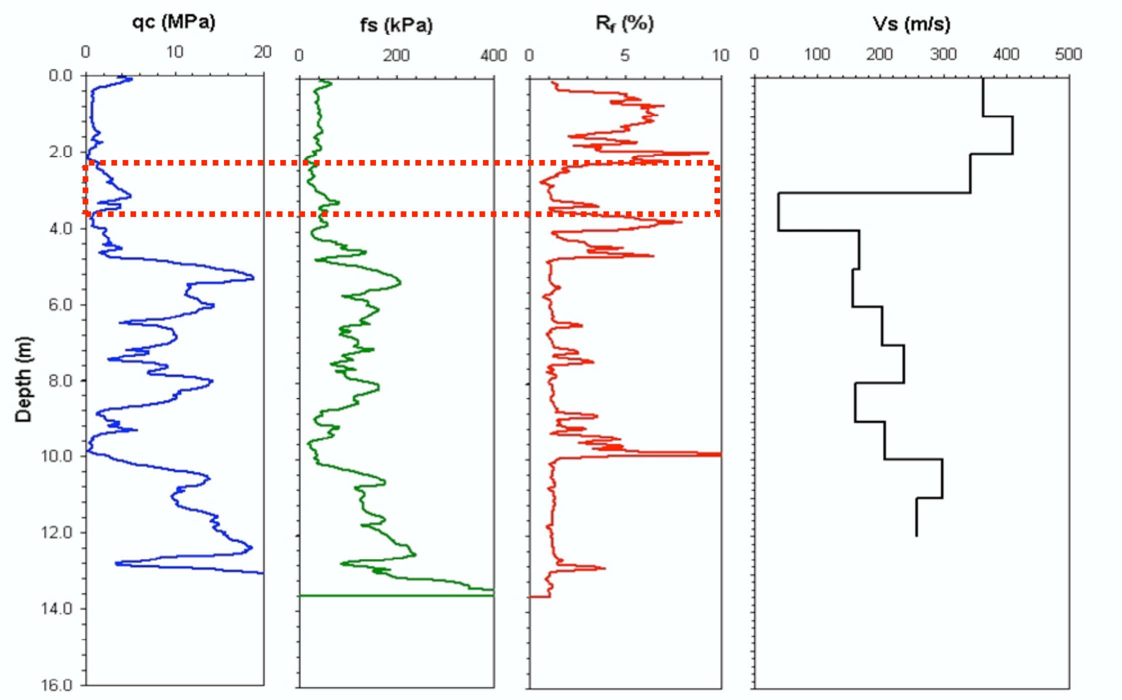

表14　12号孔勘探结果

（丰南县宣庄，Ⅸ度区，地下水位1.55米，液化，1978.9）

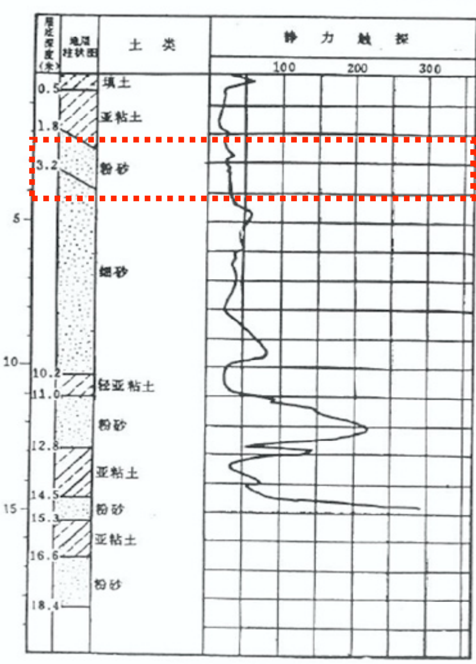

标准贯入试验 深度	标准贯入试验 击数	取样深度	含水量	容重	颗粒分析 10—2	2—0.5	0.5—0.25	0.25—0.1	0.1—0.05	<0.05
2.9	8	2.6					2	85	8	5
3.7	5	3.4					1	65	23	11
4.4	6	4.2					12	80	8	
5.0	10	4.7					8	84	8	
5.4	6	5.1					2	93	5	
5.9	5	6.1				1	2	91	6	
6.3	7	6.6					3	90	7	
6.9	10	7.1				1	10	79	10	
7.4	12	7.5					8	89	3	
7.8	7	7.9				1	6	80	8	5
8.2	14	8.4					8	89	3	
8.7	8	8.9				1	8	75	11	5
9.2	9	8.9				3	66	28	3	
10.9	16	10.6				3	13	18	44	22
12.5	30	12.2						2	73	25
12.8	15	12.7				1	3	1	53	42

Earthquake:	1976 Tanshan, China
Magnitude:	M_S=7.8
Location:	T13 Tangshan District
References:	Zhou & Zhang (1979), Shibata & Teparaska (1988)
Nature of Failure:	Liquefaction

Comments: Liquefaction documented by Zhou and Zhang.

100m from SASW measurements.

Critical layer differs from 1988 interpretation of 2.0 to 2.7m because of high fines and clay content in that upper layer.

Shear wave velocity profile questionable.

Stress		**Strength**	
Liquefied	Y	N (bpf) from 78/79	
Data Class	C	V_S (m/s)	
Critical Layer (m)	6.0 to 8.0		
Median Depth (m)	7.00		
st.dev.	0.33	q_c (MPa)	11.47
Depth to GWT (m)	1.05	st.dev.	1.02
st.dev.	0.30	f_s (kPa)	110.64
σ_v (kPa)	133.88	st.dev.	12.62
st.dev.	7.60	norm. exp. initial	0.47
σ_v' (kPa)	75.51	norm. exp. step	0.46
st.dev.	5.05	norm. exp. Final	0.46
a_{max} (g)	0.58	difference	0.00
st.dev.	0.23	C_q, C_f	1.23
r_d	0.72	C_{thin}	1.00
st.dev.	0.12	f_{s1} (kPa)	136.20
M_w	7.89	st.dev.	15.54
st.dev.	0.10	q_{c1} (MPa)	14.12
CSR_{eq}	0.48	st.dev.	1.26
st.dev.	0.21	R_f(%)	0.96
$C.O.V._{CSR}$	0.44	stdev	0.11
DWF (Moss et al.)	0.93	del qc	0.55
DWF (Youd et al.)	0.88	qc1,mod	14.67
CSR*	0.52	CRR	0.42

T13 Tangshan District

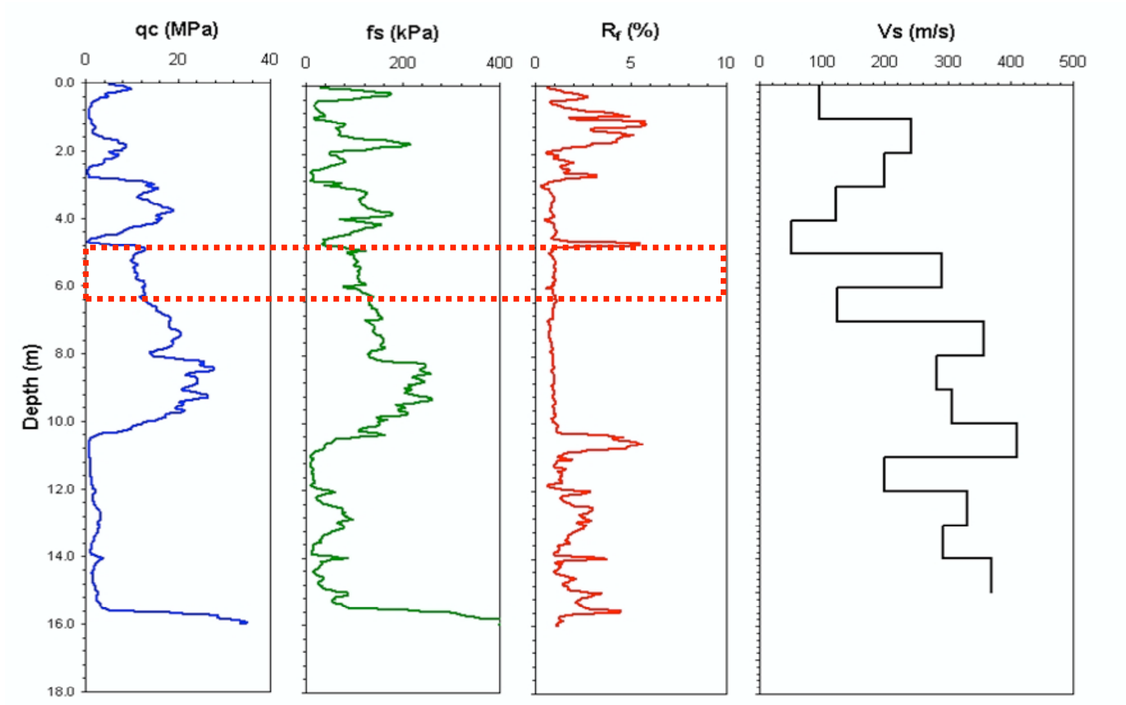

表15　13号孔勘探结果

（丰南县草各庄，Ⅹ度区，地下水位1.05米，液化，1978.9）

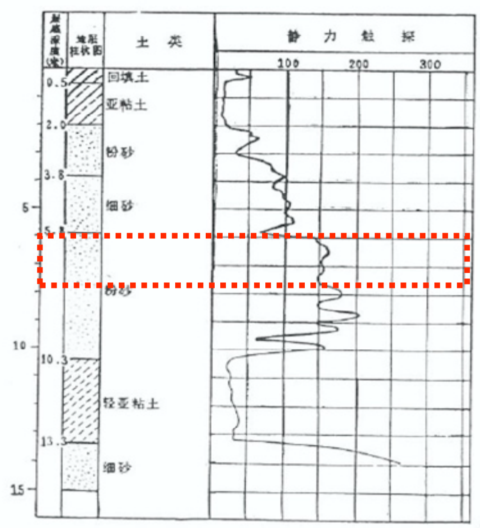

标准贯入试验		取样试验								
					颗粒分析					
深度	击数	取样深度	含水量	容重	10—2	2—0.5	0.5—0.25	0.25—0.1	0.1—0.05	<0.05
2.5	10	2.3				1	10	48	19	22
4.3	19	4.1				1	6	74	15	4
5.3	16	5.0				7	22	57	11	3
5.9	9	5.7					12	36	45	7
6.3	27	6.0					5	40	49	6
7.4	21	7.1					4	48	45	3
7.8	27	7.5				1	5	54	37	3
9.3	29	9.0				2	21	65	8	4
9.8	29	9.5					2	70	21	7

Earthquake:	1976 Tanshan, China
Magnitude:	M_S=7.8
Location:	T14 Tangshan District
References:	Zhou & Zhang (1979), Shibata & Teparaska (1988)
Nature of Failure:	Liquefaction

Comments: Liquefaction documented by Zhou and Zhang.

Hand auger sample at 2m.

Liquefiable layer may have been at the deeper 7.5m layer, below 2007 measurements.

Based on the high penetration resistance it is difficult to interpret this site as a liquefaction case history. Detailed post-earthquake observations are needed to validate this case history as liquefied.

Stress		**Strength**	
Liquefied	NA	N (bpf) from 78/79	14
Data Class	C	V_S (m/s)	167
Critical Layer (m)	1.6 to 2.0		
Median Depth (m)	1.80		
st.dev.	0.07	q_c (MPa)	10.18
Depth to GWT (m)	1.25	st.dev.	0.49
st.dev.	0.30	f_s (kPa)	77.87
σ_v (kPa)	31.98	st.dev.	7.86
st.dev.	1.74	norm. exp. initial	0.52
σ_v' (kPa)	26.58	norm. exp. step	0.48
st.dev.	2.41	norm. exp. Final	0.48
a_{max} (g)	0.54	difference	0.00
st.dev.	0.22	C_q, C_f	1.70
r_d	0.95	C_{thin}	1.00
st.dev.	0.04	f_{s1} (kPa)	132.37
M_w	7.89	st.dev.	13.36
st.dev.	0.10	q_{c1} (MPa)	17.30
CSR_{eq}	0.40	st.dev.	0.84
st.dev.	0.17	R_f(%)	0.77
C.O.V.$_{CSR}$	0.42	stdev	0.05
DWF (Moss et al.)	0.93	del qc	0.30
DWF (Youd et al.)	0.88	qc1,mod	17.59
CSR*	0.43	CRR	0.71

T14 Tangshan District

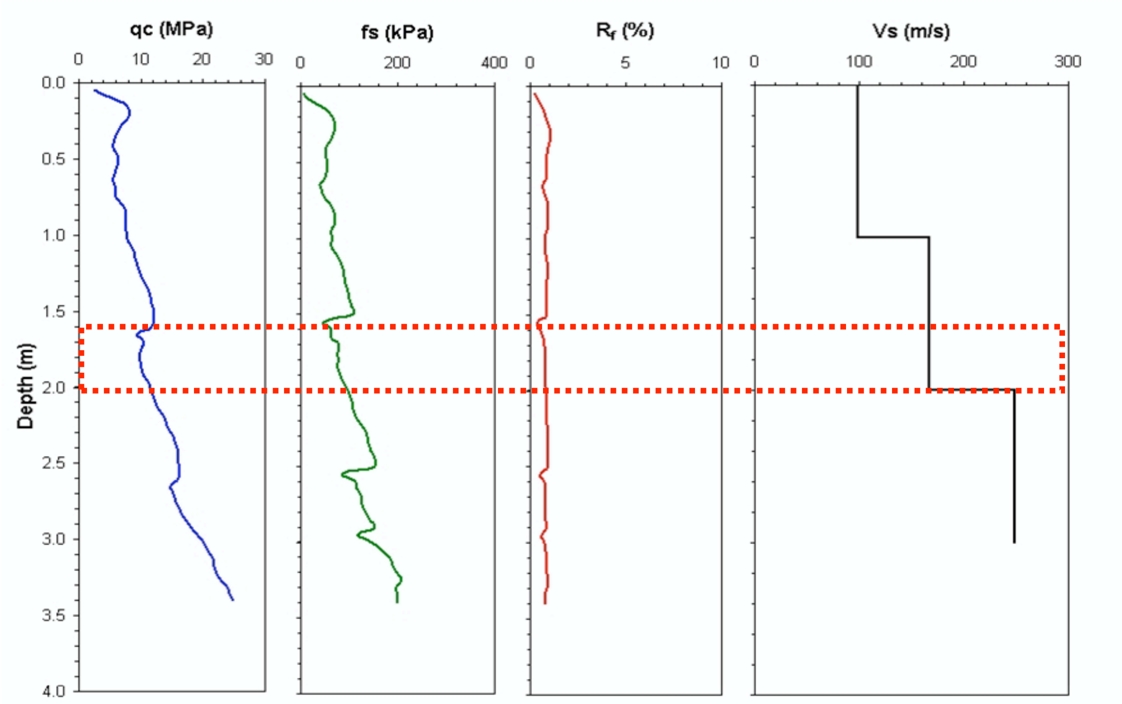

表16 14号孔勘探结果

（丰南县阎家庄，Ⅸ度区，地下水位1.25米，液化，1978.9）

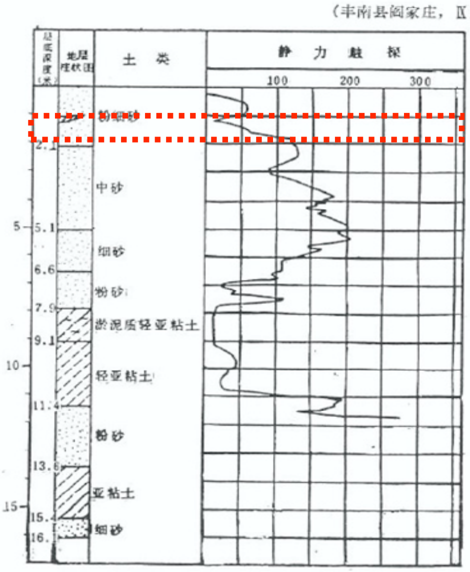

标准贯入试验		取样试验								
		取样	含水	容重	颗粒分析					
深度	击数	深度	量		10—2	2—0.5	0.5—0.25	0.25—0.1	0.1—0.05	<0.05
1.8	14	1.5					17	77	6	
2.8	15	2.5				8	51	39	2	
3.8	23	3.5				11	59	27	3	
4.8	23	4.5				1	24	71	4	
5.8	30	5.5				4	22	49	21	4
6.8	10	6.5						1	46	53

Earthquake:	1976 Tanshan, China
Magnitude:	M_S=7.8
Location:	T15 Tangshan District
References:	Zhou & Zhang (1979), Shibata & Teparaska (1988)
Nature of Failure:	Liquefaction

Comments: Liquefaction documented by Zhou and Zhang.

Very dense sand site, difficult to hand auger.

Based on the high penetration resistance it is difficult to interpret this site as a liquefaction case history. Detailed post-earthquake observations are needed to validate this case history as liquefied.

Stress		**Strength**	
Liquefied	NA	N (bpf) from 78/79	11
Data Class	C	V_S (m/s)	207
Critical Layer (m)	2.2 to 2.6		
Median Depth (m)	2.40		
st.dev.	0.07	q_c (MPa)	9.52
Depth to GWT (m)	1.00	st.dev.	0.24
st.dev.	0.30	f_s (kPa)	70.05
σ_v (kPa)	44.30	st.dev.	8.82
st.dev.	1.86	norm. exp. initial	0.53
σ_v' (kPa)	30.57	norm. exp. step	0.49
st.dev.	2.50	norm. exp. Final	0.49
a_{max} (g)	0.27	difference	0.00
st.dev.	0.11	C_q, C_f	1.70
r_d	0.95	C_{thin}	1.00
st.dev.	0.05	f_{s1} (kPa)	119.09
M_w	7.89	st.dev.	14.99
st.dev.	0.10	q_{c1} (MPa)	16.18
CSR_{eq}	0.24	st.dev.	0.40
st.dev.	0.10	R_f(%)	0.74
C.O.V.$_{CSR}$	0.41	stdev	0.10
DWF (Moss et al.)	0.93	del qc	0.22
DWF (Youd et al.)	0.88	qc1,mod	16.40
CSR*	0.26	CRR	0.58

T15 Tangshan District

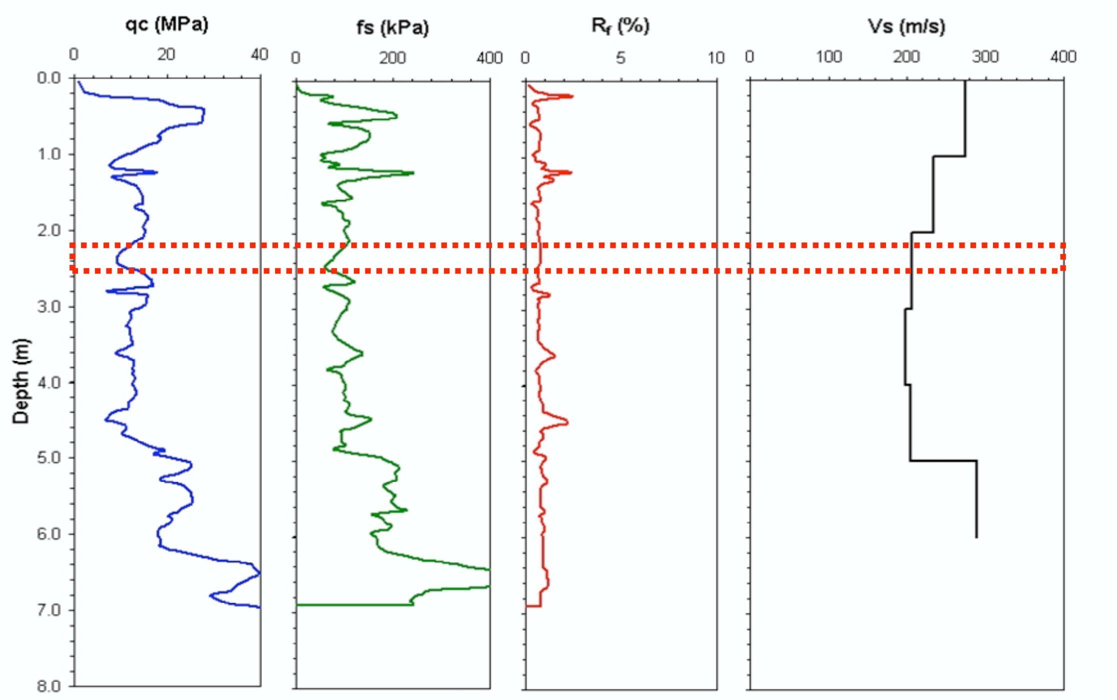

表17　15号孔勘探结果

（滦县佘庄，Ⅸ度区，地下水位1.0米，液化，1977.4）

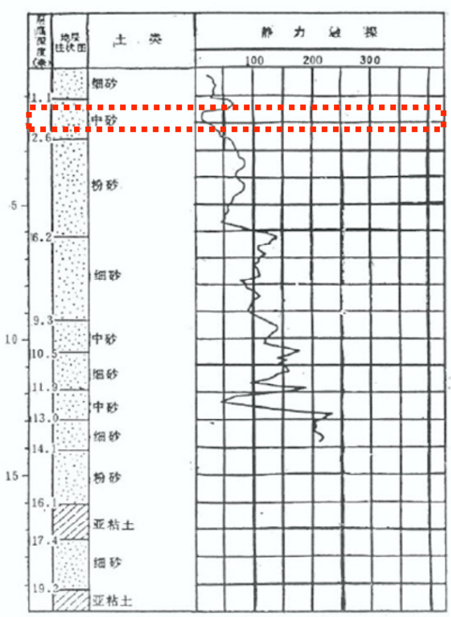

标准贯入试验		取样试验								
					颗粒分析					
深度	击数	取样深度	含水量	容重	10—2	2—0.5	0.5—0.25	0.25—0.1	<0.1	0.1—0.05
2.3	11	2.7	18.0	1.94	1.8	45.5	42.5	9.2	1.0	
3.25	15	3.4	22.7	2.01		0.7	7.7	62.2	29.4	27.9
4.3	24	4.3	23.5	1.89			16.8	65.8	17.4	14.5
5.25	23	5.3	22.8	2.07			9.5	60.9	29.6	24.2
6.25	26	6.3	19.3	2.08		2.8	36.7	47.1	13.4	11.1
7.20	43	7.4	20.4	2.05		2.1	46.2	48.2	3.5	
8.2	50	8.2	18.5	2.06		3.6	41.2	50.2	5.0	
9.3	50	9.3	21.1	2.07		4.4	46.9	43.2	5.5	
10.3	50	10.3	17.8	1.94		15.8	54.5	24.5	5.2	
11.3	50	11.3	16.7	2.09		10.6	32.7	49.5	7.2	
12.3	50	12.2	12.9	2.04	3.5	28.1	39.0	23.0	6.4	
13.3	50	13.1	21.4	2.05		0.5	36.3	54.5	8.7	
14.3	46	14.3	20.2	2.04		0.5	10.5	60.9	28.1	19.2
15.3	50	15.4	23.4	2.00		0.5	1.5	36.5	61.5	55.4
		16.4	19.2	2.00						
18.3	50	18.1	19.6	2.06		0.1	2.4	76.7	20.8	14.1

Earthquake:	1976 Tanshan, China
Magnitude:	M_S=7.8
Location:	T16 Tangshan District
References:	Zhou & Zhang (1979), Shibata & Teparaska (1988)
Nature of Failure:	
Comments:	Nonliquefaction documented by Zhou and Zhang.
	Encountered old brick foundation near the surface.

Stress		**Strength**	
Liquefied	N	N (bpf) from 78/79	32
Data Class	C	V_S (m/s)	267
Critical Layer (m)	7.2 to 8.2		
Median Depth (m)	7.50		
st.dev.	0.17	q_c (MPa)	10.26
Depth to GWT (m)	3.50	st.dev.	3.99
st.dev.	0.30	f_s (kPa)	96.78
σ_v (kPa)	137.50	st.dev.	50.72
st.dev.	4.76	norm. exp. initial	0.48
σ_v' (kPa)	98.26	norm. exp. step	0.48
st.dev.	4.22	norm. exp. Final	0.48
a_{max} (g)	0.26	difference	0.00
st.dev.	0.10	C_q, C_f	1.06
r_d	0.78	C_{thin}	1.00
st.dev.	0.13	f_{s1} (kPa)	102.62
M_w	7.89	st.dev.	53.78
st.dev.	0.10	q_{c1} (MPa)	10.88
CSR_{eq}	0.19	st.dev.	4.23
st.dev.	0.08	R_f(%)	0.94
$C.O.V._{CSR}$	0.44	stdev	0.24
DWF (Moss et al.)	0.93	del qc	0.36
DWF (Youd et al.)	0.88	qc1,mod	11.24
CSR*	0.20	CRR	0.24

T16 Tangshan District

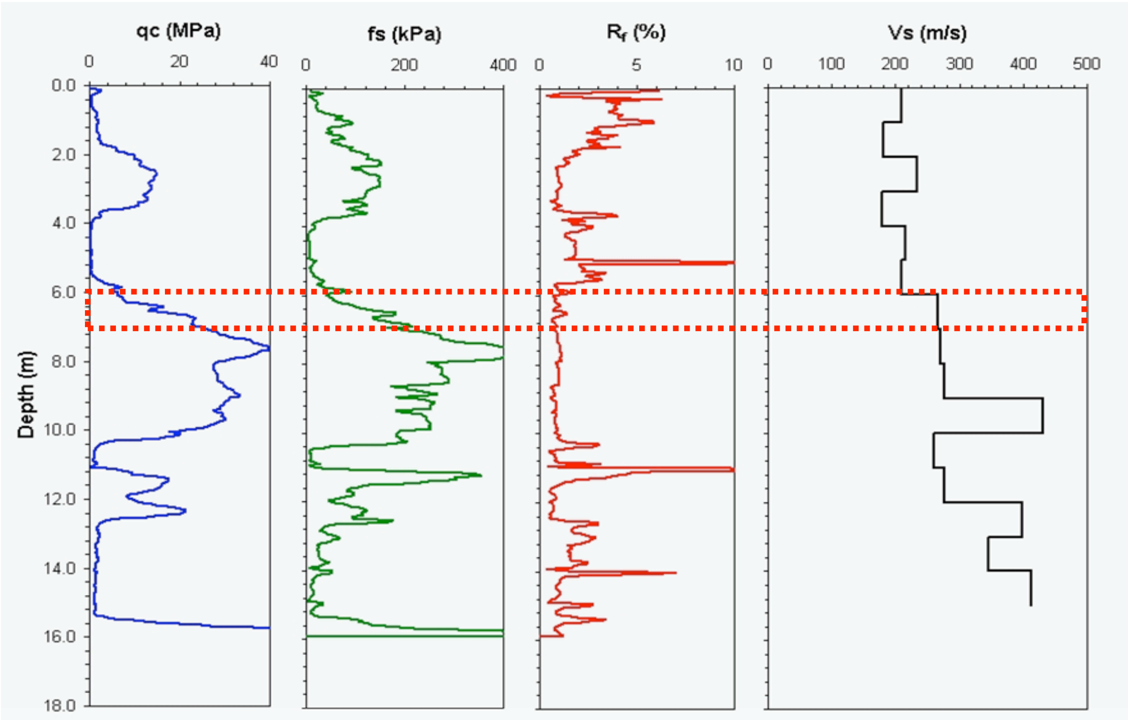

表18　16号孔勘探结果

（滦县东坨子头，Ⅸ度区，地下水位3.5米，未液化，1977.4）

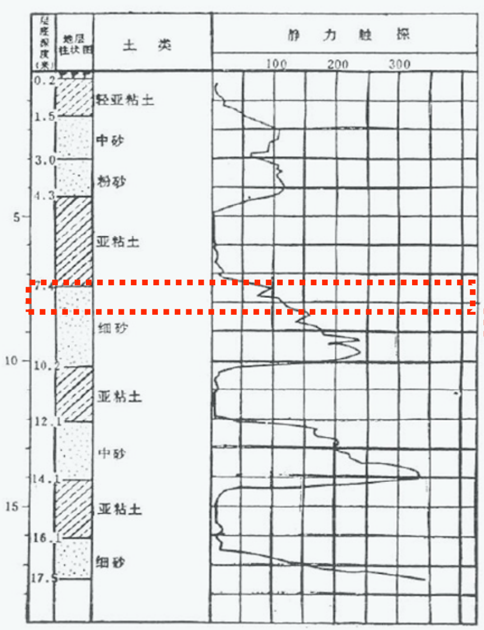

标准贯入试验		取样试验			颗粒分析					
深度	击数	取样深度	含水量	容重	10—2	2—0.5	0.5—0.25	0.25—0.1	<0.1	0.1—0.05
1.2	14	2.1	11.3	2.10		15.5	38.5	33.0	13.0	
2.25	22	3.0	19.8	1.96		0.1	10.0	60.0	29.9	25.9
3.25	23	4.1	19.6	2.13		2.4	24.8	48.9	23.9	22.1
4.25	31	7.6	14.2	2.17	0.4	10.2	31.4	38.8	19.2	15.6
5.45	10	8.2	14.6	2.09		5.4	32.4	45.2	17.0	14.5
6.3	7	9.1	19.7	2.05		0.5	36.0	47.5	16.0	12.8
7.35	32	12.1	14.7	2.12		17.2	47.0	27.7	8.1	
8.35	31	13.0	15.7	2.16		13.5	45.8	31.7	9.0	
9.3	50									
10.3	8									
12.3	46									
13.3	50									
14.3	10									
15.3	35									
16.3	50									
17.4	50									

Earthquake:	1976 Tanshan, China
Magnitude:	M_S=7.8
Location:	L1 Lutai District
References:	Zhou & Gou (1979), Shibata & Teparaska (1988)
Nature of Failure:	No Failure

Comments:

Non-liquefaction documented by Zhou and Gou

Zhou & Guo observed that a slight decrease in the PI determined what liquefied (L2) and what did not liquefy (L1).

They found silty clay ejecta that correlates to a layer at around 12m depth at L2 with a PI in the 4.7 to 5.7 range. The same layer at L1 has a PI around 8 and a slightly higher tip resistance.

Static Driving shear stresses may have contributed to the failure at L2 and not at L1.

Stress		**Strength**	
Liquefied	N?	N (bpf) from 78/79	5
Data Class	C	V_S (m/s)	148
Critical Layer (m)	7 to 12.0		
Median Depth (m)	9.75		
st.dev.	0.83	q_c (MPa)	3.55
Depth to GWT (m)	0.40	st.dev.	1.03
st.dev.	0.30	f_s (kPa)	60.68
σ_v (kPa)	189.13	st.dev.	44.69
st.dev.	17.33	norm. exp. initial	0.53
σ_v' (kPa)	97.40	norm. exp. step	0.52
st.dev.	8.75	norm. exp. Final	0.52
a_{max} (g)	0.27	difference	0.00
st.dev.	0.11	C_q, C_f	1.01
r_d	0.70	C_{thin}	1.00
st.dev.	0.16	f_{s1} (kPa)	61.52
M_w	7.80	st.dev.	45.31
st.dev.	0.10	q_{c1} (MPa)	3.60
CSR_{eq}	0.24	st.dev.	1.04
st.dev.	0.11	R_f(%)	1.71
C.O.V.$_{CSR}$	0.48	stdev	0.85
DWF (Moss et al.)	0.95	del qc	1.11
DWF (Youd et al.)	0.90	qc1,mod	4.70
CSR*	0.25	CRR	0.07

L1 Lutai District

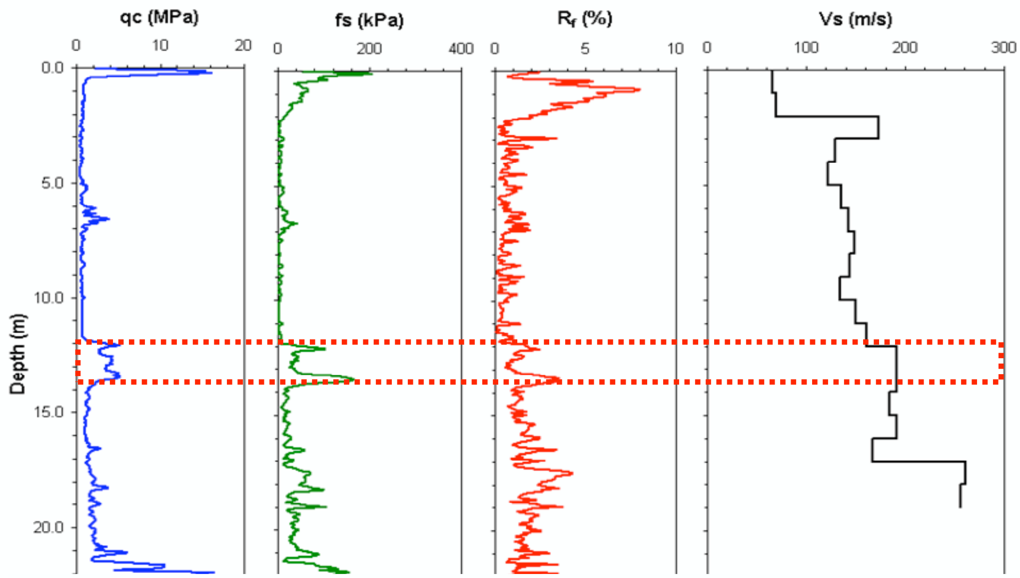

表9 勘探试验结果（芦台化肥厂，地下水位0.4米，未液化，1977.8）

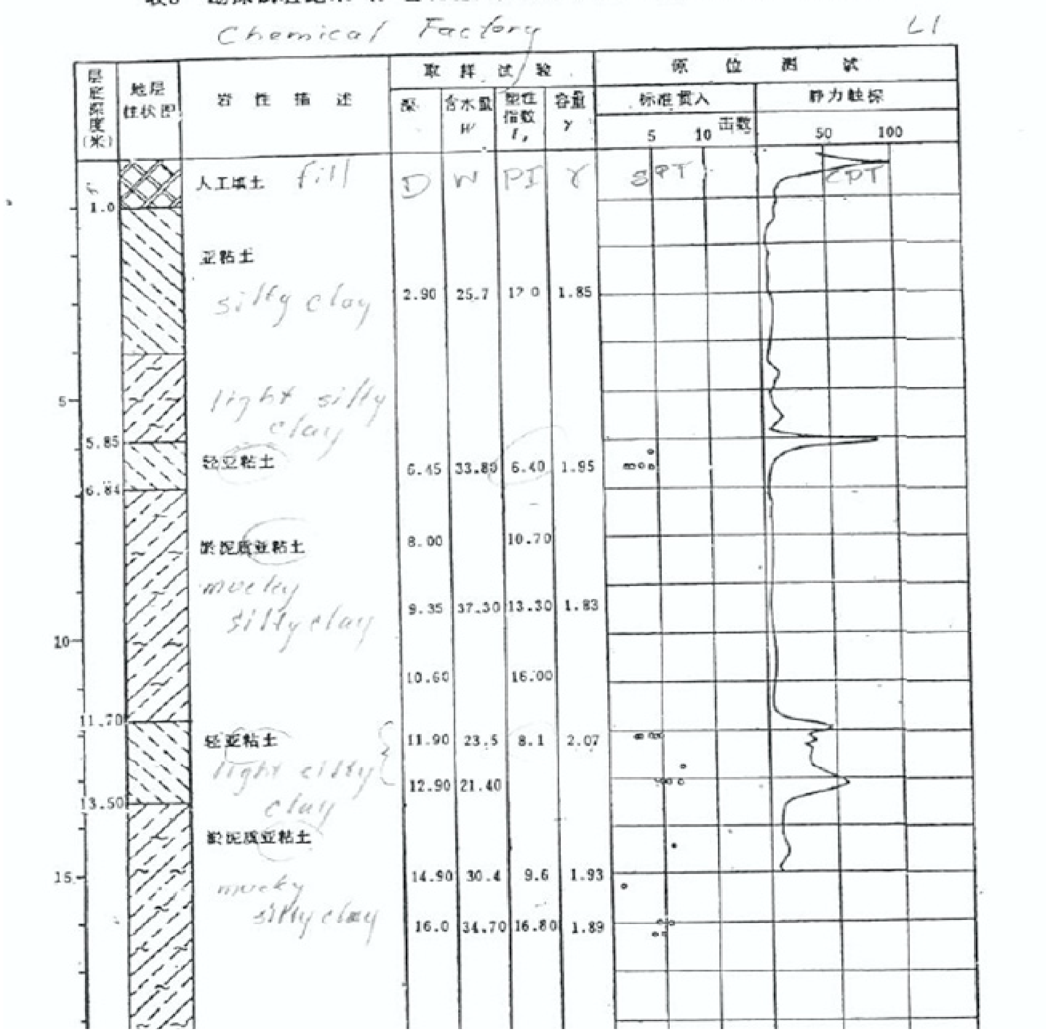

Earthquake: 1976 Tanshan, China
Magnitude: M_S=7.8
Location: L2 Lutai District
References: Zhou & Guo (1979), Shibata & Teparaska (1988)
Nature of Failure: Exhibited liquefaction traits

Comments: Liquefaction documented by Zhou and Guo.

Zhou & Guo observed that a slight decrease in the PI determined what liquefied (L2) and what did not liquefy (L1).

They found silty clay ejecta that correlates to a layer at around 12m depth at L2 with a PI in the 4.7 to 5.7 range. The same layer at L1 has a PI around 8 and a slightly higher tip resistance.

Static Driving shear stresses may have contributed to the failure at L2 and not at L1.

Stress		**Strength**	
Liquefied	Y?	N (bpf) from 78/79	
Data Class	ERR	V_S (m/s)	179
Critical Layer (m)	12.0 to 13.0		
Median Depth (m)	12.50		
st.dev.	0.17	q_c (MPa)	3.73
Depth to GWT (m)	0.21	st.dev.	1.30
st.dev.	0.30	f_s (kPa)	48.72
σ_v (kPa)	243.23	st.dev.	30.76
st.dev.	8.54	norm. exp. initial	0.55
σ_v' (kPa)	122.66	norm. exp. step	0.57
st.dev.	8.25	norm. exp. Final	0.57
a_{max} (g)	0.27	difference	0.00
st.dev.	0.11	C_q, C_f	0.89
r_d	0.63	C_{thin}	1.00
st.dev.	0.20	f_{s1} (kPa)	43.36
M_w	7.89	st.dev.	27.37
st.dev.	0.10	q_{c1} (MPa)	3.32
CSR_{eq}	0.22	st.dev.	1.16
st.dev.	0.11	R_f(%)	1.31
$C.O.V._{CSR}$	0.51	stdev	0.39
DWF (Moss et al.)	0.93	del qc	0.71
DWF (Youd et al.)	0.88	qc1,mod	4.03
CSR*	0.24	CRR	0.07

L2 Lutai District

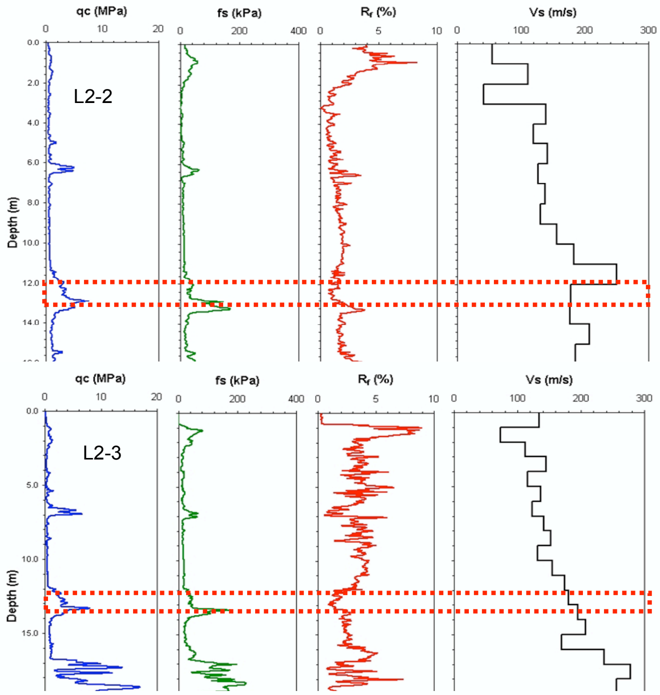

表10 勘探试验综合表（芦台农机厂，地下水位0.21米，液化，1977.8）

Agriculture Machine Factory L2

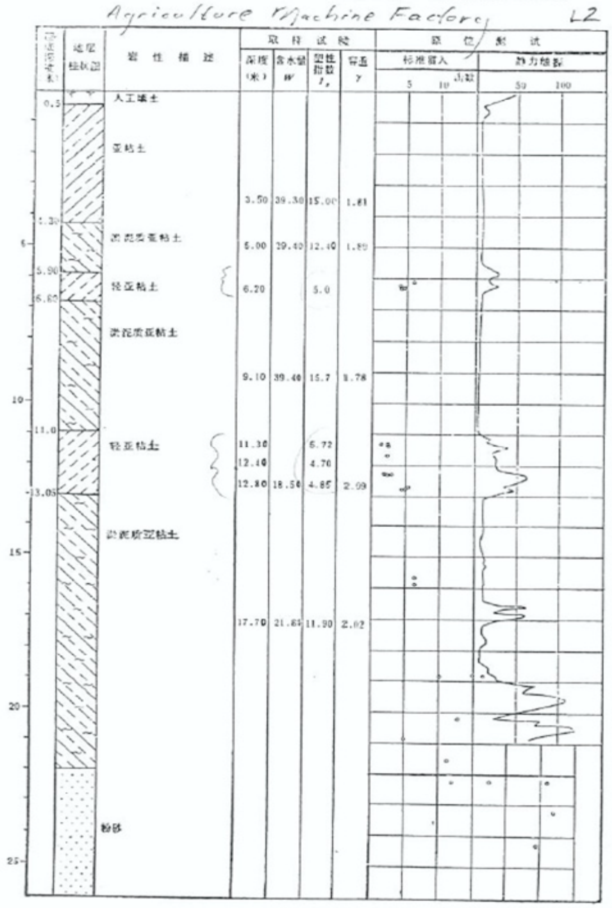

Cyclic failure calculations for L1 and L2 using Boulanger and Idriss (2006) method for CPT measurements.

L1-critical layer 7 to 11m depth

qc (MPa)	0.688065	
st.dev.	0.085278	
u (kPa)	278.0309	
st.dev.	97.83995	
a	1	area correction
qt (MPa)	0.688065	qc+(1-a)u
st.dev.	0.085278	
Nk	17.5	cone factor
su (kPa)	28.7894	(qt-sig_v)/Nk
st.dev.	4.972056	
Kalpha	1.00	
Ksigma	1.00	
CRR index	0.24	0.8*(su/p)
FS	0.93	against cyclic failure

L2-critical layer 7 to 11m depth

qc (MPa)	0.535308	
st.dev.	0.130259	
u (kPa)	251.6419	
st.dev.	143.1968	
a	1	area correction
qt (MPa)	0.535308	qc+(1-a)u
st.dev.	0.130259	
Nk	17.5	cone factor
su (kPa)	20.0333	(qt-sig_v)/Nk
st.dev.	7.459389	
Kalpha	1.00	
Ksigma	1.00	
CRR index	0.17	0.8*(su/p)
FS	0.66	against cyclic failure

Appendix B: Data Processing Techniques (Chapter 4 excerpt from Moss et al. 2003)

Chapter 4
Data Processing

4.1 INTRODUCTION

In order to have a robust unbiased estimate of the occurrence or nonoccurrence of liquefaction it is of preeminent importance to have the highest quality data. A probabilistic correlation requires powerful statistical techniques, but is only as good as the quality of data to which the techniques are applied. To this end, data processing was of utmost importance in this study. A considerable amount of time was spent processing and reviewing the database to minimize epistemic uncertainty that can creep in due to human error, biased interpretation, and poor analysis techniques.

4.2 FIELD OBSERVATIONS

The basis of a liquefaction correlation is a research engineer's observation of liquefaction or absence of liquefaction following a seismic event, and the index test measurements of the suspect critical layer. This basis is inherently fraught with uncertainty including lack of full coverage of affected area, misinterpretation of field evidence, poor index testing procedures, difficult field conditions, etc.

One of the primary discrepancies of a database of this type is that researchers tend to retrieve more liquefied than nonliquefied case histories. This can be attributed to the fact that testing in a liquefied area is much more appealing than testing at a site that hasn't experienced liquefaction. This unfortunately leads to a data bias, more liquefied case histories than nonliquefied case histories. To account for this data imbalance the procedure of bias weighting is used, as described in Chapter 5 on Bayesian analysis.

Liquefaction field correlations y are not based truly on the occurrence or nonoccurrence of liquefaction but on the observation of the manifestations of liquefaction at a particular location and the lack of manifestation at some other location. These manifestations can take the form of sand boils or sand blows, lateral spreading, building tilting or settlement, ground loss, broken lifelines, etc. Liquefaction can and does occur at depths where there is no surface evidence of the event. This of course does not make it into a liquefaction database; it fits the tree-falling-in-the-woods analogy.

The most content-rich sites are sites that are labeled as marginal. Marginal liquefaction does not exist, a soil deposit either liquefies or does not liquefy. Marginal is a research engineer's interpretation that at this location liquefaction was either incipient or occurred and resulted in minimal surface manifestations. These sites are included in the database and tend to have the most information content because they fall near the limit-state (threshold of liquefaction/nonliquefaction).

All these vagaries are incorporated into the database and can result in epistemic uncertainty. To minimize this uncertainty a panel of experts reviewed the database and came to a consensus on each site and the data it contained. This process of consensus results in a robust database that contains the best assessment of each variable to the highest standards of practice.

4.3 STRENGTH PARAMETERS

4.3.1 Choice of Logs

At any given site there can be multiple CPT and also corollary SPT logs to choose from. Proximity of the logs to the observed liquefaction/nonliquefaction is critical. The depositional environment and the properties that lead to liquefaction can vary significantly over a small distance and therefore it is important to be as close to the observed location as possible. Logs that are considered to be representative of the conditions are chosen. When there are multiple logs, the values (such as tip and sleeve resistance) are average.

CPT logs that were measured using a mechanical cone or a sleeveless cone are not used in this database because of the lack of sleeve measurements. However, when a sleeveless cone trace has a corollary SPT log that shows that the critical layer is composed of clean sand (FC<5%), then the tip resistance is used in conjunction with a prescribed median "clean sand" friction ratio ($R_f \cong 0.35\%$). This allows the use of important early CPT tip resistance data with a neutral friction ratio.

There are a few earthquake reconnaissance trips that utilized a Chinese cone. The report by Earth Technology (1985) showed that there is very little difference between tip and sleeve readings using the Chinese cone and a cone following ASTM specifications (D3441 and D5778); therefore the Chinese cone was treated no differently in this database.

4.3.2 Case Selection

The objective in case selection in this study was to end up with a group of statistically independent data points. Some previous correlations have used multiple liquefaction or nonliquefaction cases from a single site to generate more statistical data for analysis. This method can be incorrect for two reasons. First, given a site with consistent stratigraphy and a uniform depositional environment, selecting two liquefied or two nonliquefied cases from the same critical layer results in cross-correlation of these two data points. The cross-correlation must be accounted for in any form of statistical analysis and will result in much higher uncertainty or much reduced informational content for each data point. Second, if a particular layer within the site does liquefy, this then modifies the incoming seismic energy for the layers above through seismic isolation and below by blocking full reflection off the surface. This leads to a modified CSR for other layers at the site which can be difficult to determine.

4.3.3 Critical Layer Selection

Selection of the critical layer is an important step in estimating the seismic strength of a particular soil deposit. The criteria for selection is finding the strata of soil that is the weakest-link-in-the-chain from a liquefaction perspective. Finding the weakest link requires observing the tip resistance and friction ratio in conjunction, with the addition of a SPT log, for soil classification, if one is available. For most depositional environments this can be a simple matter of looking for the smallest continuous stretch of tip resistance with low friction ratio that agrees with the SPT log in terms of a liquefiable material. It can be a difficult proposal for fluvial depositional environments where the strata are thin, interbedded, and discontinuous both horizontally and vertically. A final criteria for identifying a critical layer is comparing the suspect layers to previous correlations. This aids in the more difficult sites where determining which of multiple layers liquefied or didn't liquefy.

One issue that is not commonly addressed in liquefaction correlations is that the *in situ* data are usually acquired post ground shaking. Particularly for the liquefied cases, the soil strength and properties have most likely been modified due to the process of liquefaction. Chameau et al. (1991) looked at sites that were affected by the Loma Prieta Earthquake in which previous CPT data existed. Post event CPT data were acquired and compared to the pre-event CPT data. They found that loose materials experienced the most alteration in tip resistance due to the ground shaking and subsequent liquefaction. This comes as no surprise. Recent work involving large scale liquefaction blast tests have and are being performed in Japan where pre- and post-liquefaction CPT measurements are made. Hopefully these data will resolve the bias and allow for proper accounting of the changes that occur within a liquefied layer.

If it can be assumed that tip resistance has a positive correlation with relative density for clean sands (Schmertmann 1978), then the greater the tip resistance the greater the relative density. In a critical state framework, given a constant confining stress, the higher the relative density (lower the void ratio), the less capacity the soil has for contractive behavior. Liquefaction is premised on this contractive behavior of soils. Therefore, the closer a point lies to the limit-state or liquefaction boundary the less contractive it is, and the less pre- to post-liquefaction change in resistance it is likely to experience. On the nonliquefaction side of the limit-state it is assumed that the resistance is unmodified by the ground shaking because no liquefaction has occurred. Another issue is that if a CSR value is determined for a liquefied site using the post-liquefaction *in situ* measurements for site response analysis, the value may be slightly higher than pre-liquefaction conditions because of the stiffening that has occurred.

Given all these pre- and post-liquefaction considerations, it is conjectured that the limit-state function is totally unaffected by post-liquefaction densification because:

1. near the limit-state the soils are near the critical state (small state parameter) and therefore have not significantly densified,
2. nonliquefied soils will have no post-event densification and therefore are unaffected by the event and will maintain their position near the limit-state.

The soils most affected by liquefaction, which will give vastly different post-event resistance measurements, are the loose or low tip resistance soils, and these have little impact on the limit-state function in a Bayesian-type analysis.

4.3.4 Index Measurements

Once the critical layer has been selected it is a matter of determining the appropriate statistics of the measurements within the layer. Kulansingam, Boulanger, and Idriss (1999) studied various procedures for estimating an average tip resistance over a standardized distance of cone travel. They looked at different standardized distances and came to the conclusion that having a preset distance over which the resistance is averaged works poorly.

The approach used in this study was to let the depositional environment dictate. Using the procedures described above for identifying the critical layer, the maximum distance over which the soil deposit lies is often apparent. The top and bottom depths are taken as extrema. The distribution of the tip and sleeve resistances are assumed to be normal, and the averages and standard deviations are calculated from a digitized form of the trace. Raw sleeve and tip measurements are used to calculate the friction ratio in order to eliminate aliasing that may have occurred in the field calculations.

Induced pore pressure can have an affect on the tip and sleeve measurements. This affect is pronounced in soils that respond in an undrained manner to the strain imposed by the advancing cone (i.e., fine-grained soils). For most soils that are susceptible to liquefaction, fully drained cone penetration is assumed (Lunne et al. 1997). Therefore, in general, no pore pressure corrections are necessary for materials that are potentially liquefiable. The assumption of fully drained response was checked using pore pressure measurements, when available, for each site.

4.3.5 Masked Liquefaction

In certain situations liquefaction may occur at depth but evidence may not reach the ground surface due to the monolithic or unified nature of overlying nonliquefiable strata. This masked liquefaction situation was researched and presented by Ishihara (1985). The results from that research are used to screen sites that are found to be liquefiable in terms of the index measurements, has overlying nonliquefiable material that fits the Ishihara (1985) thickness criteria, showed no surface manifestation of liquefaction, and was reported as a nonliquefied site. For reference, at a site experiencing a low level of ground shaking (PGA < 0.2 g) with a 2 m thick liquefiable layer, an overlying nonliquefiable layer of approximately 2 m could eliminate all surface manifestation of liquefaction.

4.3.6 Screening for Other Failure Mechanisms

Certain soil types are not susceptible to liquefaction but may deform via cyclic softening. These soils may exhibit surface manifestations that can appear quite similar to what may be observed in "classic" liquefaction, such as lateral spreading, and building tilting, punching, and settlement. However it has been shown that the failure mechanism is quite different from liquefaction and is primarily a function asymmetrical driving shear stresses (K_α). The soils that are susceptible to cyclic softening tend to have a high percentage of fines and these fines will tend to behave in a plastic manner. Several cases like this were observed in the 2001 Kocaeli, Turkey, earthquake and the 2001 Chi-Chi, Taiwan, earthquake. Since the limit-state and the overall correlation is based on "classic" liquefaction, it is not appropriate to include these cases in the analysis.

A criteria for screening these cases is based on research of fines content and plasticity in relation to liquefaction susceptibility (Andrews and Matin 2000; Andrianopoulos et al. 2001; Guo and Prakash 1999; Perlea 2000; Polito 2001; Sancio et al. 2003; Yamamuro and Lade 1998, Youd and Gilstrap 1999; to name a few). The criteria for soils not susceptible to liquefaction used in this study are shown graphically in Figure 4.1.

4.3.7 Normalization

The tip and sleeve are normalized using the variable normalization scheme presented with this study in Chapter 3, on Normalization. Note that the tip and sleeve values are normalized equivalently, which results in no change for a normalized friction ratio ($R_{f,1} = R_f$).

4.3.8 Thin Layer Correction

Thin layer corrections, if they were required, are performed using the method proposed in this study in Chapter 2, on Thin Layer Correction. Note that only 4% of the cases in the database required a thin layer correction. For database purposes the thin layer correction was limited to a maximum of 1.5 ($C_{thin} \leq 1.5$).

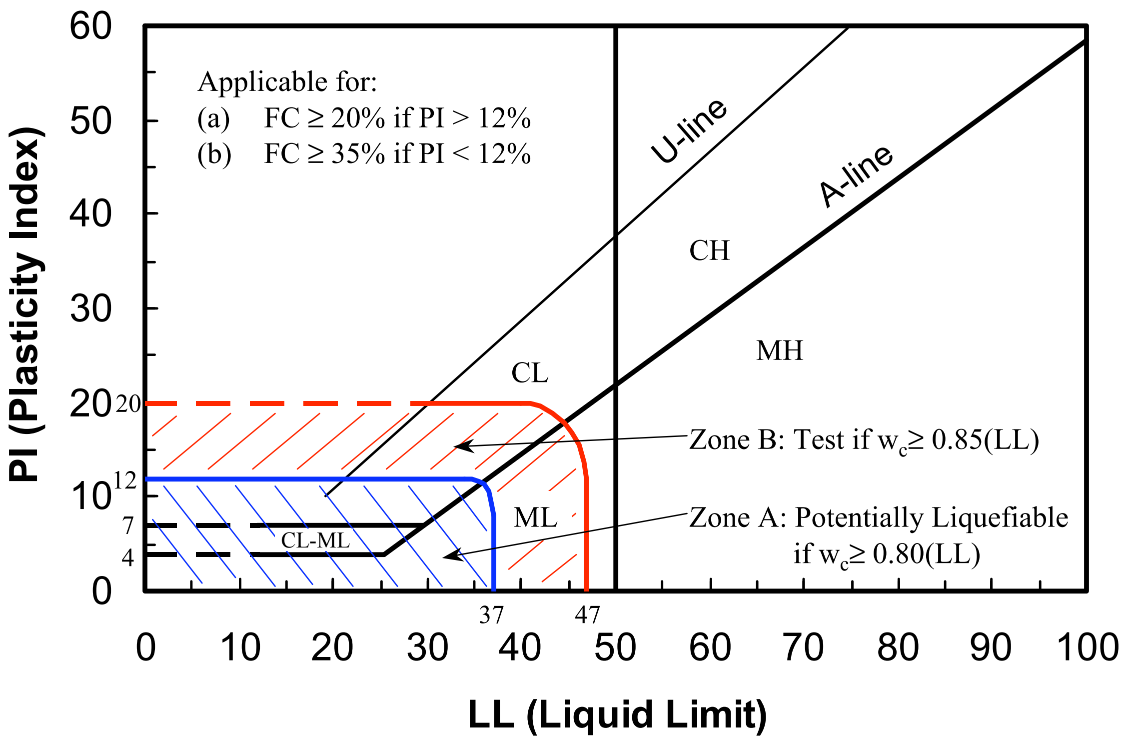

Fig. 4.1 Screening criteria for failure mechanism other than liquefaction.

4.3.9 Processed Strength Parameters

The result of this processing procedure is unbiased, statistically independent $q_{c,1}$, $f_{s,1}$, and R_f values for the liquefied and nonliquefied cases. These are mean resistance values and variances over the extent of the critical layer which have been normalized to one atmosphere and corrected for thin layer issue if required.

4.4 STRESS PARAMETERS

4.4.1 Cyclic Stress Ratio

The dynamic stress that the critical layer experienced is determined using the simplified uniform cyclic stress ratio as defined by Seed and Idriss (1971),

$$CSR = 0.65 \cdot \frac{a_{\max}}{g} \cdot \frac{\sigma_v}{\sigma'_v} \cdot r_d \tag{4.1}$$

The CSR value calculated using Equation 4.1 is assumed to be the average or mean of a normally distributed random variable as in Equation 4.2. The variance of CSR is calculated via equation 4.3, where the coefficient of variation is equal to the standard deviation divided by the mean. Both Equation 4.2 and 4.3 are using first-order Taylor series expansions about the mean point, including only the first two terms.

$$\overline{CSR} \cong 0.65 \cdot \frac{\overline{a_{\max}}}{g} \cdot \frac{\overline{\sigma_v}}{\overline{\sigma'_v}} \cdot \overline{r_d} \tag{4.2}$$

$$\delta_{CSR}{}^2 \cong \delta_{a\max}{}^2 + \delta_{rd}{}^2 + \delta_{\sigma v}{}^2 + \delta_{\sigma' v}{}^2 - 2 \cdot \rho_{\sigma v \sigma' v} \cdot \delta_{\sigma v} \cdot \delta_{\sigma' v} \tag{4.3}$$

Total and effective stress are correlated parameters, therefore the inclusion of the correlation coefficient term for these two variables is necessary.

4.4.2 Peak Ground Acceleration

The geometric mean of the peak ground acceleration is based on the best estimation of ground shaking possible. The methods of estimation are strong motion recordings, site response, calibrated attenuation relationships, adjustment of estimated site pga through general site response modeling, and general attenuation relationships. Using a calibrated attenuation relationship means using all available recordings to tune general attenuation relationships for event-specific variations and azimuth specifics when recordings permit.

The coefficient of variation of the peak ground acceleration is fixed according to the method of ground shaking estimation;

$\delta < 0.10$ for sites with strong motion stations less than 100m from site,

$\delta = 0.10$ to 0.25 for sites with strong motion stations within 100 to 500m from site or where site response analysis was performed using a nearby rock recording as input base motion ,

$\delta = 0.25$ to 0.35 for sites with strong motion stations within 500 m to 1000 m and/or estimates from calibrated attenuation relationships,

$\delta = 0.35$ to 0.5 for others.

This is a subjective determination of the variance of the ground shaking but is based on typical uncertainty bands from general attenuation relationships that have coefficient of variations of between 0.3 and 0.5 (e.g., Abrahamson and Silva 1997).

4.4.3 Total and Effective Stress

The total and effective vertical stress are correlated variables and this correlation must be accounted. The critical layer is selected using the procedures outlined above. From this the total extent of the critical layer is used to calculate the mean and variance of the critical layer, assuming that it is normally distributed. The variance is estimated using a 6 sigma approach, where the extrema of the layer are assumed to be three standard deviations away from the mean on either side. The total variance is then divided by six to give an estimate of the standard deviation.

A deterministic estimate is made of the mean unit weight of the soil above and below the water table. The variance is based on statistical studies of the measured variability of soil unit weight and is set at $\delta \cong 0.1$ (Kulhawy and Trautman 1996). The water table mean is taken as the reported field measured value (with consideration given for the depth of water table during the seismic event) and the variance is set at a fixed standard deviation of σ = 0.3 m., a reasonable estimate of water table fluctuations given relatively stable groundwater conditions. An estimate of the total and effective vertical stresses, their respective variances, and covariance can then be calculated using the expansion Equations 4.4–4.9:

$$ {}_{\sigma_v} \cong {}_{\gamma 1} \cdot {}_{h_w} + {}_{\gamma 2} \cdot \left({}_{h} - {}_{hw} \right) \tag{4.4}$$

$$ {}_{\sigma_v'} \cong {}_{\gamma 1} \cdot {}_{hw} + \left({}_{\gamma 2} - \gamma_w \right) \cdot \left({}_{h} - {}_{hw} \right) \tag{4.5}$$

$$ \sigma^2_{\sigma_v} \cong {}^2_{hw} \cdot \sigma^2_{\gamma 1} + \left({}_{h} - {}_{hw} \right)^2 \cdot \sigma^2_{\gamma 2} + {}^2_{\gamma 2} \cdot \sigma^2_{h} + \left({}_{\gamma 1} - {}_{\gamma 2} \right)^2 \cdot \sigma^2_{hw} \tag{4.6}$$

$$ \sigma^2_{\sigma_v'} \cong {}^2_{hw} \cdot \sigma^2_{\gamma 1} + \left({}_{h} - {}_{hw} \right)^2 \cdot \sigma^2_{\gamma 2} + \left({}_{\gamma 2} - \gamma_w \right)^2 \cdot \sigma^2_{h} + \left({}_{\gamma 1} + \gamma_w - {}_{\gamma 2} \right)^2 \cdot \sigma^2_{hw} \tag{4.7}$$

$$ Cov[\sigma_v, \sigma_v'] \cong \left({}^2_{hw} \cdot \sigma^2_{\gamma 1} \right) + \left({}_{\gamma 1} - {}_{\gamma 2} \right) \cdot \left({}_{\gamma 1} + \gamma_w - {}_{\gamma 2} \right) \cdot \sigma^2_{hw} + \left({}_{h} - {}_{hw} \right)^2 \cdot \sigma^2_{\gamma 2} + {}_{\gamma 2} \cdot \left({}_{\gamma 2} - \gamma_w \right) \cdot \sigma^2_{h} \tag{4.8}$$

$$ \rho_{\sigma_v \sigma_v'} = \frac{Cov[\sigma_v, \sigma_v']}{Var[\sigma_v] \cdot Var[\sigma_v']} \tag{4.9}$$

4.4.4 Nonlinear Shear Mass Participation Factor (r_d)

The nonlinear shear mass participation factor accounts for nonlinear response within a soil column and reduces the peak ground acceleration at the surface to reflect the ground acceleration that is experienced at the critical depth. This factor, denoted as r_d, has been derived from ground response analyses. In recent work, 2153 site response analyses were run using 50 sites and 42 ground motions covering a comprehensive suite of motions and soil profiles (Cetin and Seed 2000). This brute force approach allows for careful statistical analysis of the median response given the depth, peak ground acceleration, moment magnitude, and indicative shear wave velocity of the site. The variance was estimated from the dispersion of these simulations. The median values can be estimated using Equations 4.10 and 4.11, and the variance from Equations 4.12 and 4.13,

d < 65 ft (4.10)

$$r_d(d, M_w, a_{\max}) = \frac{\left[1 + \dfrac{-9.147 - 4.173 \cdot a_{\max} + 0.652 \cdot M_w}{10.567 + 0.089 \cdot e^{0.089 \cdot (-d - 7.760 \cdot a_{\max} + 78.576)}}\right]}{\left[1 + \dfrac{-9.147 - 4.173 \cdot PGA + 0.652 \cdot M_w}{10.567 + 0.089 \cdot e^{0.089 \cdot (-7.760 \cdot a_{\max} + 78.576)}}\right]} \pm \sigma_{\varepsilon r_d}$$

d ≥ 65 ft (4.11)

$$r_d(d, M_w, a_{\max}) = \frac{\left[1 + \dfrac{-9.147 - 4.173 \cdot a_{\max} + 0.652 \cdot M_w}{10.567 + 0.089 \cdot e^{0.089 \cdot (-d - 7.760 \cdot a_{\max} + 78.576)}}\right]}{\left[1 + \dfrac{-9.147 - 4.173 \cdot a_{\max} + 0.652 \cdot M_w}{10.567 + 0.089 \cdot e^{0.089 \cdot (-7.760 \cdot a_{\max} + 78.576)}}\right]} \pm \sigma_{\varepsilon r_d}$$

d < 40 ft

$$\sigma_{\varepsilon r_d}(d) = d^{0.864} \cdot 0.00814 \tag{4.12}$$

d ≥ 40 ft

$$\sigma_{\varepsilon r_d}(d) = 40^{0.864} \cdot 0.00814 \tag{4.13}$$

4.4.5 Moment Magnitude

Moment magnitude is a value that is usually reported by seismological laboratories following an event and iterated on for a week or two until the final value is set in stone. Calculating the moment magnitude involves an inverse problem to determine the seismic moment. The uncertainty in these calculations comes from the nonunique inversion based on seismograms that are recorded at various teleseismic stations. The dimensions of the fault plane and the amount of slip associated with larger magnitude events tend to be easier to define than with smaller magnitude events. A simple equation Equation 4.14, based on the variance of a series of previous events (1989 Loma Prieta, 1994 Northridge, 1999 Tehuacan, 1999 Kocaeli, 1999 Taiwan, 2001 Denali), was used to estimate this epistemic uncertainty,

$$\sigma_{M_w} \cong 0.5 - 0.45 \cdot \log(M_w) \tag{4.14}$$

4.5 DATA CLASS

After the case histories have been selected and processed they are classified according to the quality of the informational content. Four classes of data are used to group the data, A through D, with D being substandard and therefore not included in the final database. The criteria for the data classes are as follows:

Class A

1. Original CPT trace with q_c and f_s/R_f, using a ASTM D3441 and D5778 spec. cone.
2. No thin layer correction required
3. $\delta_{CSR} \leq 0.20$

Class B

1. Original CPT trace with q_c and f_s/R_f, using a ASTM D3441 and D5778 spec. cone.
2. Thin layer correction.
3. $0.20 < \delta_{CSR} \leq 0.35$

Class C

1. Original CPT trace with q_c and f_s/R_f, but using a nonstandard cone (e.g., Chinese cone or mechanical cone).
2. No sleeve data but FC ≤ 5% (i.e., “clean” sand).
3. $0.35 < \delta_{CSR} \leq 0.50$

Class D

1. Not satisfying the criteria for Classes A, B, or C.

4.6 REVIEW PROCESS

The final step in processing the data is an extensive review procedure. Each case in the database is reviewed a minimum of three times. A panel of qualified experts was assembled to do the review, this included in addition to the author and Prof. Raymond B. Seed; Prof. Jon Stewart, Prof. Les Youd, Dr. Rob Kayen, and Prof. Kohji Tokimatsu. Each case was reviewed by the author, Ray Seed, and at least one of the four independent reviewers. The objective was to remove as much human error and epistemic error from the database as possible.

A final note on the review process includes the review of the analytical and statistical procedures. The application of Bayesian analysis to SPT-based liquefaction-triggering correlations and the techniques used was reviewed extensively by the Pacific Earthquake Engineering Research Center (PEER), and peer reviewed as journal publications in the *Journal of Geotechnical and Geoenvironmental Engineering* and the *Journal of Structural Reliability.* The CPT-based liquefaction-triggering correlation, and the associated Bayesian analysis and methodology, was also reviewed extensively by PEER at quarterly meetings that included as a review panel Prof. Les Youd, Prof. Geoff Martin, and Prof. I. M. Idriss.

It is the author's belief that the power of the Bayesian framework in engineering application is to incorporate all forms of information and that the review process is one of the more important and congenial steps in reducing epistemic uncertainty.

4.7 CONCLUSION

This chapter includes all the details and procedures used to process data for an unbiased liquefaction-triggering correlation within a Bayesian framework. The methods used to generate the best estimates of the representative statistics for each parameter are presented in their entirety. Figures 4.2 through 4.4 show the processed data in $q_{c,1}$ vs. CSR space. The task of developing accurate and appropriate processing techniques was both important and involved, and the final correlation attests to the time well spent.

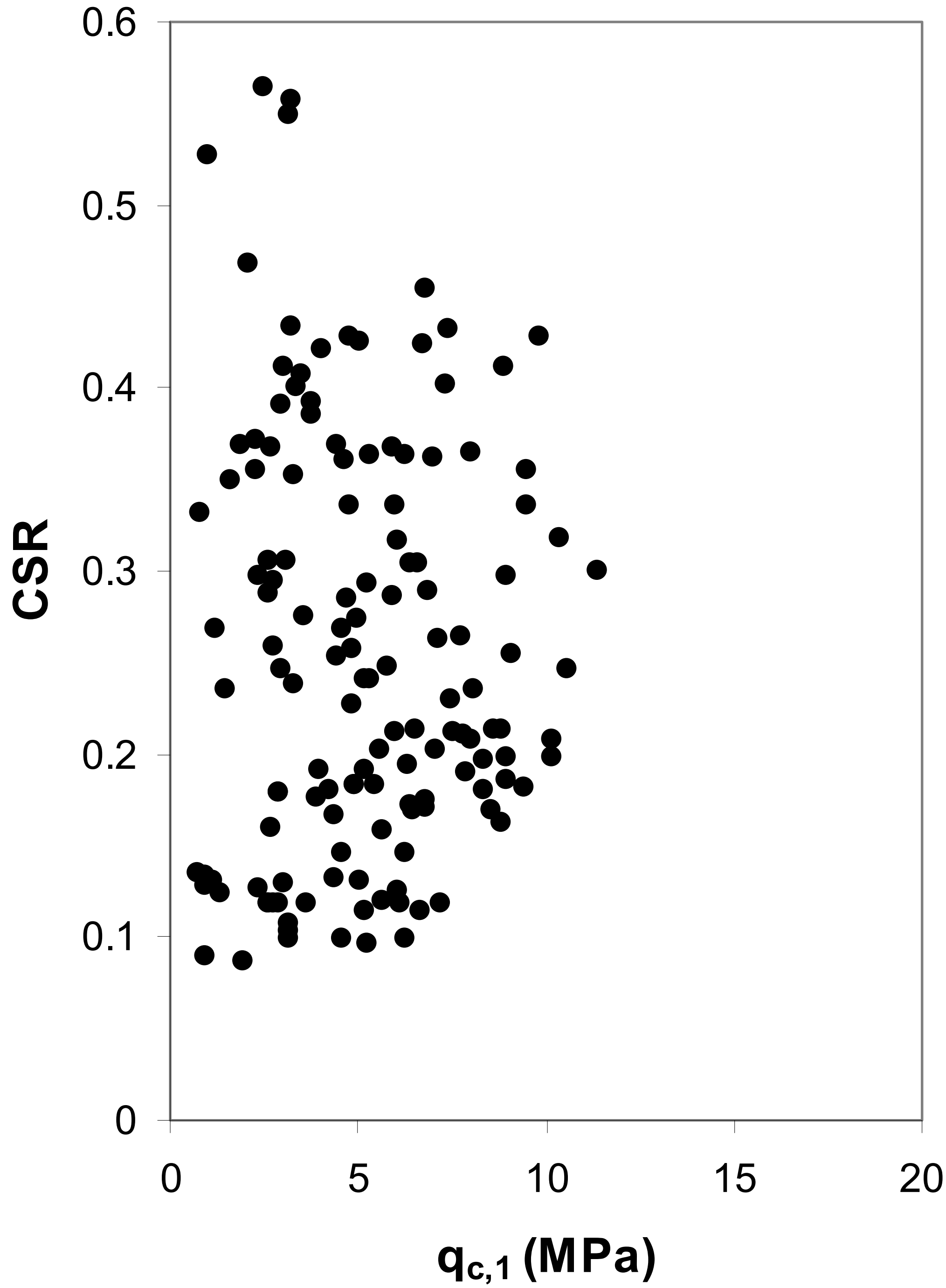

Fig. 4.2 Plot showing mean location of liquefied data points.

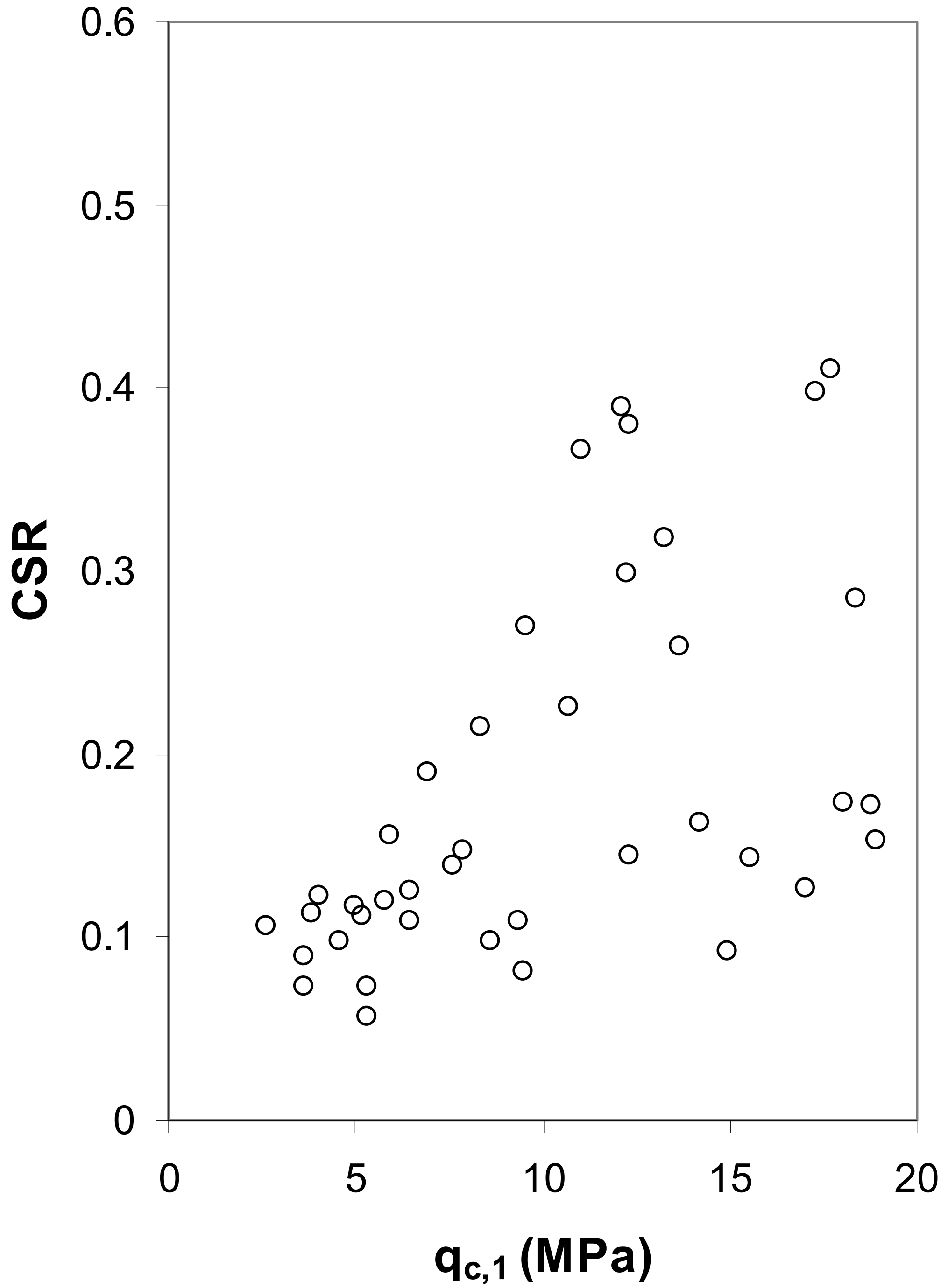

Fig. 4.3 Plot showing mean location of nonliquefied data points.

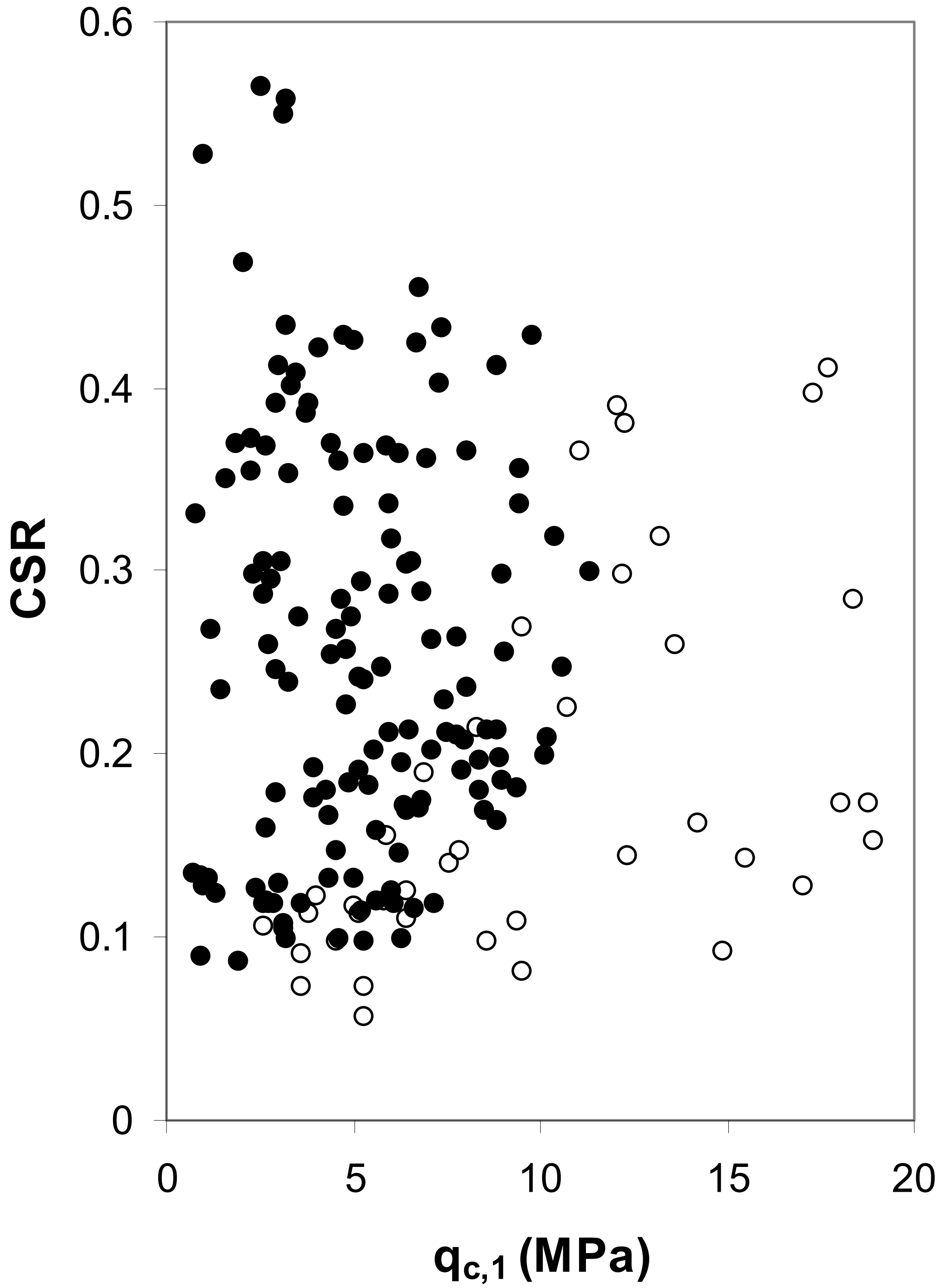

Fig. 4.4 Plot showing mean location of both liquefied (dots) and nonliquefied (circles) data points.

PEER REPORTS

PEER reports are available individually or by yearly subscription. PEER reports can be ordered at http://peer.berkeley.edu/publications/peer_reports.html or by contacting the Pacific Earthquake Engineering Research Center, 1301 South 46th Street, Richmond, CA 94804-4698. Tel.: (510) 665-3448; Fax: (510) 665-3456; Email: peer_editor@berkeley.edu

PEER 2009/01 *Evaluation of Ground Motion Selection and Modification Methods: Predicting Median Interstory Drift Response of Buildings.* Curt B. Haselton, Ed. June 2009.

PEER 2008/10 *Technical Manual for Strata.* Albert R. Kottke and Ellen M. Rathje. February 2009.

PEER 2008/09 *NGA Model for Average Horizontal Component of Peak Ground Motion and Response Spectra.* Brian S.-J. Chiou and Robert R. Youngs. November 2008.

PEER 2008/08 *Toward Earthquake-Resistant Design of Concentrically Braced Steel Structures.* Patxi Uriz and Stephen A. Mahin. November 2008.

PEER 2008/07 *Using OpenSees for Performance-Based Evaluation of Bridges on Liquefiable Soils.* Stephen L. Kramer, Pedro Arduino, and HyungSuk Shin. November 2008.

PEER 2008/06 *Shaking Table Tests and Numerical Investigation of Self-Centering Reinforced Concrete Bridge Columns.* Hyung IL Jeong, Junichi Sakai, and Stephen A. Mahin. September 2008.

PEER 2008/05 *Performance-Based Earthquake Engineering Design Evaluation Procedure for Bridge Foundations Undergoing Liquefaction-Induced Lateral Ground Displacement.* Christian A. Ledezma and Jonathan D. Bray. August 2008.

PEER 2008/04 *Benchmarking of Nonlinear Geotechnical Ground Response Analysis Procedures.* Jonathan P. Stewart, Annie On-Lei Kwok, Yousseff M. A. Hashash, Neven Matasovic, Robert Pyke, Zhiliang Wang, and Zhaohui Yang. August 2008.

PEER 2008/03 *Guidelines for Nonlinear Analysis of Bridge Structures in California.* Ady Aviram, Kevin R. Mackie, and Božidar Stojadinović. August 2008.

PEER 2008/02 *Treatment of Uncertainties in Seismic-Risk Analysis of Transportation Systems.* Evangelos Stergiou and Anne S. Kiremidjian. July 2008.

PEER 2008/01 *Seismic Performance Objectives for Tall Buildings.* William T. Holmes, Charles Kircher, William Petak, and Nabih Youssef. August 2008.

PEER 2007/12 *An Assessment to Benchmark the Seismic Performance of a Code-Conforming Reinforced Concrete Moment-Frame Building.* Curt Haselton, Christine A. Goulet, Judith Mitrani-Reiser, James L. Beck, Gregory G. Deierlein, Keith A. Porter, Jonathan P. Stewart, and Ertugrul Taciroglu. August 2008.

PEER 2007/11 *Bar Buckling in Reinforced Concrete Bridge Columns.* Wayne A. Brown, Dawn E. Lehman, and John F. Stanton. February 2008.

PEER 2007/10 *Computational Modeling of Progressive Collapse in Reinforced Concrete Frame Structures.* Mohamed M. Talaat and Khalid M. Mosalam. May 2008.

PEER 2007/09 *Integrated Probabilistic Performance-Based Evaluation of Benchmark Reinforced Concrete Bridges.* Kevin R. Mackie, John-Michael Wong, and Božidar Stojadinović. January 2008.

PEER 2007/08 *Assessing Seismic Collapse Safety of Modern Reinforced Concrete Moment-Frame Buildings.* Curt B. Haselton and Gregory G. Deierlein. February 2008.

PEER 2007/07 *Performance Modeling Strategies for Modern Reinforced Concrete Bridge Columns.* Michael P. Berry and Marc O. Eberhard. April 2008.

PEER 2007/06 *Development of Improved Procedures for Seismic Design of Buried and Partially Buried Structures.* Linda Al Atik and Nicholas Sitar. June 2007.

PEER 2007/05 *Uncertainty and Correlation in Seismic Risk Assessment of Transportation Systems.* Renee G. Lee and Anne S. Kiremidjian. July 2007.

PEER 2007/04 *Numerical Models for Analysis and Performance-Based Design of Shallow Foundations Subjected to Seismic Loading.* Sivapalan Gajan, Tara C. Hutchinson, Bruce L. Kutter, Prishati Raychowdhury, José A. Ugalde, and Jonathan P. Stewart. May 2008.

PEER 2007/03 *Beam-Column Element Model Calibrated for Predicting Flexural Response Leading to Global Collapse of RC Frame Buildings.* Curt B. Haselton, Abbie B. Liel, Sarah Taylor Lange, and Gregory G. Deierlein. May 2008.

PEER 2007/02 *Campbell-Bozorgnia NGA Ground Motion Relations for the Geometric Mean Horizontal Component of Peak and Spectral Ground Motion Parameters.* Kenneth W. Campbell and Yousef Bozorgnia. May 2007.

PEER 2007/01 *Boore-Atkinson NGA Ground Motion Relations for the Geometric Mean Horizontal Component of Peak and Spectral Ground Motion Parameters.* David M. Boore and Gail M. Atkinson. May. May 2007.

PEER 2006/12 *Societal Implications of Performance-Based Earthquake Engineering.* Peter J. May. May 2007.

PEER 2006/11 *Probabilistic Seismic Demand Analysis Using Advanced Ground Motion Intensity Measures, Attenuation Relationships, and Near-Fault Effects.* Polsak Tothong and C. Allin Cornell. March 2007.

PEER 2006/10 *Application of the PEER PBEE Methodology to the I-880 Viaduct.* Sashi Kunnath. February 2007.

PEER 2006/09 *Quantifying Economic Losses from Travel Forgone Following a Large Metropolitan Earthquake.* James Moore, Sungbin Cho, Yue Yue Fan, and Stuart Werner. November 2006.

PEER 2006/08 *Vector-Valued Ground Motion Intensity Measures for Probabilistic Seismic Demand Analysis*. Jack W. Baker and C. Allin Cornell. October 2006.

PEER 2006/07 *Analytical Modeling of Reinforced Concrete Walls for Predicting Flexural and Coupled–Shear-Flexural Responses.* Kutay Orakcal, Leonardo M. Massone, and John W. Wallace. October 2006.

PEER 2006/06 *Nonlinear Analysis of a Soil-Drilled Pier System under Static and Dynamic Axial Loading.* Gang Wang and Nicholas Sitar. November 2006.

PEER 2006/05 *Advanced Seismic Assessment Guidelines.* Paolo Bazzurro, C. Allin Cornell, Charles Menun, Maziar Motahari, and Nicolas Luco. September 2006.

PEER 2006/04 *Probabilistic Seismic Evaluation of Reinforced Concrete Structural Components and Systems.* Tae Hyung Lee and Khalid M. Mosalam. August 2006.

PEER 2006/03 *Performance of Lifelines Subjected to Lateral Spreading.* Scott A. Ashford and Teerawut Juirnarongrit. July 2006.

PEER 2006/02 *Pacific Earthquake Engineering Research Center Highway Demonstration Project.* Anne Kiremidjian, James Moore, Yue Yue Fan, Nesrin Basoz, Ozgur Yazali, and Meredith Williams. April 2006.

PEER 2006/01 *Bracing Berkeley. A Guide to Seismic Safety on the UC Berkeley Campus.* Mary C. Comerio, Stephen Tobriner, and Ariane Fehrenkamp. January 2006.

PEER 2005/16 *Seismic Response and Reliability of Electrical Substation Equipment and Systems*. Junho Song, Armen Der Kiureghian, and Jerome L. Sackman. April 2006.

PEER 2005/15 *CPT-Based Probabilistic Assessment of Seismic Soil Liquefaction Initiation.* R. E. S. Moss, R. B. Seed, R. E. Kayen, J. P. Stewart, and A. Der Kiureghian. April 2006.

PEER 2005/14 *Workshop on Modeling of Nonlinear Cyclic Load-Deformation Behavior of Shallow Foundations.* Bruce L. Kutter, Geoffrey Martin, Tara Hutchinson, Chad Harden, Sivapalan Gajan, and Justin Phalen. March 2006.

PEER 2005/13 *Stochastic Characterization and Decision Bases under Time-Dependent Aftershock Risk in Performance-Based Earthquake Engineering.* Gee Liek Yeo and C. Allin Cornell. July 2005.

PEER 2005/12 *PEER Testbed Study on a Laboratory Building: Exercising Seismic Performance Assessment.* Mary C. Comerio, editor. November 2005.

PEER 2005/11 *Van Nuys Hotel Building Testbed Report: Exercising Seismic Performance Assessment.* Helmut Krawinkler, editor. October 2005.

PEER 2005/10 *First NEES/E-Defense Workshop on Collapse Simulation of Reinforced Concrete Building Structures.* September 2005.

PEER 2005/09 *Test Applications of Advanced Seismic Assessment Guidelines.* Joe Maffei, Karl Telleen, Danya Mohr, William Holmes, and Yuki Nakayama. August 2006.

PEER 2005/08 *Damage Accumulation in Lightly Confined Reinforced Concrete Bridge Columns.* R. Tyler Ranf, Jared M. Nelson, Zach Price, Marc O. Eberhard, and John F. Stanton. April 2006.

PEER 2005/07 *Experimental and Analytical Studies on the Seismic Response of Freestanding and Anchored Laboratory Equipment.* Dimitrios Konstantinidis and Nicos Makris. January 2005.

PEER 2005/06 *Global Collapse of Frame Structures under Seismic Excitations.* Luis F. Ibarra and Helmut Krawinkler. September 2005.

PEER 2005//05 *Performance Characterization of Bench- and Shelf-Mounted Equipment.* Samit Ray Chaudhuri and Tara C. Hutchinson. May 2006.

PEER 2005/04 *Numerical Modeling of the Nonlinear Cyclic Response of Shallow Foundations.* Chad Harden, Tara Hutchinson, Geoffrey R. Martin, and Bruce L. Kutter. August 2005.

PEER 2005/03 *A Taxonomy of Building Components for Performance-Based Earthquake Engineering.* Keith A. Porter. September 2005.

PEER 2005/02 *Fragility Basis for California Highway Overpass Bridge Seismic Decision Making*. Kevin R. Mackie and Božidar Stojadinović. June 2005.

PEER 2005/01 *Empirical Characterization of Site Conditions on Strong Ground Motion.* Jonathan P. Stewart, Yoojoong Choi, and Robert W. Graves. June 2005.

PEER 2004/09 *Electrical Substation Equipment Interaction: Experimental Rigid Conductor Studies.* Christopher Stearns and André Filiatrault. February 2005.

PEER 2004/08 *Seismic Qualification and Fragility Testing of Line Break 550-kV Disconnect Switches.* Shakhzod M. Takhirov, Gregory L. Fenves, and Eric Fujisaki. January 2005.

PEER 2004/07 *Ground Motions for Earthquake Simulator Qualification of Electrical Substation Equipment.* Shakhzod M. Takhirov, Gregory L. Fenves, Eric Fujisaki, and Don Clyde. January 2005.

PEER 2004/06 *Performance-Based Regulation and Regulatory Regimes.* Peter J. May and Chris Koski. September 2004.

PEER 2004/05 *Performance-Based Seismic Design Concepts and Implementation: Proceedings of an International Workshop.* Peter Fajfar and Helmut Krawinkler, editors. September 2004.

PEER 2004/04 *Seismic Performance of an Instrumented Tilt-up Wall Building.* James C. Anderson and Vitelmo V. Bertero. July 2004.

PEER 2004/03 *Evaluation and Application of Concrete Tilt-up Assessment Methodologies.* Timothy Graf and James O. Malley. October 2004.

PEER 2004/02 *Analytical Investigations of New Methods for Reducing Residual Displacements of Reinforced Concrete Bridge Columns.* Junichi Sakai and Stephen A. Mahin. August 2004.

PEER 2004/01 *Seismic Performance of Masonry Buildings and Design Implications.* Kerri Anne Taeko Tokoro, James C. Anderson, and Vitelmo V. Bertero. February 2004.

PEER 2003/18 *Performance Models for Flexural Damage in Reinforced Concrete Columns.* Michael Berry and Marc Eberhard. August 2003.

PEER 2003/17 *Predicting Earthquake Damage in Older Reinforced Concrete Beam-Column Joints.* Catherine Pagni and Laura Lowes. October 2004.

PEER 2003/16 *Seismic Demands for Performance-Based Design of Bridges.* Kevin Mackie and Božidar Stojadinović. August 2003.

PEER 2003/15 *Seismic Demands for Nondeteriorating Frame Structures and Their Dependence on Ground Motions.* Ricardo Antonio Medina and Helmut Krawinkler. May 2004.

PEER 2003/14 *Finite Element Reliability and Sensitivity Methods for Performance-Based Earthquake Engineering.* Terje Haukaas and Armen Der Kiureghian. April 2004.

PEER 2003/13 *Effects of Connection Hysteretic Degradation on the Seismic Behavior of Steel Moment-Resisting Frames.* Janise E. Rodgers and Stephen A. Mahin. March 2004.

PEER 2003/12 *Implementation Manual for the Seismic Protection of Laboratory Contents: Format and Case Studies.* William T. Holmes and Mary C. Comerio. October 2003.

PEER 2003/11 *Fifth U.S.-Japan Workshop on Performance-Based Earthquake Engineering Methodology for Reinforced Concrete Building Structures.* February 2004.

PEER 2003/10 *A Beam-Column Joint Model for Simulating the Earthquake Response of Reinforced Concrete Frames*. Laura N. Lowes, Nilanjan Mitra, and Arash Altoontash. February 2004.

PEER 2003/09 *Sequencing Repairs after an Earthquake: An Economic Approach.* Marco Casari and Simon J. Wilkie. April 2004.

PEER 2003/08 *A Technical Framework for Probability-Based Demand and Capacity Factor Design (DCFD) Seismic Formats*. Fatemeh Jalayer and C. Allin Cornell. November 2003.

PEER 2003/07 *Uncertainty Specification and Propagation for Loss Estimation Using FOSM Methods.* Jack W. Baker and C. Allin Cornell. September 2003.

PEER 2003/06 *Performance of Circular Reinforced Concrete Bridge Columns under Bidirectional Earthquake Loading*. Mahmoud M. Hachem, Stephen A. Mahin, and Jack P. Moehle. February 2003.

PEER 2003/05 *Response Assessment for Building-Specific Loss Estimation.* Eduardo Miranda and Shahram Taghavi. September 2003.

PEER 2003/04 *Experimental Assessment of Columns with Short Lap Splices Subjected to Cyclic Loads*. Murat Melek, John W. Wallace, and Joel Conte. April 2003.

PEER 2003/03 *Probabilistic Response Assessment for Building-Specific Loss Estimation.* Eduardo Miranda and Hesameddin Aslani. September 2003.

PEER 2003/02 *Software Framework for Collaborative Development of Nonlinear Dynamic Analysis Program.* Jun Peng and Kincho H. Law. September 2003.

PEER 2003/01 *Shake Table Tests and Analytical Studies on the Gravity Load Collapse of Reinforced Concrete Frames.* Kenneth John Elwood and Jack P. Moehle. November 2003.

PEER 2002/24 *Performance of Beam to Column Bridge Joints Subjected to a Large Velocity Pulse.* Natalie Gibson, André Filiatrault, and Scott A. Ashford. April 2002.

PEER 2002/23 *Effects of Large Velocity Pulses on Reinforced Concrete Bridge Columns.* Greg L. Orozco and Scott A. Ashford. April 2002.

PEER 2002/22 *Characterization of Large Velocity Pulses for Laboratory Testing.* Kenneth E. Cox and Scott A. Ashford. April 2002.

PEER 2002/21 *Fourth U.S.-Japan Workshop on Performance-Based Earthquake Engineering Methodology for Reinforced Concrete Building Structures*. December 2002.

PEER 2002/20 *Barriers to Adoption and Implementation of PBEE Innovations.* Peter J. May. August 2002.

PEER 2002/19 *Economic-Engineered Integrated Models for Earthquakes: Socioeconomic Impacts.* Peter Gordon, James E. Moore II, and Harry W. Richardson. July 2002.

PEER 2002/18 *Assessment of Reinforced Concrete Building Exterior Joints with Substandard Details.* Chris P. Pantelides, Jon Hansen, Justin Nadauld, and Lawrence D. Reaveley. May 2002.

PEER 2002/17 *Structural Characterization and Seismic Response Analysis of a Highway Overcrossing Equipped with Elastomeric Bearings and Fluid Dampers: A Case Study.* Nicos Makris and Jian Zhang. November 2002.

PEER 2002/16 *Estimation of Uncertainty in Geotechnical Properties for Performance-Based Earthquake Engineering.* Allen L. Jones, Steven L. Kramer, and Pedro Arduino. December 2002.

PEER 2002/15 *Seismic Behavior of Bridge Columns Subjected to Various Loading Patterns*. Asadollah Esmaeily-Gh. and Yan Xiao. December 2002.

PEER 2002/14 *Inelastic Seismic Response of Extended Pile Shaft Supported Bridge Structures.* T.C. Hutchinson, R.W. Boulanger, Y.H. Chai, and I.M. Idriss. December 2002.

PEER 2002/13 *Probabilistic Models and Fragility Estimates for Bridge Components and Systems.* Paolo Gardoni, Armen Der Kiureghian, and Khalid M. Mosalam. June 2002.

PEER 2002/12 *Effects of Fault Dip and Slip Rake on Near-Source Ground Motions: Why Chi-Chi Was a Relatively Mild M7.6 Earthquake.* Brad T. Aagaard, John F. Hall, and Thomas H. Heaton. December 2002.

PEER 2002/11 *Analytical and Experimental Study of Fiber-Reinforced Strip Isolators*. James M. Kelly and Shakhzod M. Takhirov. September 2002.

PEER 2002/10 *Centrifuge Modeling of Settlement and Lateral Spreading with Comparisons to Numerical Analyses***.** Sivapalan Gajan and Bruce L. Kutter. January 2003.

PEER 2002/09 *Documentation and Analysis of Field Case Histories of Seismic Compression during the 1994 Northridge, California, Earthquake.* Jonathan P. Stewart, Patrick M. Smith, Daniel H. Whang, and Jonathan D. Bray. October 2002.

PEER 2002/08 *Component Testing, Stability Analysis and Characterization of Buckling-Restrained Unbonded Braces™.* Cameron Black, Nicos Makris, and Ian Aiken. September 2002.

PEER 2002/07 *Seismic Performance of Pile-Wharf Connections.* Charles W. Roeder, Robert Graff, Jennifer Soderstrom, and Jun Han Yoo. December 2001.

PEER 2002/06 *The Use of Benefit-Cost Analysis for Evaluation of Performance-Based Earthquake Engineering Decisions*. Richard O. Zerbe and Anthony Falit-Baiamonte. September 2001.

PEER 2002/05 *Guidelines, Specifications, and Seismic Performance Characterization of Nonstructural Building Components and Equipment*. André Filiatrault, Constantin Christopoulos, and Christopher Stearns. September 2001.

PEER 2002/04 *Consortium of Organizations for Strong-Motion Observation Systems and the Pacific Earthquake Engineering Research Center Lifelines Program: Invited Workshop on Archiving and Web Dissemination of Geotechnical Data, 4–5 October 2001*. September 2002.

PEER 2002/03 *Investigation of Sensitivity of Building Loss Estimates to Major Uncertain Variables for the Van Nuys Testbed.* Keith A. Porter, James L. Beck, and Rustem V. Shaikhutdinov. August 2002.

PEER 2002/02 *The Third U.S.-Japan Workshop on Performance-Based Earthquake Engineering Methodology for Reinforced Concrete Building Structures*. July 2002.

PEER 2002/01 *Nonstructural Loss Estimation: The UC Berkeley Case Study.* Mary C. Comerio and John C. Stallmeyer. December 2001.

PEER 2001/16 *Statistics of SDF-System Estimate of Roof Displacement for Pushover Analysis of Buildings.* Anil K. Chopra, Rakesh K. Goel, and Chatpan Chintanapakdee. December 2001.

PEER 2001/15 *Damage to Bridges during the 2001 Nisqually Earthquake.* R. Tyler Ranf, Marc O. Eberhard, and Michael P. Berry. November 2001.

PEER 2001/14 *Rocking Response of Equipment Anchored to a Base Foundation.* Nicos Makris and Cameron J. Black. September 2001.

PEER 2001/13 *Modeling Soil Liquefaction Hazards for Performance-Based Earthquake Engineering.* Steven L. Kramer and Ahmed-W. Elgamal. February 2001.

PEER 2001/12 *Development of Geotechnical Capabilities in OpenSees.* Boris Jeremi . September 2001.

PEER 2001/11 *Analytical and Experimental Study of Fiber-Reinforced Elastomeric Isolators*. James M. Kelly and Shakhzod M. Takhirov. September 2001.

PEER 2001/10 *Amplification Factors for Spectral Acceleration in Active Regions.* Jonathan P. Stewart, Andrew H. Liu, Yoojoong Choi, and Mehmet B. Baturay. December 2001.

PEER 2001/09 *Ground Motion Evaluation Procedures for Performance-Based Design.* Jonathan P. Stewart, Shyh-Jeng Chiou, Jonathan D. Bray, Robert W. Graves, Paul G. Somerville, and Norman A. Abrahamson. September 2001.

PEER 2001/08 *Experimental and Computational Evaluation of Reinforced Concrete Bridge Beam-Column Connections for Seismic Performance*. Clay J. Naito, Jack P. Moehle, and Khalid M. Mosalam. November 2001.

PEER 2001/07 *The Rocking Spectrum and the Shortcomings of Design Guidelines.* Nicos Makris and Dimitrios Konstantinidis. August 2001.

PEER 2001/06 *Development of an Electrical Substation Equipment Performance Database for Evaluation of Equipment Fragilities*. Thalia Agnanos. April 1999.

PEER 2001/05 *Stiffness Analysis of Fiber-Reinforced Elastomeric Isolators.* Hsiang-Chuan Tsai and James M. Kelly. May 2001.

PEER 2001/04 *Organizational and Societal Considerations for Performance-Based Earthquake Engineering.* Peter J. May. April 2001.

PEER 2001/03 *A Modal Pushover Analysis Procedure to Estimate Seismic Demands for Buildings: Theory and Preliminary Evaluation.* Anil K. Chopra and Rakesh K. Goel. January 2001.

PEER 2001/02 *Seismic Response Analysis of Highway Overcrossings Including Soil-Structure Interaction.* Jian Zhang and Nicos Makris. March 2001.

PEER 2001/01 *Experimental Study of Large Seismic Steel Beam-to-Column Connections.* Egor P. Popov and Shakhzod M. Takhirov. November 2000.

PEER 2000/10 *The Second U.S.-Japan Workshop on Performance-Based Earthquake Engineering Methodology for Reinforced Concrete Building Structures.* March 2000.

PEER 2000/09 *Structural Engineering Reconnaissance of the August 17, 1999 Earthquake: Kocaeli (Izmit), Turkey.* Halil Sezen, Kenneth J. Elwood, Andrew S. Whittaker, Khalid Mosalam, John J. Wallace, and John F. Stanton. December 2000.

PEER 2000/08 *Behavior of Reinforced Concrete Bridge Columns Having Varying Aspect Ratios and Varying Lengths of Confinement.* Anthony J. Calderone, Dawn E. Lehman, and Jack P. Moehle. January 2001.

PEER 2000/07 *Cover-Plate and Flange-Plate Reinforced Steel Moment-Resisting Connections.* Taejin Kim, Andrew S. Whittaker, Amir S. Gilani, Vitelmo V. Bertero, and Shakhzod M. Takhirov. September 2000.

PEER 2000/06 *Seismic Evaluation and Analysis of 230-kV Disconnect Switches.* Amir S. J. Gilani, Andrew S. Whittaker, Gregory L. Fenves, Chun-Hao Chen, Henry Ho, and Eric Fujisaki. July 2000.

PEER 2000/05 *Performance-Based Evaluation of Exterior Reinforced Concrete Building Joints for Seismic Excitation.* Chandra Clyde, Chris P. Pantelides, and Lawrence D. Reaveley. July 2000.

PEER 2000/04 *An Evaluation of Seismic Energy Demand: An Attenuation Approach.* Chung-Che Chou and Chia-Ming Uang. July 1999.

PEER 2000/03 *Framing Earthquake Retrofitting Decisions: The Case of Hillside Homes in Los Angeles.* Detlof von Winterfeldt, Nels Roselund, and Alicia Kitsuse. March 2000.

PEER 2000/02 *U.S.-Japan Workshop on the Effects of Near-Field Earthquake Shaking.* Andrew Whittaker, ed. July 2000.

PEER 2000/01 *Further Studies on Seismic Interaction in Interconnected Electrical Substation Equipment.* Armen Der Kiureghian, Kee-Jeung Hong, and Jerome L. Sackman. November 1999.

PEER 1999/14 *Seismic Evaluation and Retrofit of 230-kV Porcelain Transformer Bushings*. Amir S. Gilani, Andrew S. Whittaker, Gregory L. Fenves, and Eric Fujisaki. December 1999.

PEER 1999/13 *Building Vulnerability Studies: Modeling and Evaluation of Tilt-up and Steel Reinforced Concrete Buildings.* John W. Wallace, Jonathan P. Stewart, and Andrew S. Whittaker, editors. December 1999.

PEER 1999/12 *Rehabilitation of Nonductile RC Frame Building Using Encasement Plates and Energy-Dissipating Devices.* Mehrdad Sasani, Vitelmo V. Bertero, James C. Anderson. December 1999.

PEER 1999/11 *Performance Evaluation Database for Concrete Bridge Components and Systems under Simulated Seismic Loads.* Yael D. Hose and Frieder Seible. November 1999.

PEER 1999/10 *U.S.-Japan Workshop on Performance-Based Earthquake Engineering Methodology for Reinforced Concrete Building Structures.* December 1999.

PEER 1999/09 *Performance Improvement of Long Period Building Structures Subjected to Severe Pulse-Type Ground Motions*. James C. Anderson, Vitelmo V. Bertero, and Raul Bertero. October 1999.

PEER 1999/08 *Envelopes for Seismic Response Vectors.* Charles Menun and Armen Der Kiureghian. July 1999.

PEER 1999/07 *Documentation of Strengths and Weaknesses of Current Computer Analysis Methods for Seismic Performance of Reinforced Concrete Members.* William F. Cofer. November 1999.

PEER 1999/06 *Rocking Response and Overturning of Anchored Equipment under Seismic Excitations.* Nicos Makris and Jian Zhang. November 1999.

PEER 1999/05 *Seismic Evaluation of 550 kV Porcelain Transformer Bushings.* Amir S. Gilani, Andrew S. Whittaker, Gregory L. Fenves, and Eric Fujisaki. October 1999.

PEER 1999/04 *Adoption and Enforcement of Earthquake Risk-Reduction Measures.* Peter J. May, Raymond J. Burby, T. Jens Feeley, and Robert Wood.

PEER 1999/03 *Task 3 Characterization of Site Response General Site Categories*. Adrian Rodriguez-Marek, Jonathan D. Bray, and Norman Abrahamson. February 1999.

PEER 1999/02 *Capacity-Demand-Diagram Methods for Estimating Seismic Deformation of Inelastic Structures: SDF Systems*. Anil K. Chopra and Rakesh Goel. April 1999.

PEER 1999/01 *Interaction in Interconnected Electrical Substation Equipment Subjected to Earthquake Ground Motions.* Armen Der Kiureghian, Jerome L. Sackman, and Kee-Jeung Hong. February 1999.

PEER 1998/08 *Behavior and Failure Analysis of a Multiple-Frame Highway Bridge in the 1994 Northridge Earthquake.* Gregory L. Fenves and Michael Ellery. December 1998.

PEER 1998/07 *Empirical Evaluation of Inertial Soil-Structure Interaction Effects.* Jonathan P. Stewart, Raymond B. Seed, and Gregory L. Fenves. November 1998.

PEER 1998/06 *Effect of Damping Mechanisms on the Response of Seismic Isolated Structures.* Nicos Makris and Shih-Po Chang. November 1998.

PEER 1998/05 *Rocking Response and Overturning of Equipment under Horizontal Pulse-Type Motions.* Nicos Makris and Yiannis Roussos. October 1998.

PEER 1998/04 *Pacific Earthquake Engineering Research Invitational Workshop Proceedings, May 14–15, 1998: Defining the Links between Planning, Policy Analysis, Economics and Earthquake Engineering.* Mary Comerio and Peter Gordon. September 1998.

PEER 1998/03 *Repair/Upgrade Procedures for Welded Beam to Column Connections.* James C. Anderson and Xiaojing Duan. May 1998.

PEER 1998/02 *Seismic Evaluation of 196 kV Porcelain Transformer Bushings.* Amir S. Gilani, Juan W. Chavez, Gregory L. Fenves, and Andrew S. Whittaker. May 1998.

PEER 1998/01 *Seismic Performance of Well-Confined Concrete Bridge Columns.* Dawn E. Lehman and Jack P. Moehle. December 2000.

ONLINE REPORTS

The following PEER reports are available by Internet only at http://peer.berkeley.edu/publications/peer_reports.html

PEER 2009/102 *Reinvestigation of Liquefaction and Nonliquefaction Case Histories from the 1976 Tangshan Earthquake.* Robb Eric Moss, Robert E. Kayen, Liyuan Tong, Songyu Liu, Guojun Cai, and Jiaer Wu. August 2009.

PEER 2009/101 *Report of the First Joint Planning Meeting for the Second Phase of NEES/E-Defense Collaborative Research on Earthquake Engineering.* Stephen A. Mahin et al. July 2009.

PEER 2008/104 *Experimental and Analytical Study of the Seismic Performance of Retaining Structures.* Linda Al Atik and Nicholas Sitar. January 2009.

PEER 2008/103 *Experimental and Computational Evaluation of Current and Innovative In-Span Hinge Details in Reinforced Concrete Box-Girder Bridges. Part 1: Experimental Findings and Pre-Test Analysis.* Matias A. Hube and Khalid M. Mosalam. January 2009.

PEER 2008/102 *Modeling of Unreinforced Masonry Infill Walls Considering In-Plane and Out-of-Plane Interaction.* Stephen Kadysiewski and Khalid M. Mosalam. January 2009.

PEER 2008/101 *Seismic Performance Objectives for Tall Buildings.* William T. Holmes, Charles Kircher, William Petak, and Nabih Youssef. August 2008.

PEER 2007/101 *Generalized Hybrid Simulation Framework for Structural Systems Subjected to Seismic Loading.* Tarek Elkhoraibi and Khalid M. Mosalam. July 2007.

PEER 2007/100 *Seismic Evaluation of Reinforced Concrete Buildings Including Effects of Masonry Infill Walls.* Alidad Hashemi and Khalid M. Mosalam. July 2007.